A LABORATORY STUDY OF THE POTENTIAL OF TIME-RESOLVED LASER FLUOROSENSORS

D. M. Rayner and A. G. Szabo

Division of Biological Sciences
National Research Council Canada
Ottawa, Canada K1A OR6

Prepared for: The Sensor Working Group
Canada Centre for Remote Sensing

November 1976

Report Number By-76-2 (RC)

A LABORATORY STUDY OF THE POTENTIAL OF TIME-RESOLVED LASER FLUOROSENSORS

D. M. Rayner and A. G. Szabo

Division of Biological Sciences
National Research Council Canada
Ottawa, Canada K1A OR6

Prepared for: The Sensor Working Group
Canada Centre for Remote Sensing

November 1976

Report Number By-76-2 (RC)

CONTENTS

1. Introduction

The extension of the capabilities of laser fluorosensors to include the measurement of fluorescence decay parameters has been suggested as a means of improving the selectivity of such sensors[1,2]. In our Interim Report[3] we reported the results of a careful investigation of the decay parameters of a small selection of oils likely to be discharged in Canadian waters. These measurements were made at high resolution and established that the oils did indeed show fluorescence decay properties which allowed all but the bunker oils to be individually characterised in the laboratory. However theoretical consideration of the practical operation of airborne remote time-resolved fluorosensors, especially the low signal-to-noise ratio (S/N) to be expected (~20:1 cf. 400:1 for the laboratory measurements), the wide bandpass required to obtain even this S/N, and the possible distortion of the fluorescence signal due to the sea state, may cause limitations in the utility of laser fluorosensors in the remote classification of oils.

In this Final Report we present the results of an investigation of the fluorescence properties of a large selection of oils under conditions estimated to be close to those expected in practice. We also report the results of a study of the effects of aging on these properties for a few oils. In the light of these results we discuss the degree of discrimination with which the present fluorosensors should be able to identify and characterize oil. The possible lowering of this degree of discrimination due

to the sea state is discussed more fully than in the Interim Report. Finally we report some preliminary studies on the fluorescence properties of chlorophyll in vivo and consider other roles of fluorosensing whose feasibility could be determined by further laboratory studies.

2. Experimental

Fluorescence emission spectra were measured using the NRC built fluorimeter described in our Interim Report[3]. All the spectra have been corrected for the variation of the instrument response function with wavelength. The units of fluorescence intensity are relative quanta/second. All the oil samples were of sufficient thickness to be optically dense at the excitation wavelength of 337 nm, chosen for these experiments as being the wavelength of the nitrogen laser. For all the spectra reported the excitation bandwidth was 1.4 nm and the emission bandwidth was 7 nm.

Fluorescence decay profiles were measured using a simplified version of the single photon counting fluorescence lifetime apparatus used for our previous high resolution study of oil fluorescence and described previously[4]. The fluorosensor presently under development has two temporal channels. These channels have a broad spectral bandwidth of as yet undetermined wavelength. To mimic this system we therefore substituted the emission monochromator in our apparatus with one of two broad bandpass filter combinations: a) a Corning glass 0-51 filter followed by a Corning glass 7-54 filter (in that order since the 0-51 filter fluorescences); b) a solution of potassium chromate (0.1% w/v in water) of 10 mm path length. The transmission curves of these two filter systems are shown in Figure 1. When using a broad bandwidth one must also consider the quantum efficiency of the photomultiplier across the bandwidth. Multiplying the filter

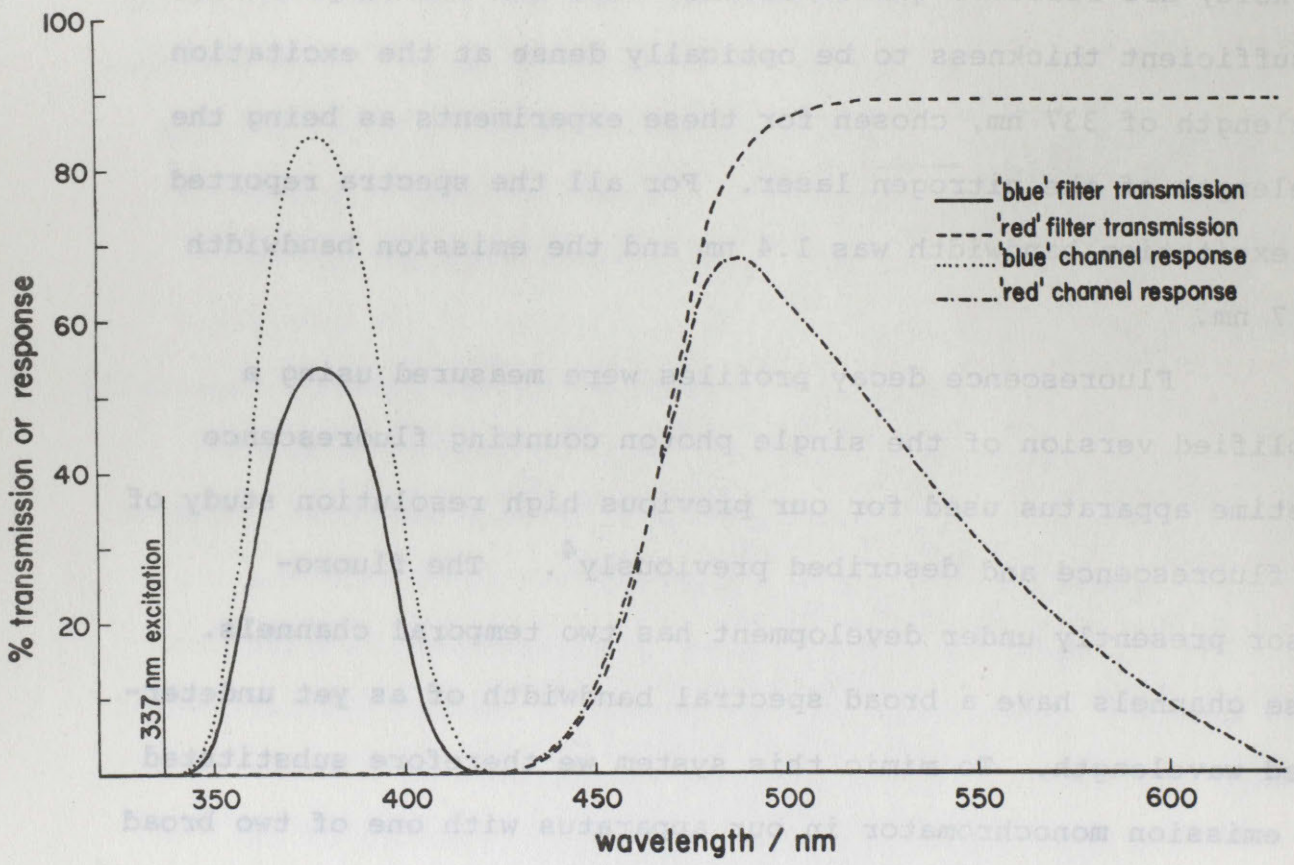

Figure 1: The transmission and response curves for the blue and red channel filter combinations. The response at a given wavelength is the product of the filter transmission and the cathode quantum efficiency of the PMT (RCA 8850) at that wavelength.

transmission and the quantum efficiency of the tube we obtain the bandpass envelope or response in which the measurements are effectively made. The choice of filters was based on the results of our preliminary studies and is explained in section 5. All decay profiles were collected to give 400 counts in the peak which, assuming a Poisson distribution for the noise, gives an S/N ratio of 20. This relatively low number of counts could be collected in a short period of time thus removing the need to alternate the sample and scatterer (to measure the lamp profile) to compensate for lamp drift. The lamp profile was collected independently immediately prior to making each sample measurement. The low S/N ratios also masked the effect of the variation of the photomultiplier time response variation with wavelength. The correction procedure described previously[4] and used for our earlier precise measurements on oils was therefore not applied. The oil sample was contained in a small open dish as before and the emission was collected using a front surface arrangement.

3. Oil Selection

A much larger selection of crude oils and refined products was investigated than in the preliminary study. The oils can be grouped by their origin and physical properties into three main groups; crude oils (CO): heavy refined oils (HO), and light refined oils (LO). Table 1 gives the name, type, and code number used in this report. Where the oil was one of the selection provided by the RCMP their identification number (PP #) is also recorded.

Table 1. Selection of oils used in this study

Code #	Description	RCMP #
CO1	Venezuelan 'Lago Medio' Crude	-
CO2	Texaco Transmountain Crude	-
CO3	Texaco Arabian Crude	-
CO4	Texaco Nigerian Crude	-
CO5	Texaco Venezuelan 'Lago Medio' Crude	-
CO6	Gulf Oil Redwater Crude	PP19
CO7	Gulf Oil B.C. Light Crude	PP20
CO8	B.P. Light Sour Crude	PP21
CO9	B.P. Medium Sweet Crude	PP22
CO10	B.P. Chagrin Crude	PP23
CO11	Texaco Common Sweet Crude	PP24
CO12	I.P. #2 Blend Crude	PP28
CO13	Gulf Oil Company Coleville/Smiley Crude	PP29
CO14	Imperial Oil Venezuelan Crude	PP32
CO15	Brega Ligbian Crude	PP41
CO16	Shell Canada Midal Crude	PP44
CO17	Shell Canada I.P. Crude	PP44
CO18	Shell Oil Boundary Lake Crude	PP72

Code #	Description	RCMP #
CO19	Shell Oil Peace River Crude	PP73
CO20	Shell Oil Gulf Alberta Crude	PP74
CO21	Imperial Oil Crude (IOCO Blend Redwater and Gulf Alberta)	PP78
HO1	Medium Bunker C	-
HO2	Esso Bunker Fuel	-
HO3	Esso Fuel Int. 2	-
HO4	Esso Fuel Int. 10	-
HO5	Esso Fuel Int. 12	-
HO6	Esso Fuel Int. 15	-
HO7	Esso Fuel Int. 20	-
HO8	Gulf Oil #5B Bunker Fuel	PP17
HO9	Gulf Oil #6C Bunker Fuel	PP18
HO10	B.P. Bunker 6C	PP25
HO11	Gulf Oil Company Bunker 6C	PP26
HO12	Gulf Oil Company Bunker 6C-1.5	PP30
HO13	Imperial Oil Venezuelan Bunker #6	PP31
HO14	Imperial Oil Venezuelan Bunker #5	PP33
HO15	Golden Eagle Refinery Venezuelan High S Content Bunker C	-
HO16	Shell 1.5% Bunker	PP42
HO17	Texaco Heavy Bunker 6C	PP52
HO18	Gulf Bunker #5	PP54
HO19	Gulf Bunker 6C	PP57
HO20	Shell Oil Bunker C	PP69
HO21	Shell Oil #5 Fuel	PP70
HO22	Shell Oil 1500 Sec. Fuel	PP71
HO23	Imperial Oil Bunker C	PP75
HO24	Imperial Oil Fuel 46 (Bunker B or #5)	PP76
HO25	Standard Light Fuel Oil	PP79
HO26	Standard Fuel Oil	PP80
HO27	Standard Oil Chevron Intermediate Bunker Fuel 4	PP81
HO28	Standard Oil Chevron Intermediate Bunker Fuel 10	PP82

Code #	Description	RCMP #
LO1	Esso Marine Gas/Oil	
LO2	Furnace Fuel Oil #2B (Winter)	
LO3	Esso Marine Diesel	
LO4	Lubricating Oil taken on Russian Ship	PP61
LO5	Circulated Lubricating Oil taken on Russian Ship	PP62
LO6	Light Diesel taken on Russian Ship	PP63
LO7	Marine Diesel taken on Swedish Ship	PP64
LO8	Diesel (Gas/Oil) taken on Russian Ship	PP68
LO9	Imperial Oil Marine Diesel Oil	PP77
LO10	Standard Oil Chevron Marine Diesel	PP84
UO3	Unknown liquid	PP91

4. Fluorescence Emission Spectra

The fluorescence emission spectra for the selection of oils are recorded in the lower frames of the Figures presented in Appendix I. All the spectra are recorded in relative quanta per second so that intensity comparisons can be made between any two spectra. Four ranges were used for the intensity ordinate, the scale being successively multiplied by 5. Any intensity reading can be converted to relative energy units by dividing by the wavelength at which that reading is taken.

The final spectrum reported in Appendix I is that recorded, in the same units, for a solution of quinine sulphate (10^{-4} M in 0.5 M H_2SO_4). This is a commonly used standard and has a quantum yield of fluorescence of 0.55. The standard can be used to estimate the quantum yield of fluorescence of an oil by comparison of the spectra or more rigorously by comparison of the areas under the curves. If we ignore differences in the refractive indices between an oil and the standard solution (and hence differences in the reflective losses at the interface) then the quantum yield of fluorescence of the oil (ϕ_{OIL}) is given by

$$\phi_{OIL} = \frac{\text{Area under oil spectrum}}{\text{Area under standard spectrum}} \times \phi_s$$

where ϕ_s is the quantum yield of fluorescence of the standard. ϕ_{OIL} values give an overall indication of the strength of fluorescence signal to be expected from an oil and are listed in Table 2 along with the wavelength of maximum fluorescence intensity.

Table 2. Quantum efficiencies of fluorescence and wavelengths of maximum fluorescence intensity of oils

Code #	ϕ_{OIL}	λ_{max}/nm		ϕ_{OIL}	λ_{max}/nm
CO1	0.023	511	CO12	0.054	520
CO2	0.083	508	CO13	0.015	536
CO3	0.034	535	CO14	0.017	507
CO4	0.095	484	CO15	0.032	508
CO5	0.021	508	CO16	0.017	538
CO6	0.041	535	CO17	0.037	508
CO7	0.107	468	CO18	0.032	511
CO8	0.038	510	CO19	0.0642	511
CO9	0.044	510	CO20	0.072	510
CO10	0.013	563	CO21	0.031	510
CO11	0.047	508			
HO1	0.002	525	HO15	0.005	545
HO2	0.003	540	HO16	0.006	580
HO3	0.014	530	HO17	0.004	570
HO4	0.007	570	HO18	0.010	570
HO5	0.006	560	HO19	0.006	580
HO6	0.006	560	HO20	0.009	585
HO7	0.006	560	HO21	0.013	580
HO8	0.015	590	HO22	0.008	580
HO9	0.010	580	HO23	0.009	590
HO10	0.004	580	HO24	0.005	560
HO11	0.003	535	HO25	0.016	555
HO12	0.007	565	HO26	0.012	560
HO13	0.004	535	HO27	0.018	560
HO14	0.006	545	HO28	0.009	585
LO1	0.048	395	LO6	0.076	400
LO2	0.053	400	LO7	0.058	419
LO3	0.085	400	LO8	0.072	404
LO4	0.044	407	LO9	0.064	415
LO5	0.117	407	LO10	0.103	452

Where a fluorosensor has spectral channels of specific wavelength and bandwidth the relative size of the signal to be expected in any channel can be found by integrating between the wavelength boundaries of that channel. The corrected spectra are stored in digital form on magnetic tape at the NRCC Computer Centre and this type of calculation can be made easily once any particular fluorosensor's specifications are known.

By inspection of the spectra, of which typical examples are shown in Figure 2, or by just comparing the wavelengths of maximum emission, λ_{max}, and the quantum yields of fluorescence, ϕ_{OIL}, we can divide the oils into three main groups, confirming with a larger oil selection the results of our Interim Report:

1. The light refined petroleum products which show partly structured emission with λ_{max} less than 455 nm in all cases and typically about 410 nm and with ϕ_{OIL} greater than 0.04 and less than 0.12.

2. The crude oils which show broad, unstructured emission with λ_{max} between 480 nm and 565 nm and with ϕ_{OIL} greater than 0.015 and less than 0.11. Where crude oils show ϕ_{OIL} values comparable to those of the light oils they have lower but broader spectra than the light oils.

3. The heavy refined petroleum products which show weaker, broad, unstructured emission with λ_{max} between 525 nm and 600 nm and with ϕ_{OIL} less than 0.02 and greater than 0.02.

The larger oil selection used in this study shows that there is no distinct boundary in spectral properties between the

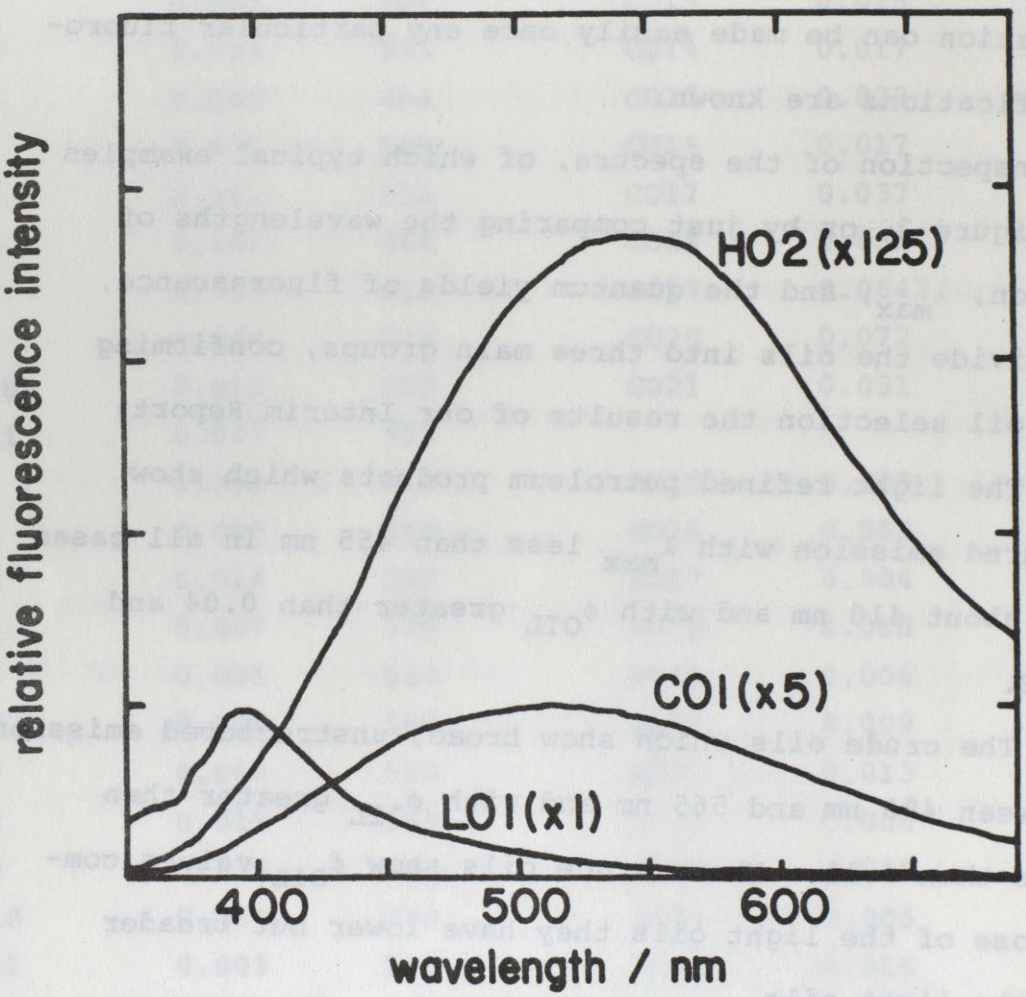

Figure 2: Typical spectra of oils from the three groups.

heavier crude oils and the lighter of the heavy refined petroleum products. Apart from these boundary cases fluorescence spectral measurements can therefore, as previously shown, be used to place an unknown oil in one of the three groups.

5. Fluorescence Decay Measurements

Given the present power capabilities of nitrogen lasers and other practical limitations of remote fluorosensing, decay measurements can only be made with a workable S/N ratio in practice by monitoring over a large spectral bandwidth. We chose to study the decay properties of our large selection of oils in two spectral regions, as the sensor under development is intended to do.

Our spectral studies demonstrated that the light oils show strong emission in the region below 450 nm. In this region the light oils have fluorescence decay times expected to be greater than 10 ns[1,2]. The crude oils also emit strongly enough to be monitored by a remote sensor in this region although with shorter decay times. The 'blue' channel was therefore chosen to be of relatively small bandwidth (~50 nm) and centred at ~380 nm (Figure 1) and was expected to perform best for light oils and to yield some information on the crude oils. The heavy oils show weaker broad emission towards the red end of the spectrum. Preliminary results also showed a lengthening of decay times for all types of oil on monitoring to the red. The 'red' channel was therefore chosen to be as wide as possible (to collect as much signal as possible from the weakly emitting heavy oils). A short wavelength cut-off filter with 50% transmission at 470 nm was used, being the shortest filter possible which does not overlap the 'blue' channel (Figure 1). Light and crude oils also emit efficiently enough in this 'red' region for decay measurements to be made.

We measured the fluorescence decay profiles of our large selection of oils in each of the above two channels. A S/N ratio 20:1, comparable to that expected from a remote sensor, was aimed for. The decay profiles are recorded in the top frames of the figures presented in Appendix I along with the profile of the exciting flash lamp. By inspection it can be seen that in any one spectral channel the fluorescence of the light oils decays slower than that of the crude oils which in turn decays slower than that of the heavy oils. In our Interim Report (p. 20) we discussed the extraction of decay parameters from decay profiles especially the deconvolution of the exciting lamp profile from the measured profile. We showed that adequate fits, even for our low noise data, could be obtained for all our oil fluorescence decay profiles by fitting to a two-exponential function (F(t));

$$F(t) = F_a e^{-t/a} + F_b e^{-t/b}.$$

It was pointed out that this function is just being used to describe an unknown decaying function (theoretically expected to be multiexponential) and that although the parameters a, b, F_a and F_b can be used to describe F(t) they have no direct photophysical meaning. However since the data in the present study have a relatively high noise level we found that a one-exponential fit was adequate for all but the longest decay profiles (where more information is available). The oil fluorescence decay times listed in Table 3 are the results of such one-exponential fits to our decay profiles using a non-linear least squares re-iterative convolution technique.

Table 3. Fluorescence decay times of oils from one-exponential fits

Oil	Blue channel			Red channel		
	decay time/ns	95% support plane limits/ns		decay time/ns	95% support plane limits/ns	
		upper	lower		upper	lower
C01	1.07	1.21	0.96	3.44	3.67	3.23
C02	1.48	1.65	1.34	5.95	6.26	5.68
C03	0.90	1.05	0.78	3.09	3.29	2.91
C04	2.00	2.22	1.81	7.47	7.84	7.13
C05	1.76	1.92	1.63	3.33	3.59	3.11
C06	1.18	1.33	1.06	4.19	4.47	3.93
C07	2.60	2.83	2.40	8.23	8.60	7.89
C08	1.38	1.52	1.27	4.39	4.64	4.17
C09	1.55	1.72	1.42	5.34	5.63	5.09
C010	0.86	0.98	0.76	2.26	2.42	2.11
C011	1.47	1.88	1.20			
C012	1.43	1.58	1.30	5.24	5.51	5.00
C013	0.82	0.97	0.71	2.28	2.44	2.14
C014	0.96	1.09	0.87	3.30	3.53	3.10
C015	1.85	2.13	1.64	4.84	5.13	4.59
C016	0.92	1.17	0.76	2.39	2.57	2.24
C017	2.26	2.63	1.98	4.81	5.09	4.55
C018	1.46	1.64	1.31	4.16	4.42	3.93
C019	2.09	2.35	1.89	5.93	6.23	5.66
C020	2.08	2.28	1.92	6.40	6.72	6.12
C021	1.32	1.47	1.20	4.46	4.70	4.24
L01	13.0	14.1	12.1			
L02	12.5	13.4	11.8	19.7	20.3	19.1
L03	11.9	12.9	10.9	31.4	32.3	30.5
L04	3.23	3.66	2.89	9.22	9.92	8.61
L05	7.91	8.81	7.18	16.1	16.9	15.4
L06	8.56	9.19	8.01	21.7	22.5	20.9
L07	4.26	4.64	3.94	7.66	8.15	7.23
L08	7.91	8.49	7.40	18.2	18.8	17.6

Oil	Blue channel			Red channel		
	decay time/ns	95% support plane limits/ns		decay time/ns	95% support plane limits/ns	
		upper	lower		upper	lower
L09	9.81	10.7	9.04	23.4	24.2	22.7
L010	5.69	6.23	5.24	10.4	9.90	11.0
H01				1.07	1.20	0.96
H02				1.00	1.12	0.91
H03	0.845	0.97	0.75	2.58	2.75	2.43
H04				1.37	1.53	1.24
H05				1.59	1.74	1.46
H06				1.36	1.52	1.23
H07				3.19	2.59	2.87
H08				1.76	1.92	1.63
H09				1.52	1.70	1.38
H010				1.09	1.21	0.99
H011				1.07	1.22	0.96
H012				1.37	1.52	1.25
H013				1.19	1.34	1.07
H014				1.59	1.75	1.45
H015				1.75	1.91	1.62
H016				1.47	1.61	1.36
H017				1.02	1.15	0.91
H018				2.10	2.27	1.95
H019				1.29	1.43	1.18
H020				1.28	1.42	1.18
H021				1.86	2.01	1.73
H022				1.44	1.57	1.33
H023				1.40	1.54	1.28
H024				1.17	1.33	1.05
H025				2.38	2.56	2.23
H026				1.98	2.13	1.84
H027				2.46	2.66	2.28
H028				1.70	1.86	1.57
H029				3.50	3.99	3.12

The limits quoted are the extremes of the 95% support plane for the two-parameter fit. Although this technique has been shown to be the best for dealing with high quality fluorescence decay data the high noise on the present data would allow the use of a simpler deconvolution method - possibly one involving transforms of some sort or even the full width half maximum method (FWHM) if the exciting flash is reproducible. It should be noted that the FWHM method can only be expected to give the same answer as methods which fit all the data when the decay can be adequately described by one exponential.

The histogram plots in Figure 3 show the spread in the decay times that were found for the oils using the 'blue channel'. Only the light and crude oil results are shown as the heavy oils' emission was too weak in this channel. From the full time scale plot it can be seen that the light oils all show longer decay times between 3 and 14 ns in the blue than the crude oils which have them bunched lower than 3 ns. There is very little overlap between one light oil and another. On the expanded plot the crude oil decay times appear to separate into small groups allowing some characterization in this class of oils with only one channel at low resolution.

In the 'red channel' it was possible to measure decay times for all the oils (Figure 4). All the oil decays that had been measured in the blue proved longer in the red. Again the light oils showed the longest decay times, coming between 7 and 32 ns. The heavy oils all have short decay times, less than 4 ns and the crude oils have intermediate decay times slightly overlapping both the heavy and light oils. The extent of this overlap is best seen on the expanded plots of Figure 4.

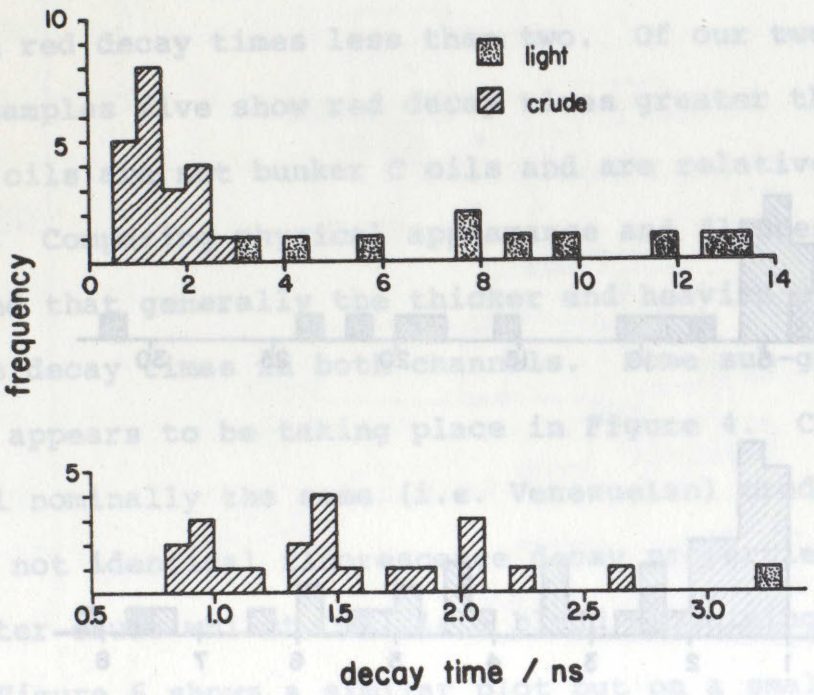

Figure 3: Distribution of oil fluorescence decay times in the blue channel.

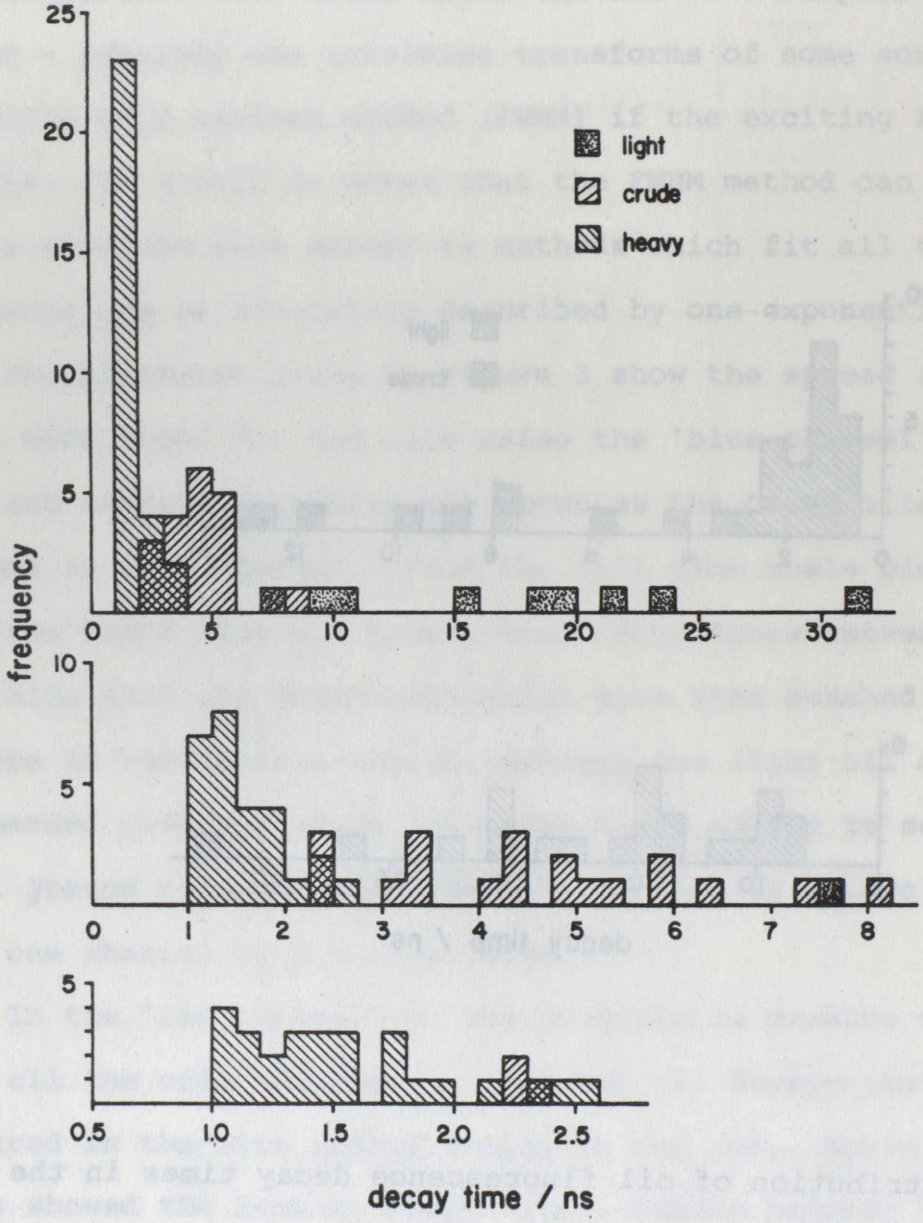

Figure 4: Distribution of oil fluorescence decay times in the red channel.

For the oils which could be studied in both channels the results can be presented as plots of 'red' decay time vs. blue decay time. In Figure 5 such a plot is shown for the crude oils. The boxes delineate the calculated confidence limits for the parameters taken from their 95% support plane values. The range covered by the crude oils can be seen from this plot. The light oil with the shortest decay times is shown in the top right hand corner whilst the heavy oils would be found at the bottom left, mostly with red decay times less than two. Of our twenty-eight heavy oil samples five show red decay times greater than two. These five heavy oils are not bunker C oils and are relatively light for that group. Comparing physical appearance and fluorescence properties we find that generally the thicker and heavier a crude oil the shorter its decay times in both channels. Some sub-grouping of the crude oils appears to be taking place in Figure 4. CO14, CO1 and CO5 are all nominally the same (i.e. Venezuelan) crude oil and show similar if not identical fluorescence decay properties. Again CO6 is a Redwater crude whilst CO21 is a blend containing Redwater crude.

Figure 6 shows a similar plot but on a smaller scale allowing the study of the light petroleum products. Under this presentation each light oil appears to have unique decay properties measurable even with low S/N ratios. The two crude oils included in the bottom left hand corner show the longest lifetimes found for the crude oils. Certainly light oils can be classified as a group by their fluorescence decay properties. However it should be noted that LO3, LO9, LO10 and LO7 are all nominally Marine Diesel fuels despite their showing widely different fluorescence decay properties.

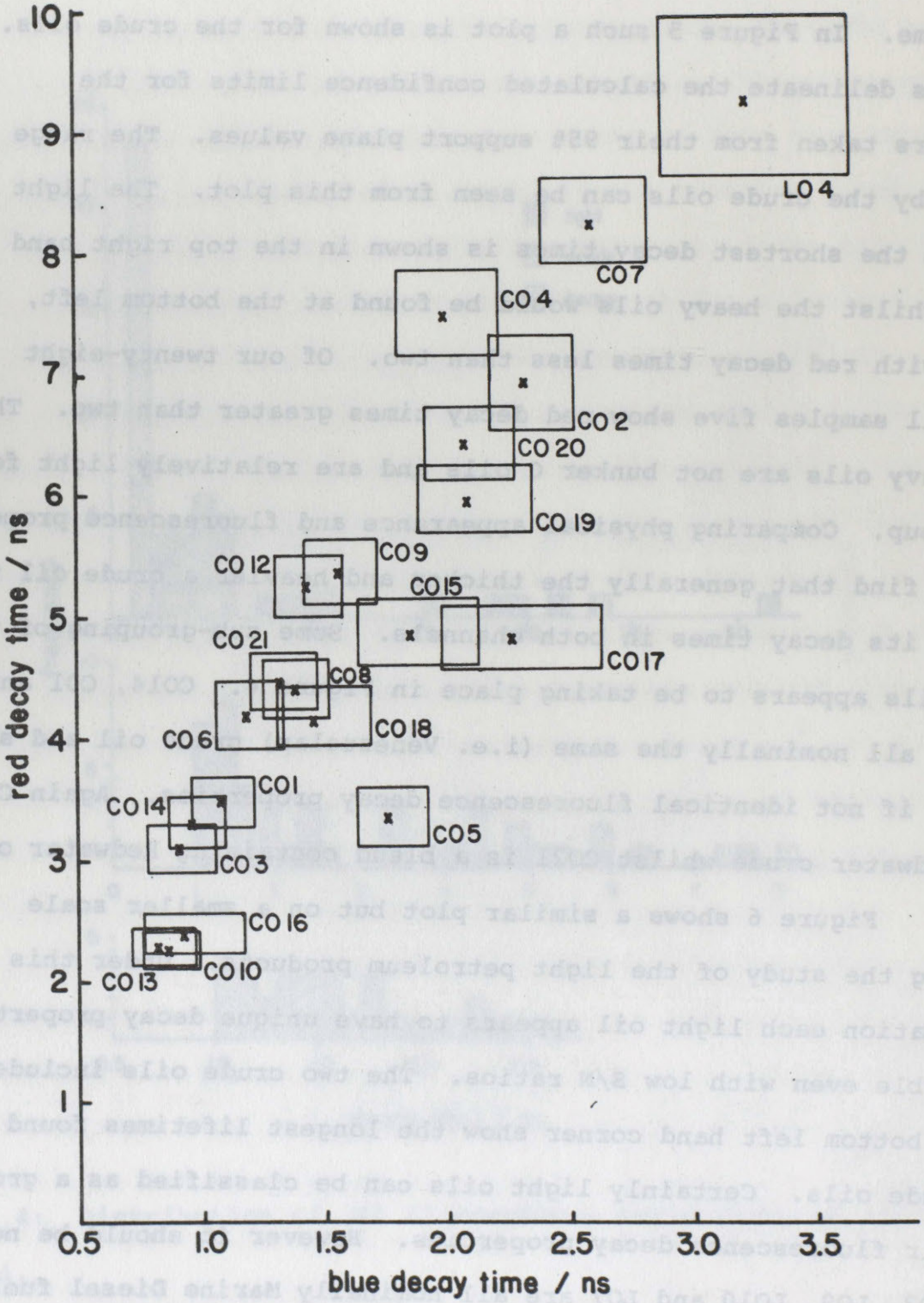

Figure 5: Red and blue channel oil fluorescence decay times of crude oils.

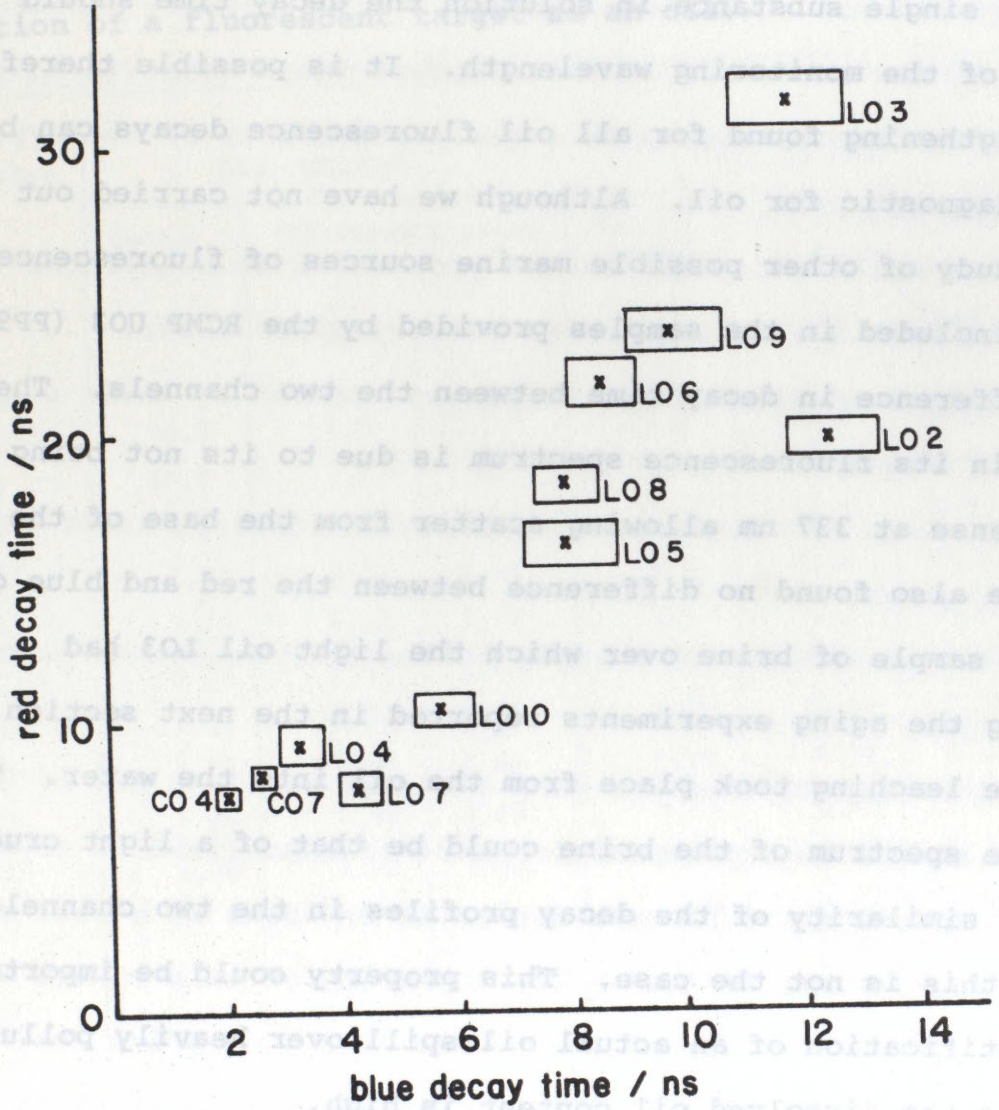

Figure 6: Red and blue channel oil fluorescence decay times of light oils.

It is also possible that the lubricating oils (LO4 and LO5) may contain some added dye which contributes to their fluorescence.

The lengthening of fluorescence decay times towards the red end of the spectrum is not a general property of fluorescence. Indeed for a single substance in solution the decay time should be independent of the monitoring wavelength. It is possible therefore that the lengthening found for all oil fluorescence decays can be used as a diagnostic for oil. Although we have not carried out an extensive study of other possible marine sources of fluorescence an unknown included in the samples provided by the RCMP UO3 (PP91) shows no difference in decay time between the two channels. The high background in its fluorescence spectrum is due to its not being optically dense at 337 nm allowing scatter from the base of the cuvette. We also found no difference between the red and blue decay times for a sample of brine over which the light oil LO3 had stood during the aging experiments reported in the next section. Considerable leaching took place from the oil into the water. The fluorescence spectrum of the brine could be that of a light crude oil but the similarity of the decay profiles in the two channels shows that this is not the case. This property could be important in the identification of an actual oil spill over heavily polluted waters where the dissolved oil content is high.

The lifetime studies on the large selection of oils therefore show that even at the low S/N ratios to be expected practically, fluorescence decay measurements can be predicted to allow the classification of oils into the same three groups as

possible using spectral measurement. Both methods will involve some uncertainty for the few oils whose properties are intermediate between those of the heavy and crude oils. Lifetime measurements could also prove more effective than spectral measurements in the identification of a fluorescent target as an oil.

6. Effect of Aging on the Fluorescence Properties of Oils

In order to predict the changes in the fluorescence properties of an oil which might occur whilst the oil is spilt we carried out model aging experiments on three oils (LO3, CO2, HO2), one representative of each group. While it is extremely difficult to simulate in the laboratory the conditions which exist in a spill in mid-ocean our experiments give a qualitative idea of the type of changes to be expected.

In a spill the fluorescence properties of an oil can be expected to change due mainly to the following processes:

i) loss of fluorescent components caused by their evaporation into the atmosphere,

ii) loss of fluorescent components caused by their leaching into the sea-water,

iii) photochemical changes in the fluorescent components due to sunlight.

Our aging experiments were designed to allow all of the above processes to take place although it is impossible to reproduce the surface area/spill thickness ratios to be found in a real spill. The rates of all three processes are dependent on this ratio. The oil was spread at a thickness of 5 mm over 1.3 l of brine (salinity adjusted to a typical sea-water value) contained in a straight-sided dish 18 cm in diameter. The relatively large thickness was necessary to have sufficient oil for the periodic removal of samples for measurements. The containers were exposed on the roof of our Ottawa laboratory to typical July weather. Samples were taken after 0, 24,

48, 72 and 144 hours for the measurement of their fluorescence spectra and their fluorescence decay profiles in the blue and red channels. The spectra and profiles are shown in Appendix II. The decay times for a one-exponential fit are shown in Table 4.

Table 4. Fluorescence decay times of aging oils from one-exponential fits

Oil	After/hrs	Blue channel			Red channel		
		decay time/ns	95% support plane limits/ns		decay time/ns	95% support plane limits/ns	
			upper	lower		upper	lower
LO3	0	10.9	11.8	10.2	29.6	30.5	28.8
LO3	24	10.1	11.0	9.3	29.3	30.0	28.5
LO3	48	8.24	9.01	7.60	23.2	24.1	22.4
LO3	72	7.27	8.02	6.64	20.5	21.4	19.7
LO3	144	3.75	4.14	3.43	10.5	11.2	9.95
CO2	0	2.33	2.51	2.18	6.89	7.31	6.52
CO2	24	2.11	2.32	1.93	6.20	6.50	5.93
CO2	48	1.83	2.10	1.63	5.88	6.22	5.57
CO2	72	1.65	1.93	1.45	5.53	5.85	5.24
CO2	144	1.69	1.90	1.53	5.42	5.73	5.15
HO2	0				1.39	1.50	1.29
HO2	24				1.28	1.41	1.18
HO2	48				1.18	1.37	1.04
HO2	72				1.17	1.42	0.99
HO2	144				1.37	1.58	1.21
Brine	48	7.76	8.56	7.10	9.02	9.84	8.34
Under	72	10.5	11.7	9.56	8.59	9.27	7.98
LO3	144	7.35	8.04	6.76	8.05	8.54	7.62

The largest effect of aging is shown for the light oil LO3. This is not surprising as processes i) and ii) will be more important for the volatile components to be found in light oils. The strength of the fluorescence decreases appreciably although its spectral distribution does not change. Decay times, in both channels have reduced by a factor of 3 after 144 hours as seen in Figure 7 which is on the same scale as Figure 6. By comparison it can be seen that the progressively aging oil spans the range covered by the light oils. This may mean that the large spread in marine diesel fluorescence decay times can be explained just by the age and history of each sample. Fluorescence was also detected, after 48 hours, from the brine over which the light oil was aged. As mentioned and discussed in the preceding section this emission was broad and unstructured and showed identical decay profiles in both channels. This difference in its properties from those of straight oil may prove useful in the identification of oil.

The crude oil CO2 showed the same type of aging as the light oil but the extent of the changes was not as marked. This can be seen in Figure 8 which is on the same scale as Figure 5. It can be seen that the aged CO2 spans about five different crude oils but remains well in the crude oil group.

The heavy oil HO2 showed very little if any change on aging. Differences in the spectra can be accounted for by the effect, at the high sensitivity required for the heavy oil, of dirt collected whilst the oil was on the roof.

These simplified aging experiments predict that even given an oil with discrete decay properties unique identification

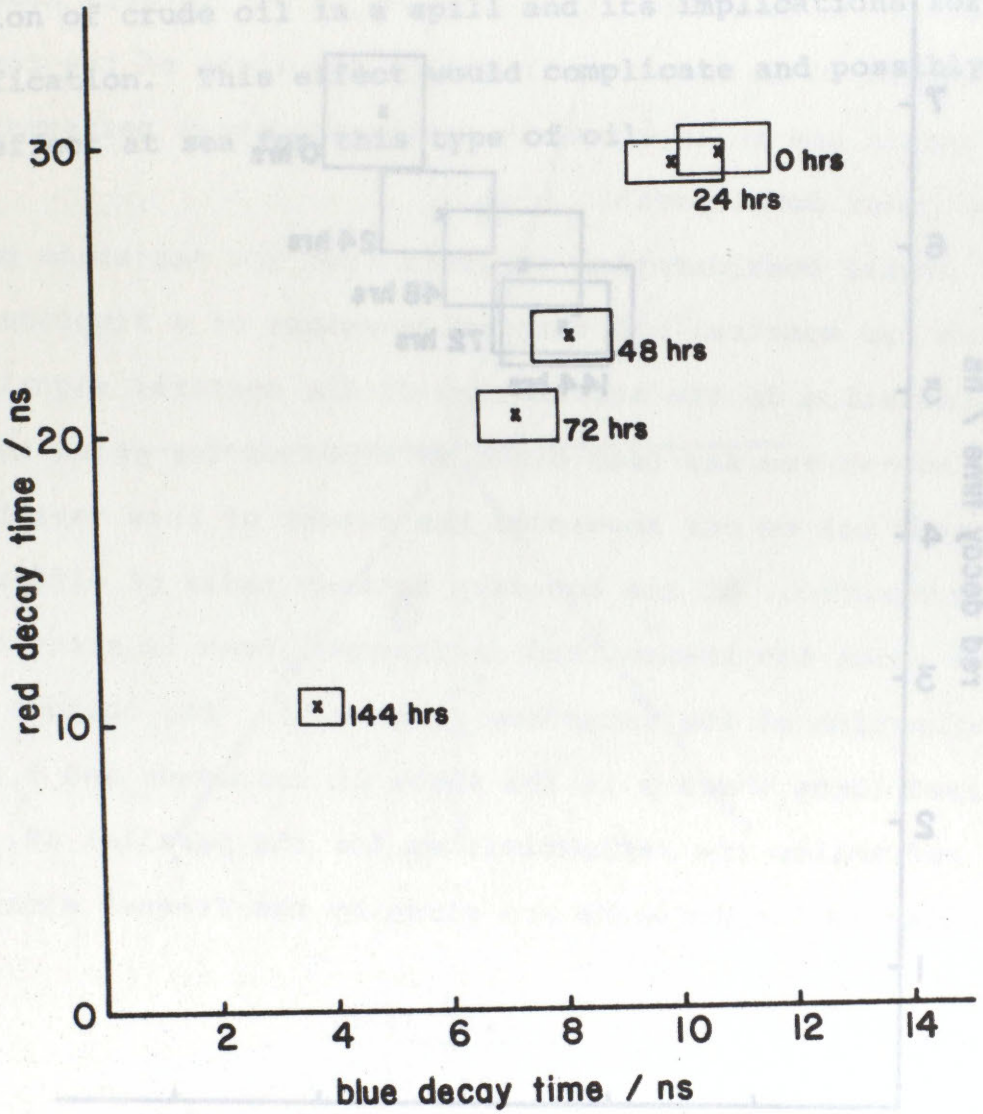

Figure 7: Effect of aging on the red and blue channel oil fluorescence decay times of light oils.

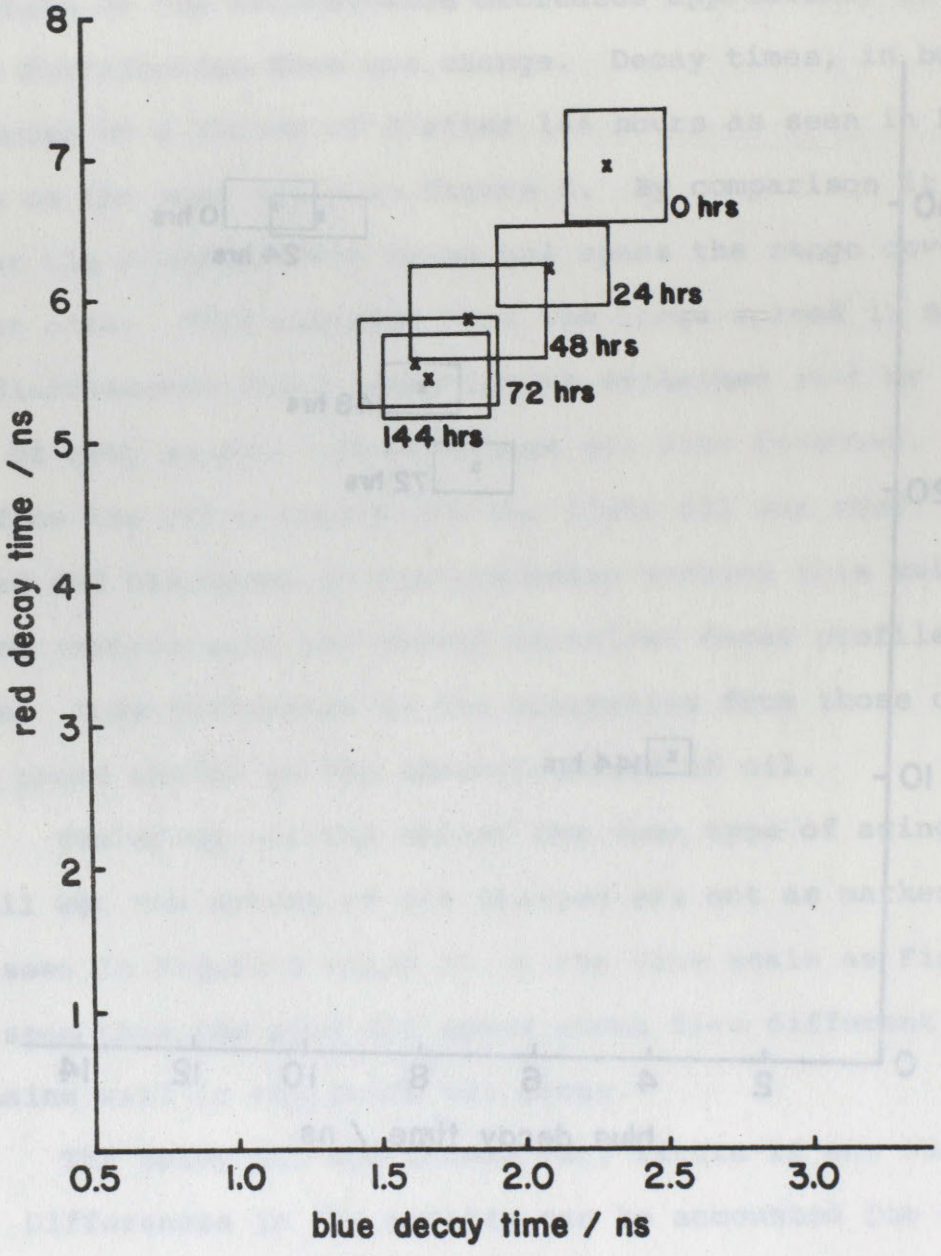

Figure 8: Effect of aging on the red and blue channel oil fluorescence decay times of light oils.

at sea would be impossible due to the effect of aging. However the three oils studied here retained the properties of their original group. Further studies on the aging of oils with borderline properties would be useful. In our Interim Report we discussed the surface fractionation of crude oil in a spill and its implications for crude oil identification. This effect would complicate and possibly mask the aging effect at sea for this type of oil.

7. The Effect of the Sea-State on Fluorosensor Performance

Whilst the present study has attempted to use data of a similar bandwidth and noise level to that expected in practice, measurements made over the ocean will in addition be effected by the sea-state. We mentioned this problem in our Interim Report but wish to discuss it in more detail and in the light of the results reported herein and an improvement in the predicted performance of the sensor under development.

Simple consideration suggests that the sea-state may effect both the spectral and temporal response of a fluorosensor. Possible variation in the attenuation of the spectral signal due to different sea-states has been cited as a reason for going to temporal measurements[2] but to our knowledge the extent of this variation has not been estimated. At the boundary between media of different refractive index the transmitted (refracted) beam is attenuated due to reflection at the interface (Figure 9). For oblique incidence of polarised light where ϕ is the angle of incidence and θ is the angle of refraction the reflectivities for the parallel ($R_{||}$) and perpendicular ($R_{\perp}$) components are given by the Fresnel equations:

$$R_{||} = \frac{\tan^2 (\phi-\theta)}{\tan^2 (\phi+\theta)}$$

$$R_{\perp} = \frac{\sin^2 (\phi-\theta)}{\sin^2 (\phi+\theta)}.$$

The relative contribution of the two components depends on the angle α which the electric vector of the incident beam forms with the plane

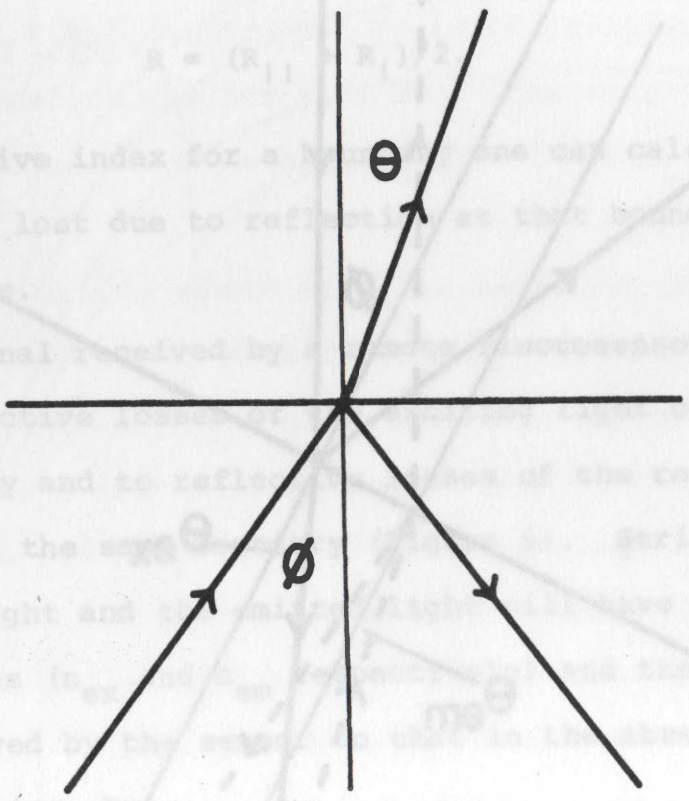

Figure 9: Reflection and refraction at a boundary between media of different refractive index.

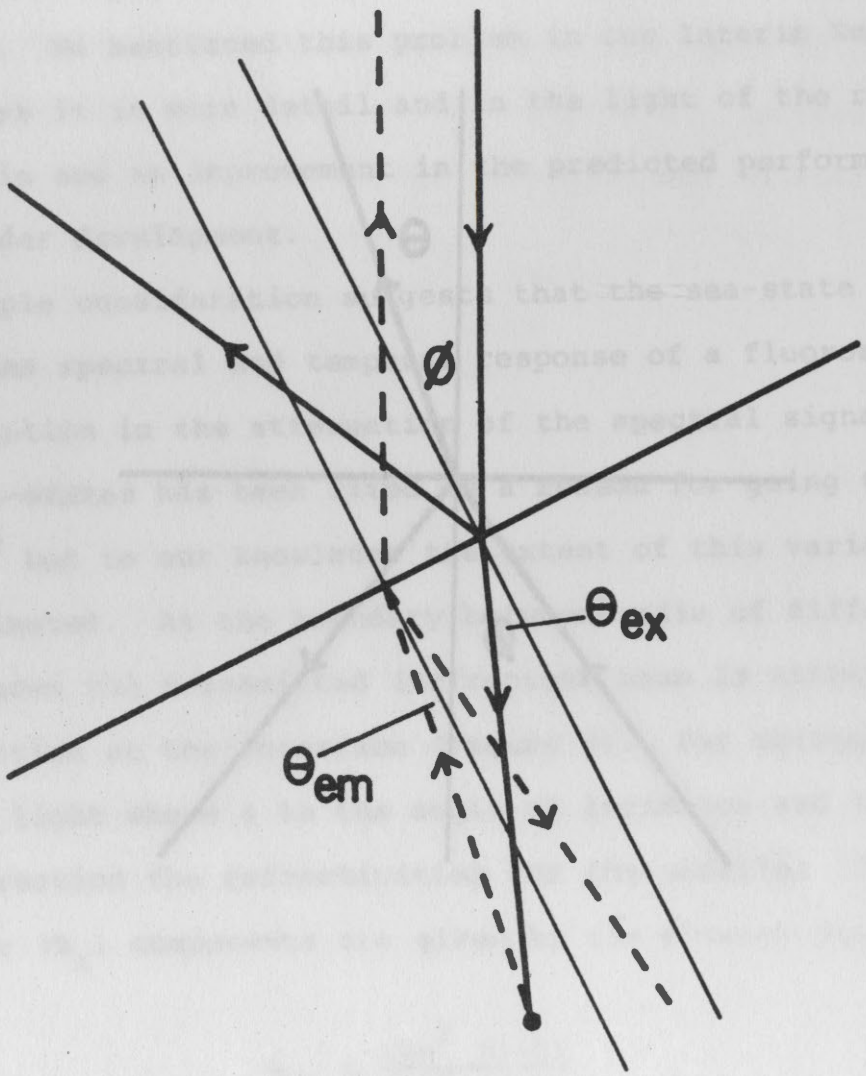

Figure 10: Excitation and emission light paths for a laser fluorosensor over an inclined target.

of incidence such that the total reflectivity is given by:

$$R = R_{||} \cos^2\alpha + R_{\perp} \sin^2\alpha. \qquad (.3)$$

For black-body (non-polarised) incident light equation (.3) reduces to give

$$R = (R_{||} + R_{|})/2. \qquad (.4)$$

Given the refractive index for a boundary one can calculate the fraction of light lost due to reflection at that boundary for any angle of incidence.

The signal received by a remote fluorosensor is attenuated due both to reflective losses of the exciting light on entering the medium under study and to reflective losses of the returning fluorescence signal at the same boundary (Figure 9). Strictly speaking the excitation light and the emitted light will have different refractive indices (n_{ex} and n_{em} respectively) and the fraction of the signal received by the sensor to that in the absence of the boundary (T) is given by:

$$T = (1 - R_{ex})(1 - R_{em}) \qquad (.5)$$

If we assume that $n_{ex} = n_{em} = n$ equation (.5) reduces to

$$T = (1 - R)^2$$

Figure 11 shows a plot of T against ϕ the angle of incidence for a series of values of n which spans those expected for envisaged fluorosensing targets. In deep water (defined as being where the

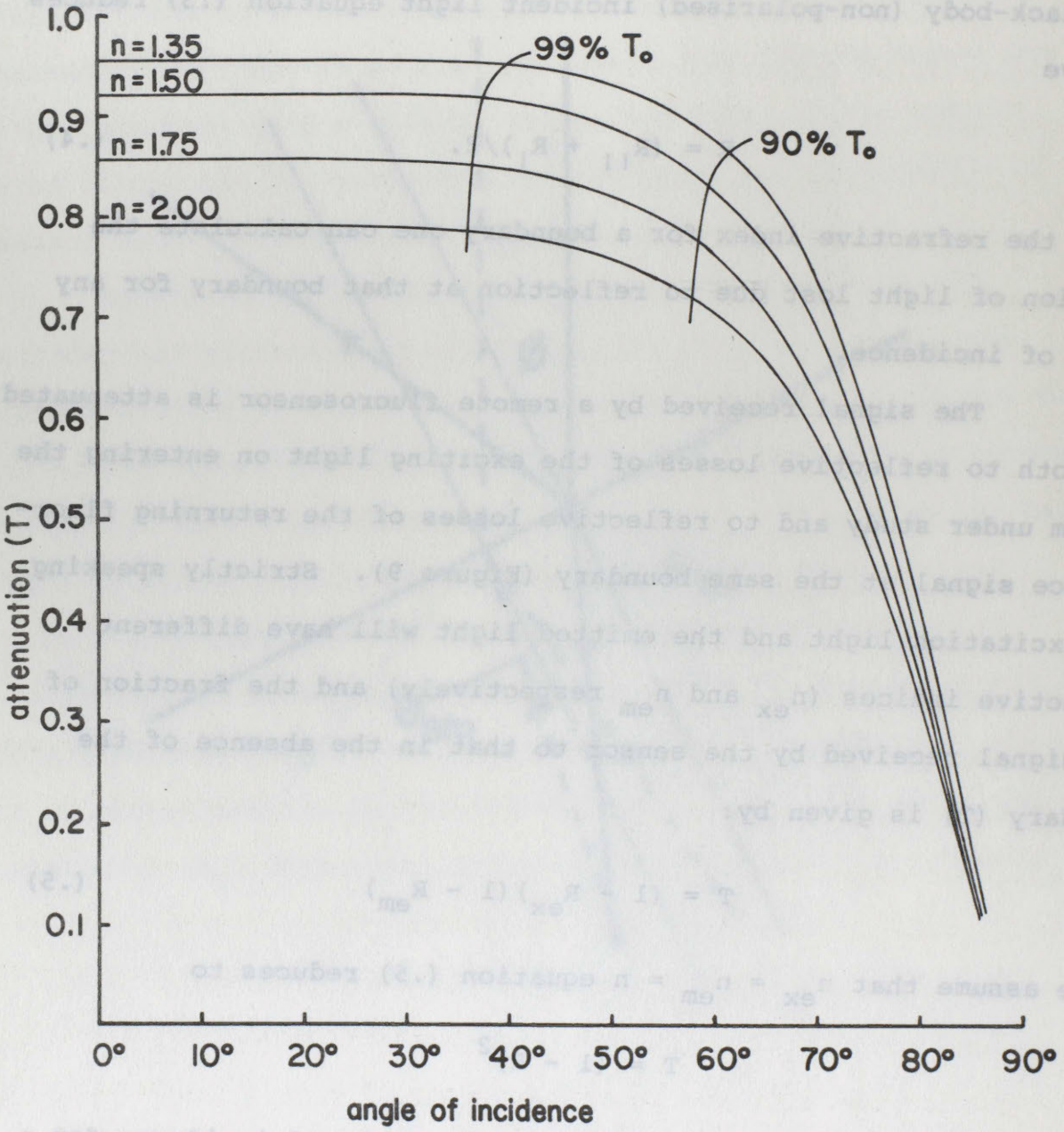

Figure 11: The attenuation of the signal received by a laser fluorosensor due to reflective losses over an inclined target as a function of the angle of inclination.

depth is greater than half the wavelength) wind waves reach a maximum slope of 1 in 7 before breaking[5]. Superimposed on these waves are smaller waves but these cannot be expected to increase the slope past 2 in 7. A slope of 1 in 7 means an angle of incidence of 8°, 2 in 7 15° and 3 in 7 22° and it can be seen that even at $\phi = 22°$ and n = 2 T has not dropped by 1% of its flat calm value (T_o). We can therefore predict that over deep water the sea-state will have negligible effect on spectra measurements as long as breaking water is avoided.

Temporal measurements will, as mentioned before, also be effected by the sea-state. A difference in the path length between the sensor and different parts of the target area will result in a distortion of the measured decay profile due to the finite speed of light. Lasers now available for fluorosensing have a beam divergence of about 1.5 mrad x 2.5 mrad. At an altitude of 1000' this would give a target area of 2.5' x 1.5' and, with the maximum wave slope of 1 in 7, a maximum there and back path length difference (over the diagonal) of 0.8'. This can give a maximum distortion in the measured decay time of 0.8 ns taking the speed of light as 1 ns per ft. A maximum error in the lifetimes of this size would hardly effect the grouping of the oils as discussed in the previous section. Only in the borderline region between the heavy and crude oils, where the red decay times are of the order of 2 to 3 ns, would ambiguity arise. The improved laser specifications and the longer decay times found in the red channel mean that the effect of the sea-state on temporal measurements will not be as restrictive as predicted in the Interim Report.

8. Chlorophyll Fluorescence

Many of the other roles envisaged for laser fluorosensors involve the monitoring of chlorophyll fluorescence. Such roles include the measurement of water quality, the detection of plant stress and the identification of vegetation. Their feasibility depends on the fluorescence properties of chlorophyll *in vivo* which differ markedly from its properties as an extract in solution. Studies of chlorophyll fluorescence *in vivo* have been conducted in attempts to elucidate the mechanism of photosynthesis. Emission with a lifetime of the order of 1 ns has been observed by many workers[6] whilst recently picosecond laser studies have been reported to show a component in the fluorescence with a lifetime of about 100 ps[7]. Most of these studies have been carried out on suspensions of unicellular algae and no large scale survey of the fluorescence properties of algae or vegetation has been conducted.

We conducted trial experiments on two types of algae, one a floating mat forming filament type (algae 1) and one which aggregated to form clumps (algae 2). Both were cultured in our laboratory from water taken from a local lake. Their fluorescence spectra are shown in Figure 12. The excitation wavelength for these experiments was 490 nm. Excitation at 337 nm gave very little fluorescence signal due to the very low absorption of chlorophyll in that region. Algae fluorescence appears to have two main peaks at 680 and 710 nm whose relative height depends on the algae. Little can be learned from quantum efficiencies due to the widely different nature of the surfaces and hence light absorbancy of the two algae. A fluorosensor

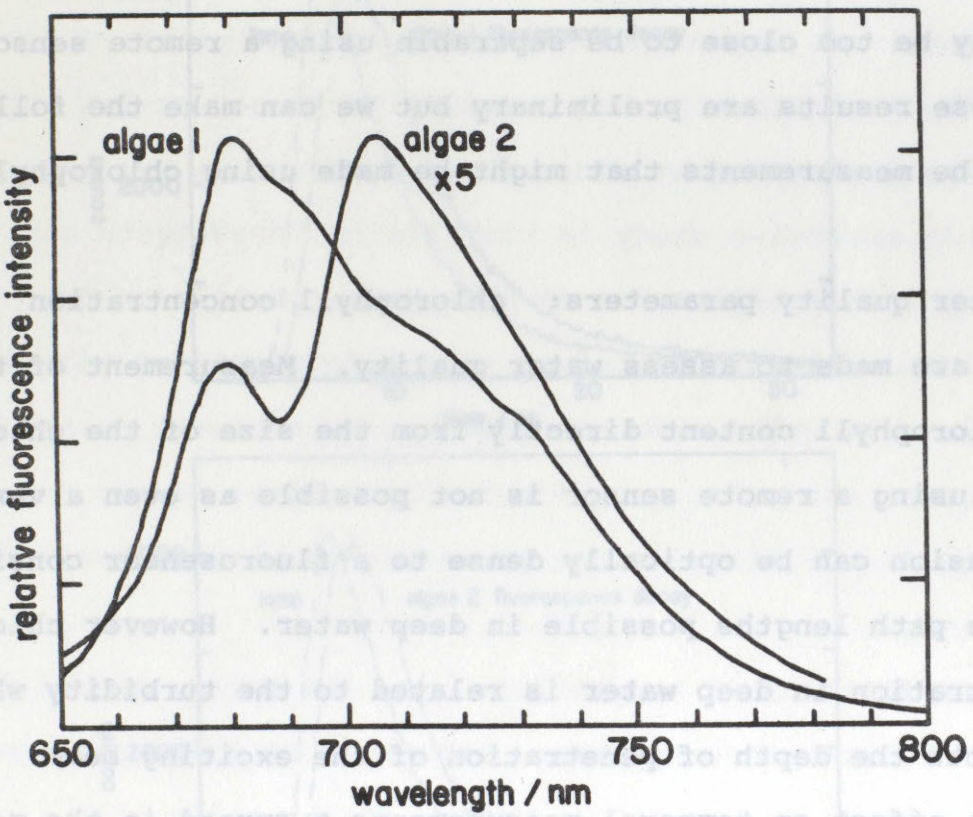

Figure 12: The fluorescence spectra of two typical algae.

intended solely for chlorophyll studies would therefore best employ a laser with output at about 500 nm and would scan the spectral region 650 to 800 nm.

Fluorescence decay profiles were collected for both algae and are shown in Figure 13. Reasonable fits to one-exponential functions were found for both samples; algae 1 giving a decay time of 1.37 ns and algae 2 1.23 ns. These decay times are short and would probably be too close to be separable using a remote sensor.

These results are preliminary but we can make the following comments on the measurements that might be made using chlorophyll fluorescence:

Water quality parameters: chlorophyll concentration measurements are made to assess water quality. Measurement of the suspended chlorophyll content directly from the size of the chlorophyll fluorescence using a remote sensor is not possible as even a very dilute suspension can be optically dense to a fluorosensor considering the large path lengths possible in deep water. However chlorophyll concentration in deep water is related to the turbidity which in turn affects the depth of penetration of the exciting beam. Like the sea-state effect on temporal measurements a spread in the measured decay time will occur due to the finite pathlength in the fluorescing medium (unlike oil where the penetration is small). Knowing the fluorescence lifetime the depth of penetration and hence the turbidity could theoretically be estimated from the measured decay profile. Knowing the fluorescence lifetime of the algae it is also possible to arrange for the returning fluorescence spectral signal to be

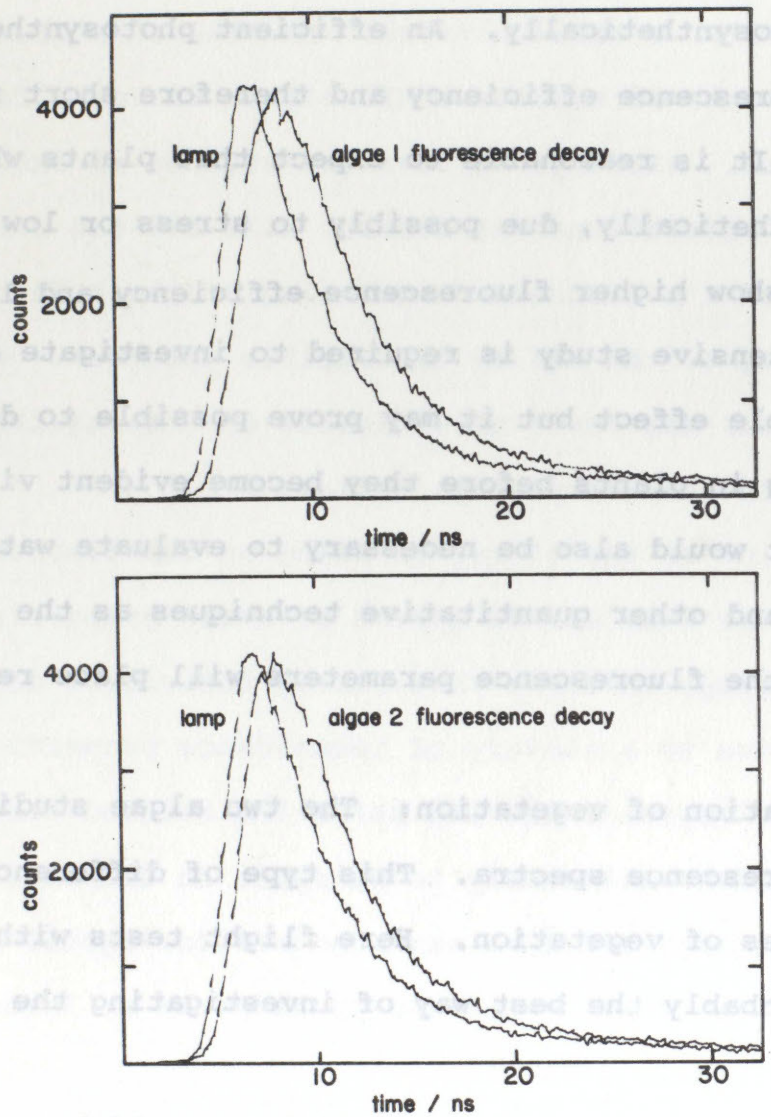

Figure 13: The fluorescence decay profiles of two typical algae.

gated so that fluorescence is only collected over a certain depth. Then chlorophyll concentrations can be estimated over that depth range. For this application the shorter the lifetimes, the smaller the depth ranges that become possible.

Plant stress: Generally the healthier a plant the more efficient it is photosynthetically. An efficient photosynthesizer must have a low fluorescence efficiency and therefore short fluorescence lifetimes. It is reasonable to expect that plants which are not active photosynthetically, due possibly to stress or low ambient light levels, will show higher fluorescence efficiency and longer decay times. An extensive study is required to investigate and quantify this possible effect but it may prove possible to detect disease or poisoning in plants before they become evident visually. A study of this sort would also be necessary to evaluate water quality monitoring and other quantitative techniques as the day to day fluctuation in the fluorescence parameters will place restrictions on their accuracy.

Identification of vegetation: The two algae studied here show different fluorescence spectra. This type of difference may be found between species of vegetation. Here flight tests with a fluorosensor are probably the best way of investigating the possibilities.

The three applications discussed above would best suit a fluorosensor designed for chlorophyll studies. Where a general fluorosensor has only one channel for chlorophyll fluorescence less information will be available especially with 337 nm excitation.

Such a channel would however be useful in oil spill detection to prevent possible false alarms due to floating seaweed rafts which might be indistinguishable from spills to other sensors. To this end studies on the fluorescence properties of seaweeds and other marine vegetation would be useful.

9. Conclusions

The fluorescence properties of the large selection of oils used in this study confirm that remote fluorosensors should be capable of characterising an oil into one of three main groups. Our results show that this should be possible using a fluorosensor in either a spectral or a temporal mode. The use of a fluorosensor capable of operating in both modes would add to the confidence in any characterisation. Although we have not studied an exhaustive selection of other possible marine fluors, oils are the only targets which have exhibited a pronounced lengthening of their fluorescence decay time on moving to the red in the visible spectrum. Thus a temporal fluorosensor may prove more capable of distinguishing oils from non-oil targets than a spectral device.

Our studies on the effect of aging on the fluorescence properties of oils as well as the spread of these properties within any of the three groups indicate that remote individual oil identification by reference to a library of fluorescence properties will not prove feasible. However the oil selection studied here is representative of most oils likely to be spilt in Canadian waters. Their fluorescence properties, as reported herein, should prove helpful in the further development and application of laser fluorosensors for oil spill surveillance.

Of other possible targets we have only made preliminary studies on the fluorescence properties of chlorophyll *in vivo* using two algae species but have been able to suggest three areas in which remote fluorosensors might exploit these properties: water quality

parameter measurement; plant stress measurement; and vegetation identification.

It is hoped that the work presented in this report will be of immediate and long term use in laser fluorosensor development and that consequently we have also demonstrated the value of laboratory studies in assessing and aiding remote sensor projects.

References

1. J.F. Fantasia, T.M. Hard and H.G. Ingrao; D.O.T./Transportation Systems Centre, Report No. TSC-USCG-71-7; 1971
2. R.M. Measures, W.R. Houston, and D.G. Stephenson; Optical Engineering 494, 13, 1974
3. D.M. Rayner and A.G. Szabo; Report No. BY-76-1, 1976, Division of Biological Sciences, NRCC
4. D.M. Rayner, A.E. McKinnon, A.G. Szabo and P.A. Hackett; Can. J. Chem. in press
5. B. Kinsman; 'Wind Waves - their generation and propagation on the ocean surface', Prentice-Hall, 1965
6. e.g. J-M. Briantias, H. Merkelo, and Govindjee; Photosynthetica 133, 6, 1972
7. G.S. Beddard, G. Porter, C.J. Tredwell, and J. Barber; Nature 167, 258, 1975

Appendix I

Oil Fluorescence Decay Profiles and Spectra

Notes:

i) Where possible decay profiles were collected in both blue and red channels as described in the text. In this Appendix the profiles are labeled B and R respectively and the lamp profiles are labeled L.

ii) The spectra are all relative to each other and to the quinine sulphate standard spectrum shown in the last figure of the Appendix. When making comparisons one should note that each spectra is plotted using one of four vertical scales.

References

Appendix I

Oil Fluorescence Decay Profiles and Spectra

Notes:

i) Where possible decay profiles were collected in both blue and red channels as described in the text. In this Appendix the profiles are labeled B and R respectively and the lamp profiles are labeled L.

ii) The spectra are all relative to each other and to the quinine sulphate standard spectrum shown in the last figure of the Appendix. When making comparisons one should note that each spectra is ploted using one of four vertical scales.

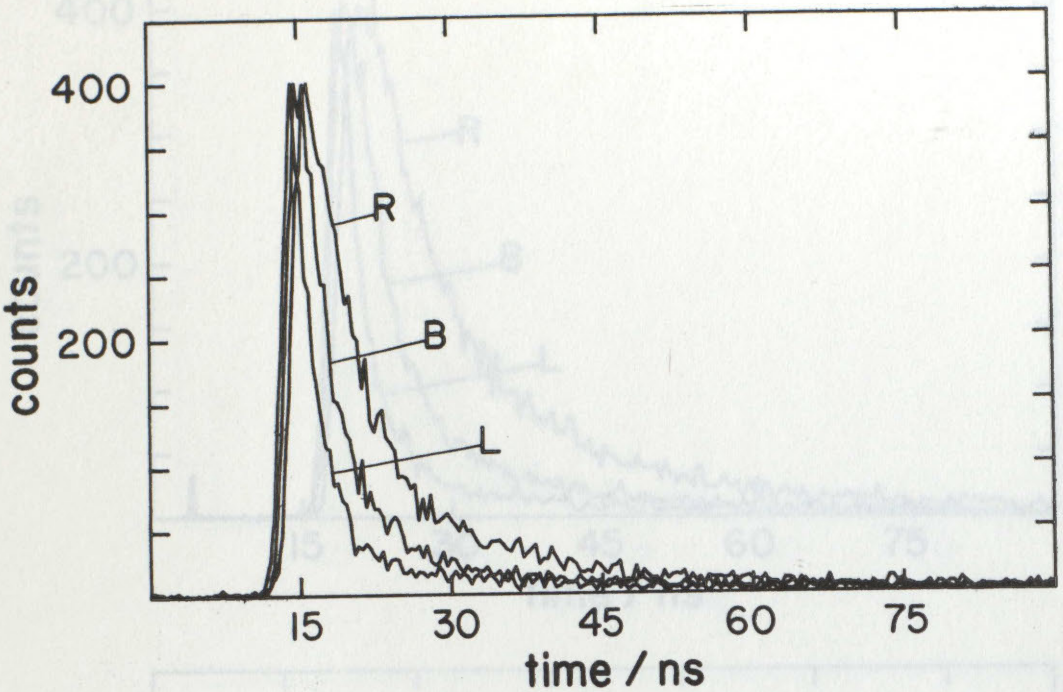

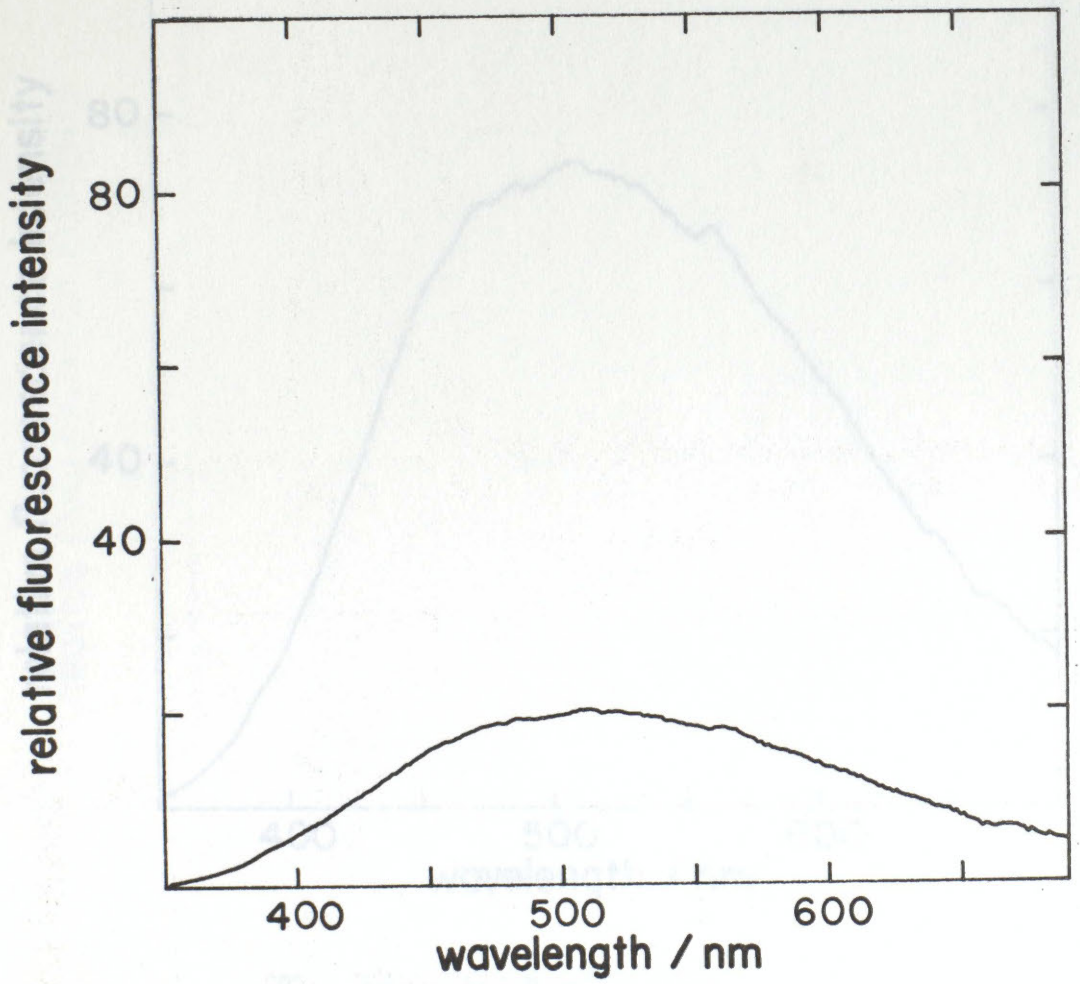

C01. VENEZUELAN 'LAGO MEDIO' CRUDE

counts
400
200
R
B
L
15
30
45
60
75
time / ns

relative fluorescence intensity
80
40
400
500
600
wavelength / nm

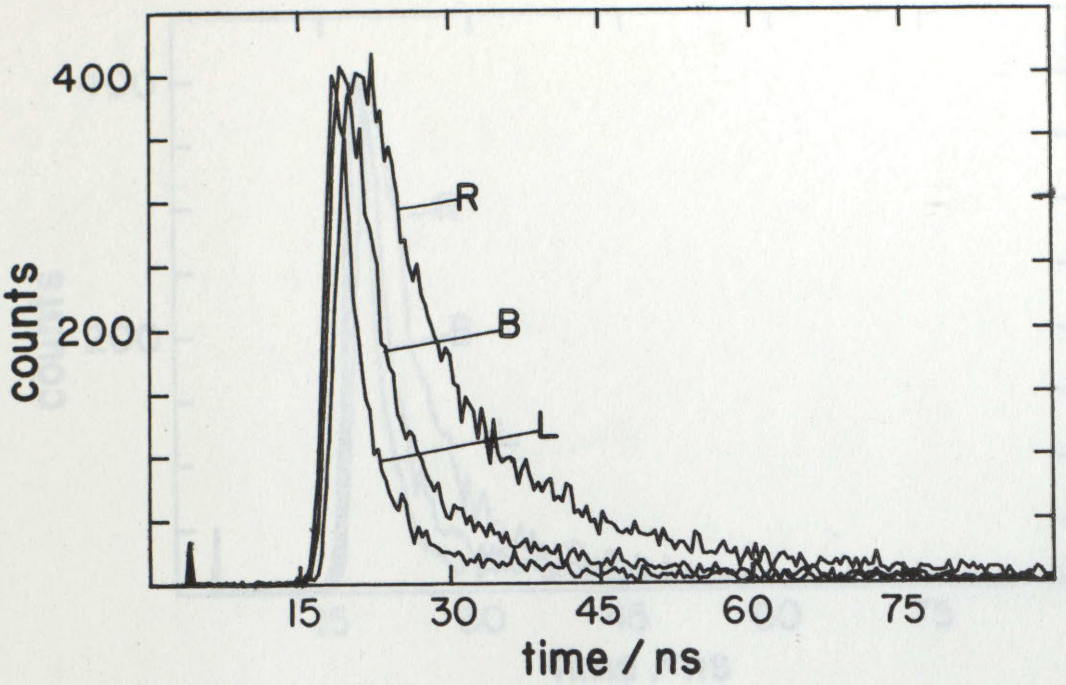

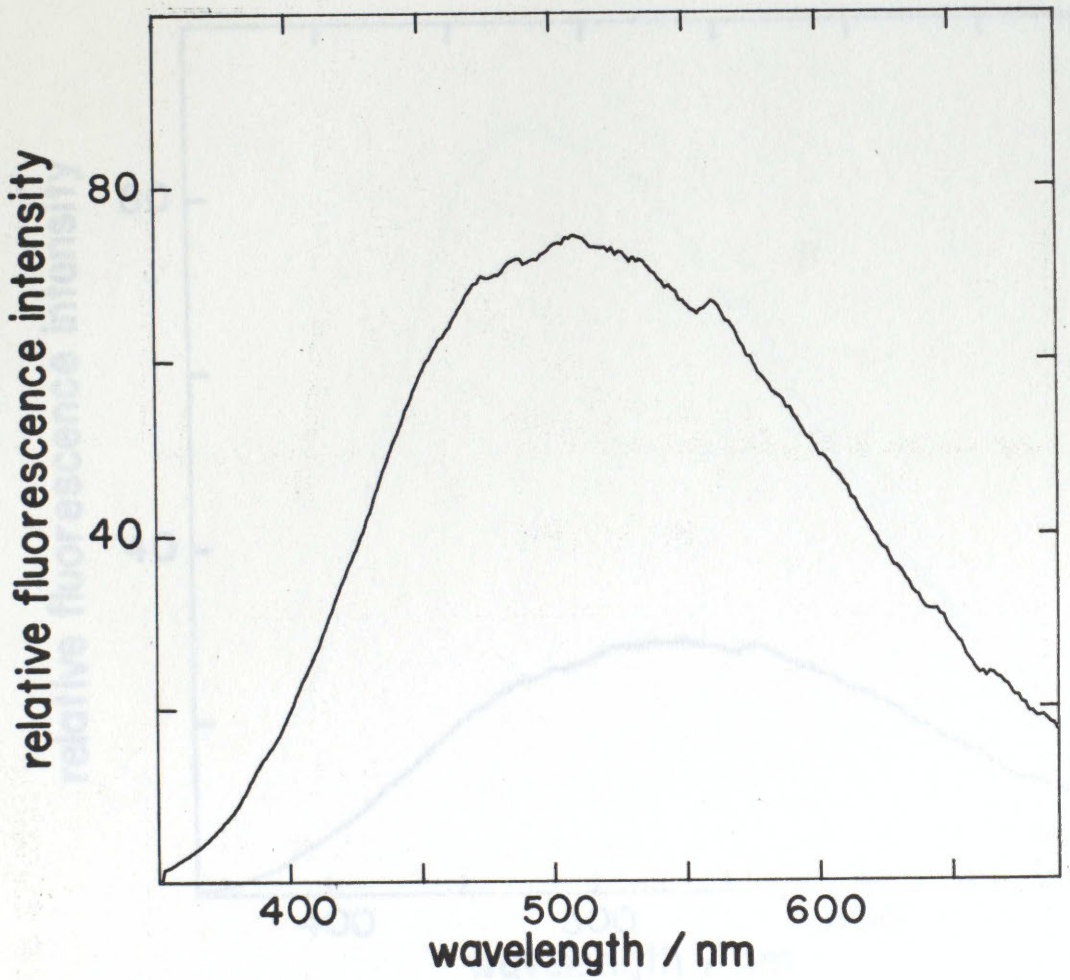

CO2. TEXACO TRANSMOUNTAIN CRUDE

counts
time / ns

relative fluorescence intensity
wavelength / nm

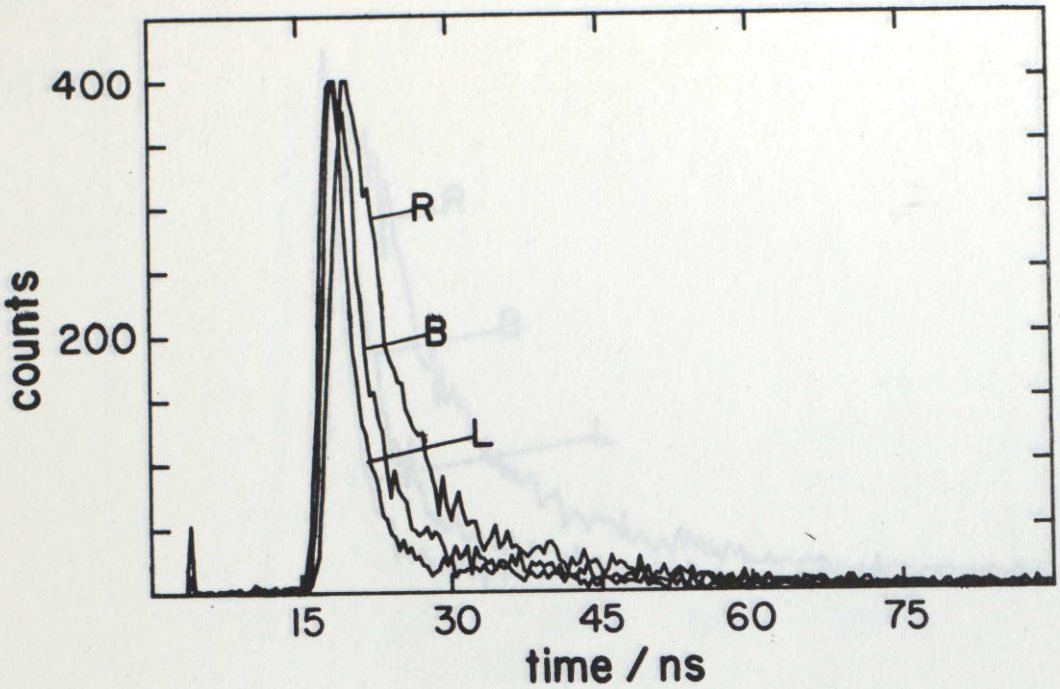

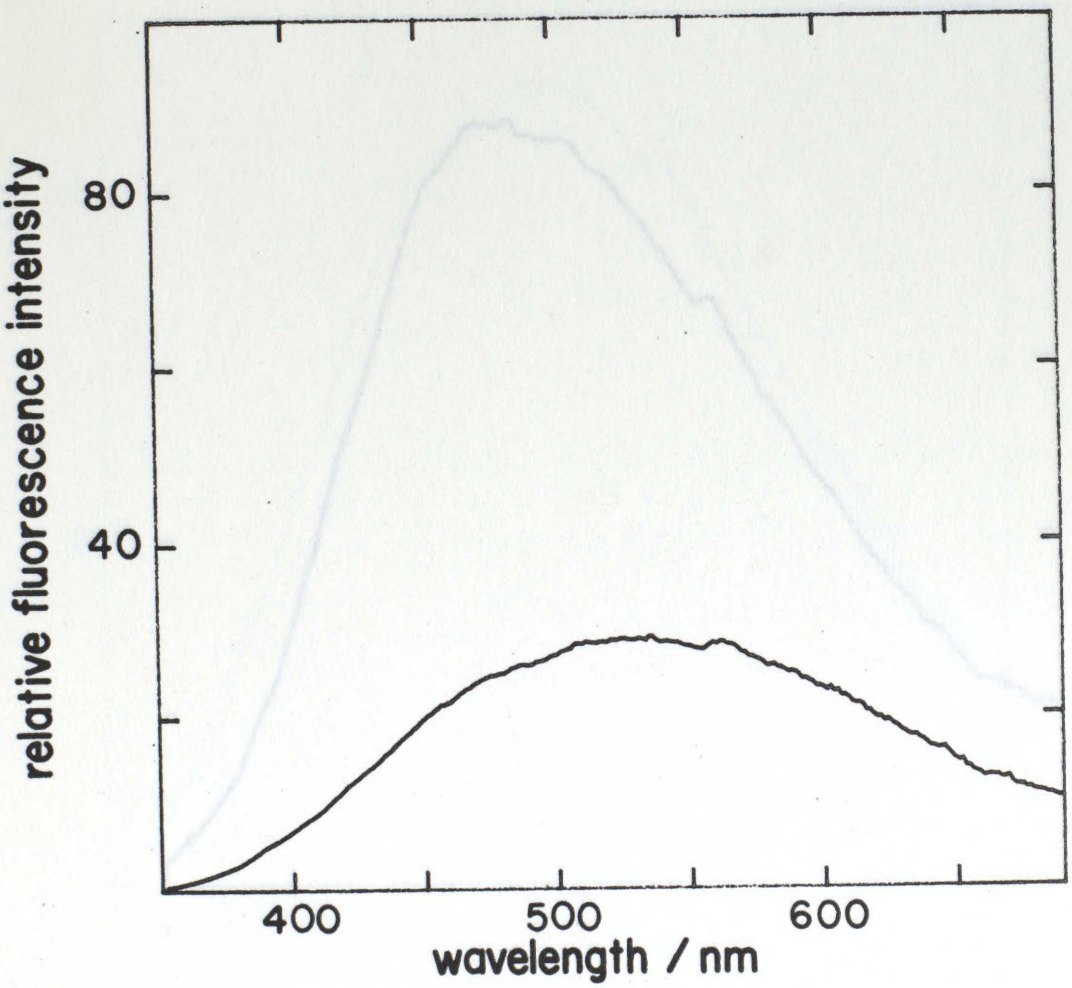

C03. TEXACO ARABIAN CRUDE

400
200
counts
15
30
45
60
75
time / ns

80
40
relative fluorescence intensity
400
500
600
wavelength / nm

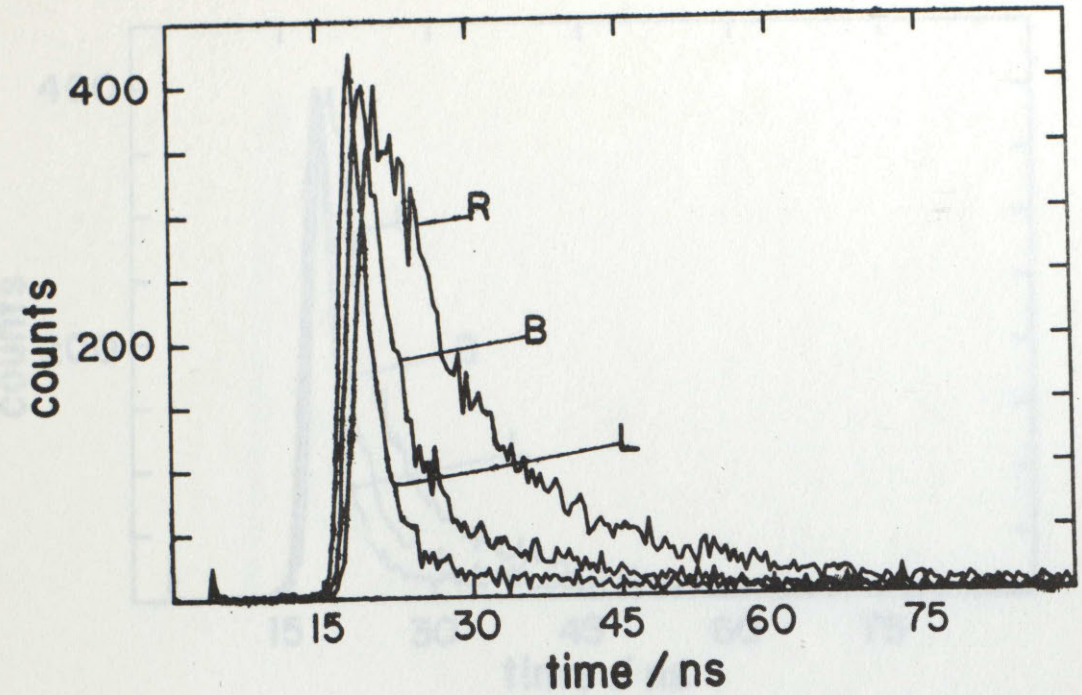

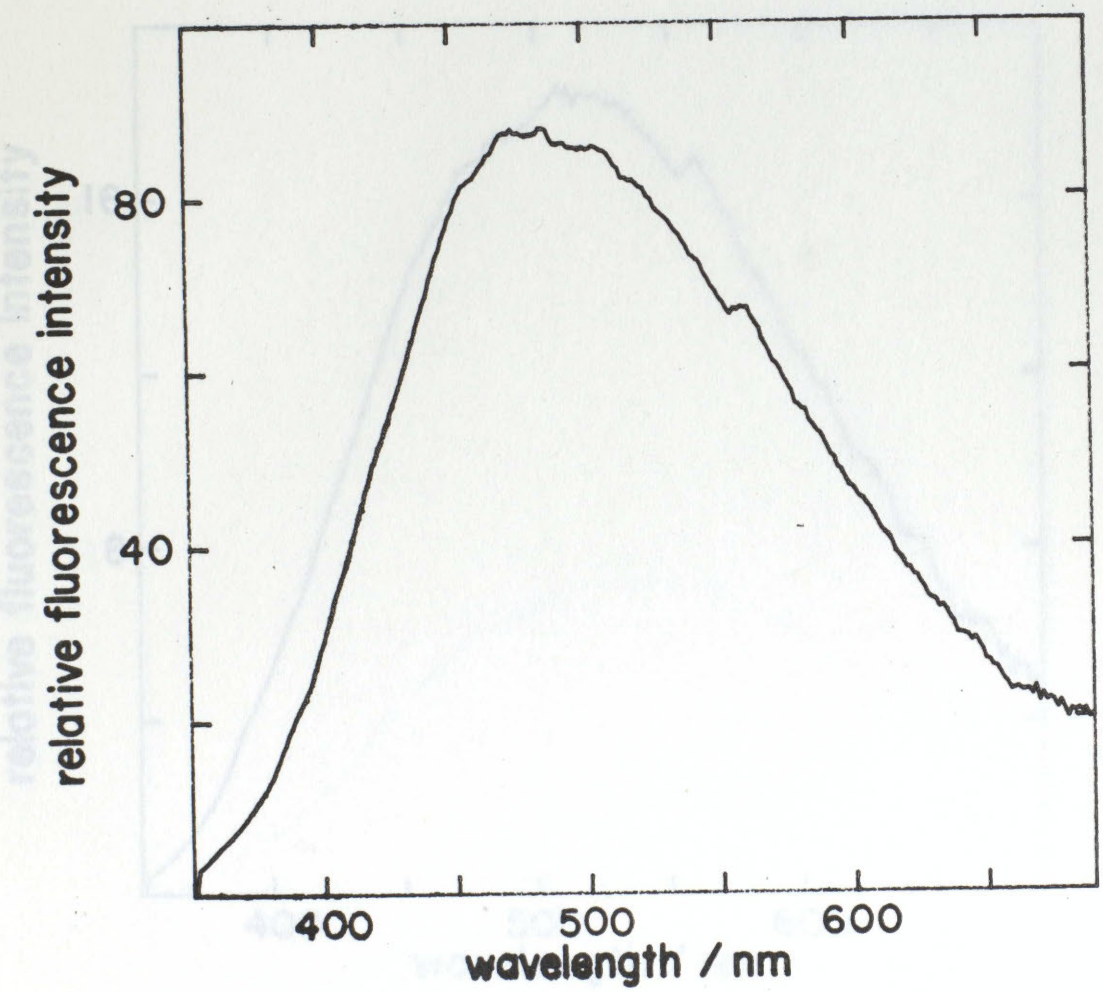

C04. TEXACO NIGERIAN CRUDE

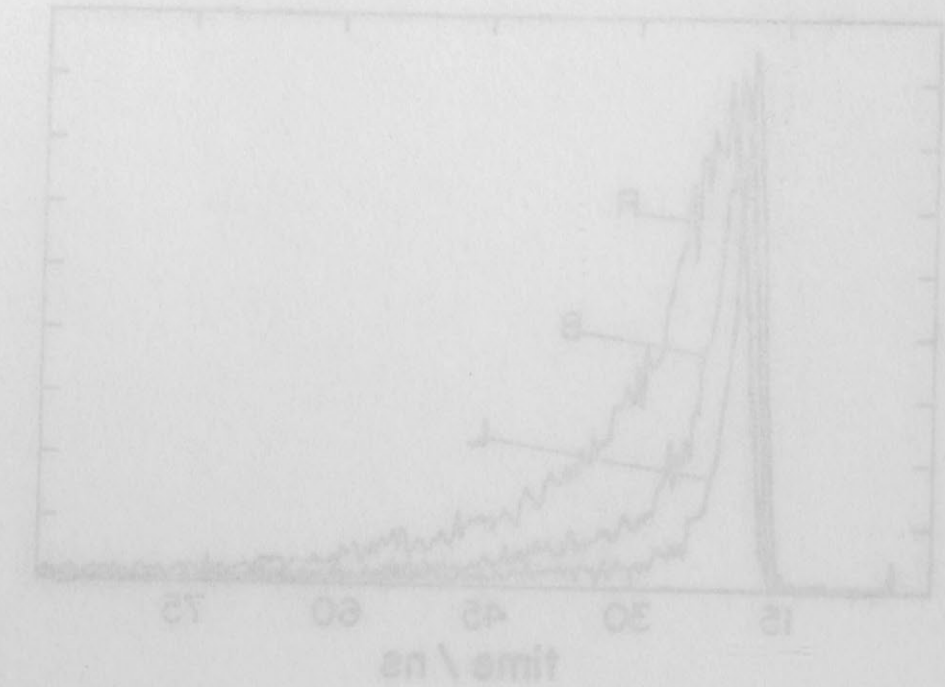
R
S
J
400
200
counts
15
30
45
60
75
time \ ns

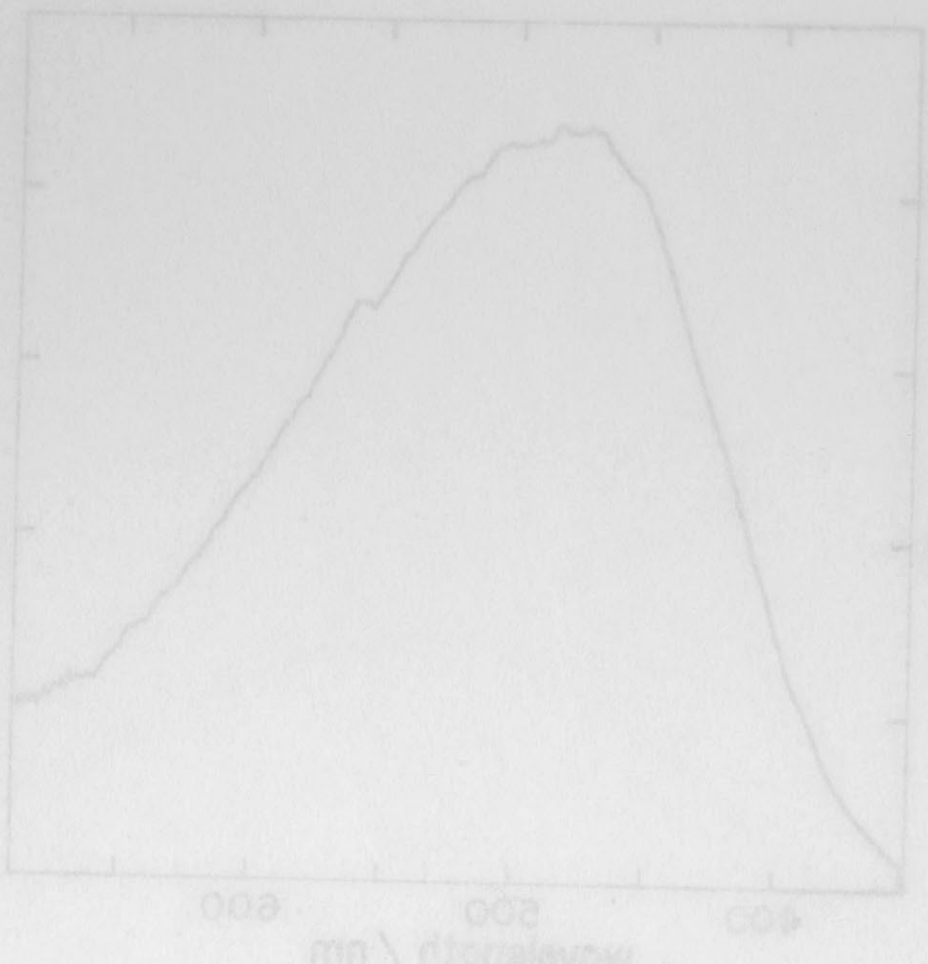
80
40
relative fluorescence intensity
600
550
500
wavelength \ nm

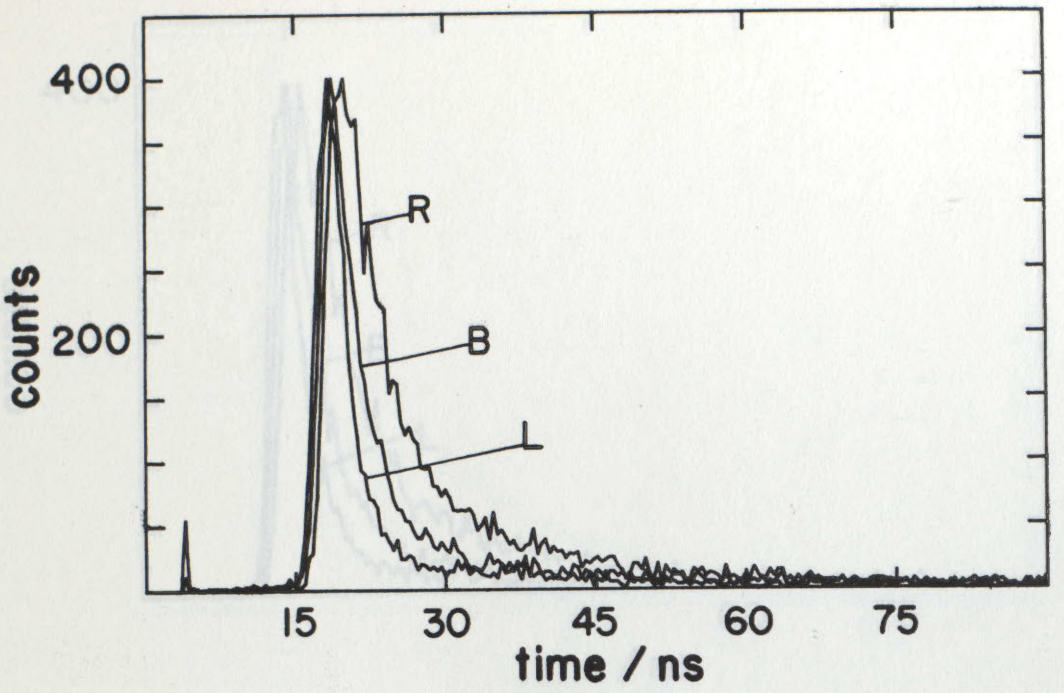

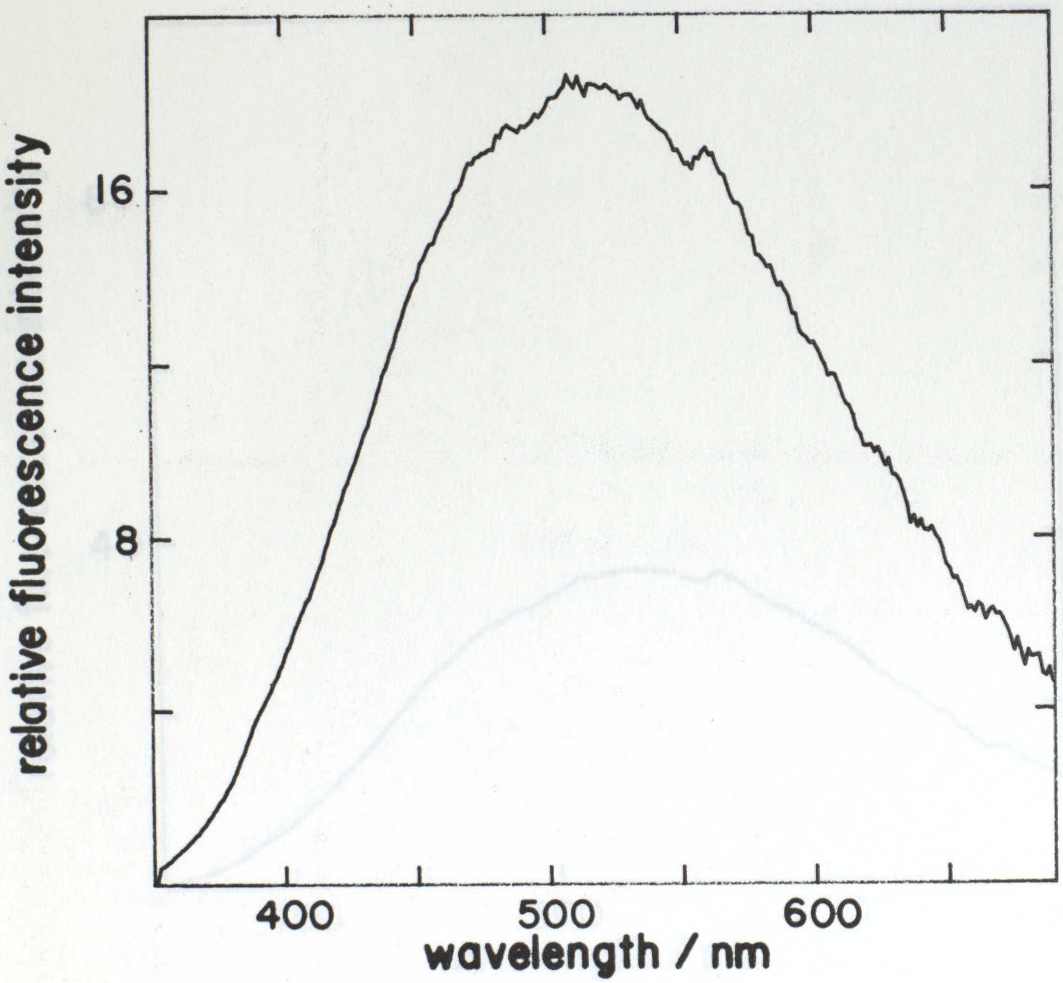

C05. TEXACO VENEZUELAN 'LAGO MEDIO' CRUDE

counts
400
200
R
S
I
15
30
45
60
75
time / ns

relative fluorescence intensity
16
8
400
500
600
wavelength / nm

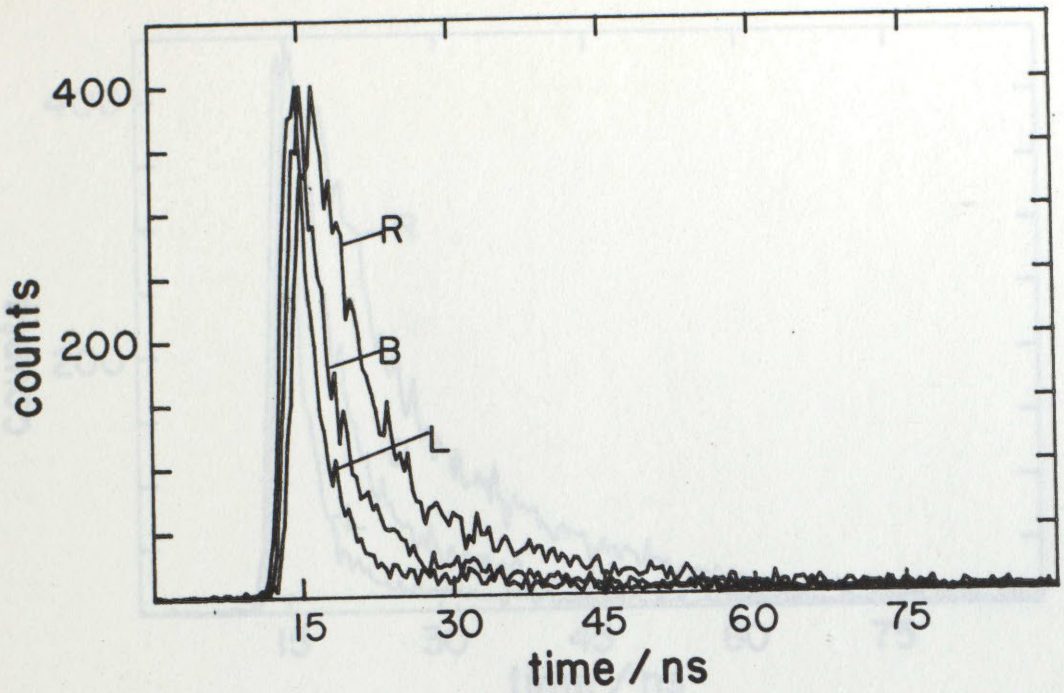

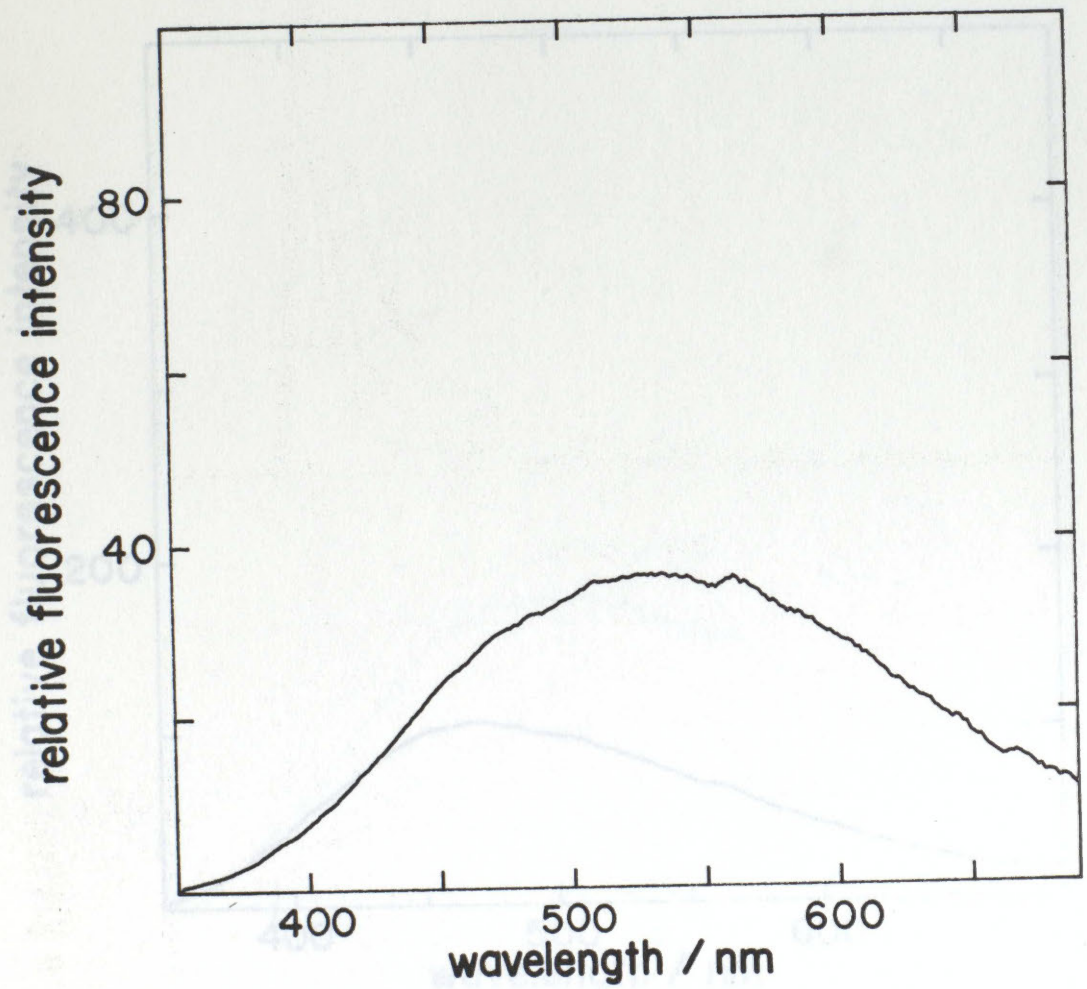

C06. GULF OIL REDWATER CRUDE (PP19)

counts
time / ns
R
B

relative fluorescence intensity
wavelength / nm

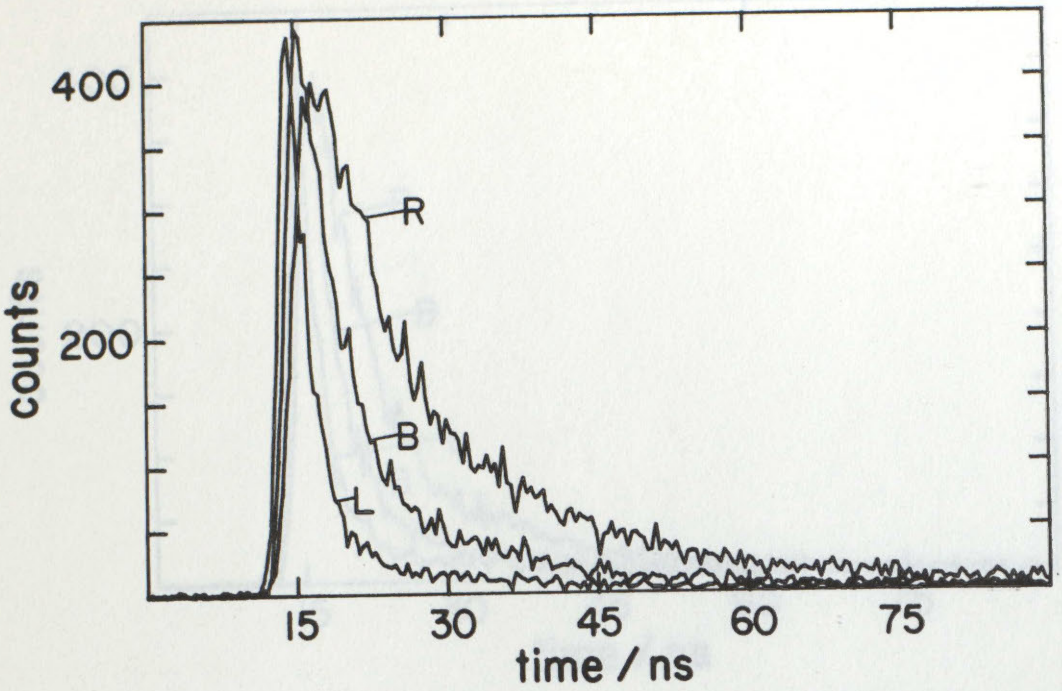

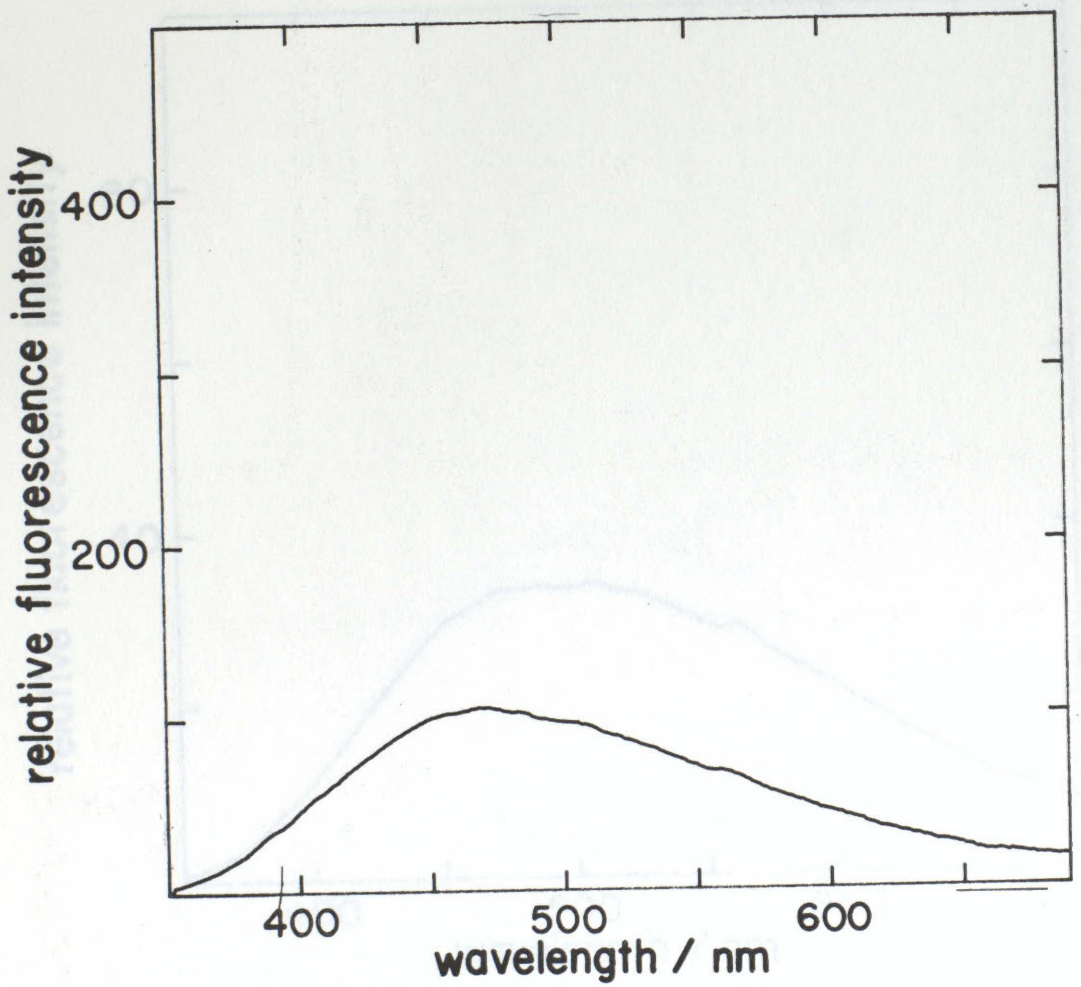

C07. GULF OIL B.C. LIGHT CRUDE (PP20)

400
200
counts
R
D
15
30
45
60
75
time / ns

400
200
relative fluorescence intensity
400
500
600
wavelength / nm

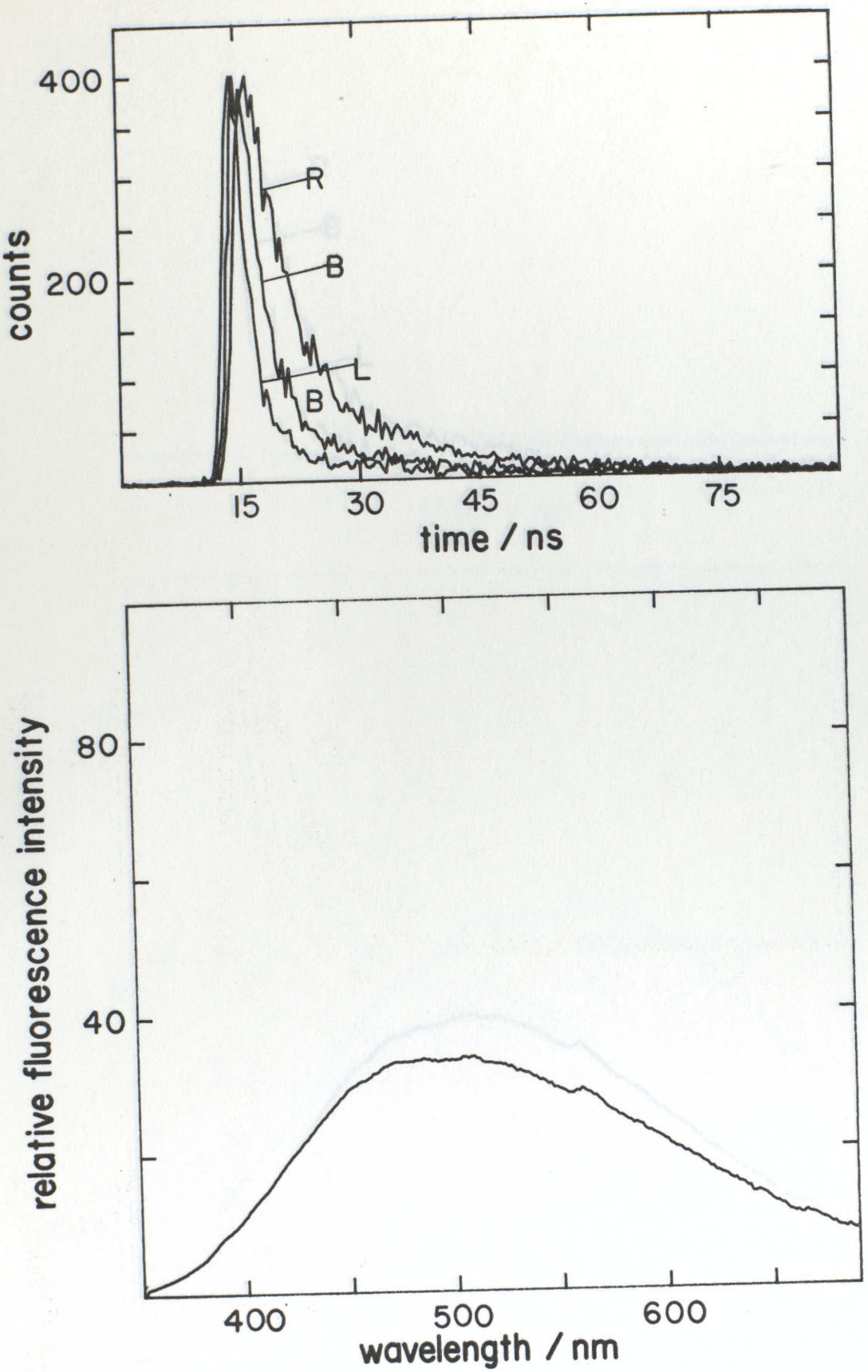

C08. B.P. LIGHT SOUR CRUDE (PP21)

counts
time / ns

relative fluorescence intensity
wavelength / nm

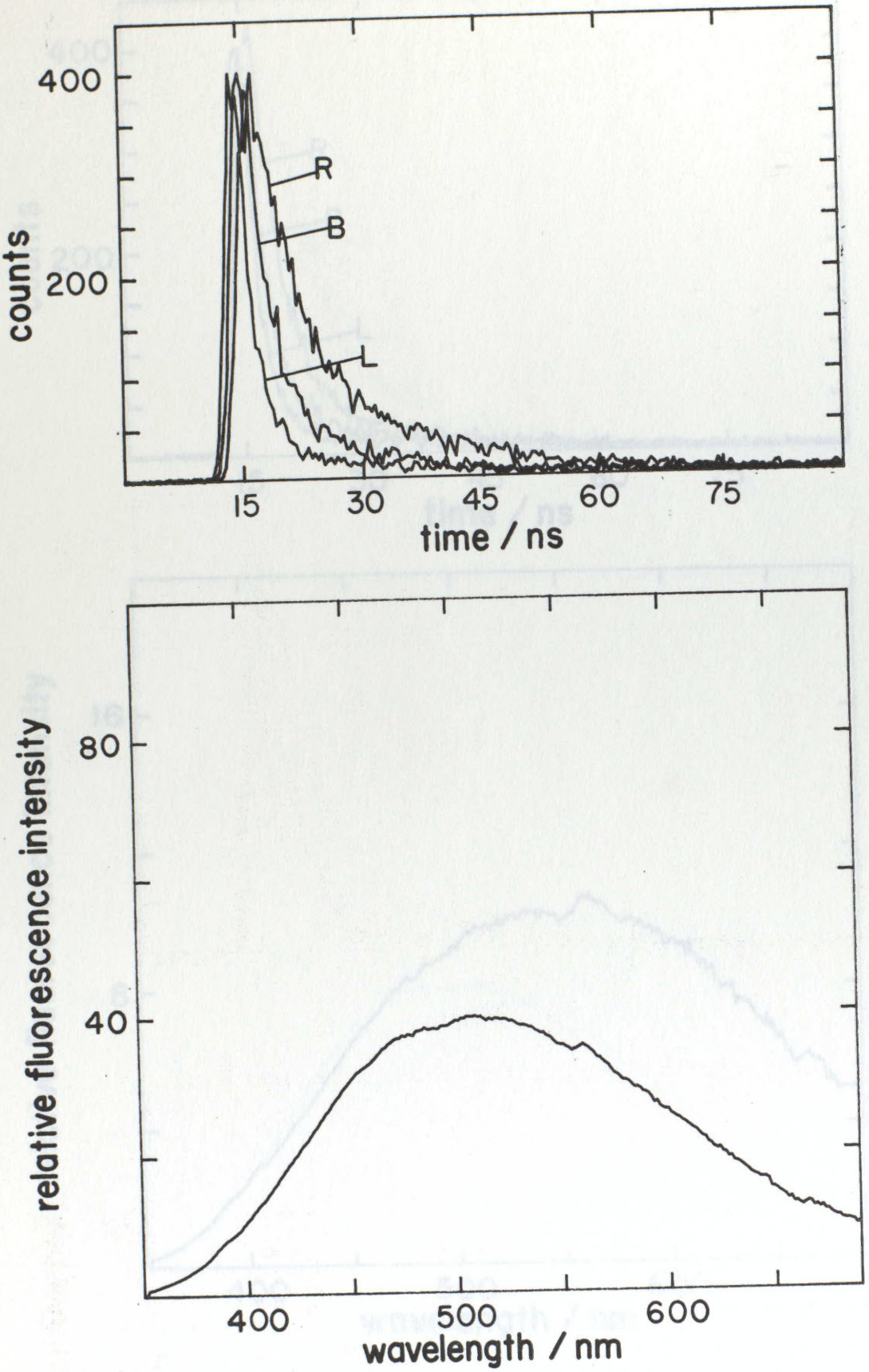

C09. B.P. MEDIUM SWEET CRUDE (PP22)

counts
400
200
time / ns
15
30
45
60
75

relative fluorescence intensity
80
40
wavelength / nm
400
500
600

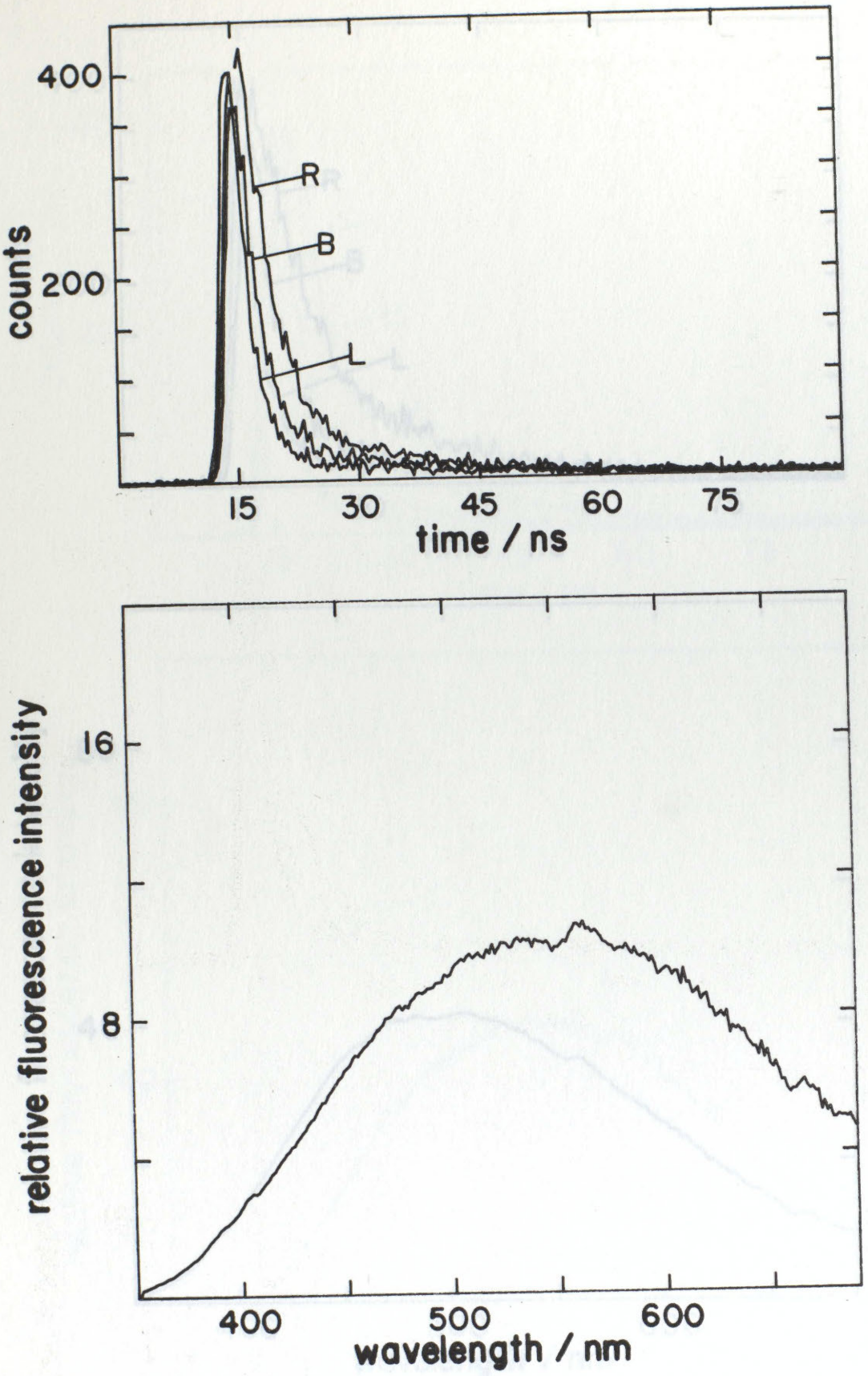

C010. B.P. CHAGRIN CRUDE (PP23)

counts
400
200
R
S
L
15
30
45
60
75
time / ns

relative fluorescence intensity
16
8
400
500
600
wavelength / nm

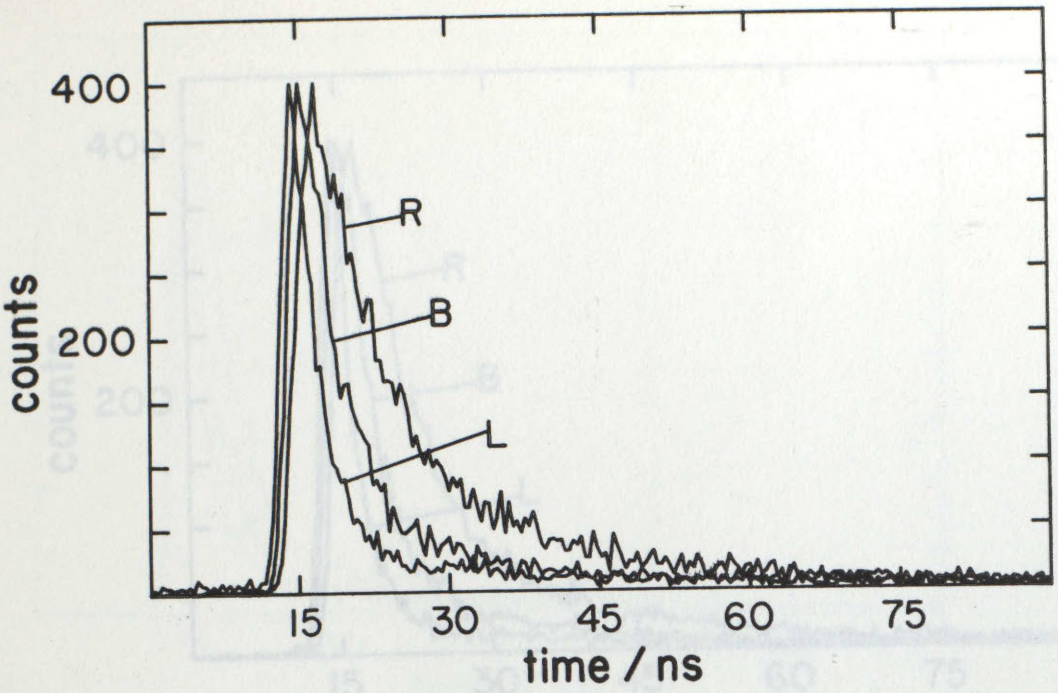

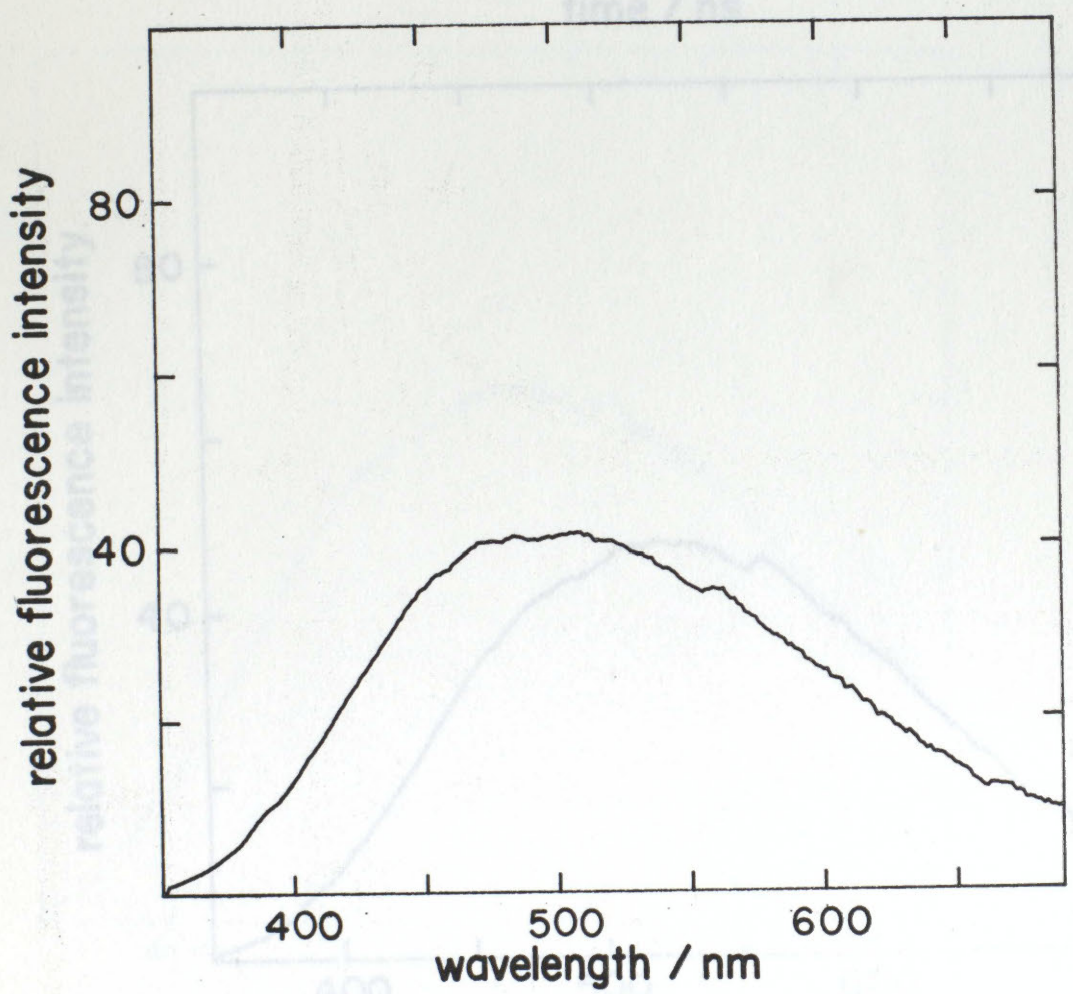

C011. TEXACO COMMON SWEET CRUDE (PP24)

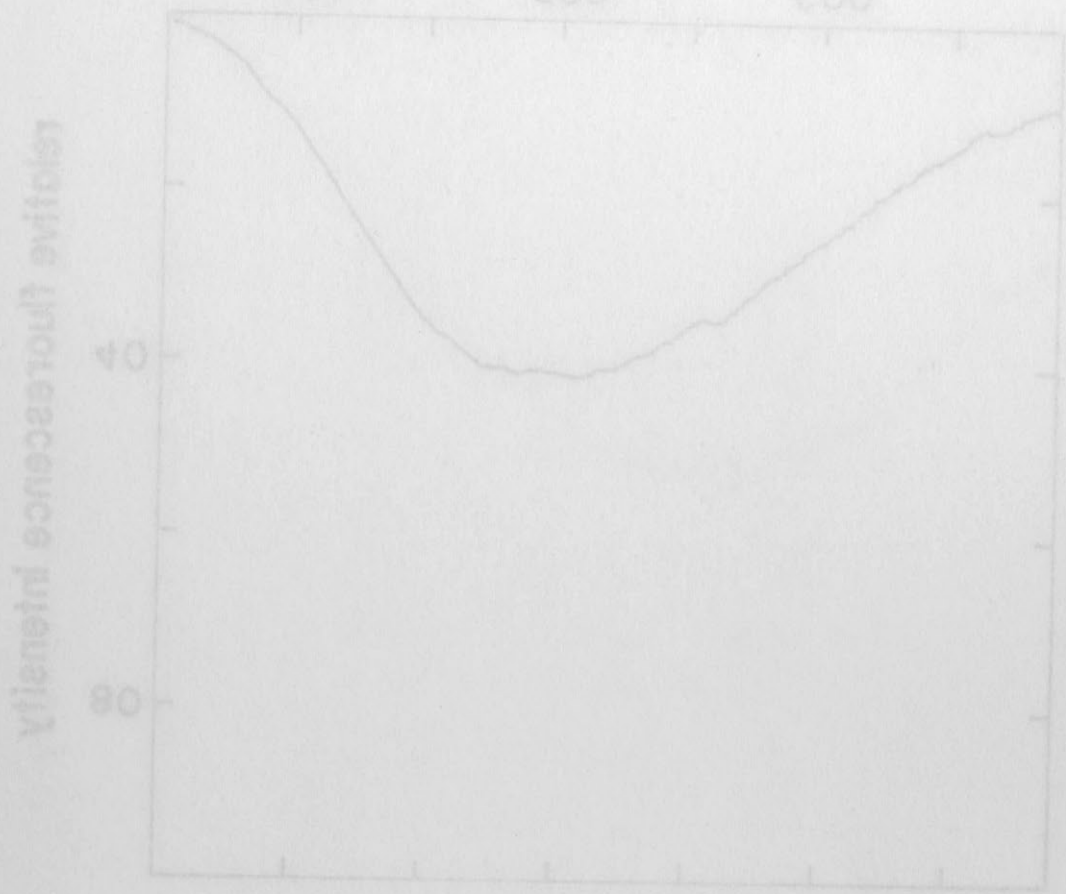
relative fluorescence intensity
80
40

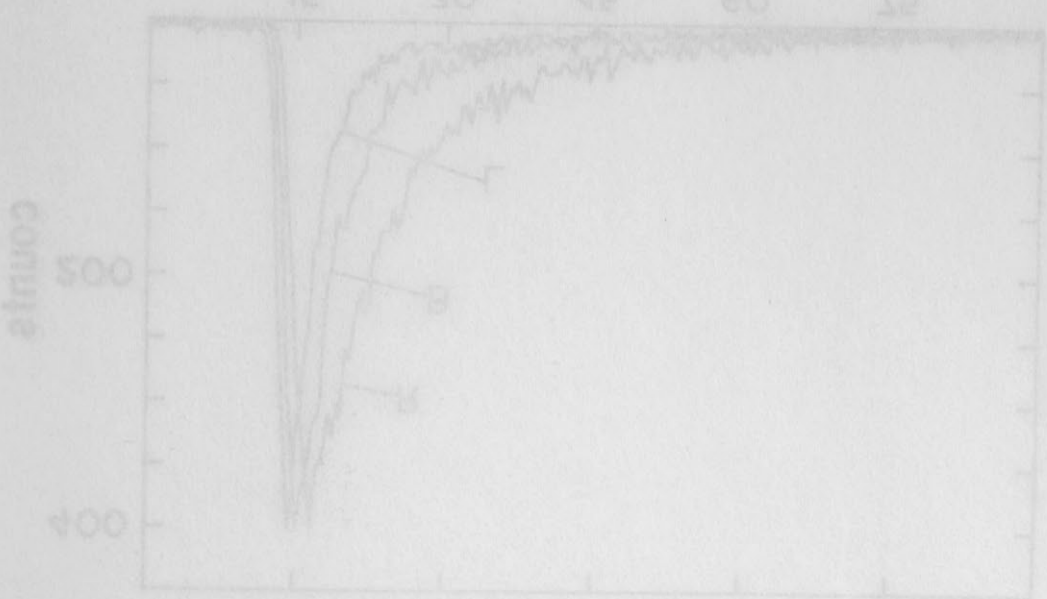
counts
500

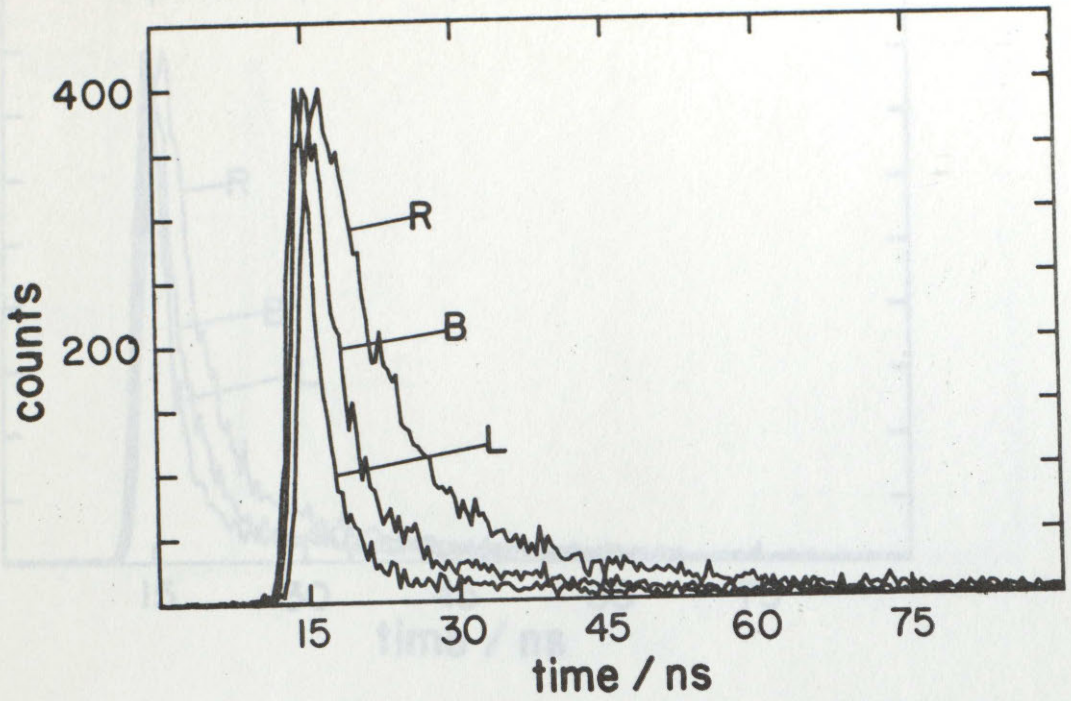

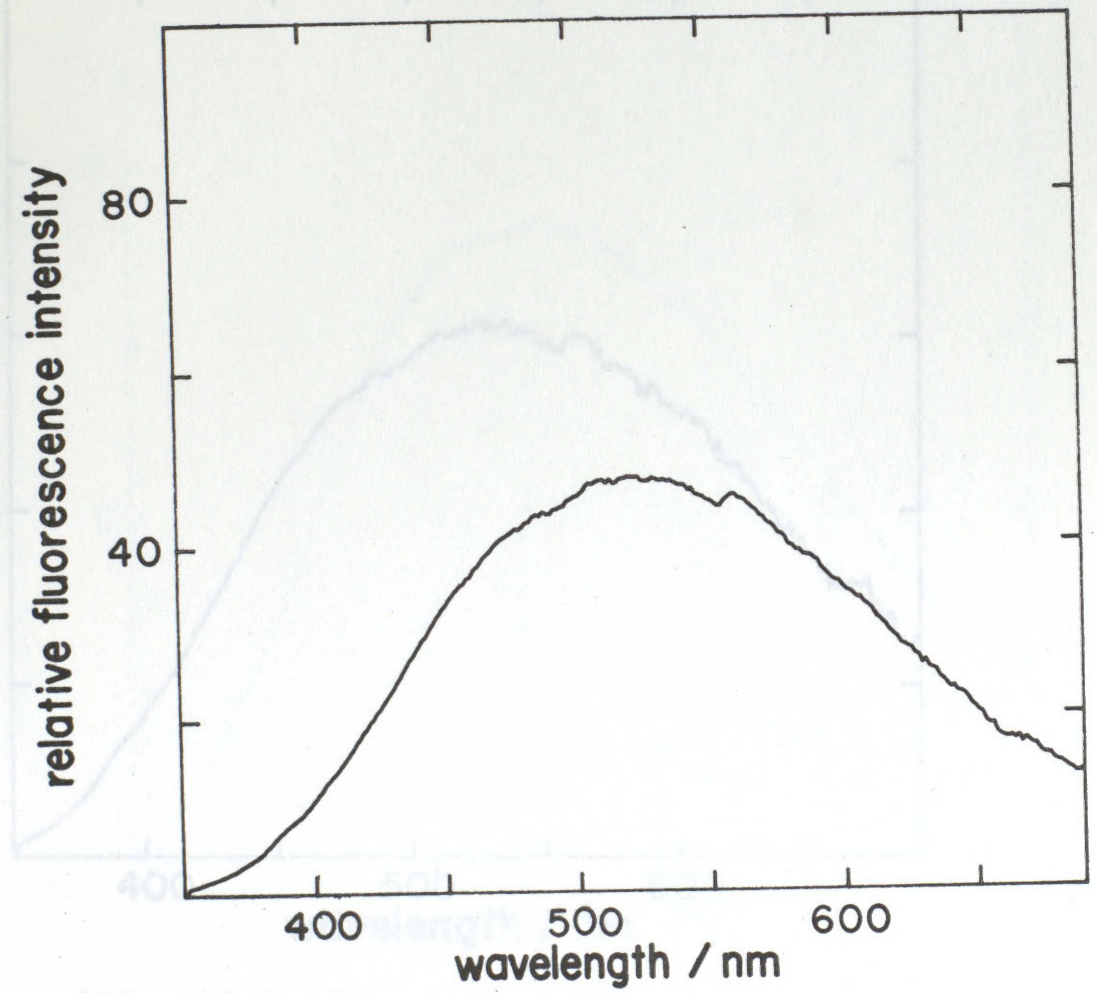

C012. I.P. #2 BLEND CRUDE, K842, CKM483 (PP28)

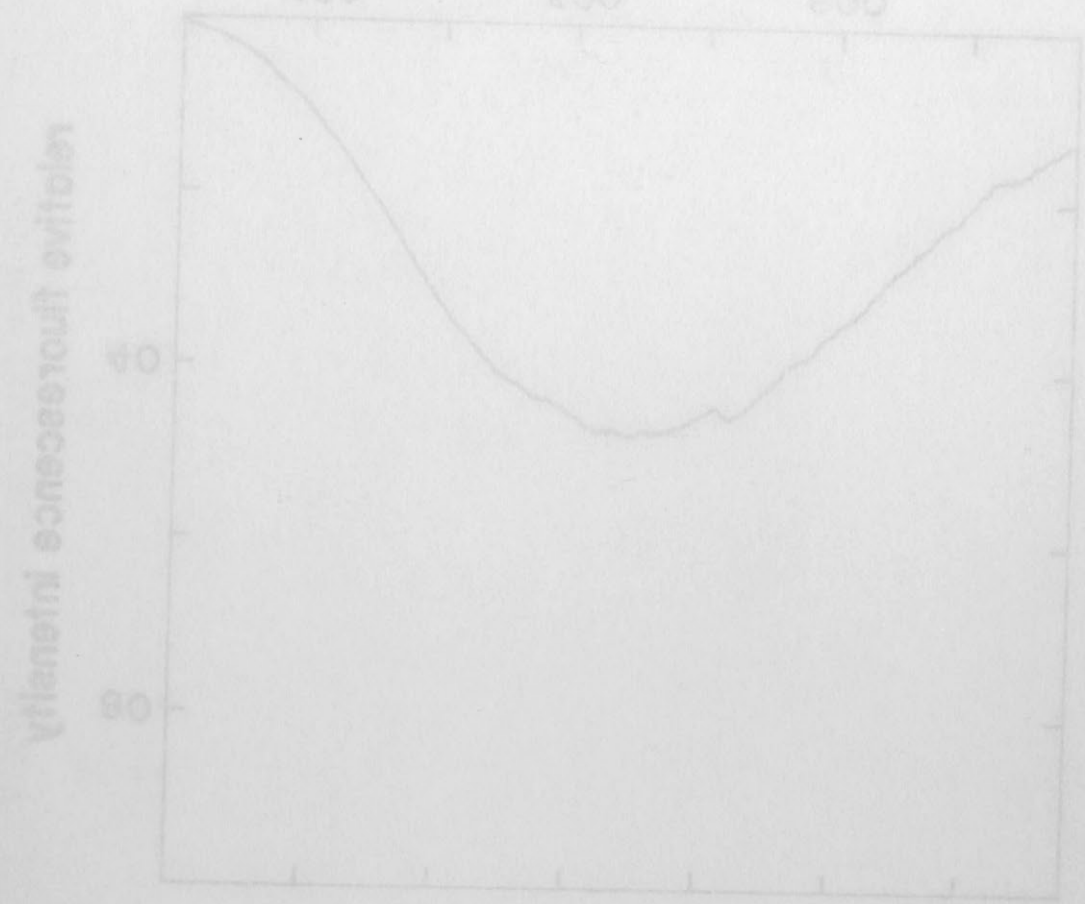

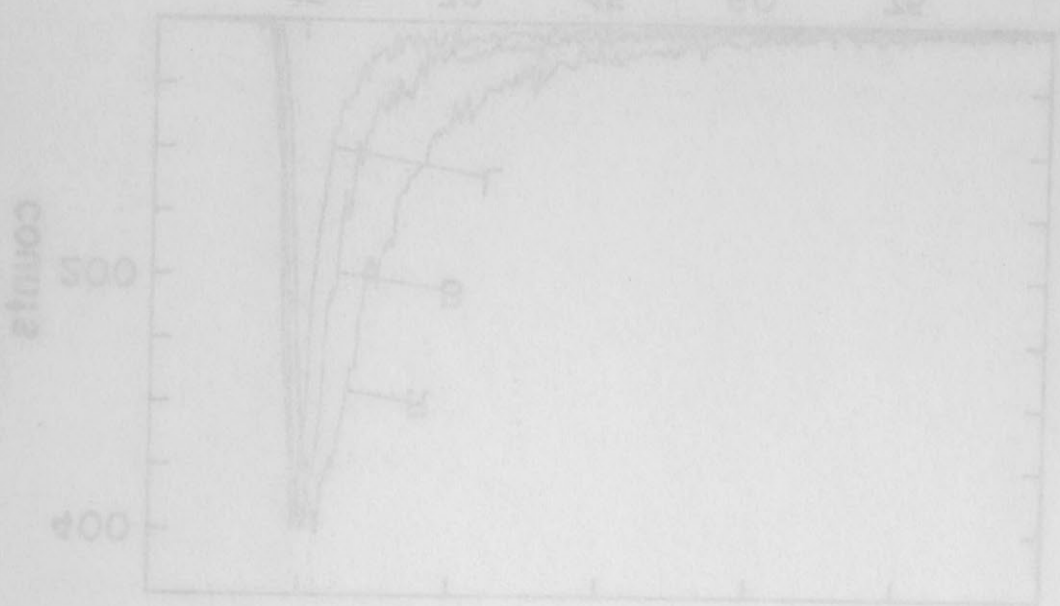

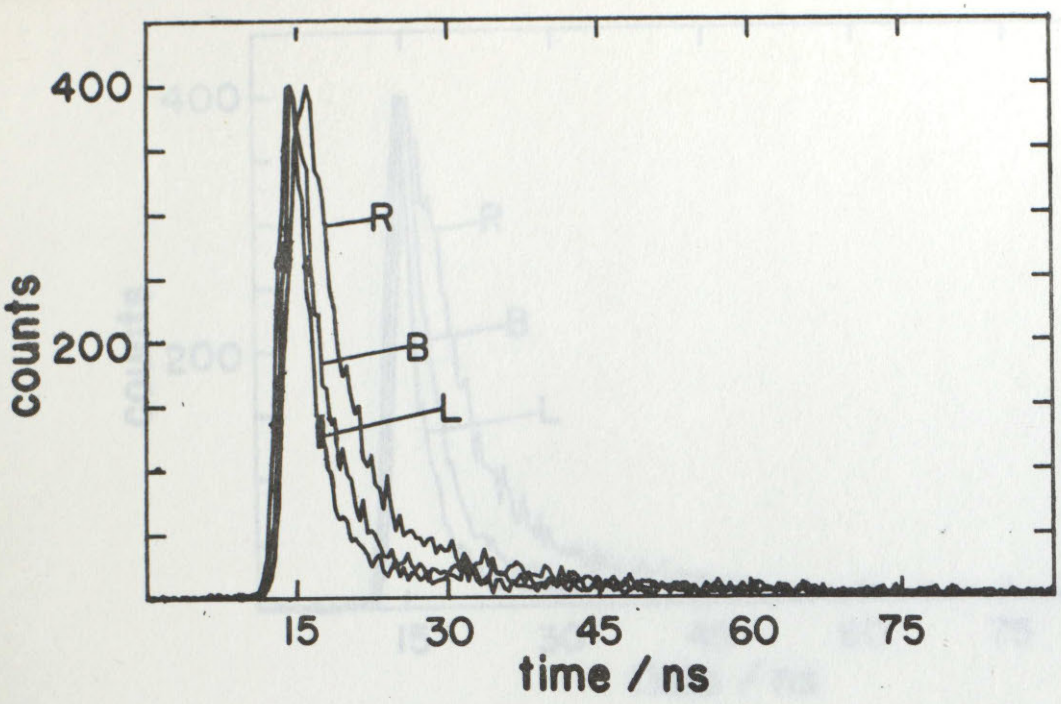

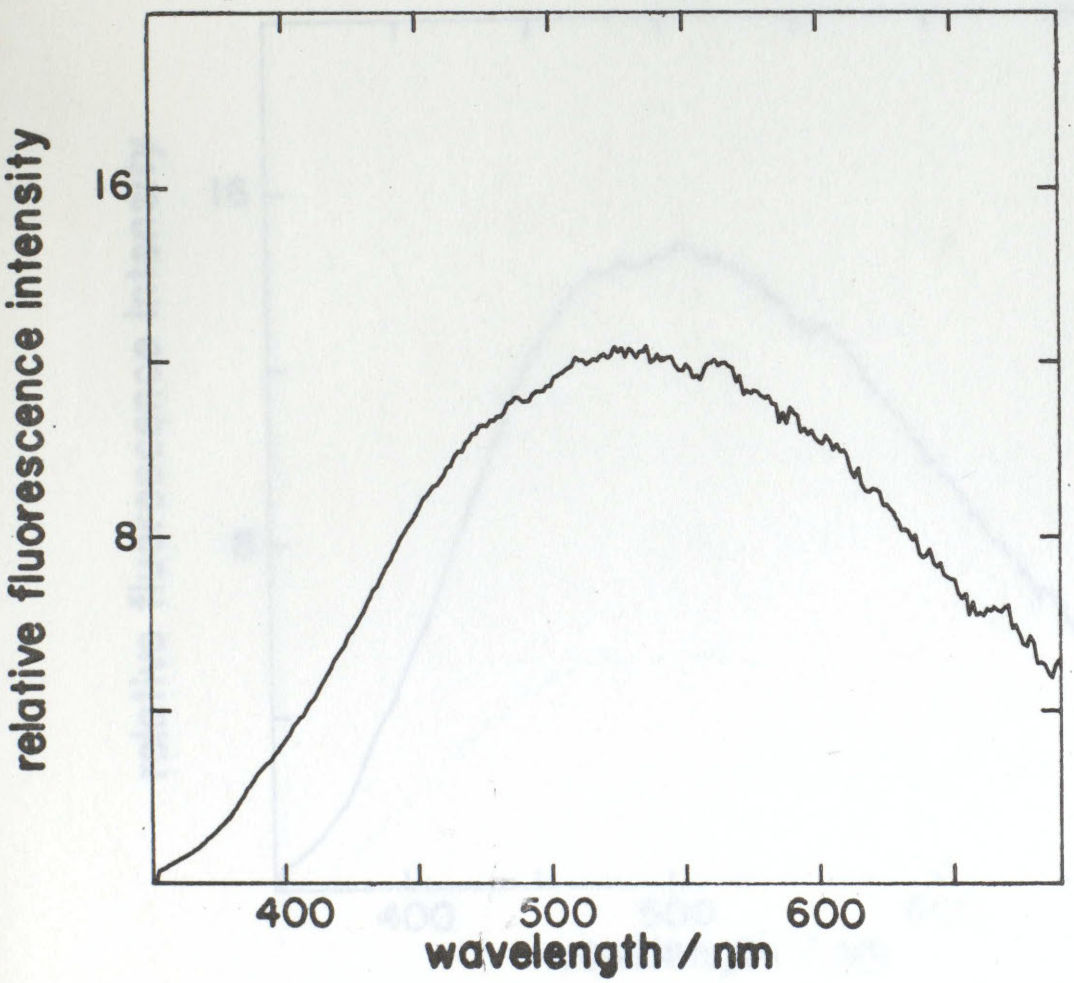

C013. GULF OIL COMPANY COLEVILLE/SMILEY CRUDE (PP29)

400
200
counts
R
B
Y
15
30
45
60
75
time / ns

relative fluorescence intensity
16
8
400
500
600
wavelength / nm

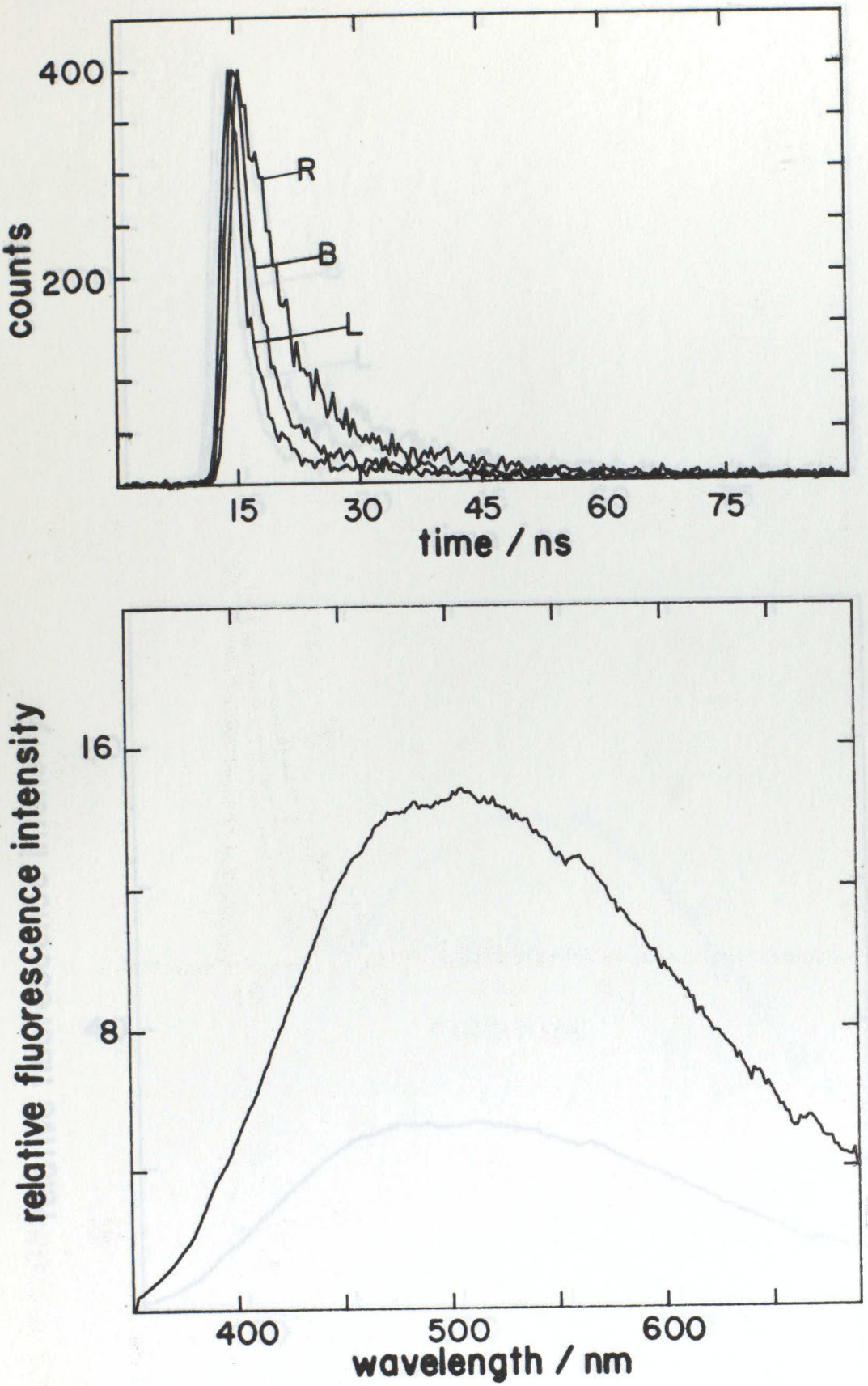

C014. IMPERIAL OIL VENEZUELAN CRUDE (PP32)

counts
400
200
R
B
L
15
30
45
60
75
time / ns

relative fluorescence intensity
15
9
400
500
600
wavelength / nm

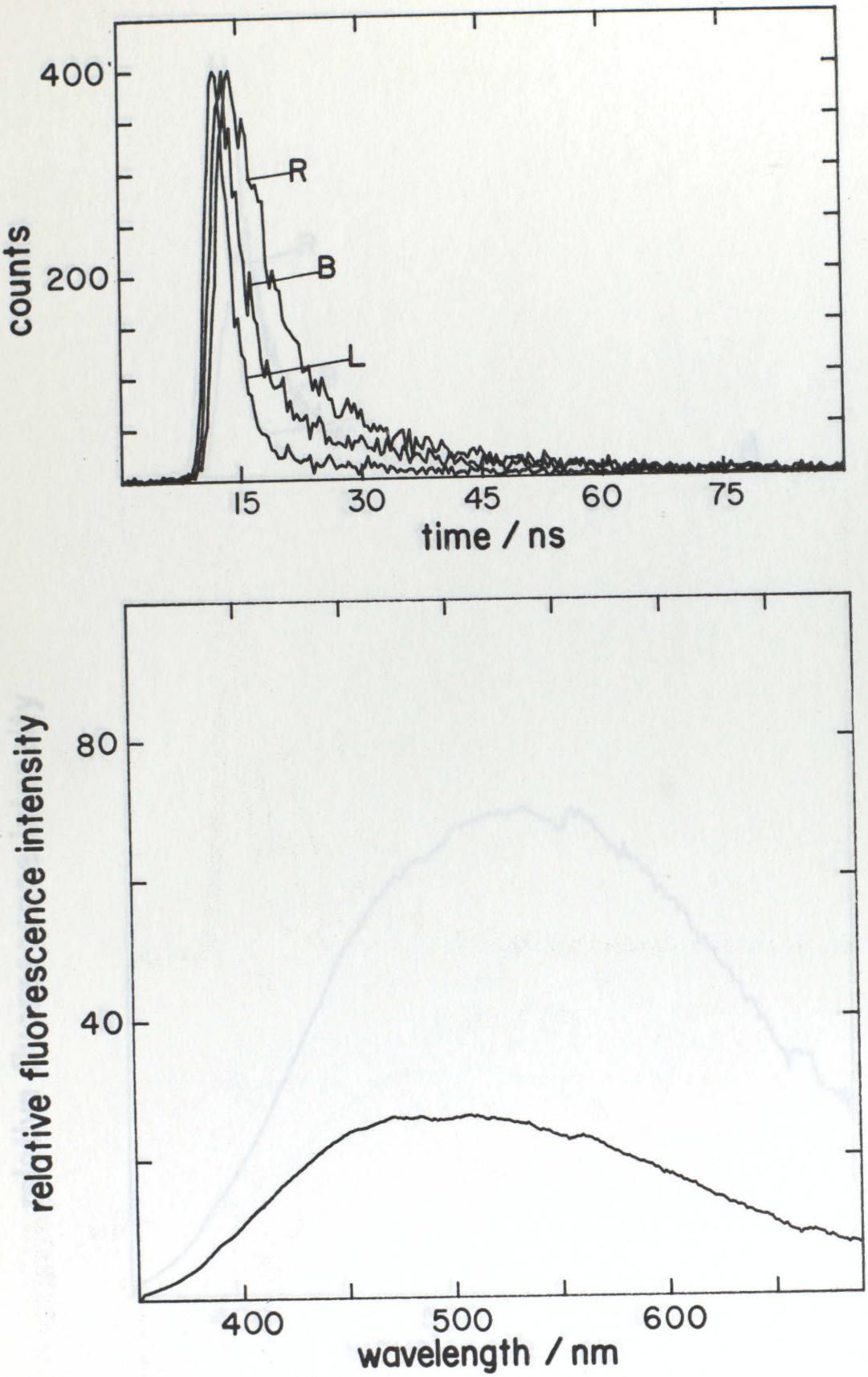

C015. BREGA LIGBIAN CRUDE (PP41).

counts
time / ns

relative fluorescence intensity
wavelength / nm

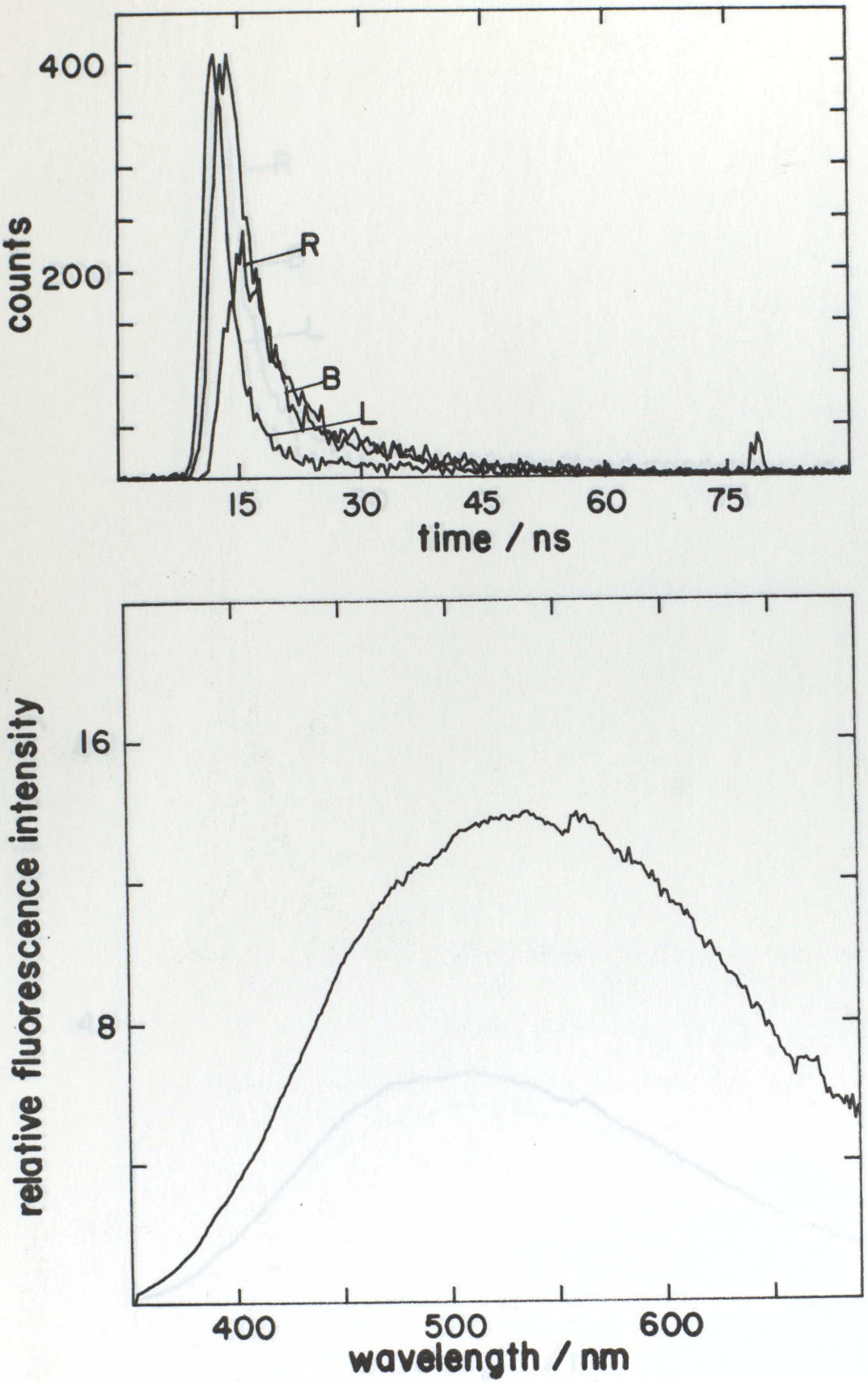

C016. SHELL CANADA MIDAL CRUDE (PP44)

counts
400
200
time / ns
15
30
45
60
75
A
B
C

relative fluorescence intensity
15
5
wavelength / nm
400
500
600

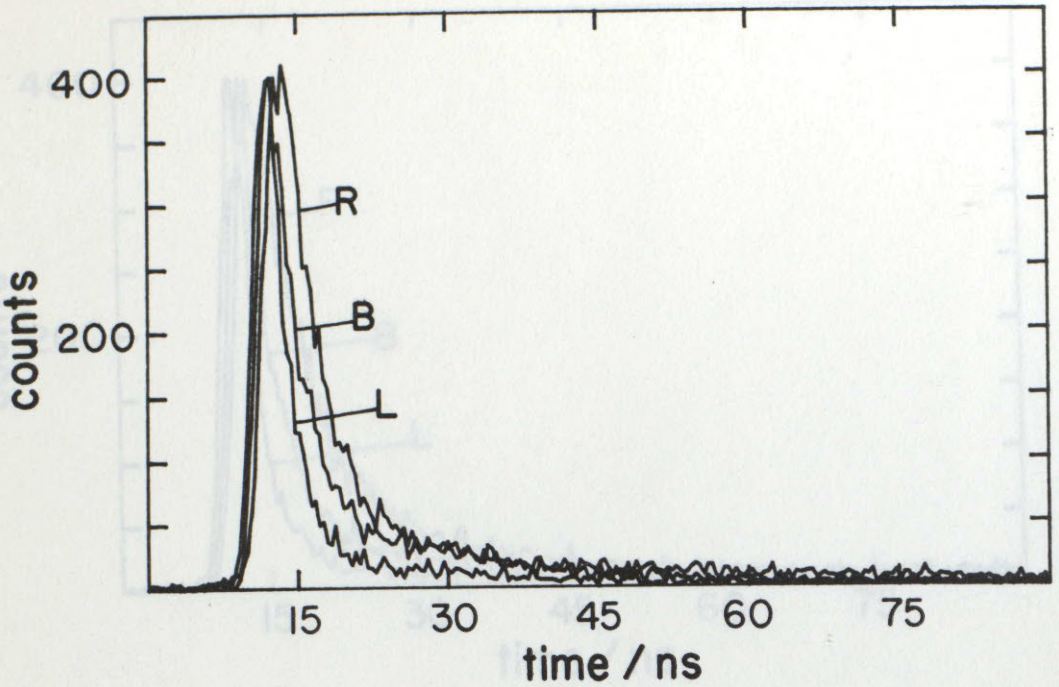

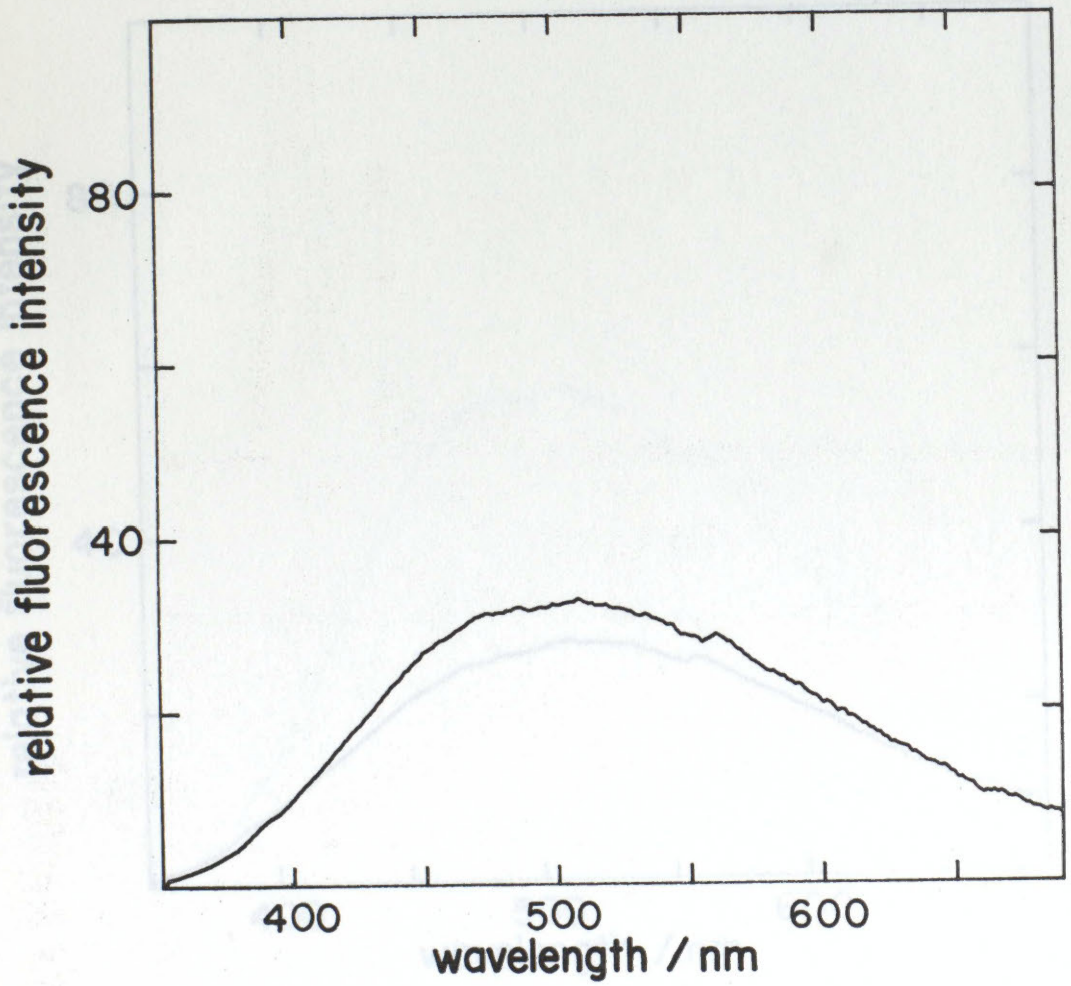

C017. SHELL CANADA I.P. CRUDE (PP45)

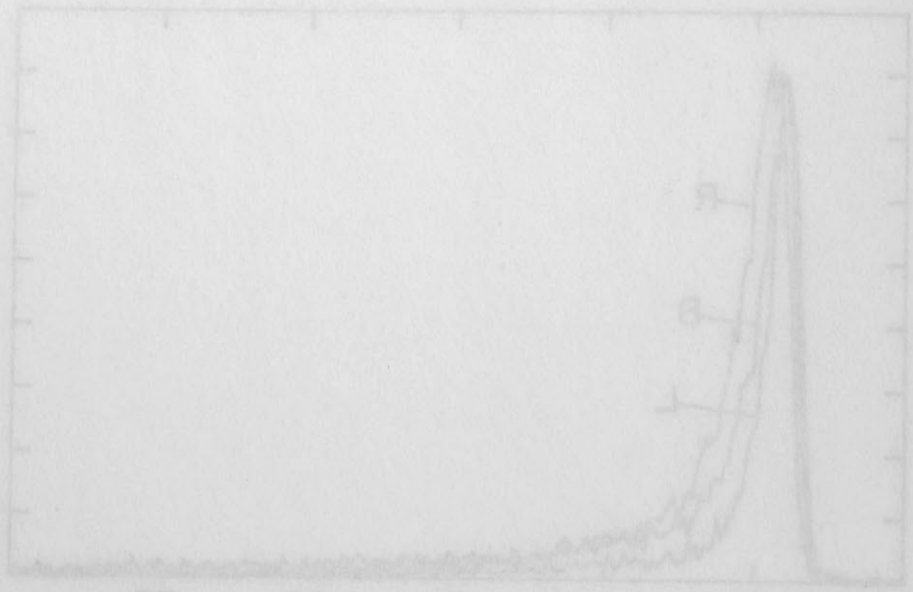
400
200
counts
15
30
45
60
75
time / ns

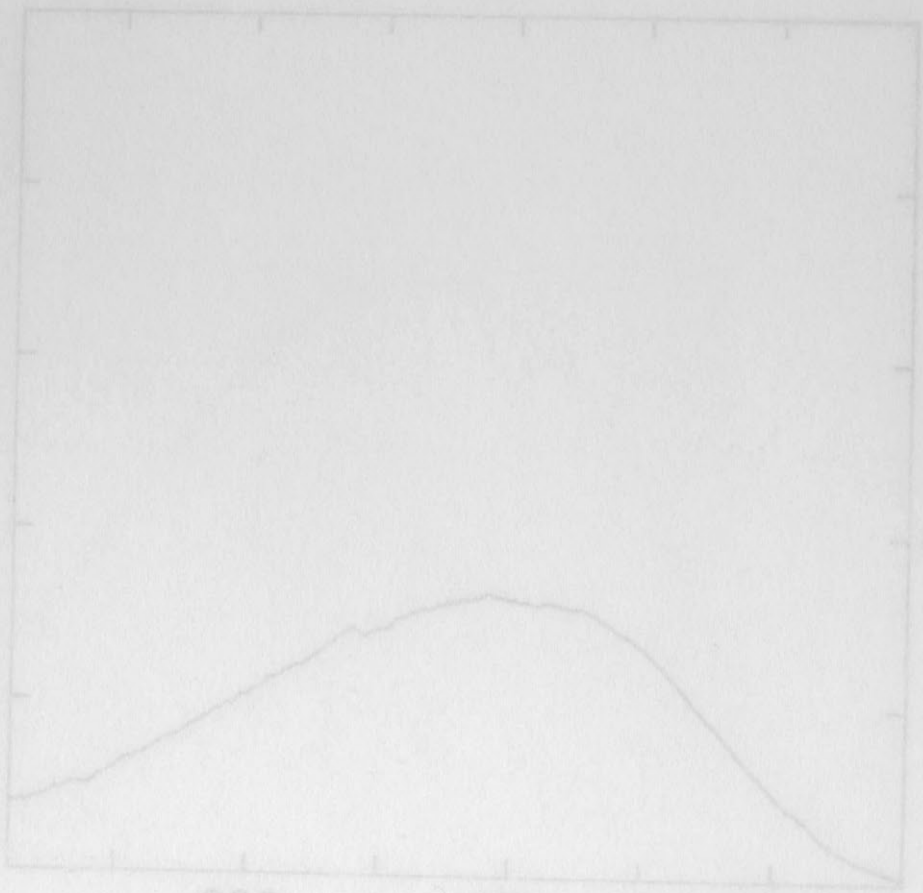
80
40
relative fluorescence intensity
400
500
600
wavelength / nm

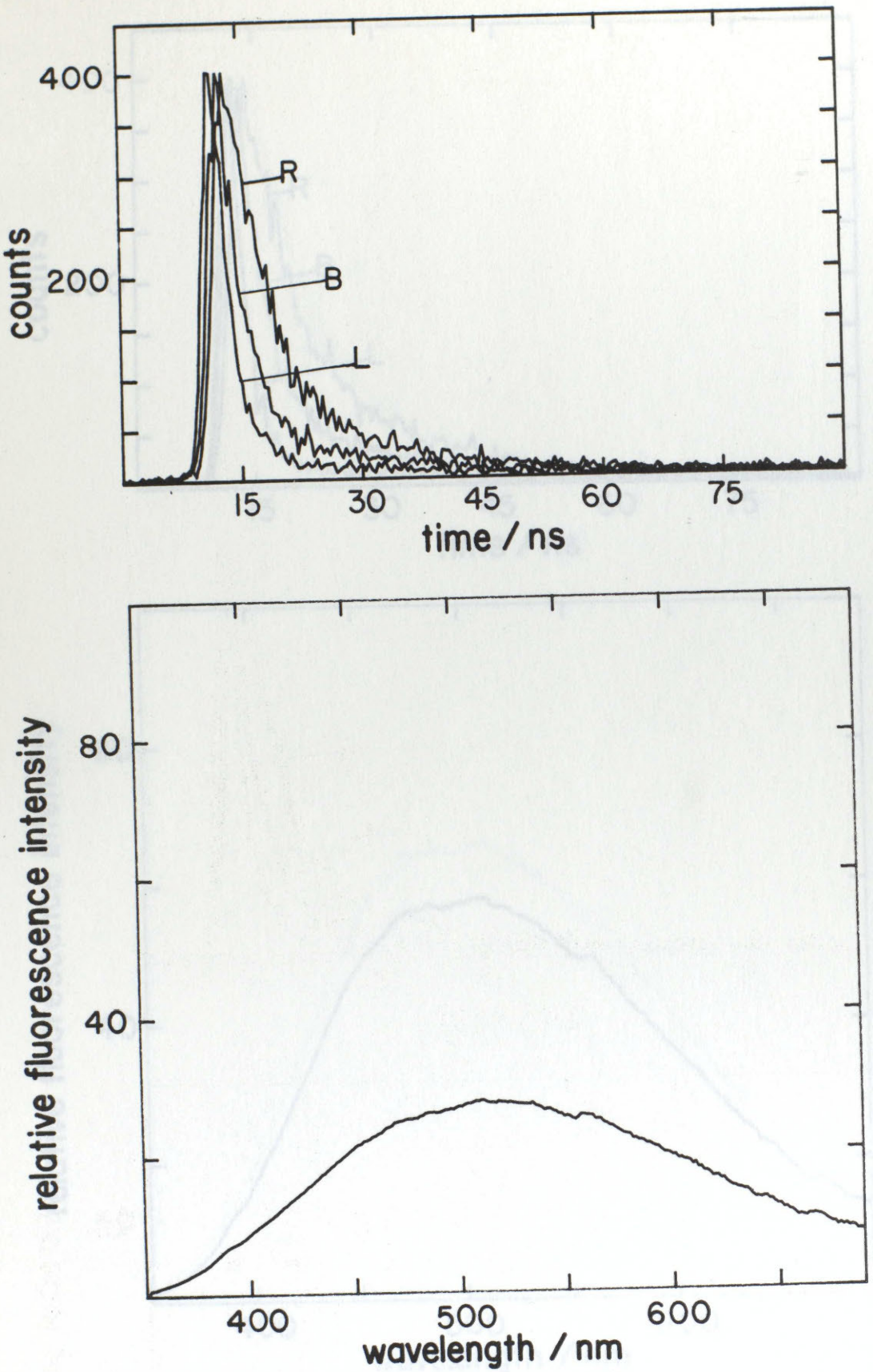

C018. SHELL OIL BOUNDARY LAKE CRUDE (PP72)

counts
time / ns

relative fluorescence intensity
wavelength / nm

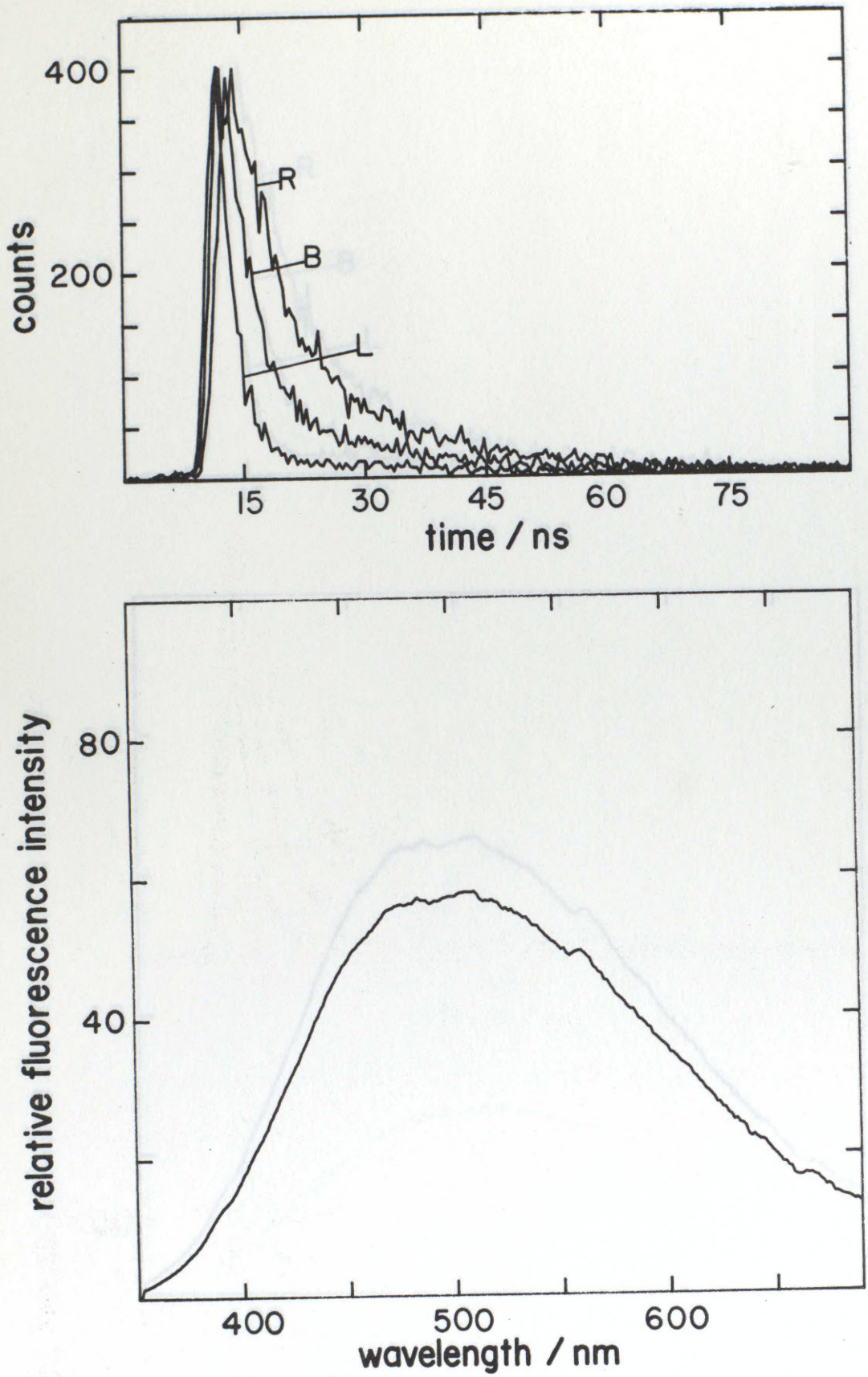

C019. SHELL OIL PEACE RIVER CRUDE (PP73)

counts
400
200
time / ns
15
30
45
60
75

relative fluorescence intensity
80
40
wavelength / nm
400
500
600

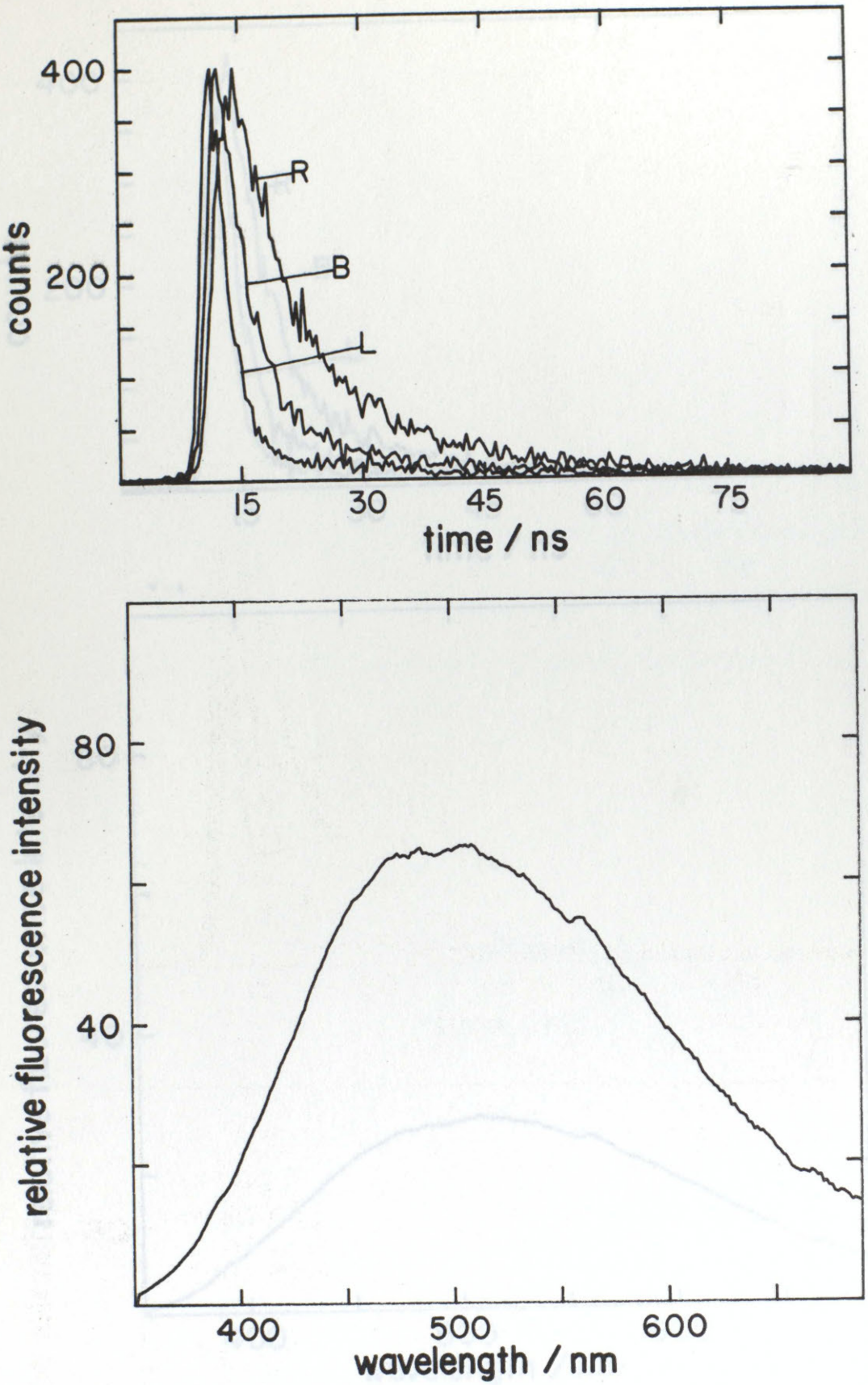

C020. SHEFF OIL GULF ALBERTA CRUDE (PP74)

400
200
counts
R
S
I
15
30
45
60
75
time / ns

80
40
relative fluorescence intensity
400
500
600
wavelength / nm

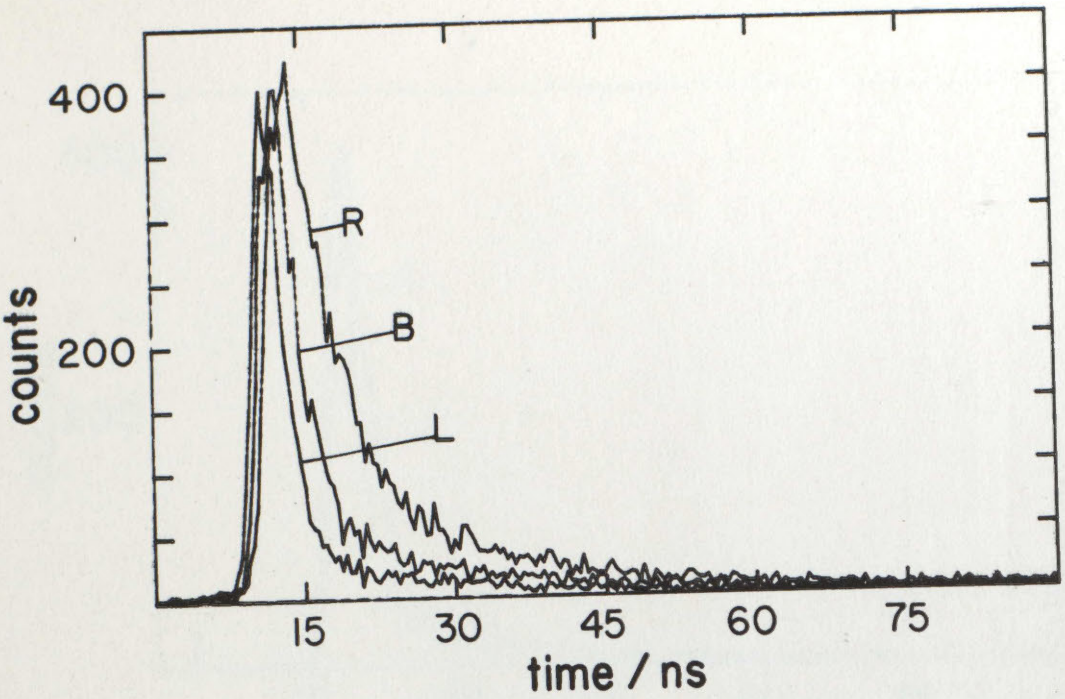

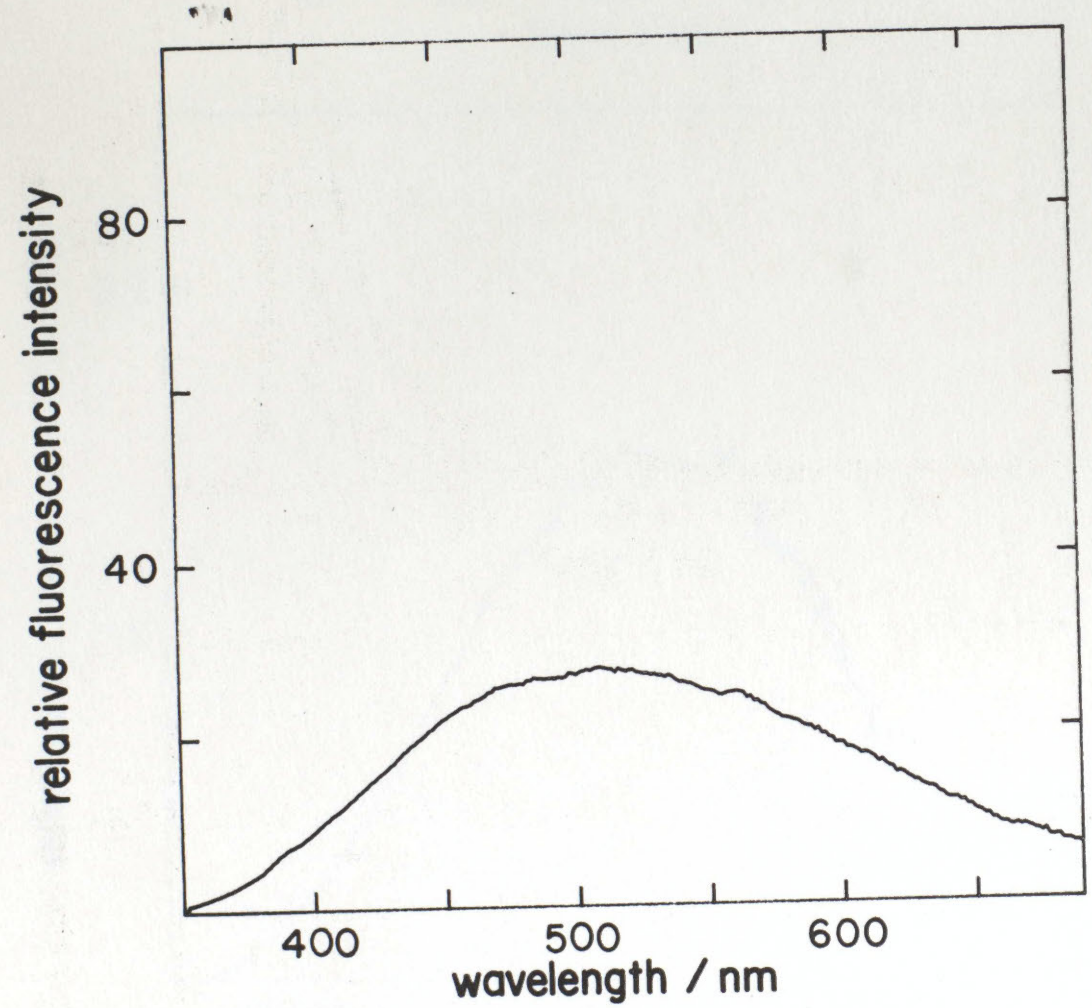

C021. IMPERIAL OIL CRUDE (IOCO BLEND REDWATER AND GULF ALBERTA (PP78)

counts
400
200
R
B
15
30
45
60
75
time / ns

relative fluorescence intensity
80
40
400
500
600
wavelength / nm

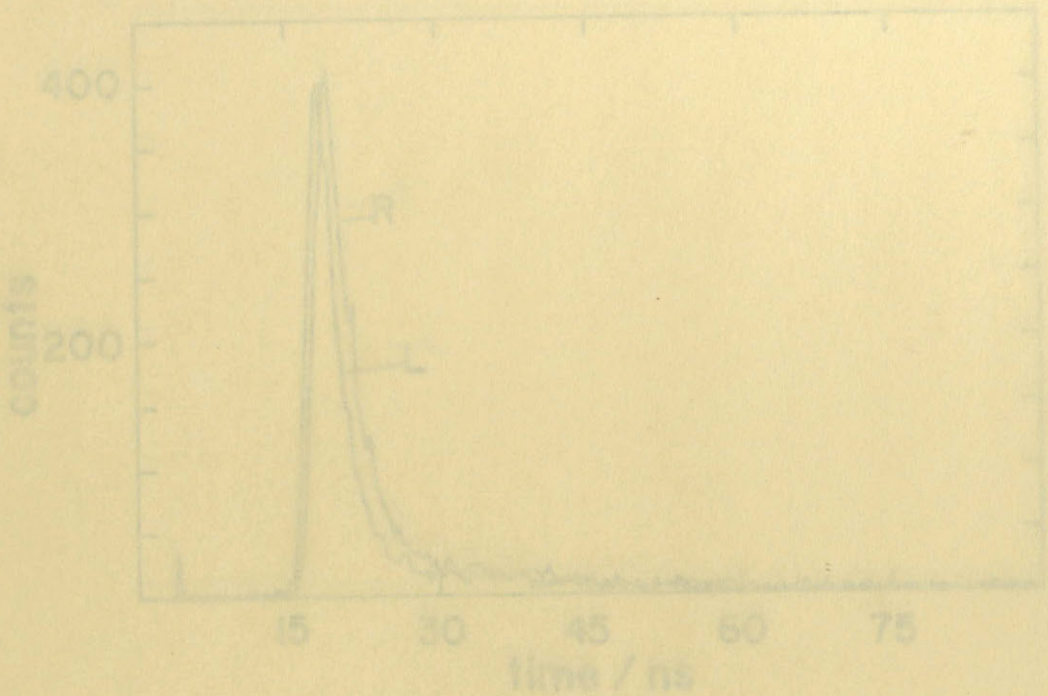
400
200
counts
R
L
15
30
45
60
75
time / ns

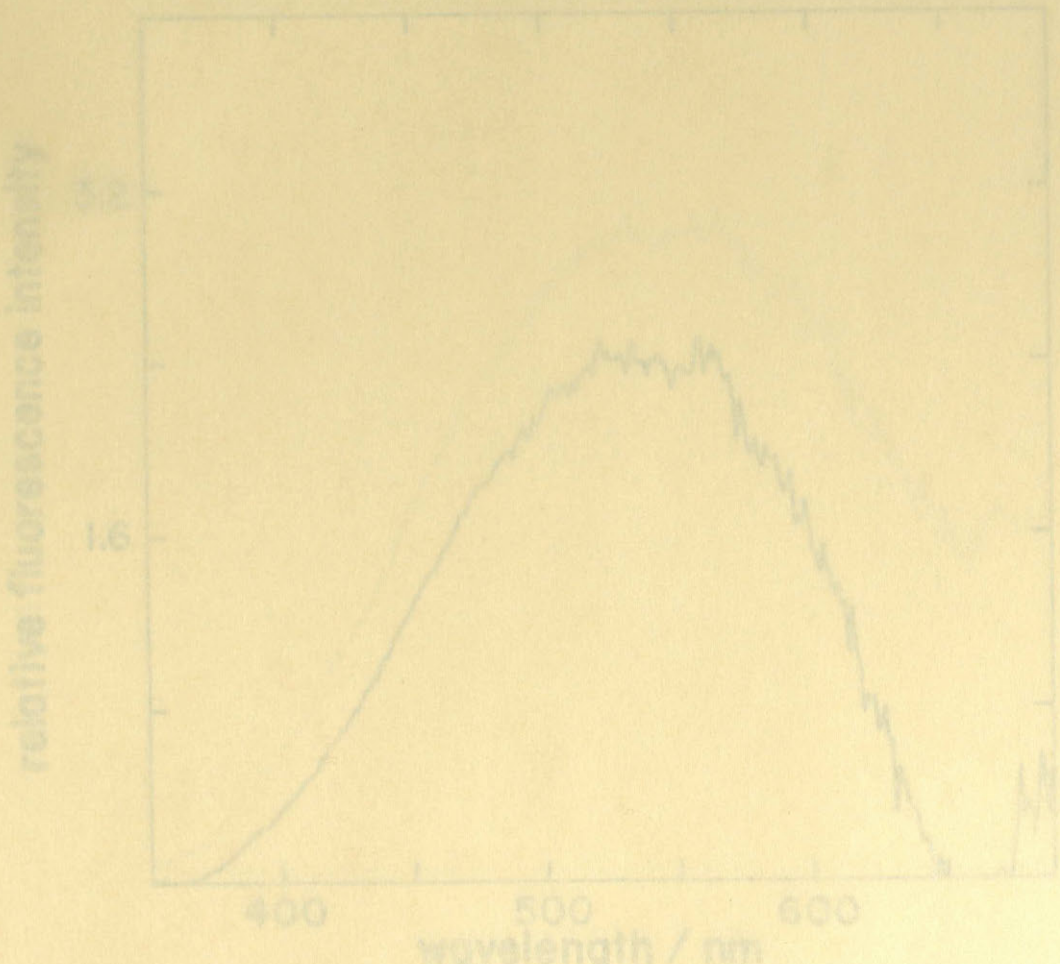
3.2
1.6
relative fluorescence intensity
400
500
600
wavelength / nm

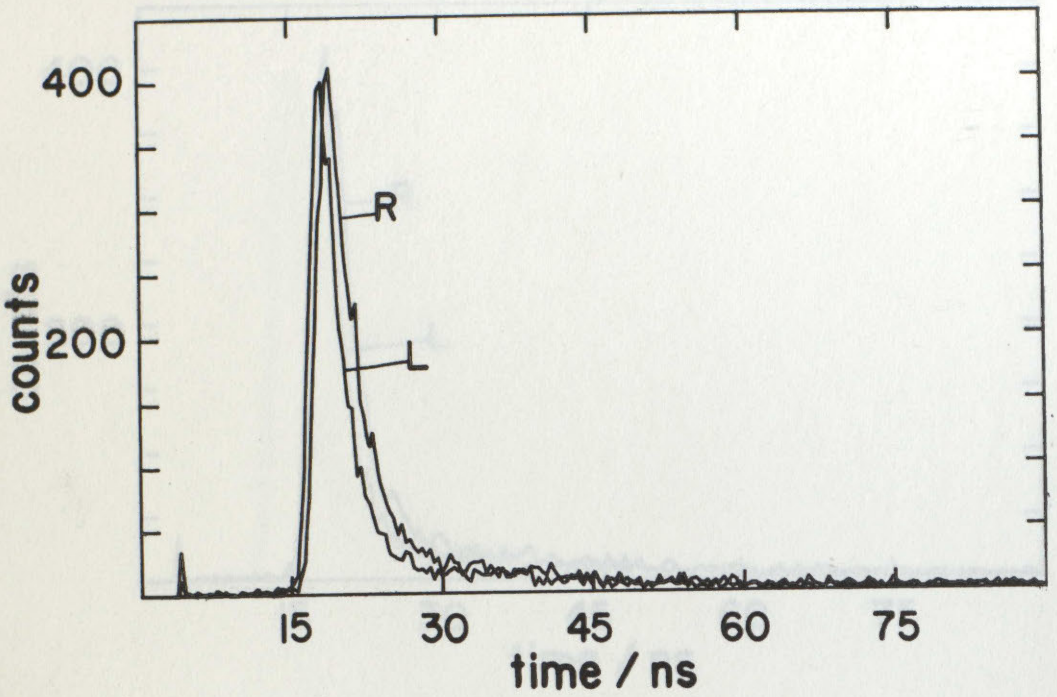

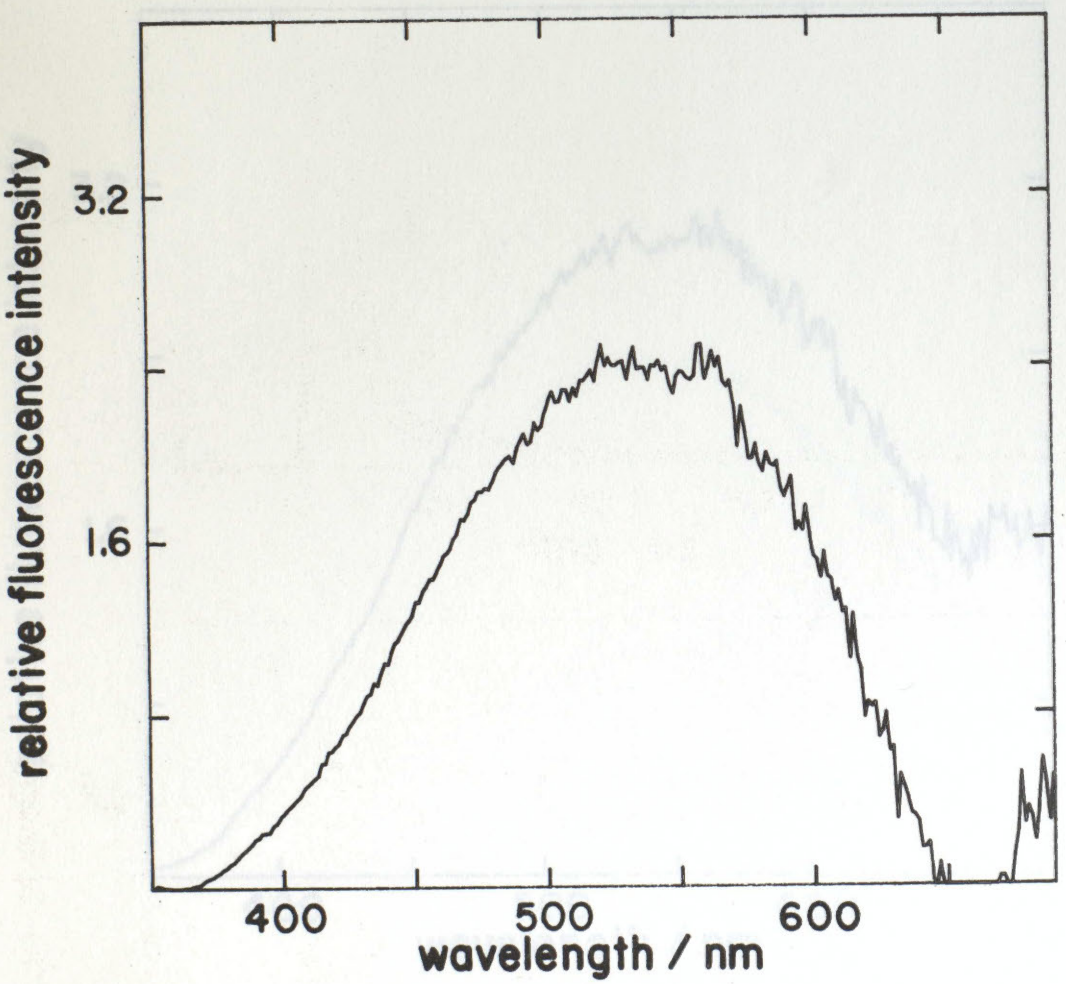

HO1. MEDIUM BUNKER C

400
200
counts
R
I
15
30
45
60
75
time / ns

3.2
1.6
(arbitrary units) fluorescence intensity
400
500
600
wavelength / nm

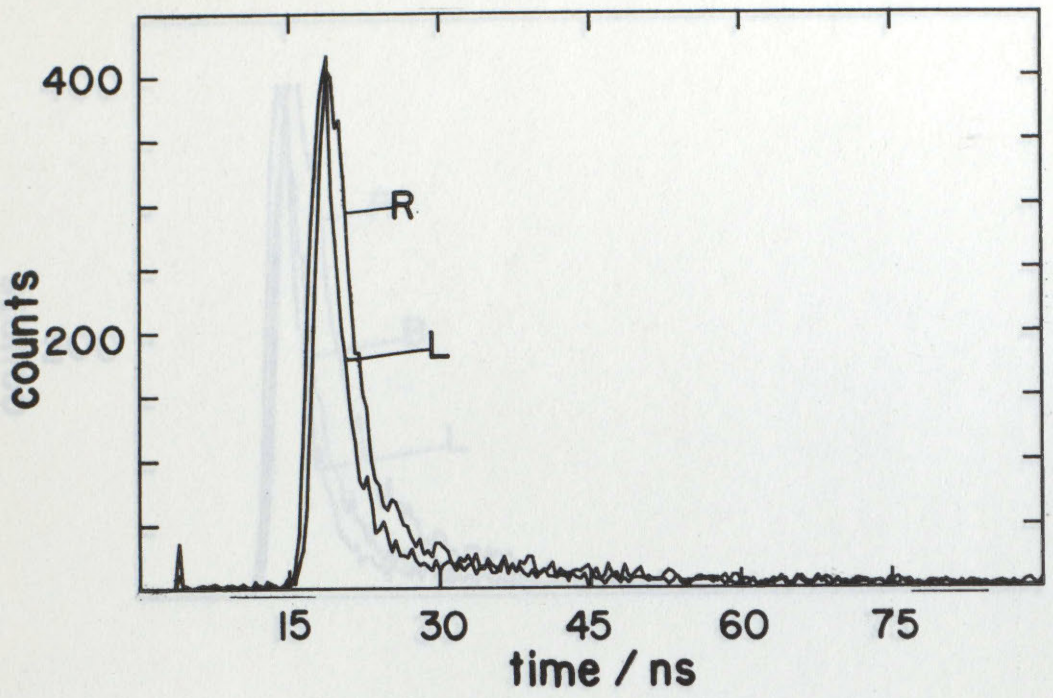

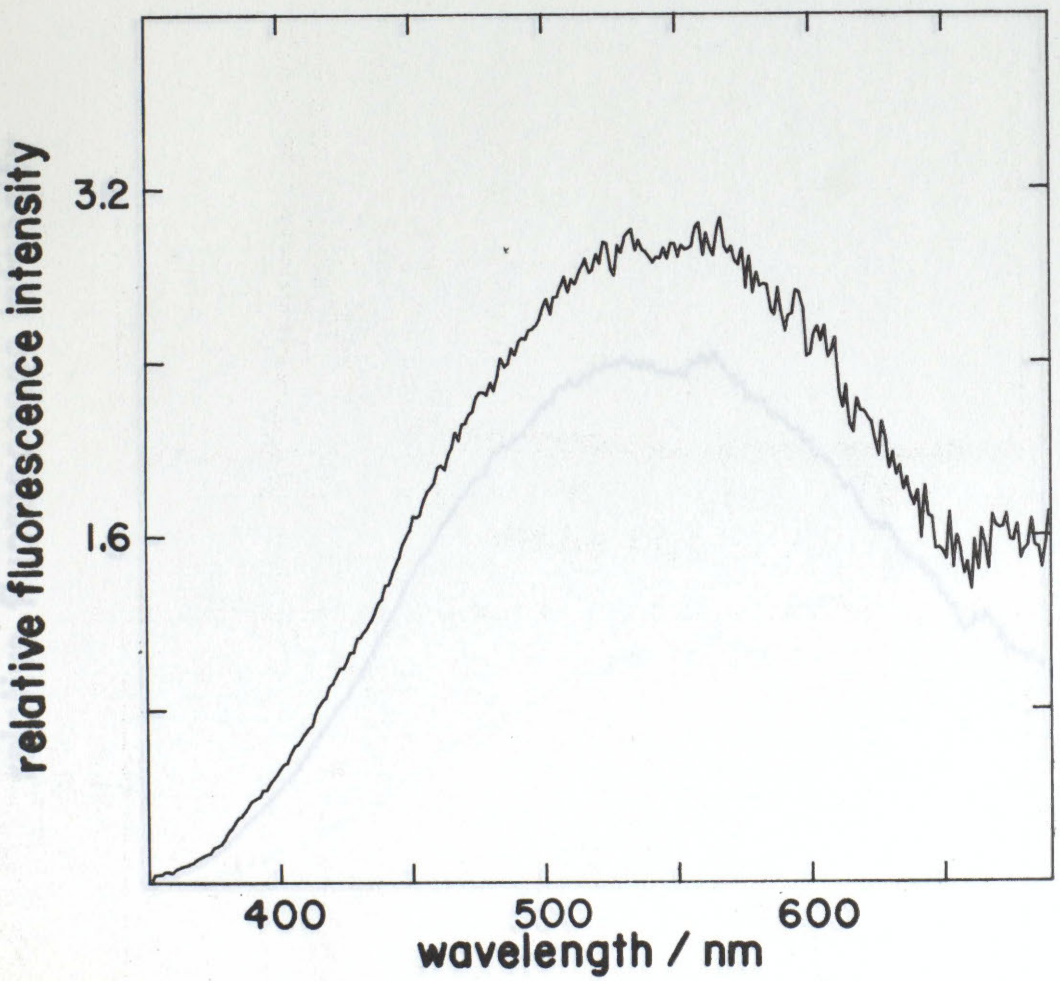

H02. ESSO BUNKER FUEL

400
200
counts
15
30
45
60
75
time / ns

3.2
1.6
Relative fluorescence intensity
400
500
600
wavelength / nm

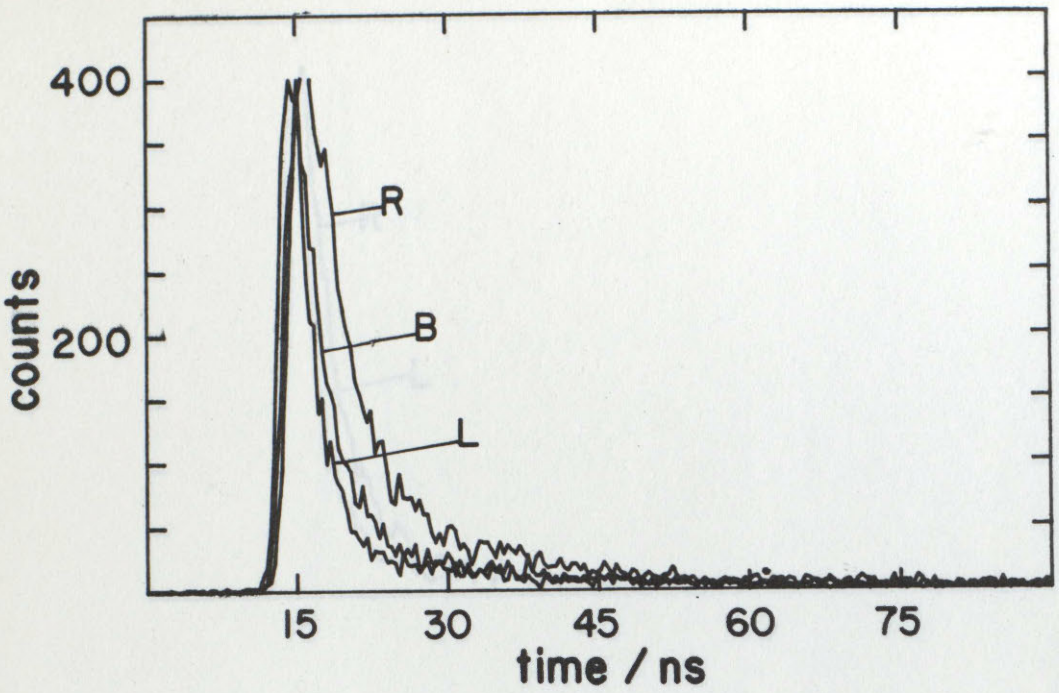

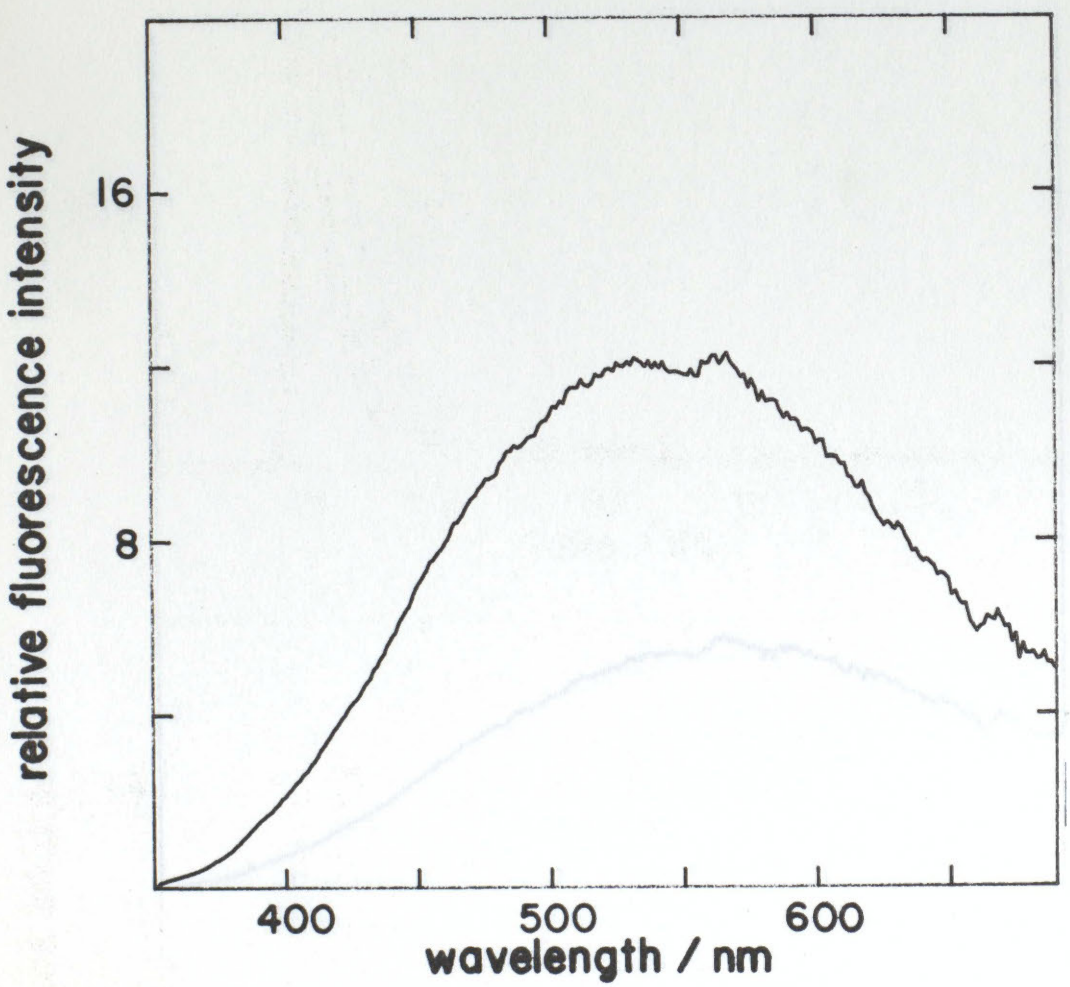

H03. ESSO FUEL INT. 2

counts
time / ns

relative fluorescence intensity
wavelength / nm

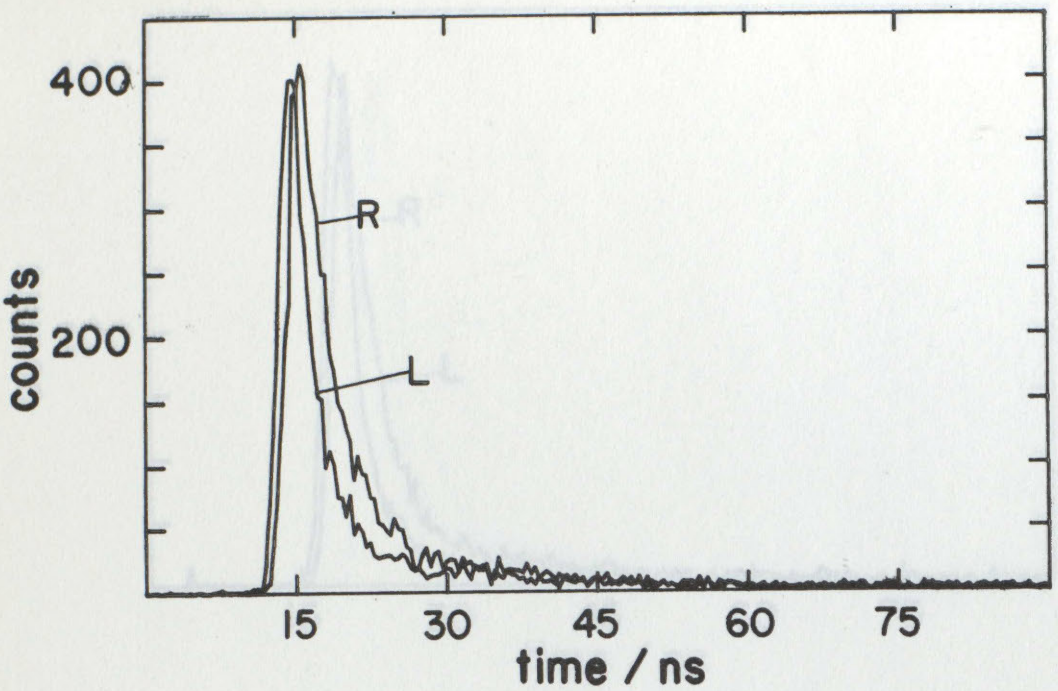
400
200
counts
R
L
15
30
45
60
75
time / ns

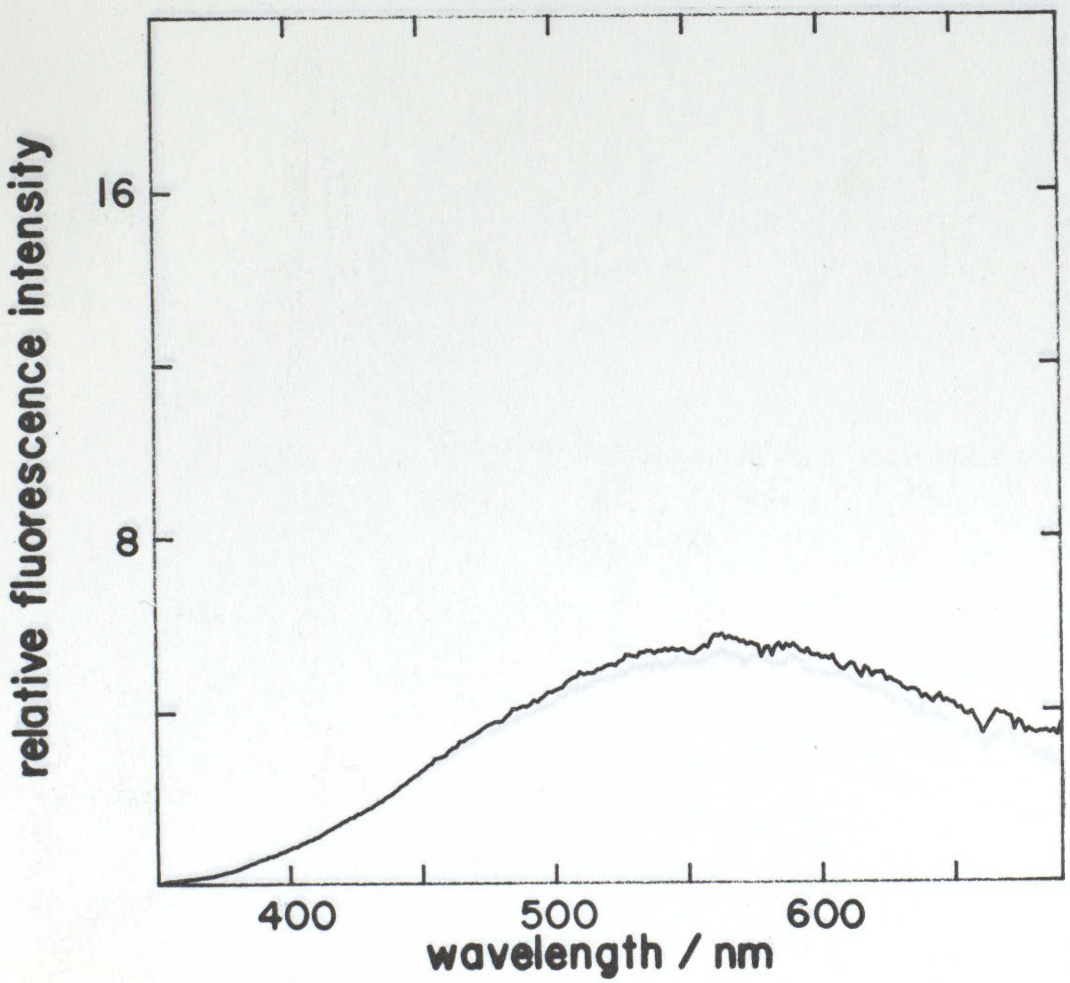
16
8
relative fluorescence intensity
400
500
600
wavelength / nm

400
200
counts
15
30
45
60
75
time / ns

15
0
relative fluorescence intensity
400
500
600
wavelength / nm

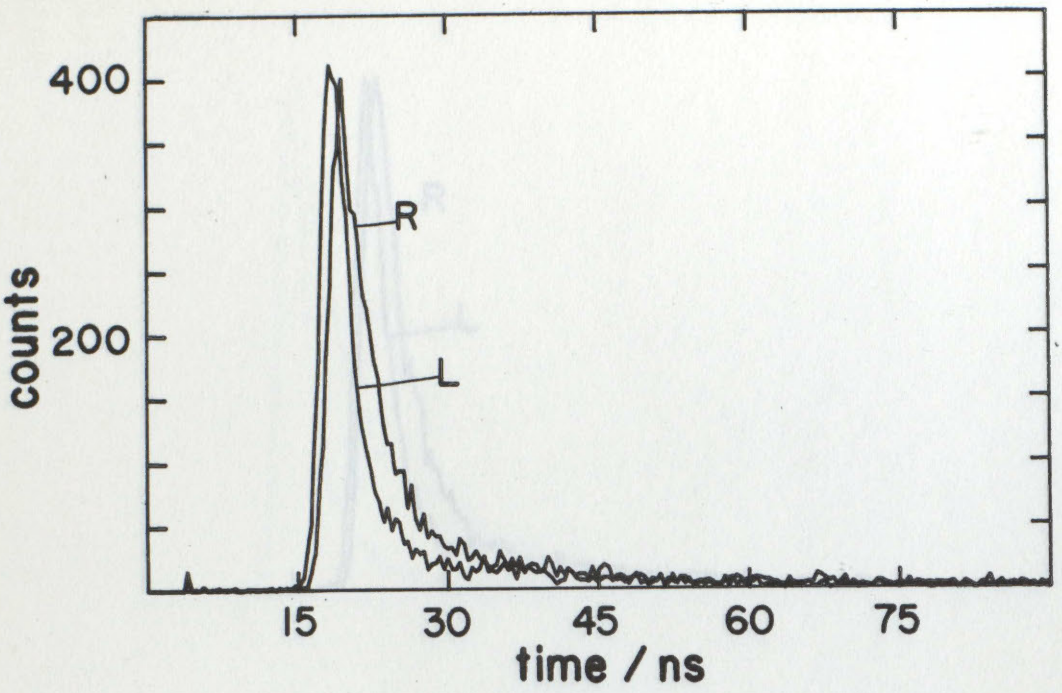

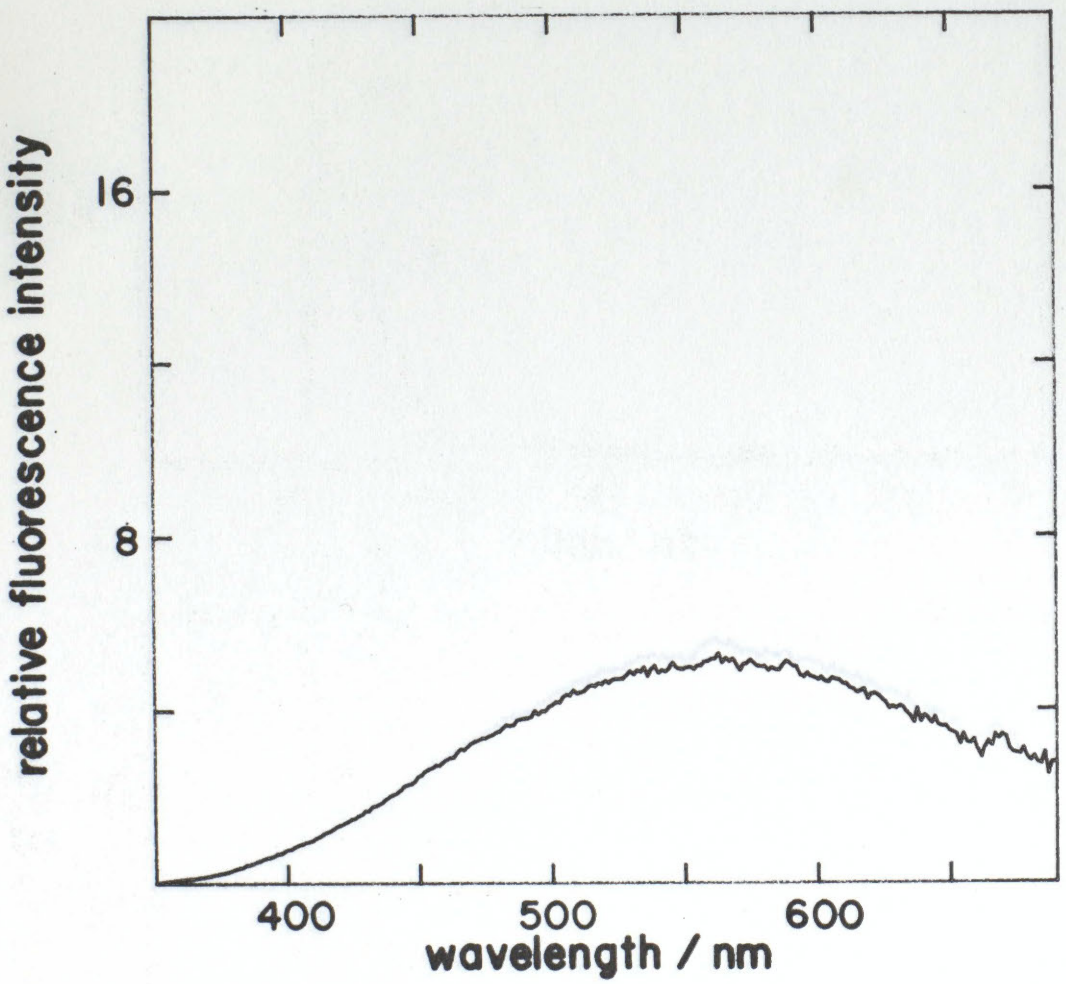

H05. ESSO FUEL INT. 12

400
200
counts
R
L
15
30
45
60
75
time / ns

16
8
relative fluorescence intensity
400
500
600
wavelength / nm

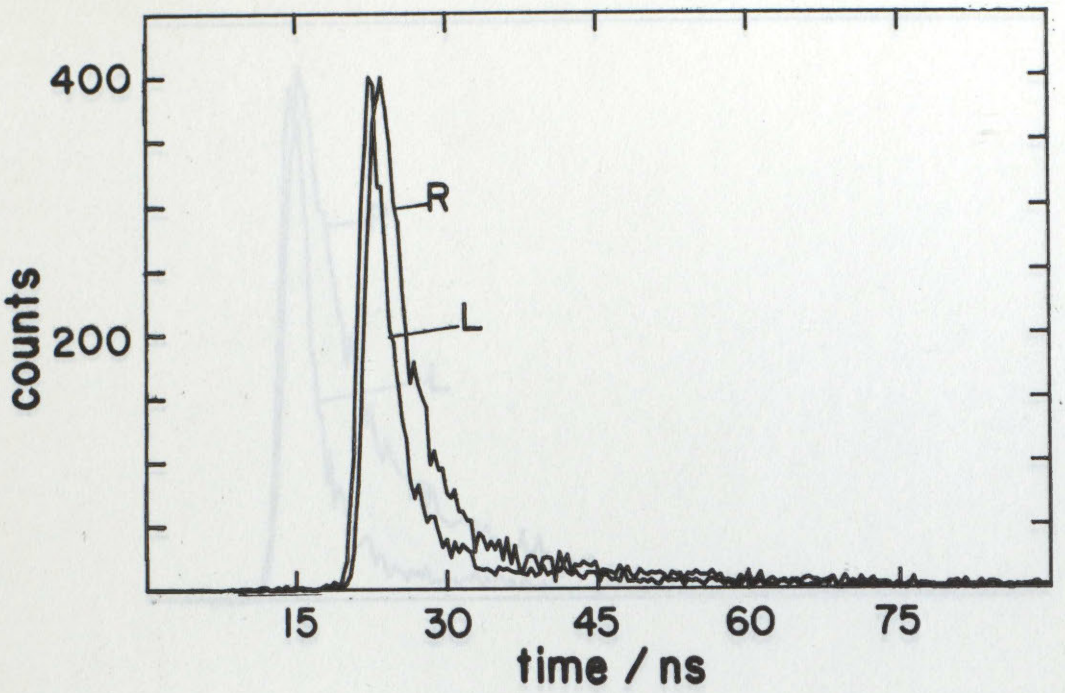

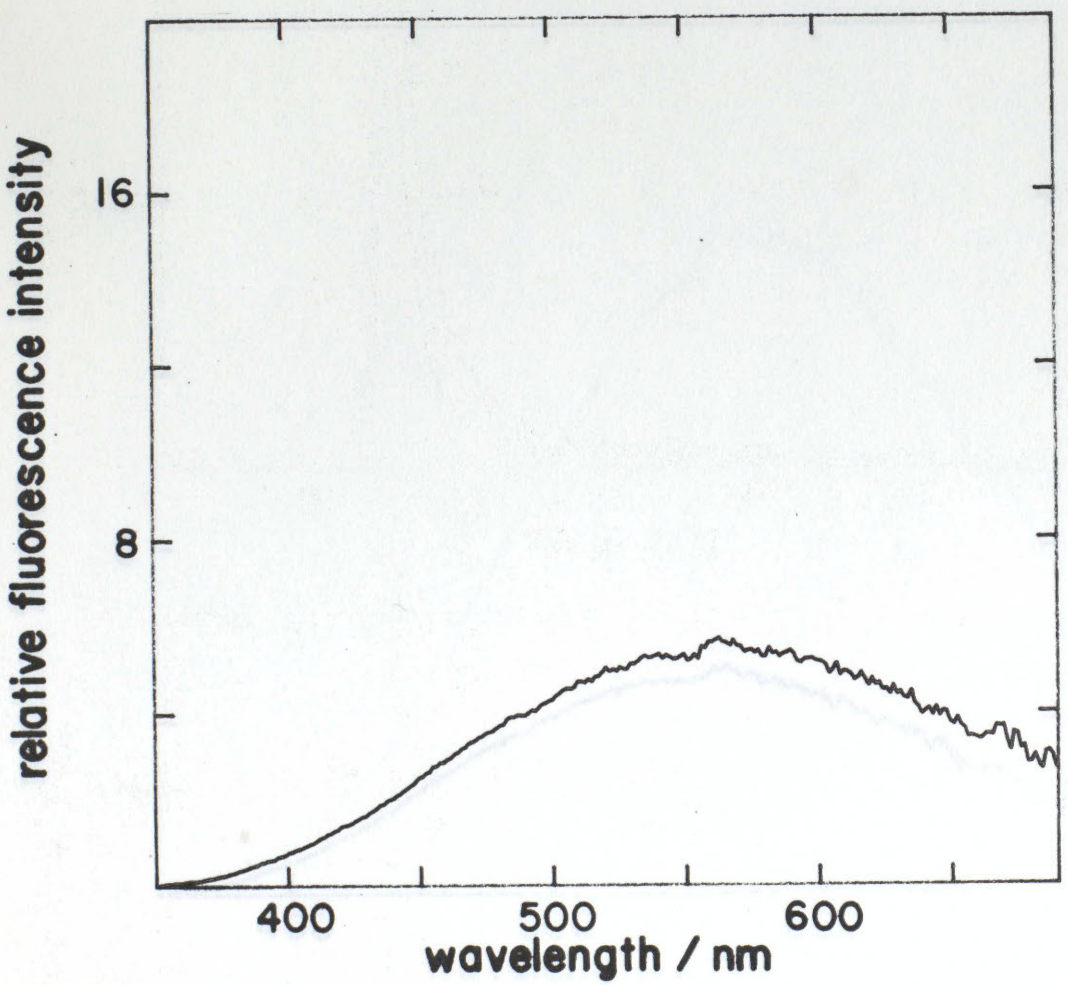

H06. ESSO FUEL INT. 15

400
200
counts
15
20
45
60
75
time / ns

15
8
relative fluorescence intensity
400
500
600
wavelength / nm

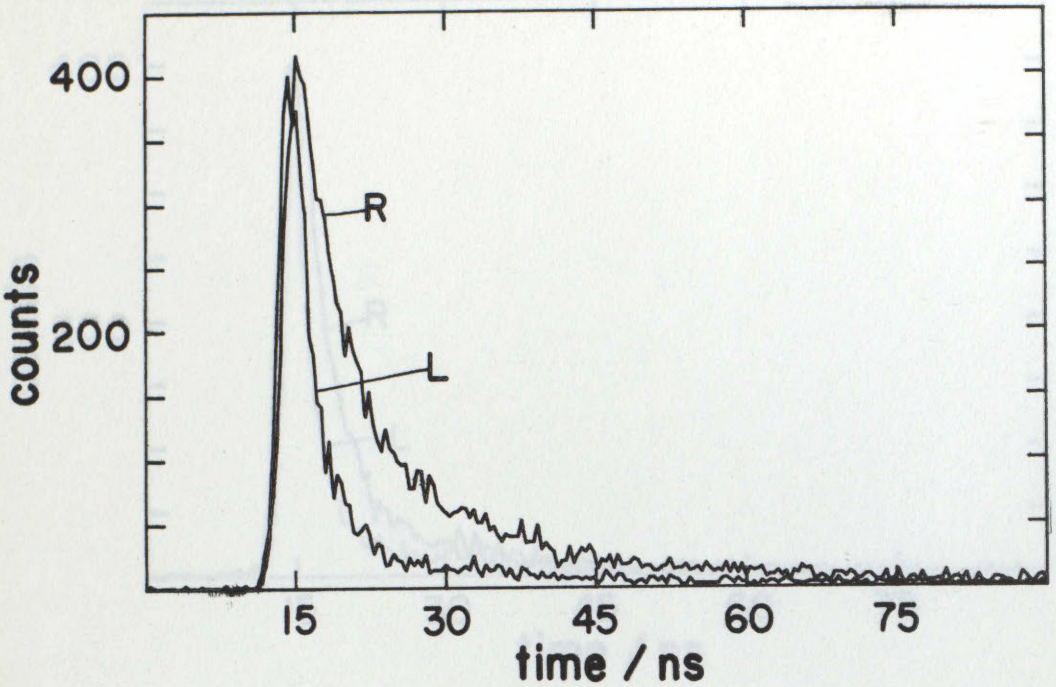

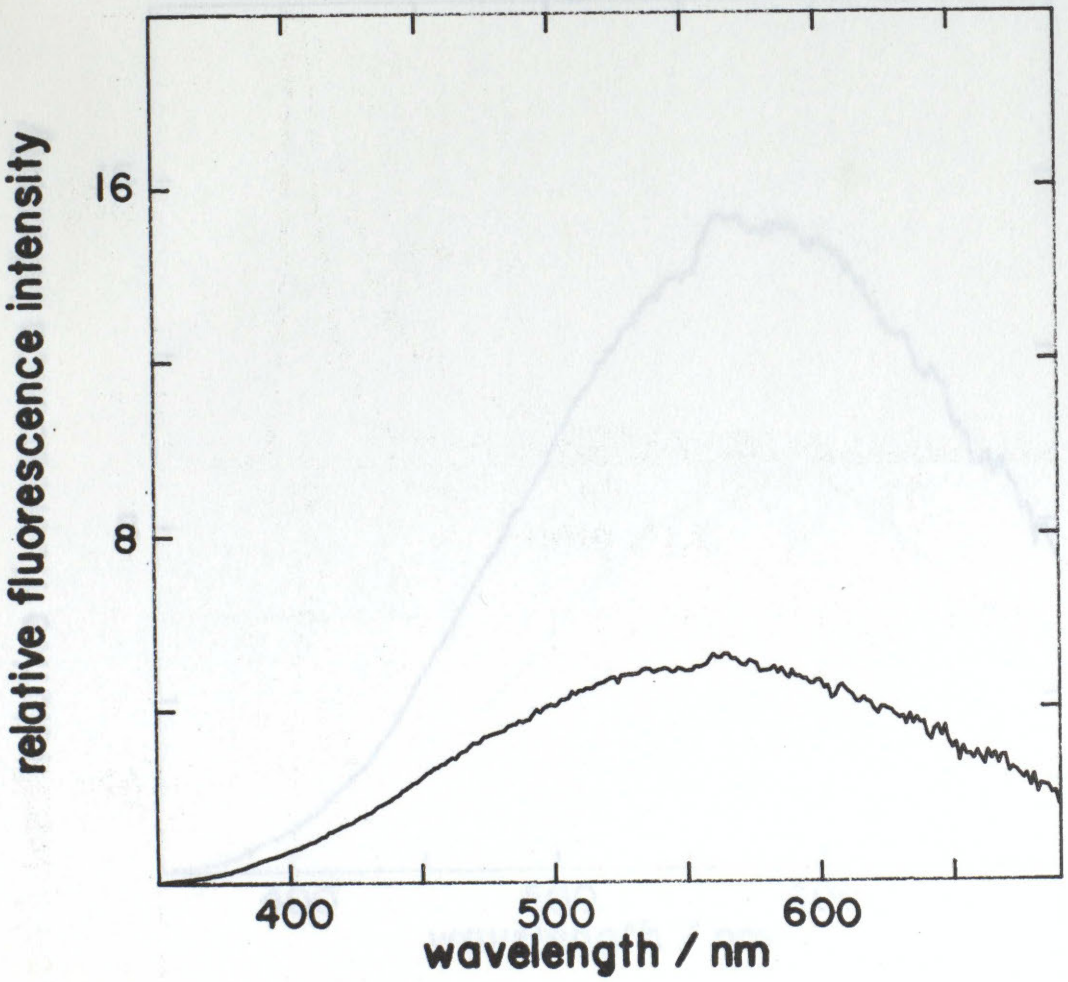

H07. ESSO FUEL INT. 20

400
200
counts
15
30
45
60
75
time / ns

16
8
relative fluorescence intensity
400
500
600
wavelength / nm

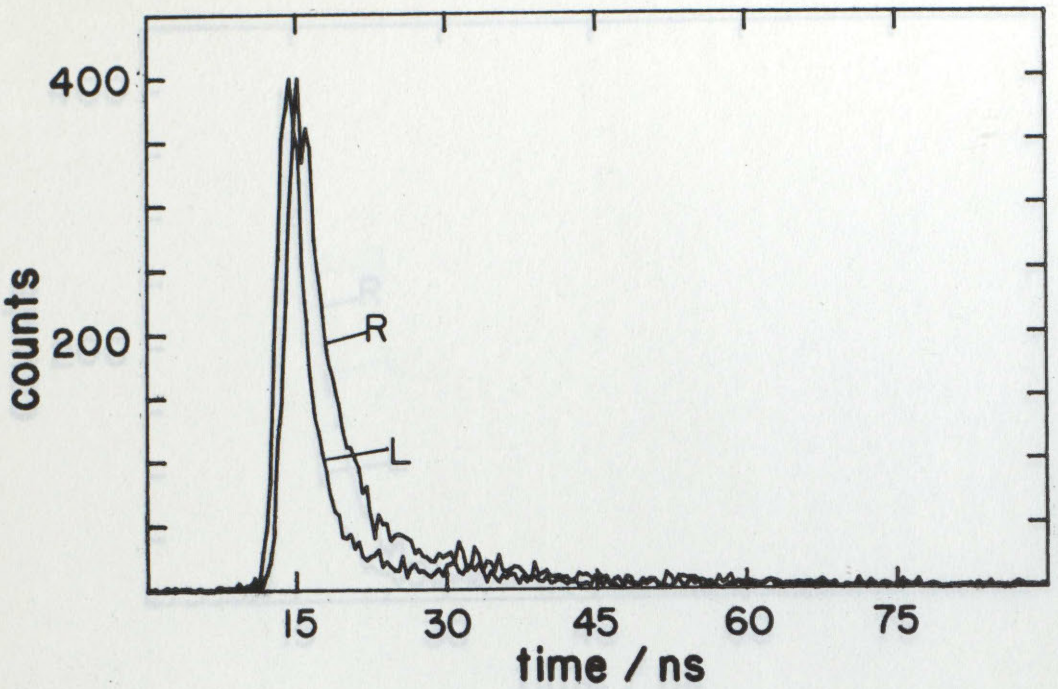

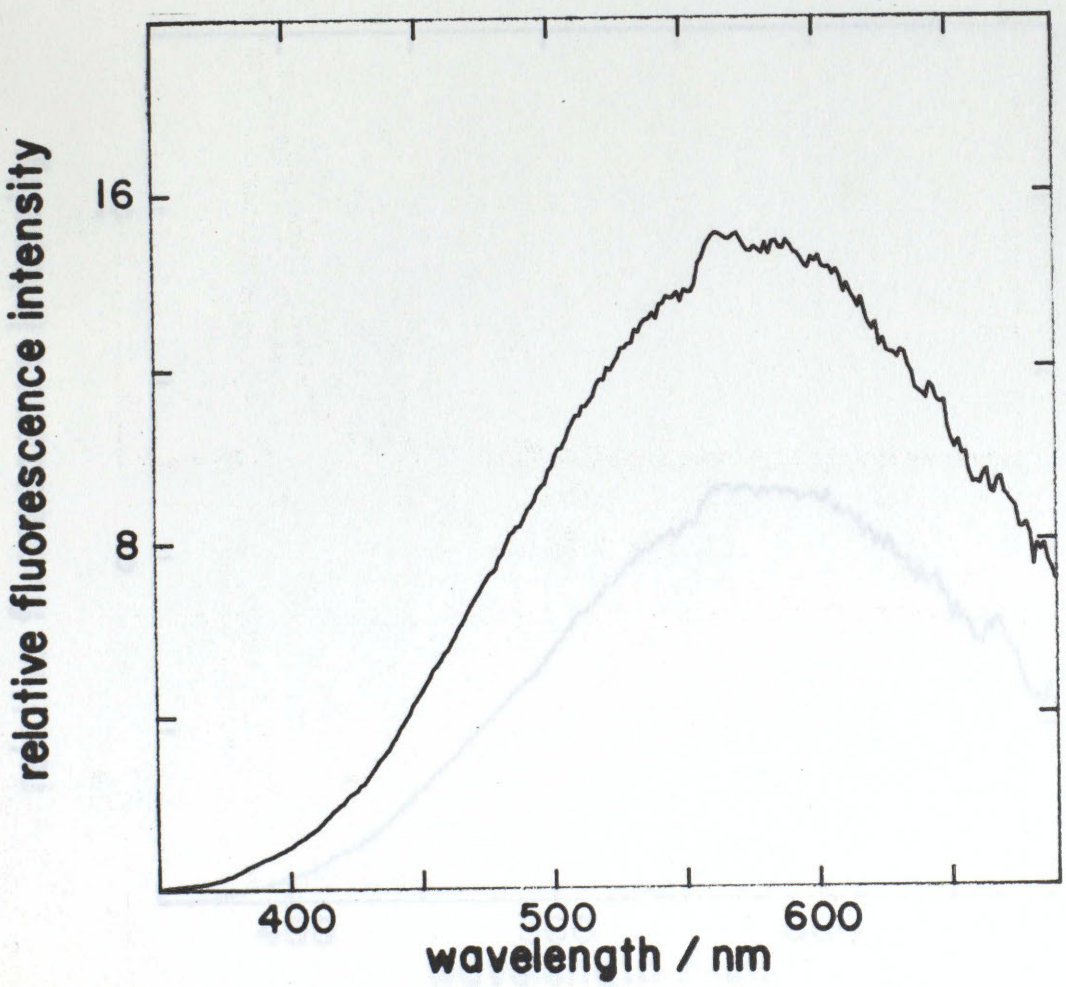

H08. GULF OIL #5B BUNKER FUEL (PP17)

400
200
counts
15
30
45
60
75
time / ns

16
8
relative fluorescence intensity
400
500
600
wavelength / nm

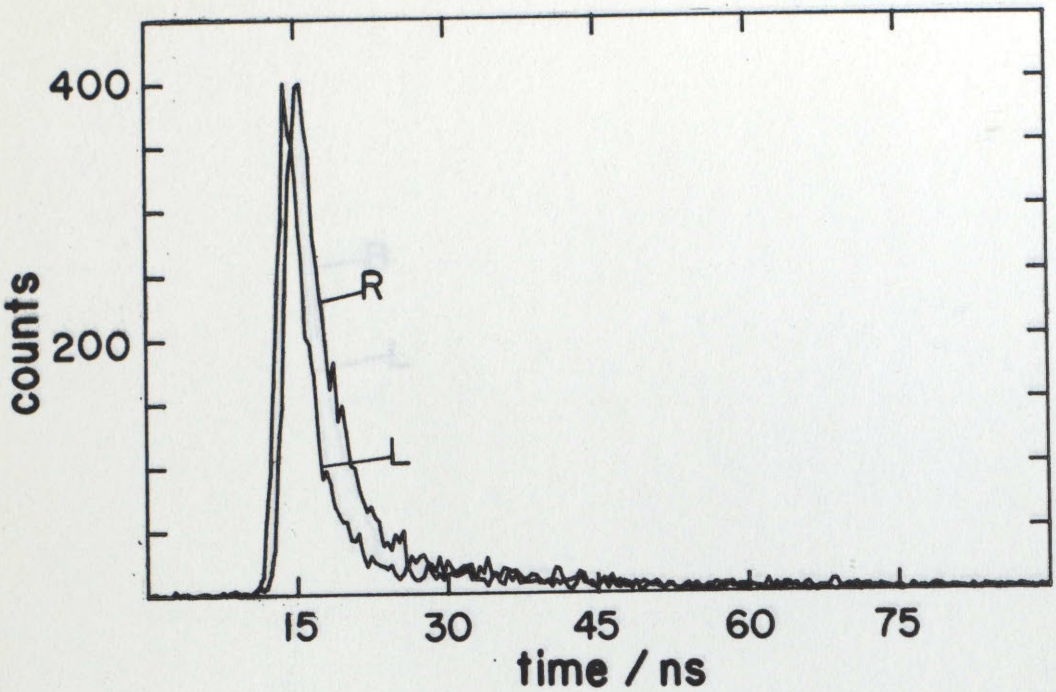

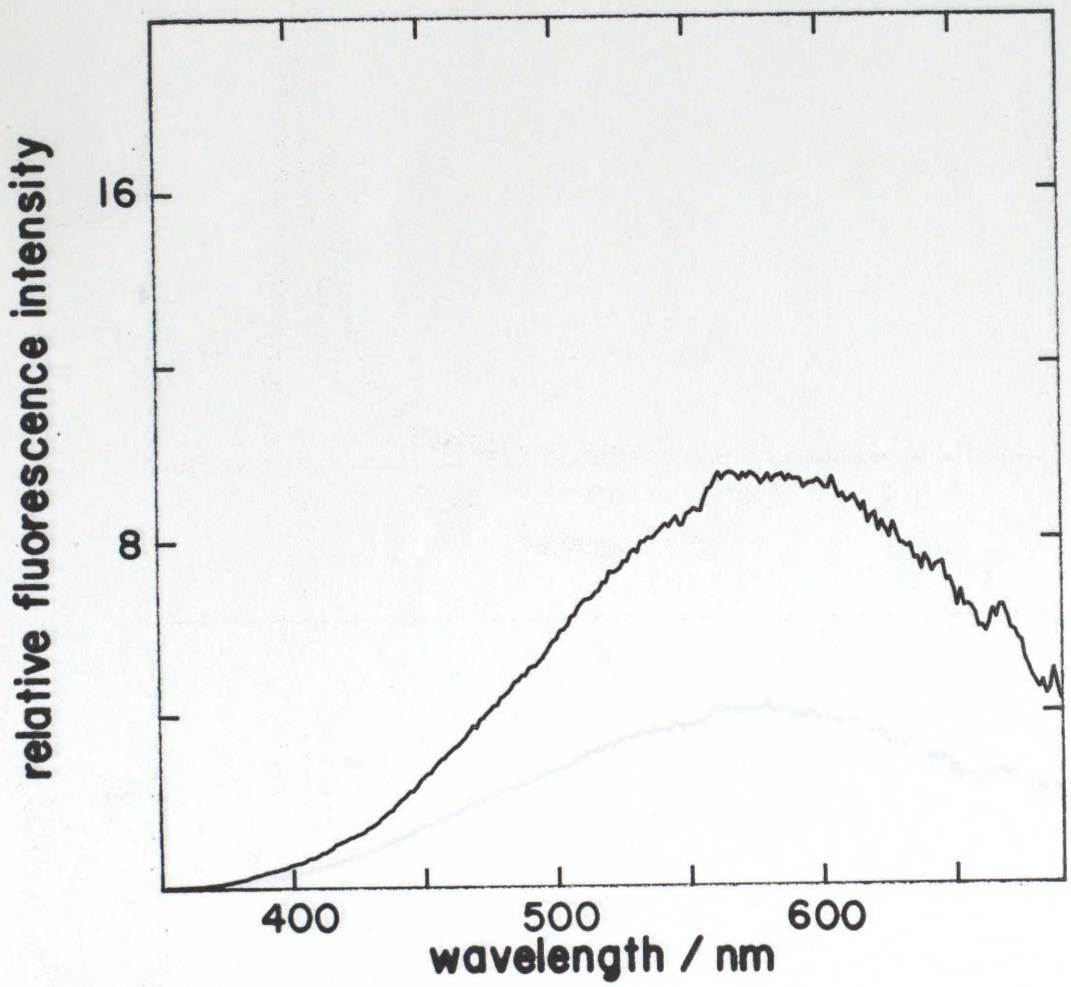

H09. GULF OIL #6C BUNKER FUEL (PP18)

counts
400
200
time / ns
15
30
45
60
75

relative fluorescence intensity
15
8
wavelength / nm
400
500
600

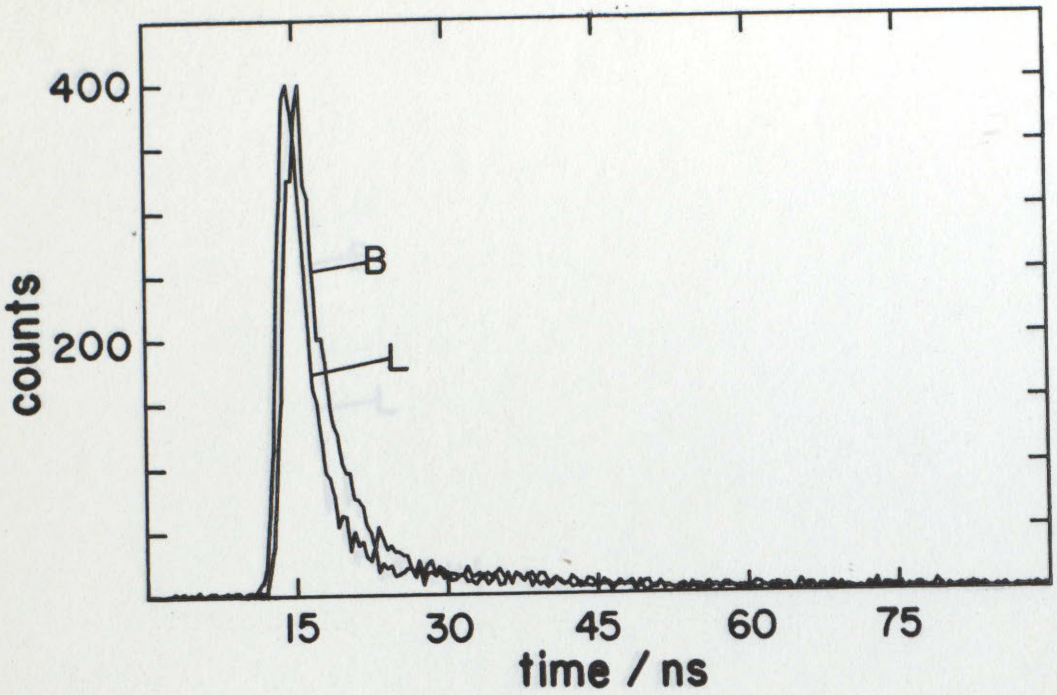

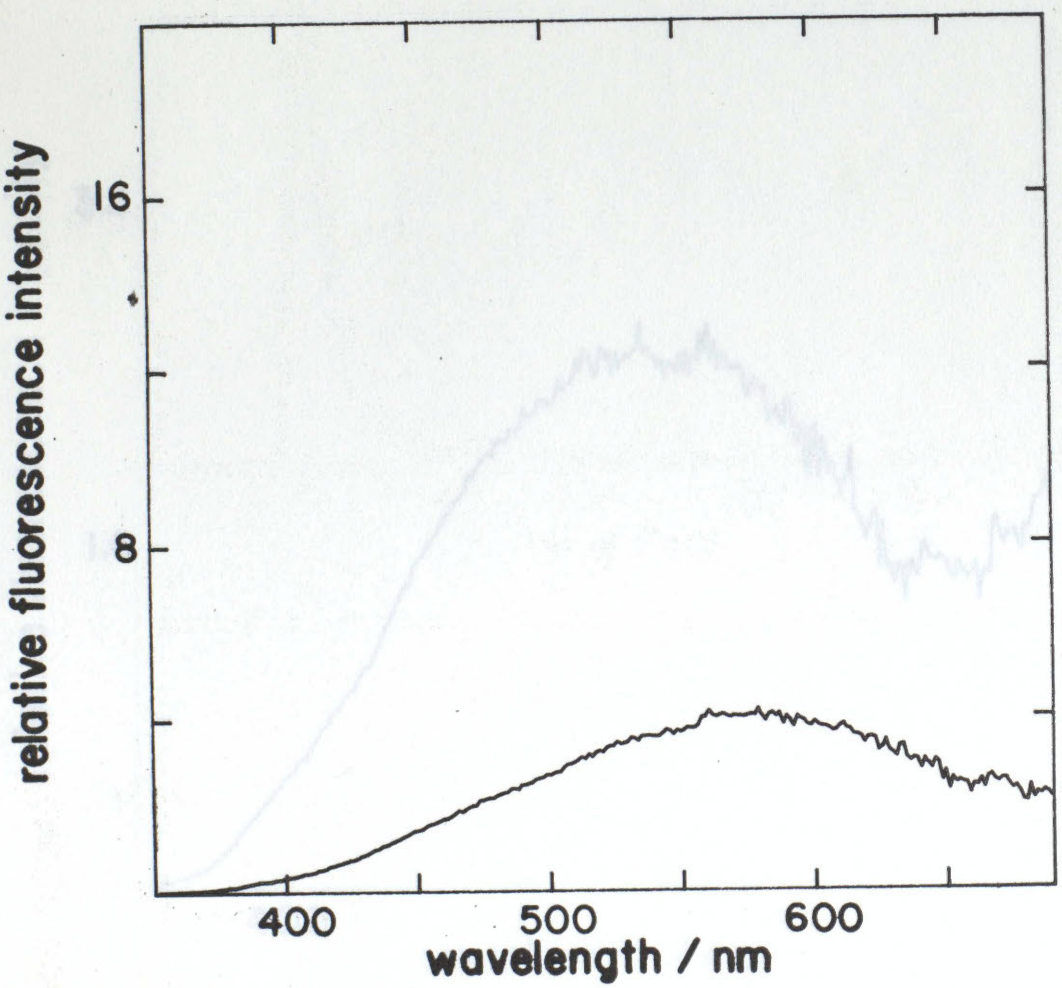

H010. B.P. BUNKER 6C (PP25)

400
200
counts
15
30
45
60
75
time / ns

16
8
relative fluorescence intensity
400
500
600
wavelength / nm

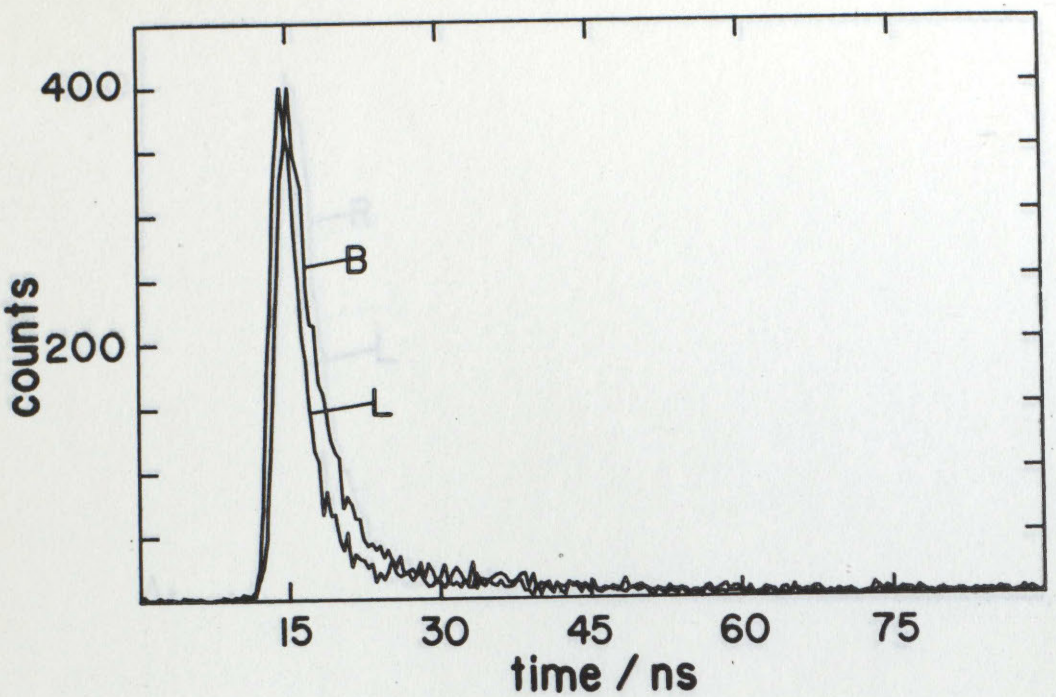

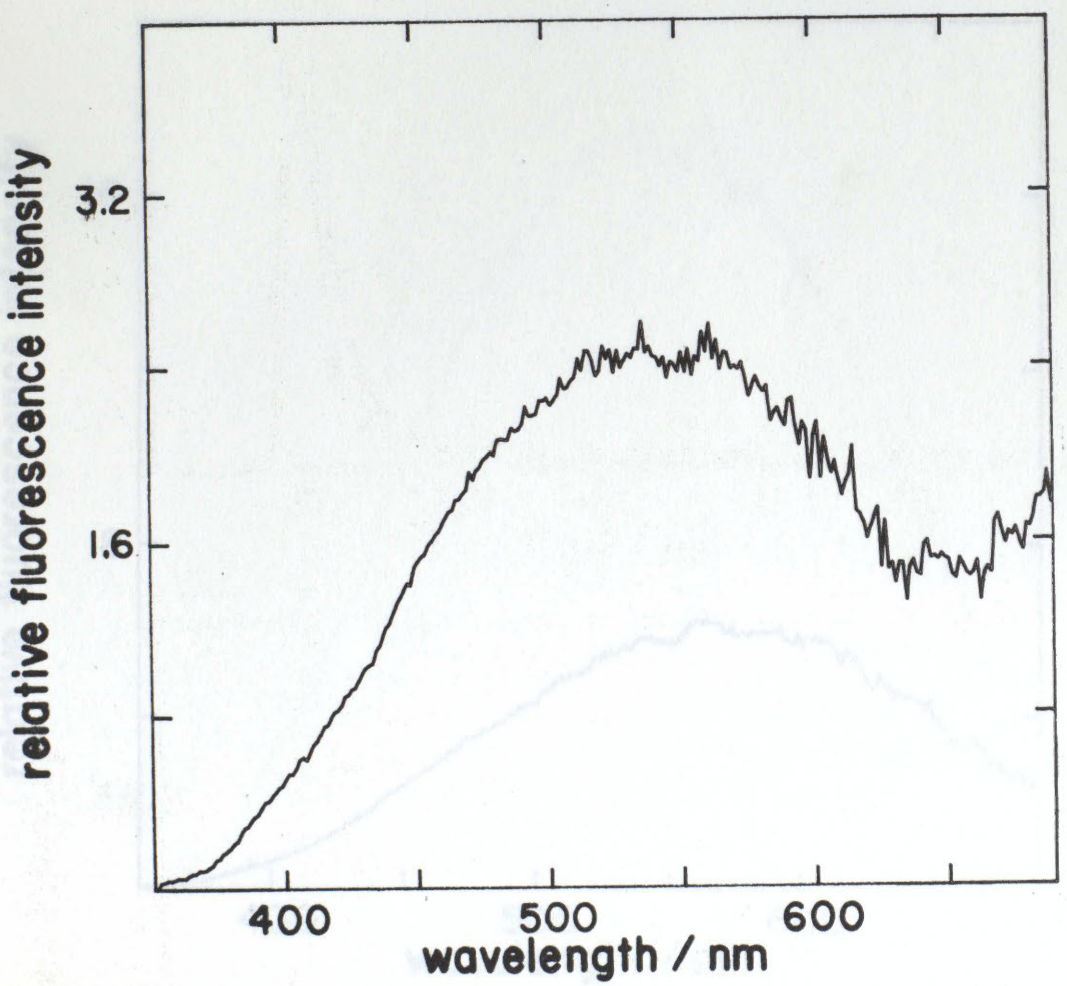

H011. GULF OIL COMPANY BUNKER 6C, K33, CKM481 (PP26)

400
200
counts
15
30
45
60
75
time / ns

3.2
1.6
relative fluorescence intensity
400
500
600
wavelength / nm

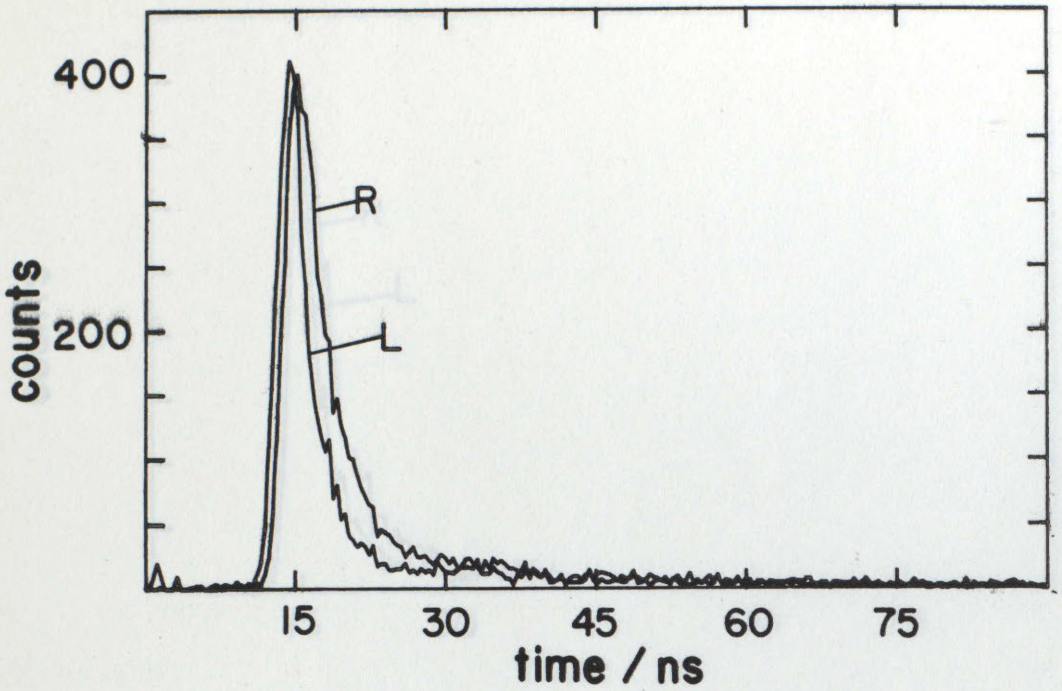

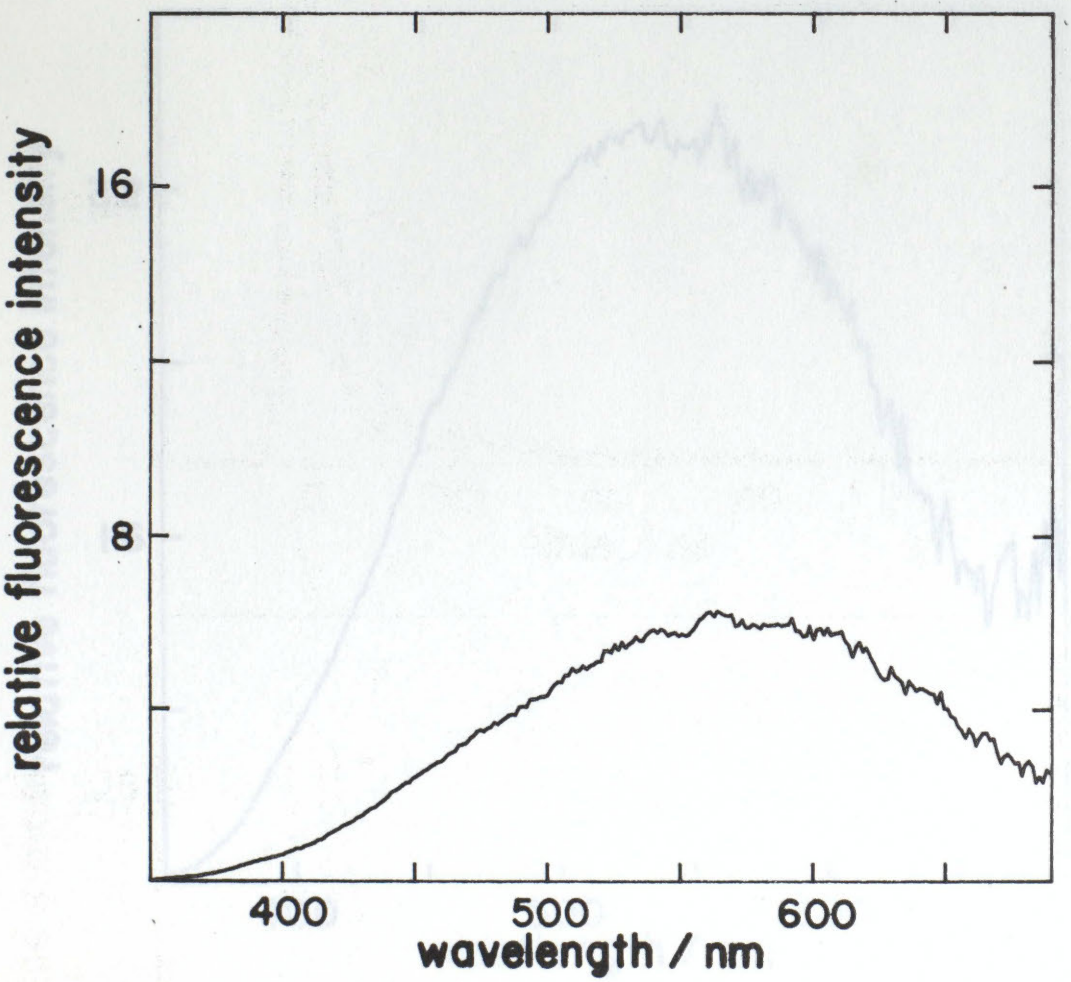

H012. GULF OIL COMPANY BUNKER 6C -1.5, K23, CKM482 (PP30)

400
200
counts
15
30
45
60
75
time / ns

16
8
relative fluorescence intensity
400
500
600
wavelength / nm

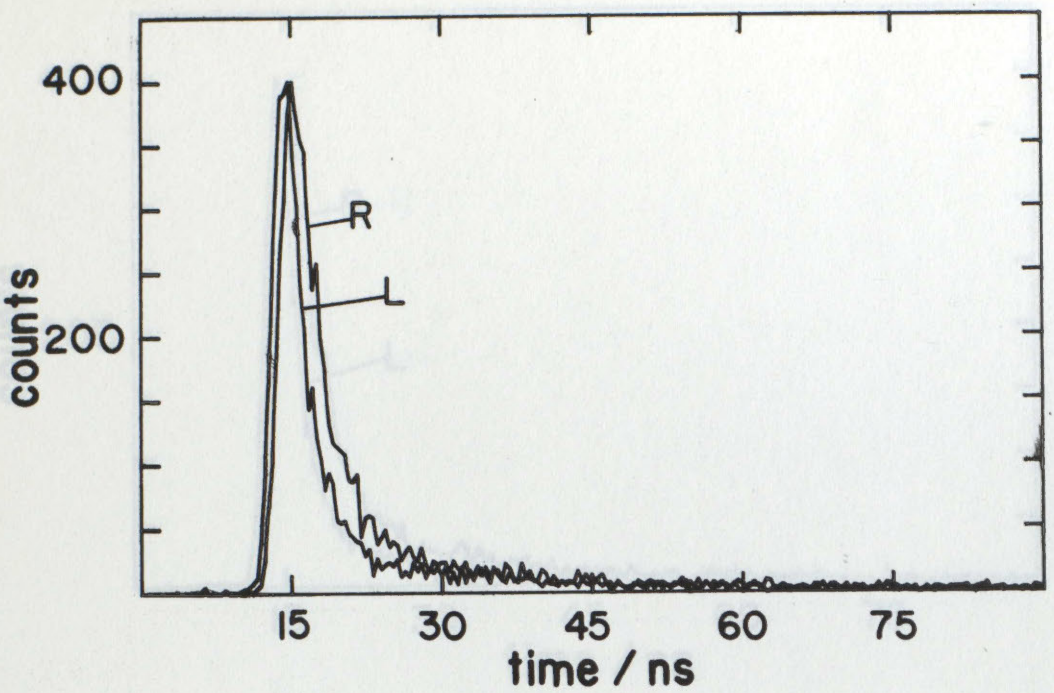

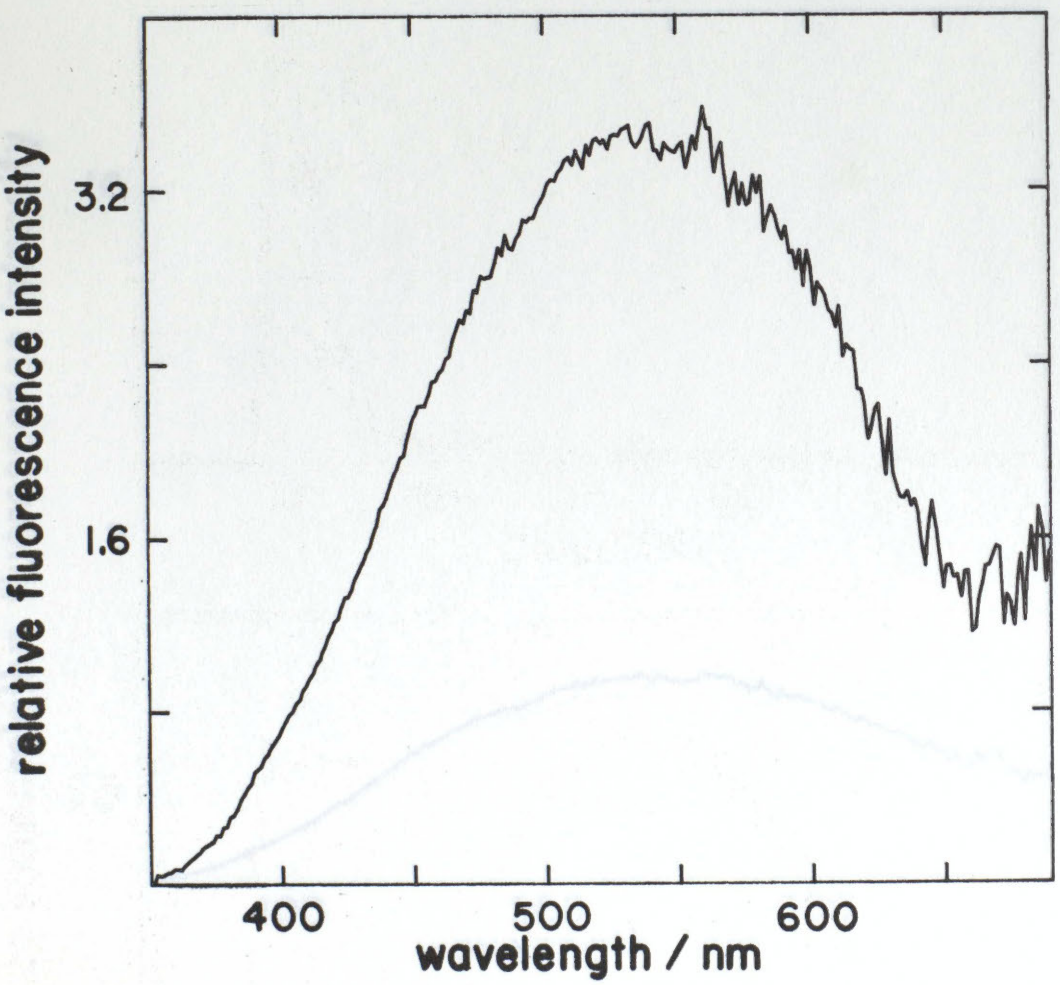

H013. IMPERIAL OIL VENEZUELAN BUNKER #6 (PP31)

400
200
counts
15
30
45
60
75
time / ns

3.2
1.6
(arbitrary) fluorescence intensity
400
500
600
wavelength / nm

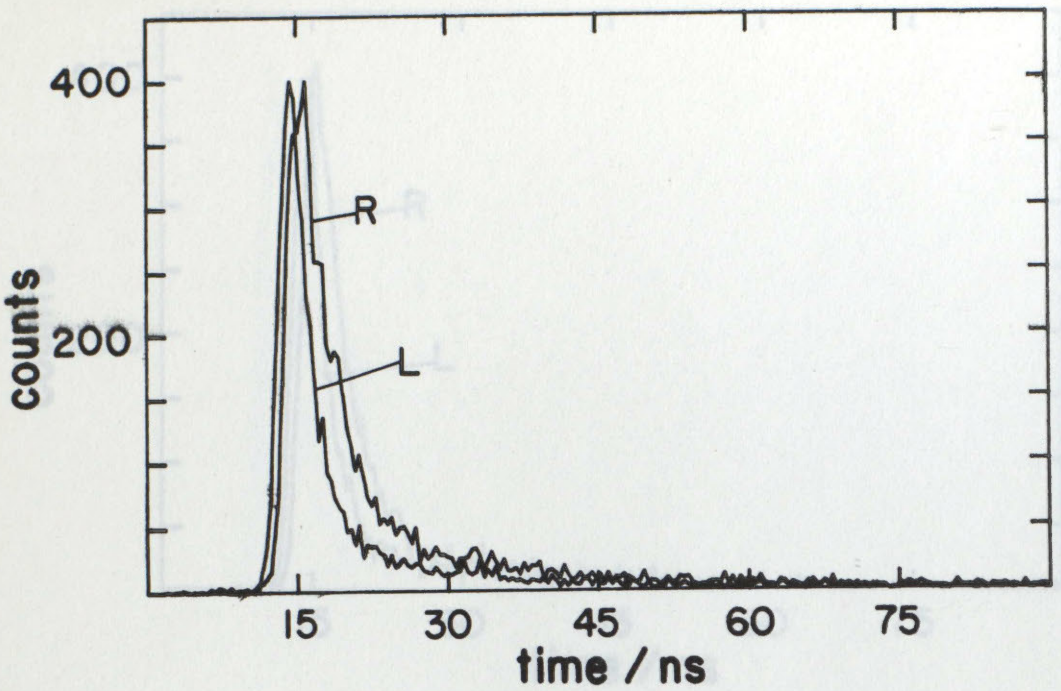

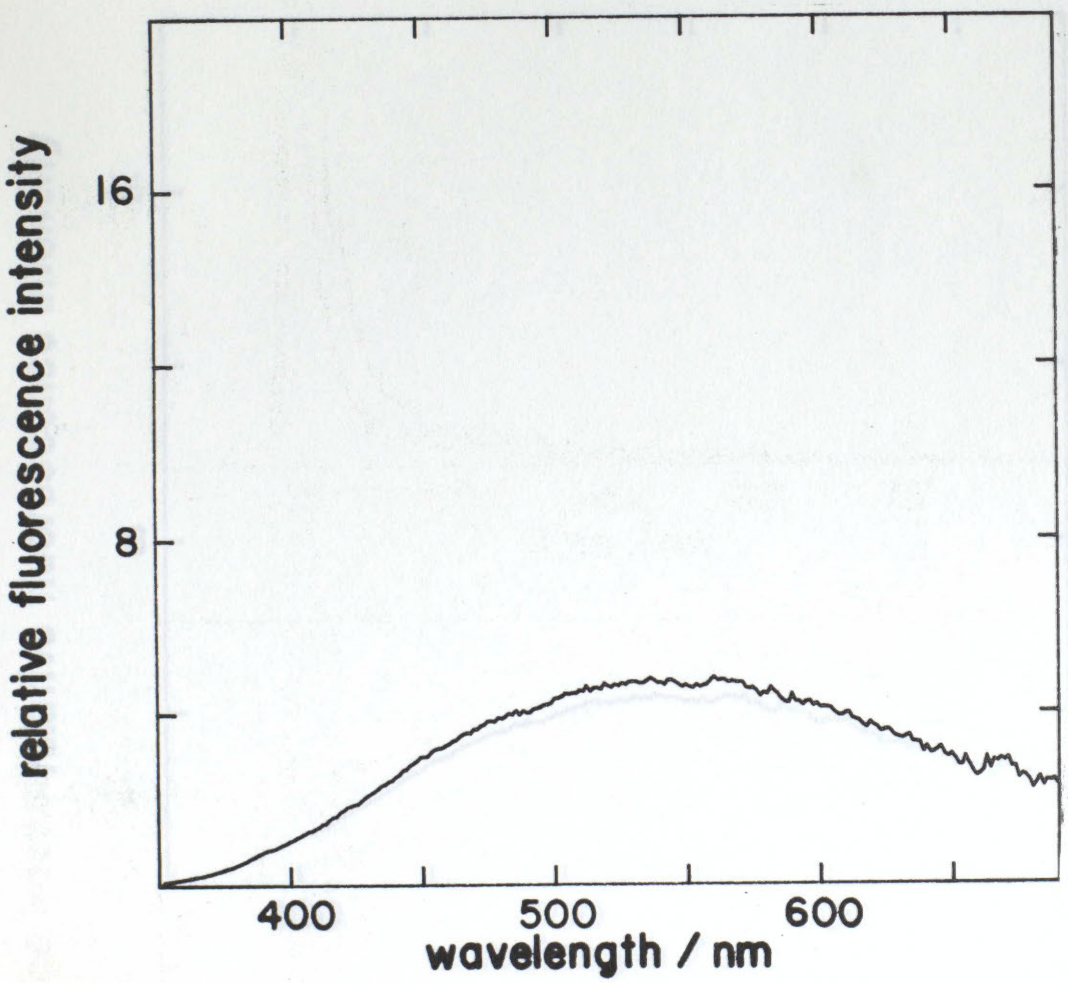

H014. IMPERIAL OIL VENEZUELAN BUNKER #5 (PP33)

400
200
counts
R
L
15
30
45
60
75
time / ns

16
8
relative fluorescence intensity
400
500
600
wavelength / nm

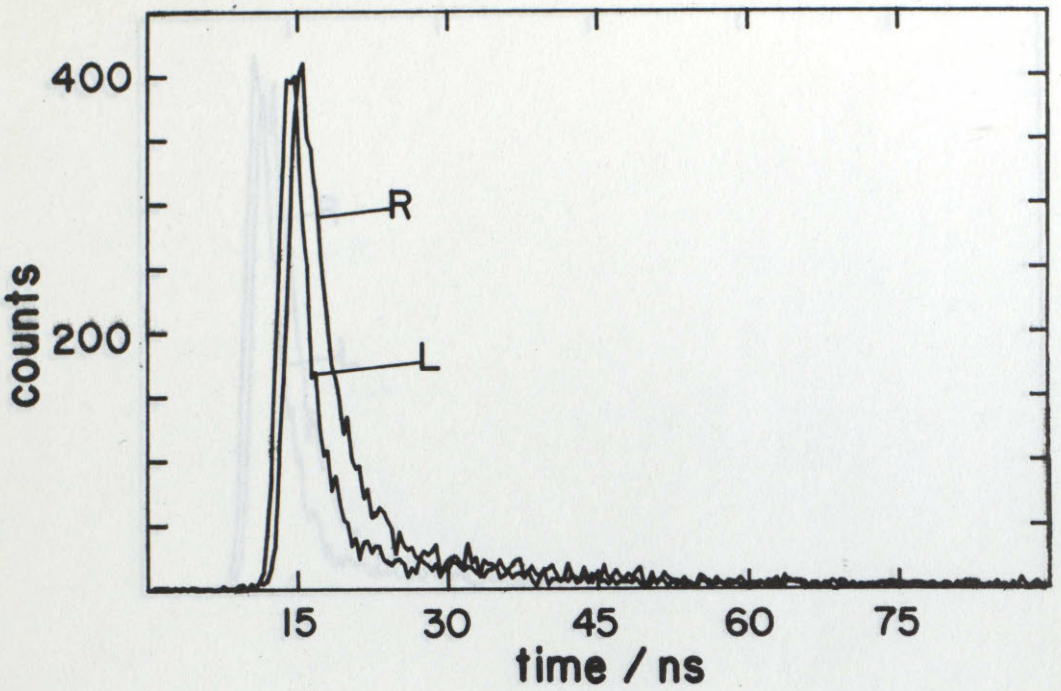

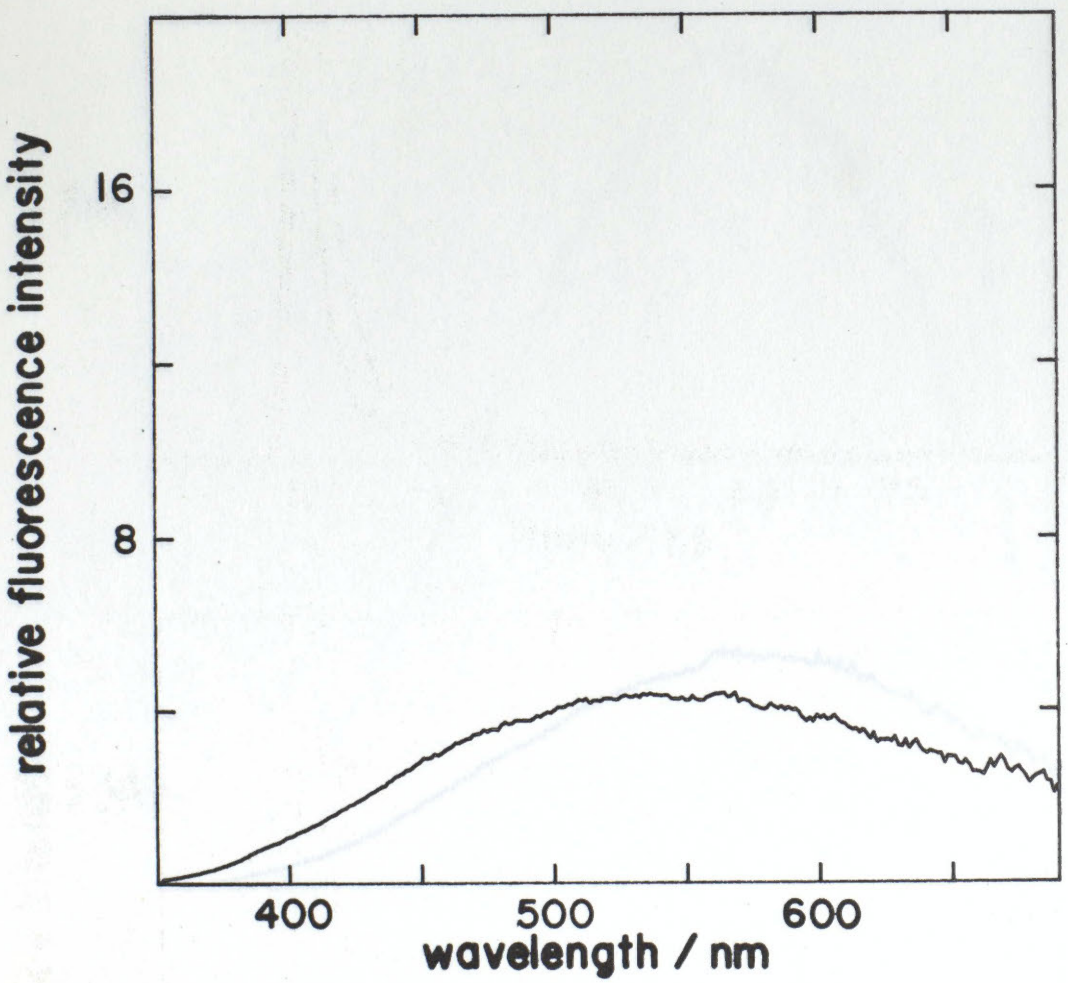

H015. GOLDEN EAGLE REFINERY VENEZUELAN HIGH S CONTENT BUNKER C (6C)

counts
400
200
R
L
15
30
45
60
75
time / ns

relative fluorescence intensity
15
8
400
500
600
wavelength / nm

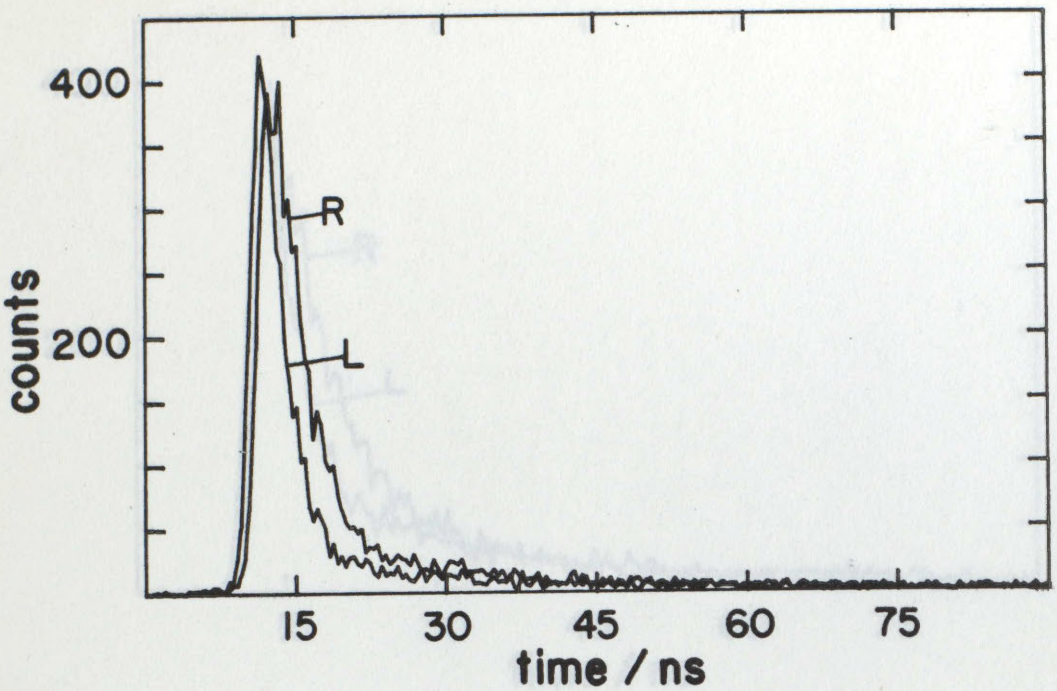

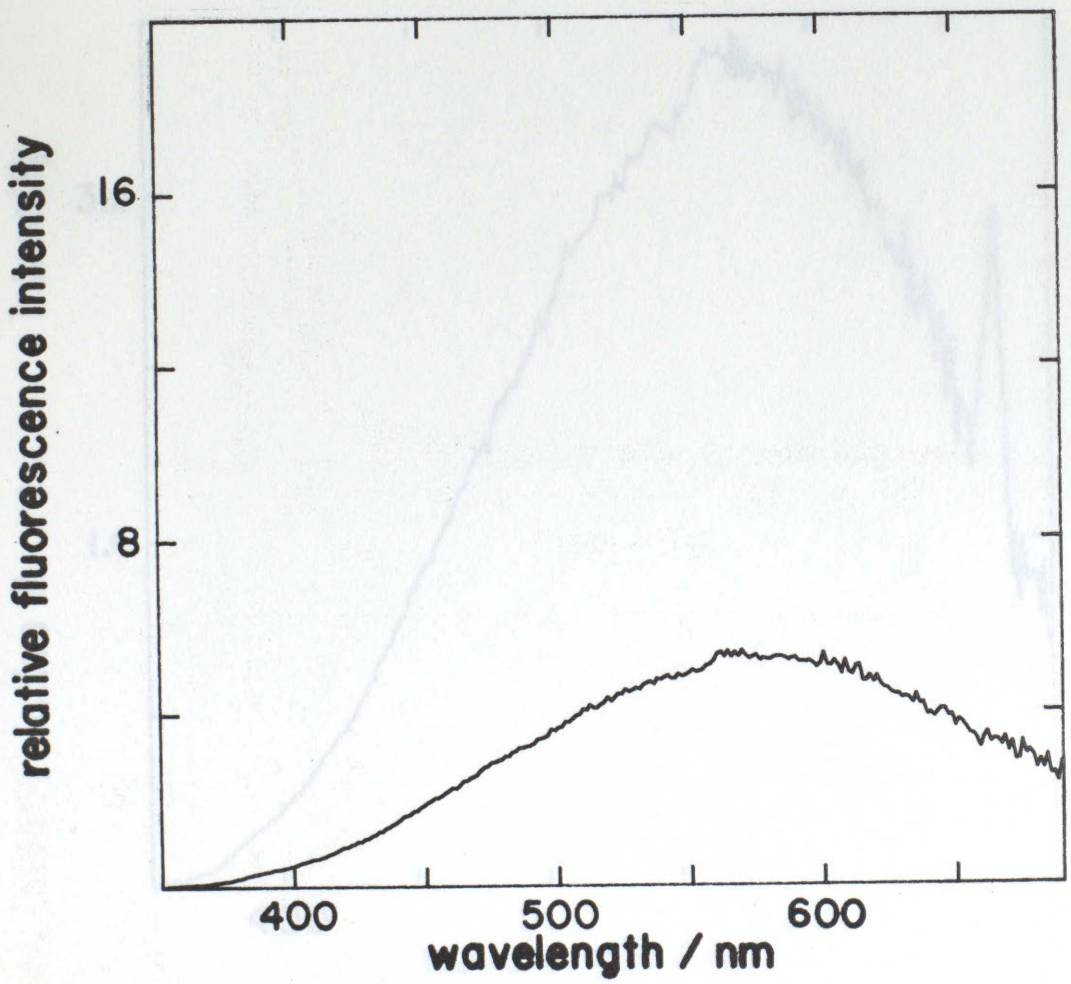

H016. SHELL 1.5% BUNKER K8016 (PP42)

400
200
counts
15
30
45
60
75
time / ns
16
0
relative fluorescence intensity
400
500
600
wavelength / nm

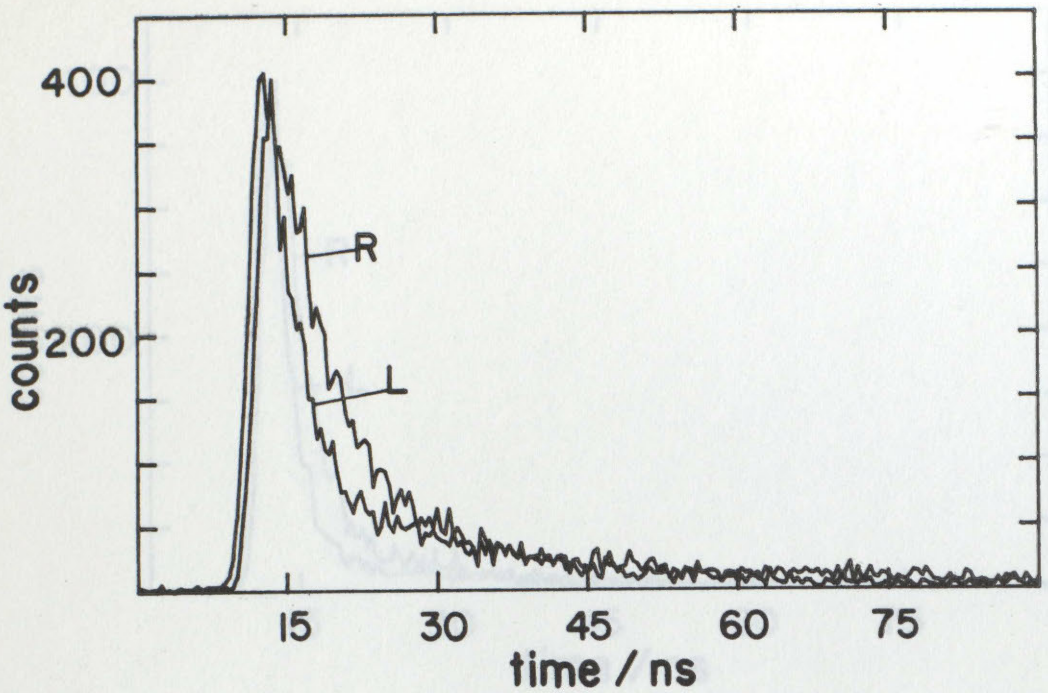

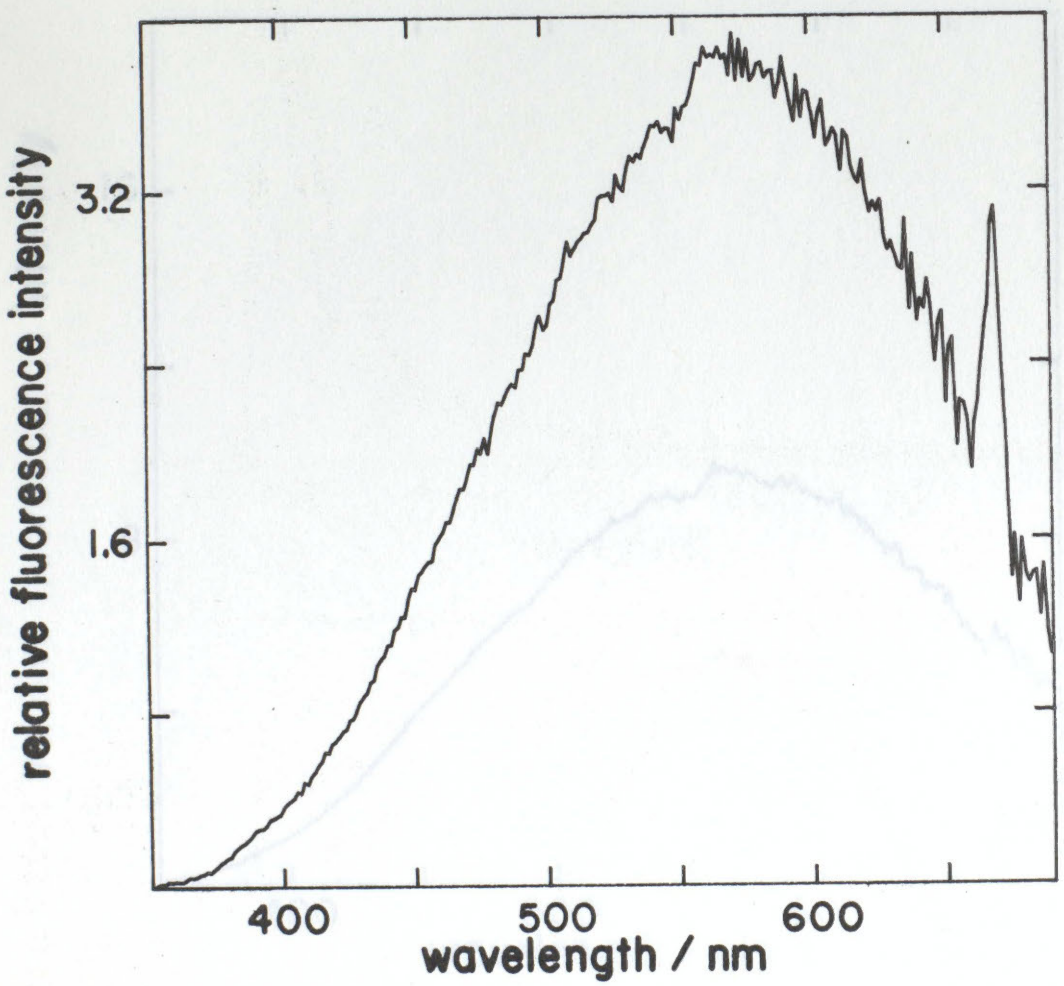

H017. TEXACO HEAVY BUNKER 6C (PP52)

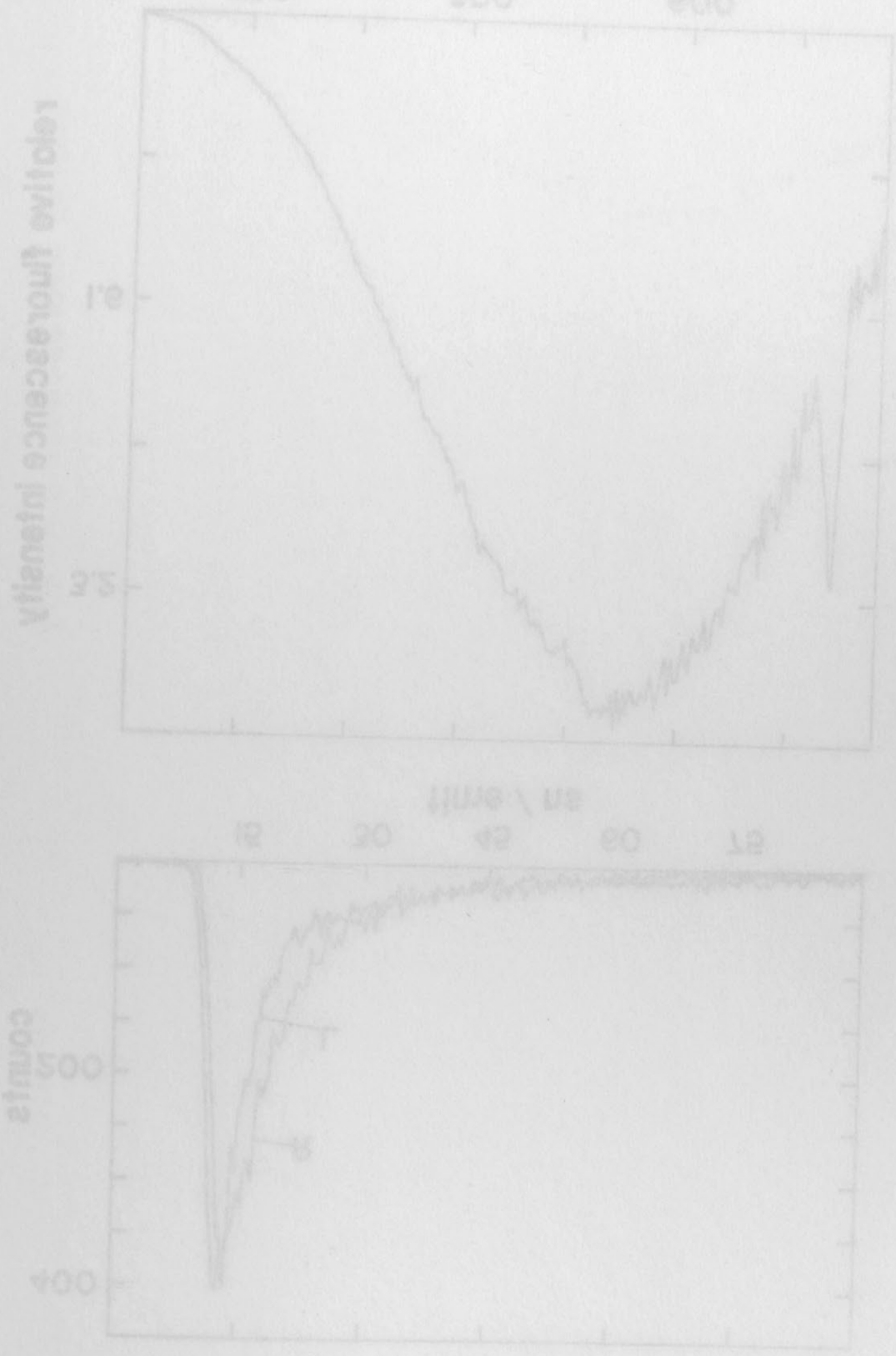

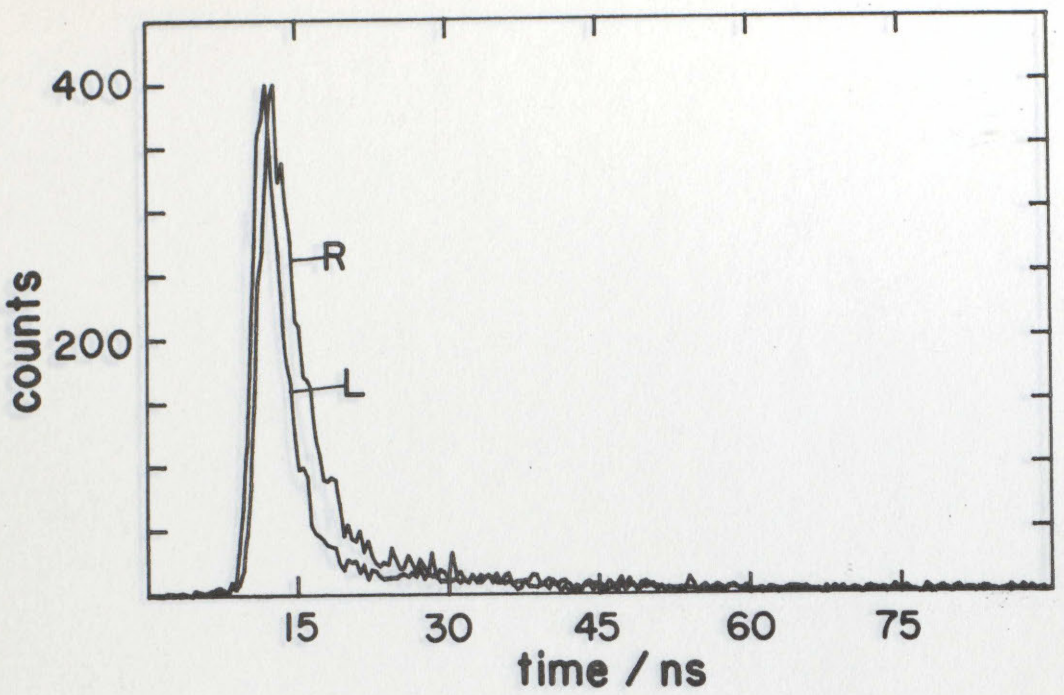

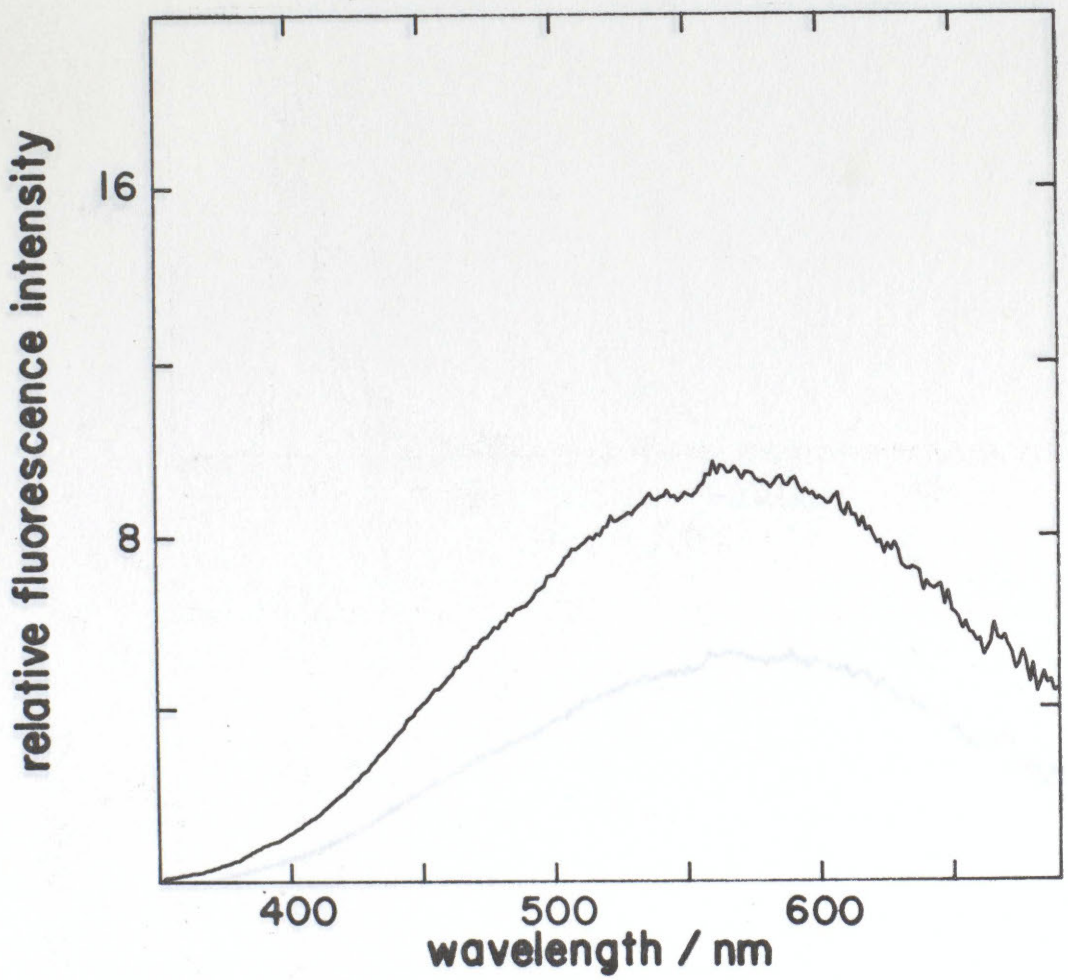

H018. GULF BUNKER #5 (PP54)

400
200
counts
15
30
45
60
75
time / ns

16
8
relative fluorescence intensity
400
500
600
wavelength / nm

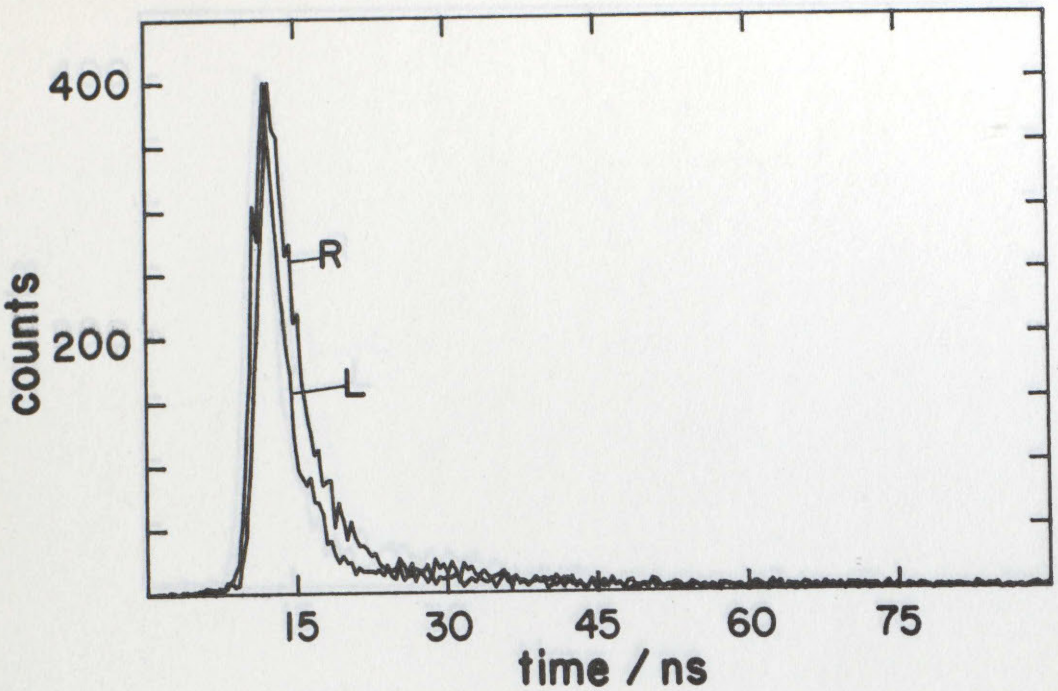

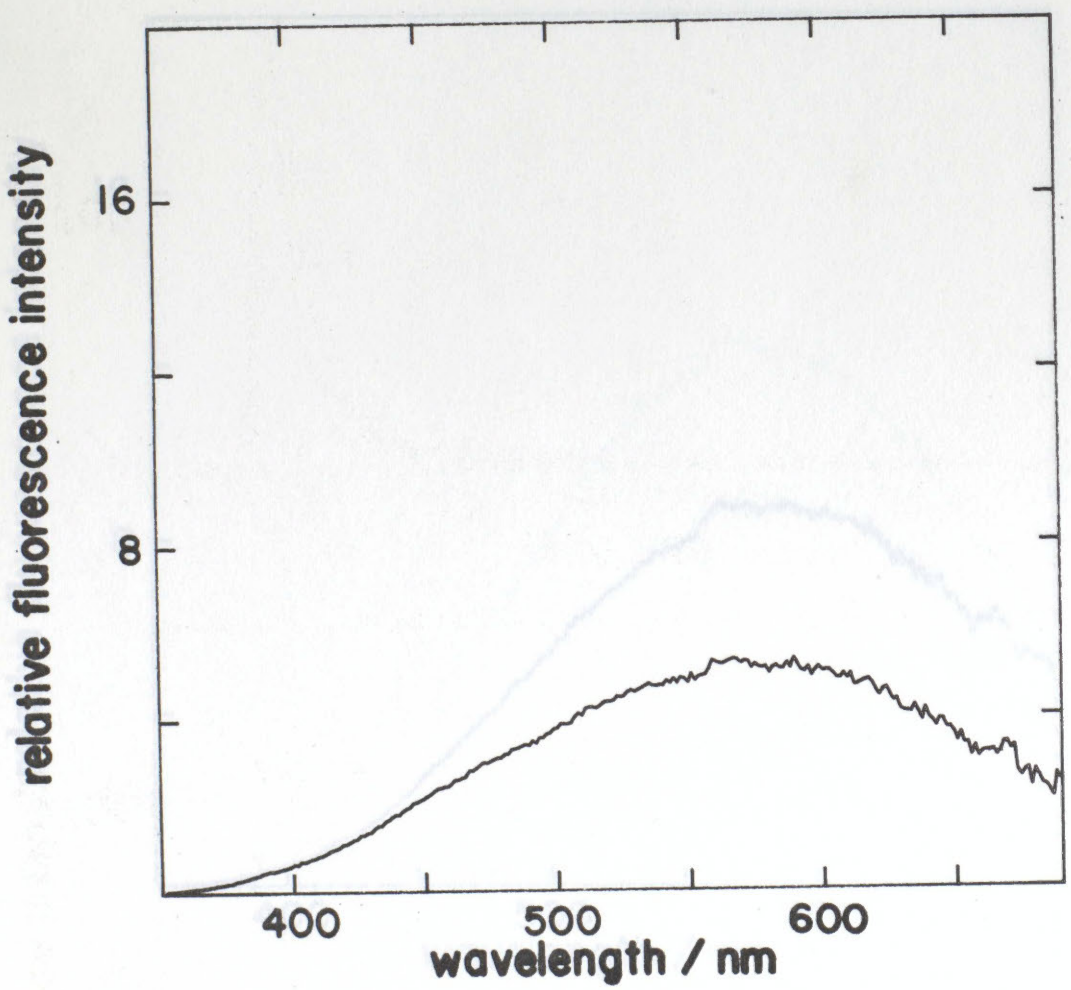

H019. GULF BUNKER 6C (PP57)

400
200
counts
15
30
45
60
75
time / ns

15
5
relative fluorescence intensity
400
500
600
wavelength / nm

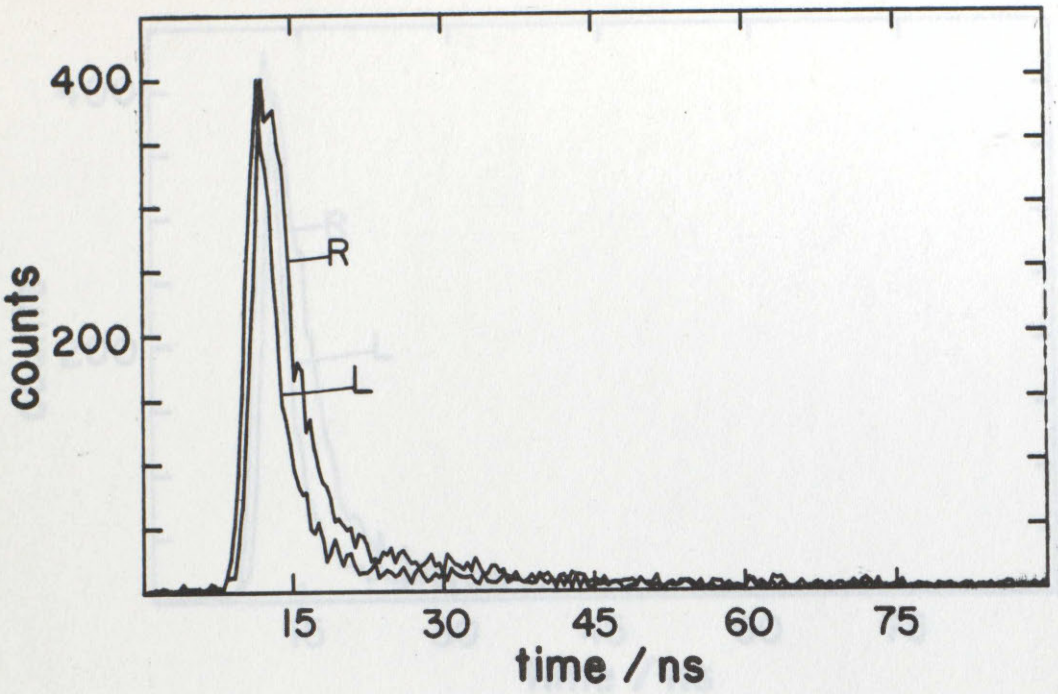

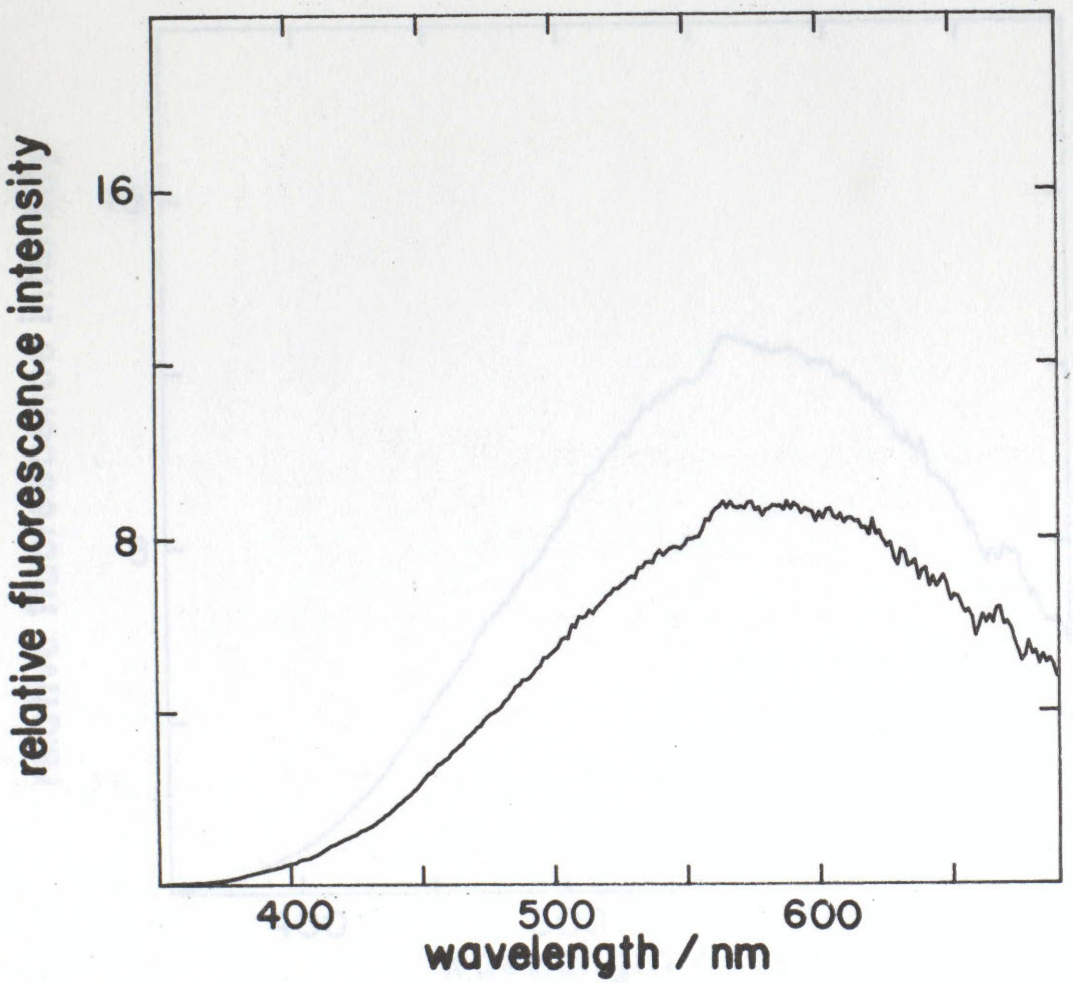

H020. SHELL OIL BUNKER C (#6) (PP69)

400
200
counts
R
L
15
30
45
60
75
time / ns

16
8
relative fluorescence intensity
400
500
600
wavelength / nm

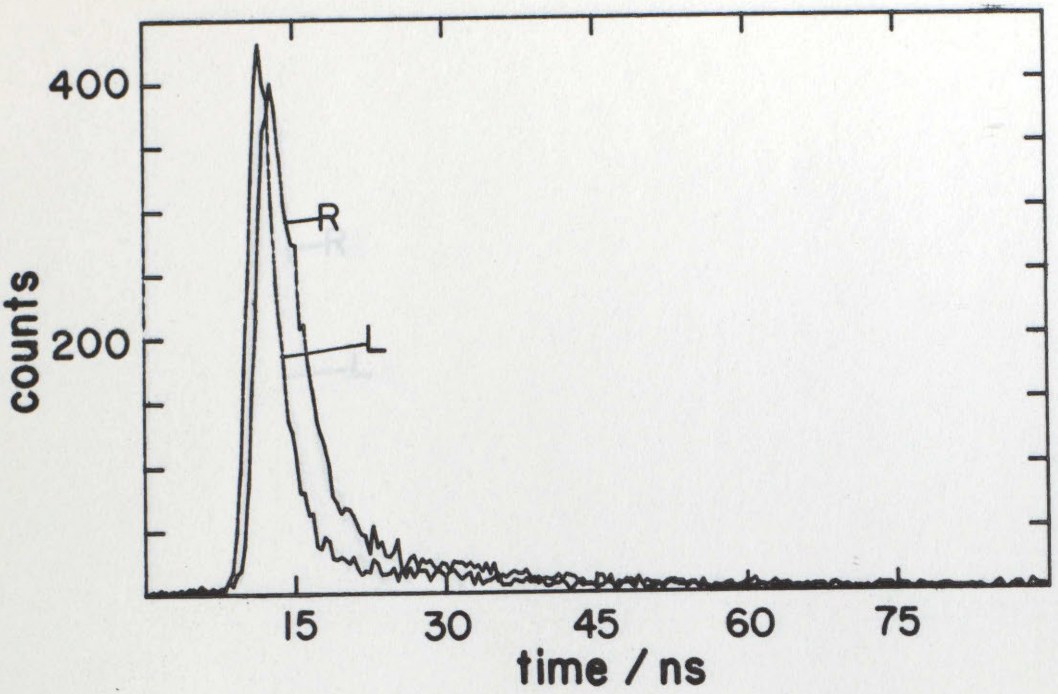

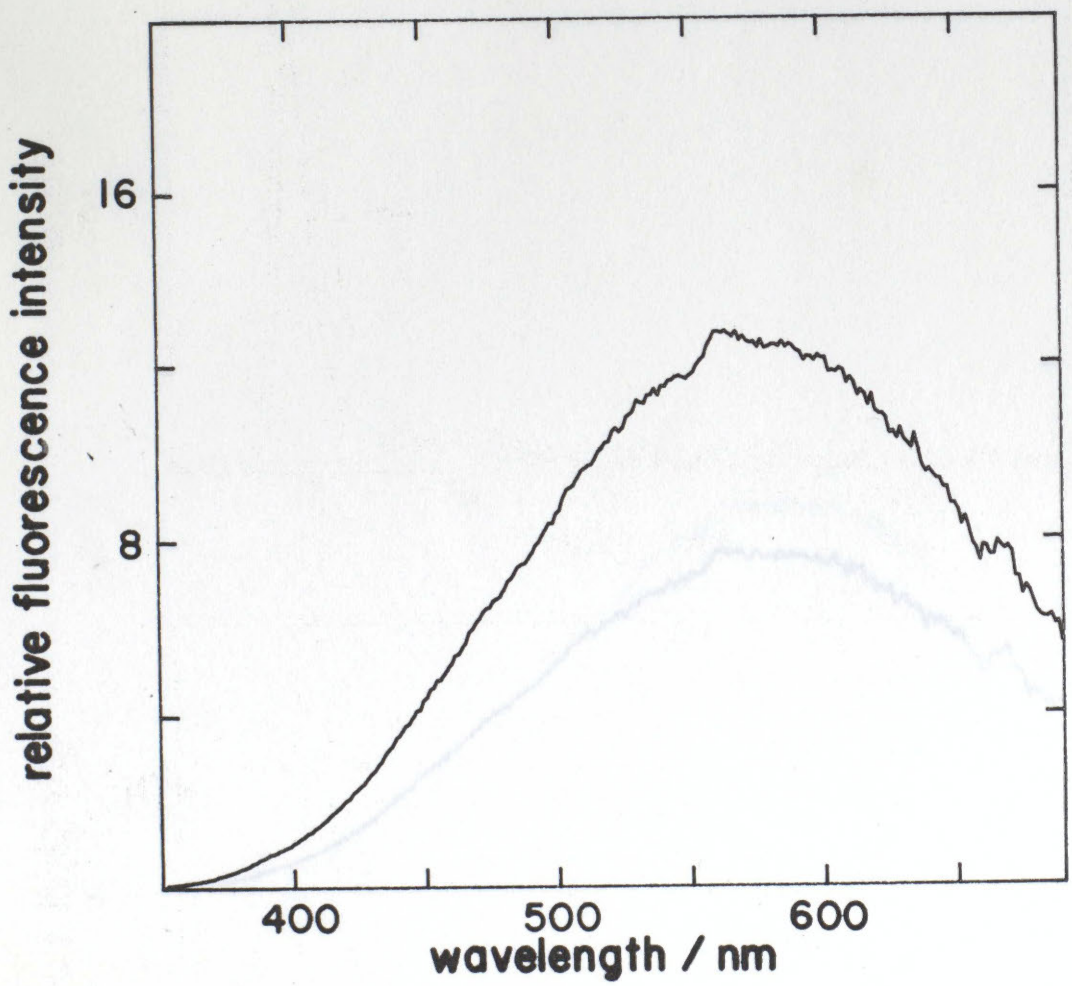

H021. SHELL OIL #5 FUEL (PP70)

400
200
counts
15
30
45
60
75
time / ns

15
0
relative fluorescence intensity
400
500
600
wavelength / nm

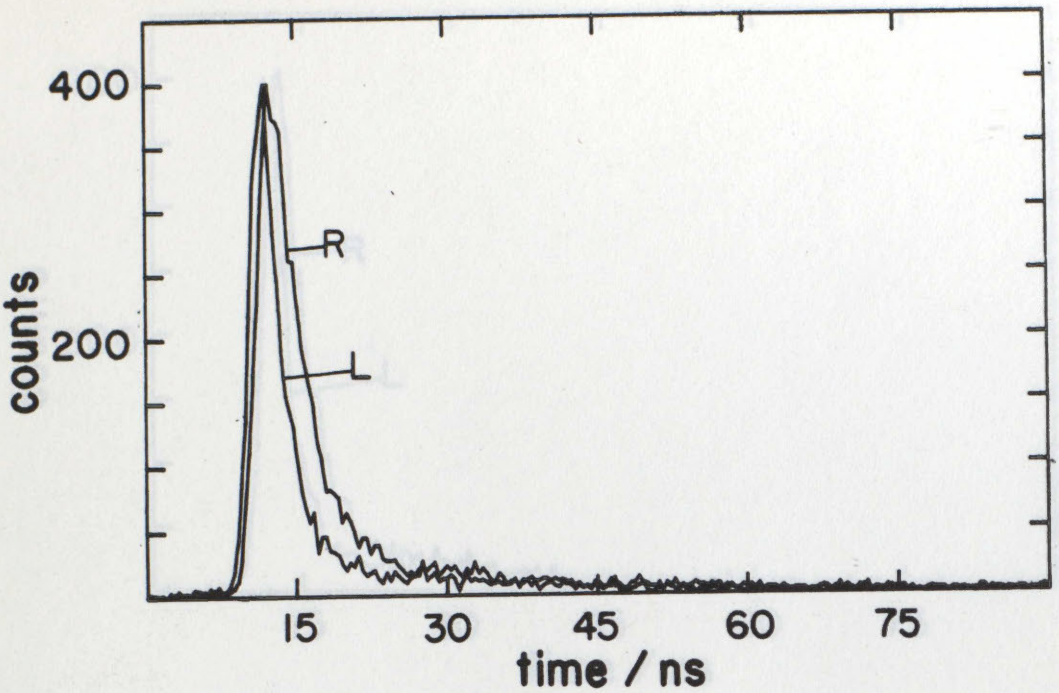

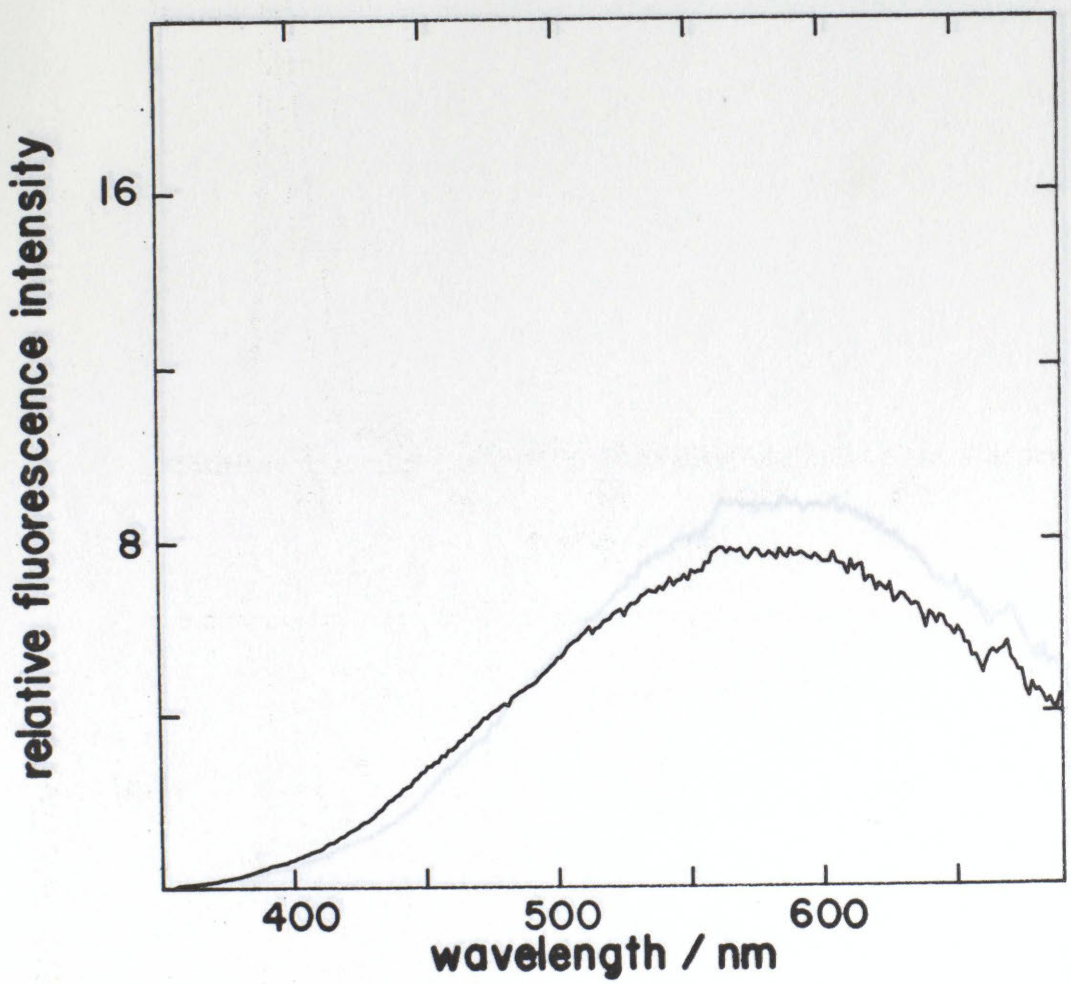

H022. SHELLOIL 1500 SEC. FUEL (PP71)

400
200
counts
15
30
45
60
75
time / ns

16
8
relative fluorescence intensity
400
500
600
wavelength / nm

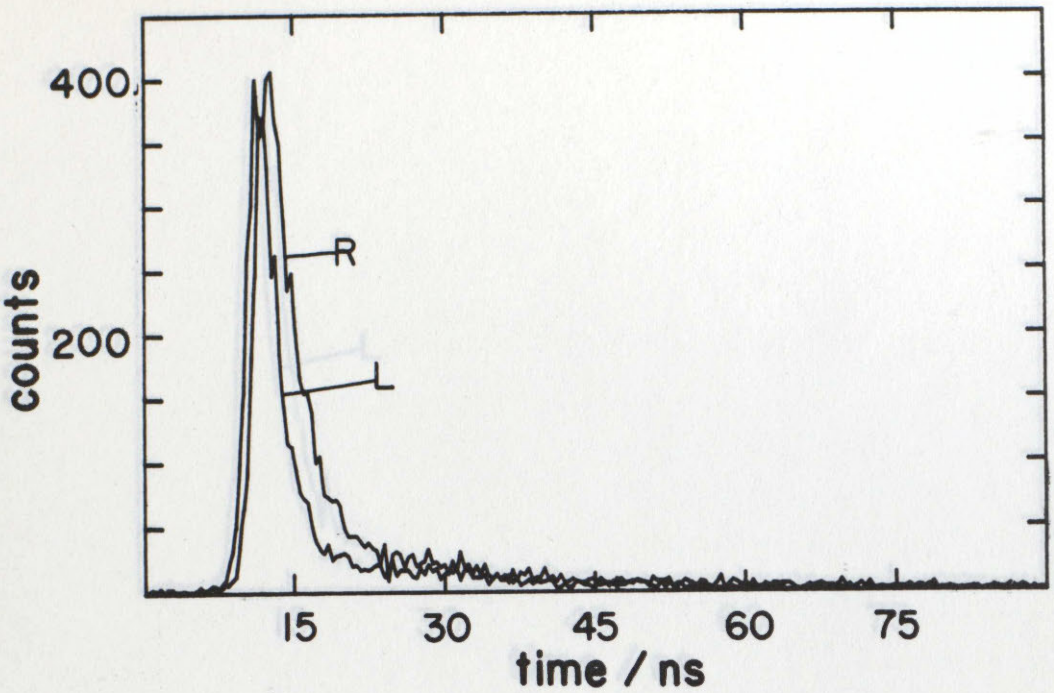

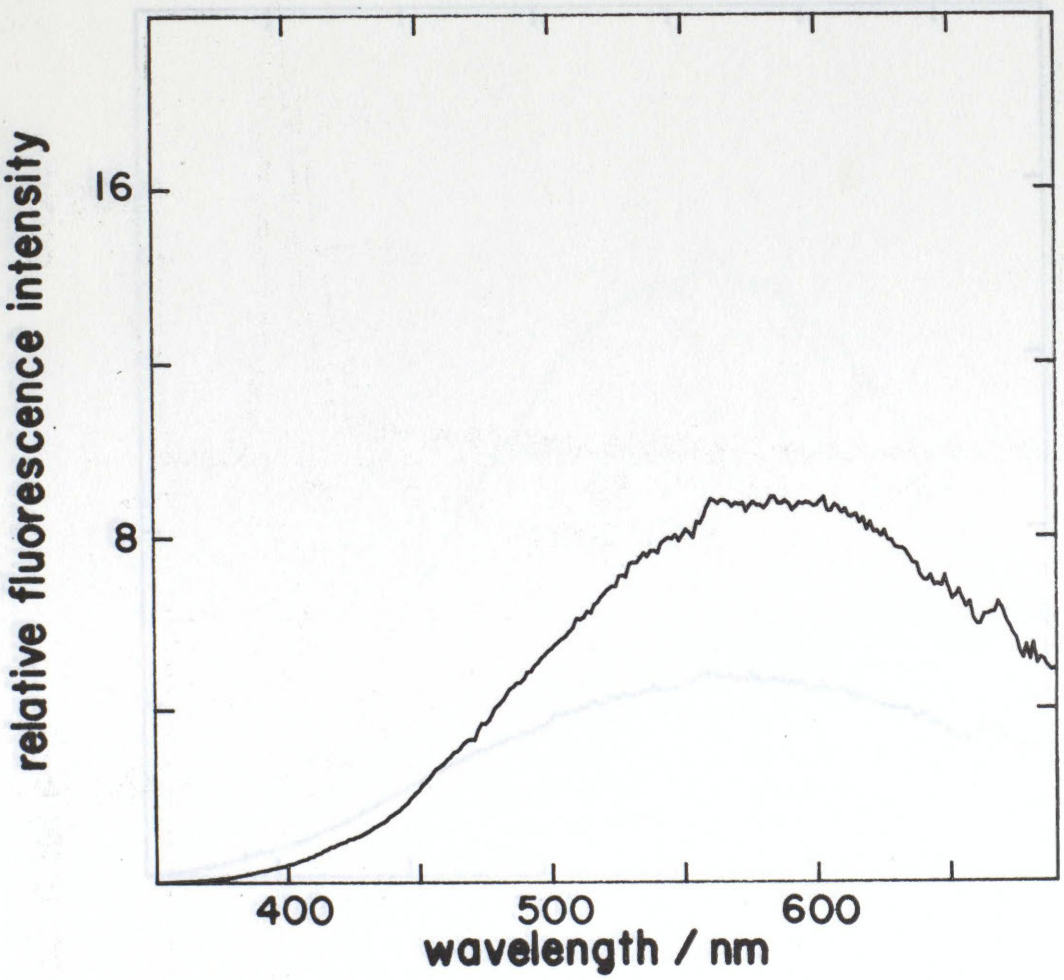

H023. IMPERIAL OIL BUNKER C (#6) (PP75)

400
200
counts
15
30
45
60
75
time / ns

16
8
relative fluorescence intensity
400
500
600
wavelength / nm

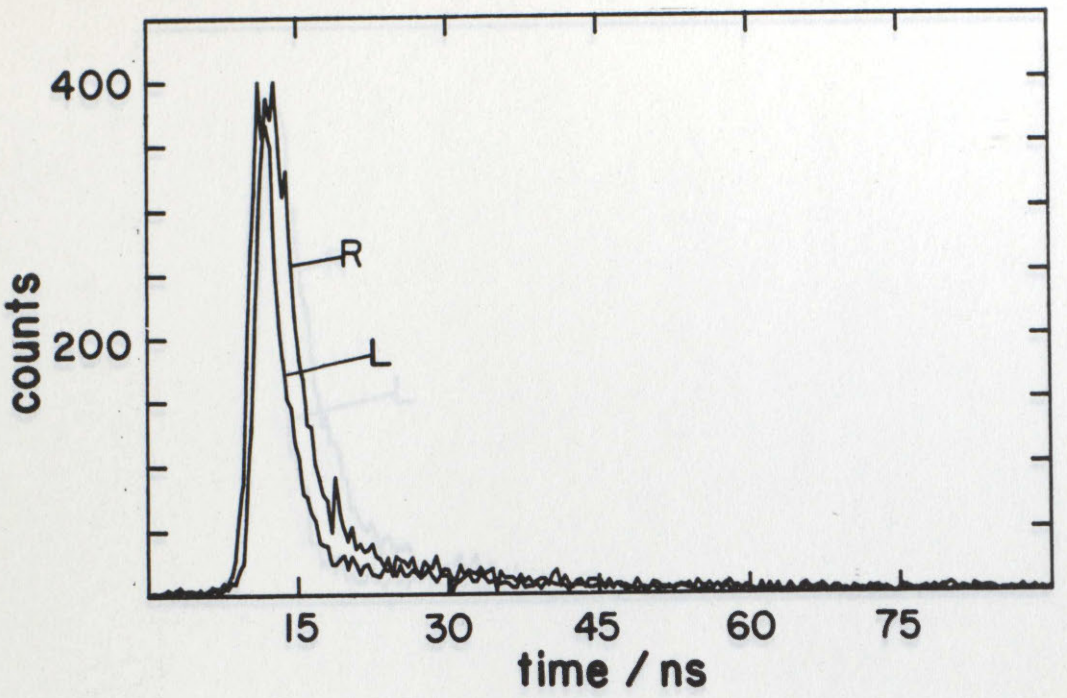

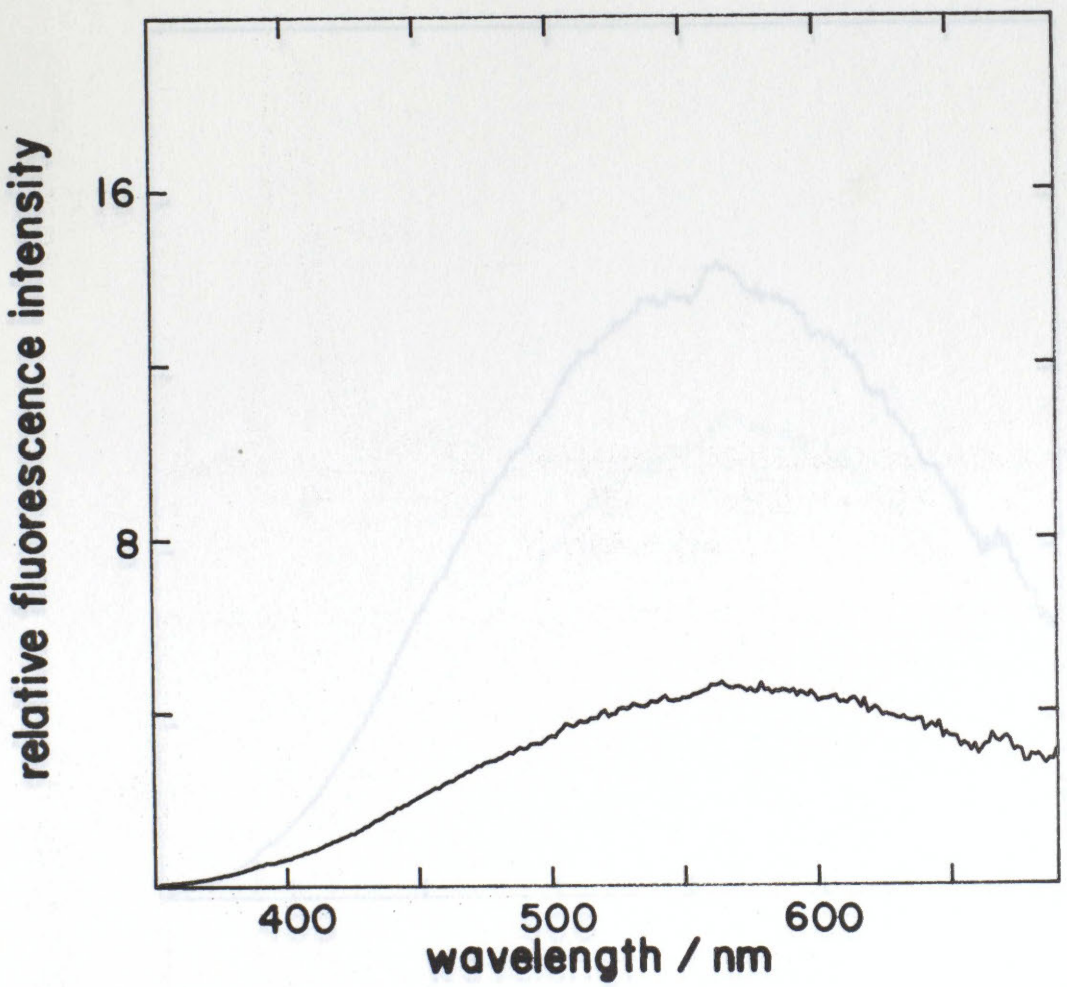

H024. IMPERIAL OIL FUEL 46 (BUNKER B OR #5) (PP76)

counts
400
200
R
I
15
30
45
60
75
time \ ns

relative fluorescence intensity
16
8
400
500
600
wavelength \ nm

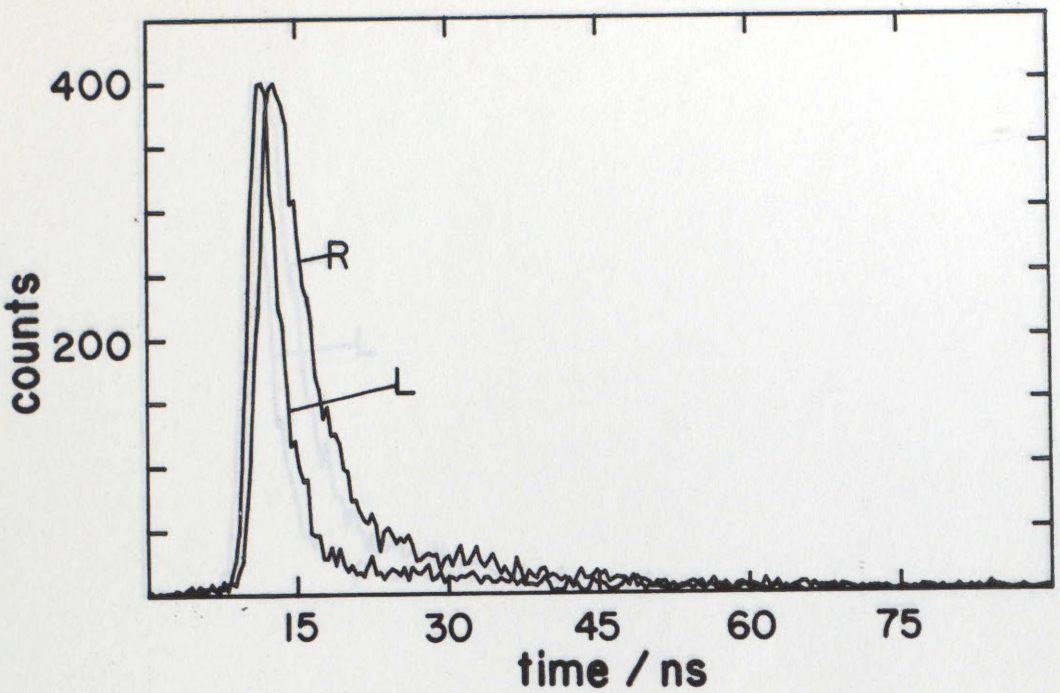

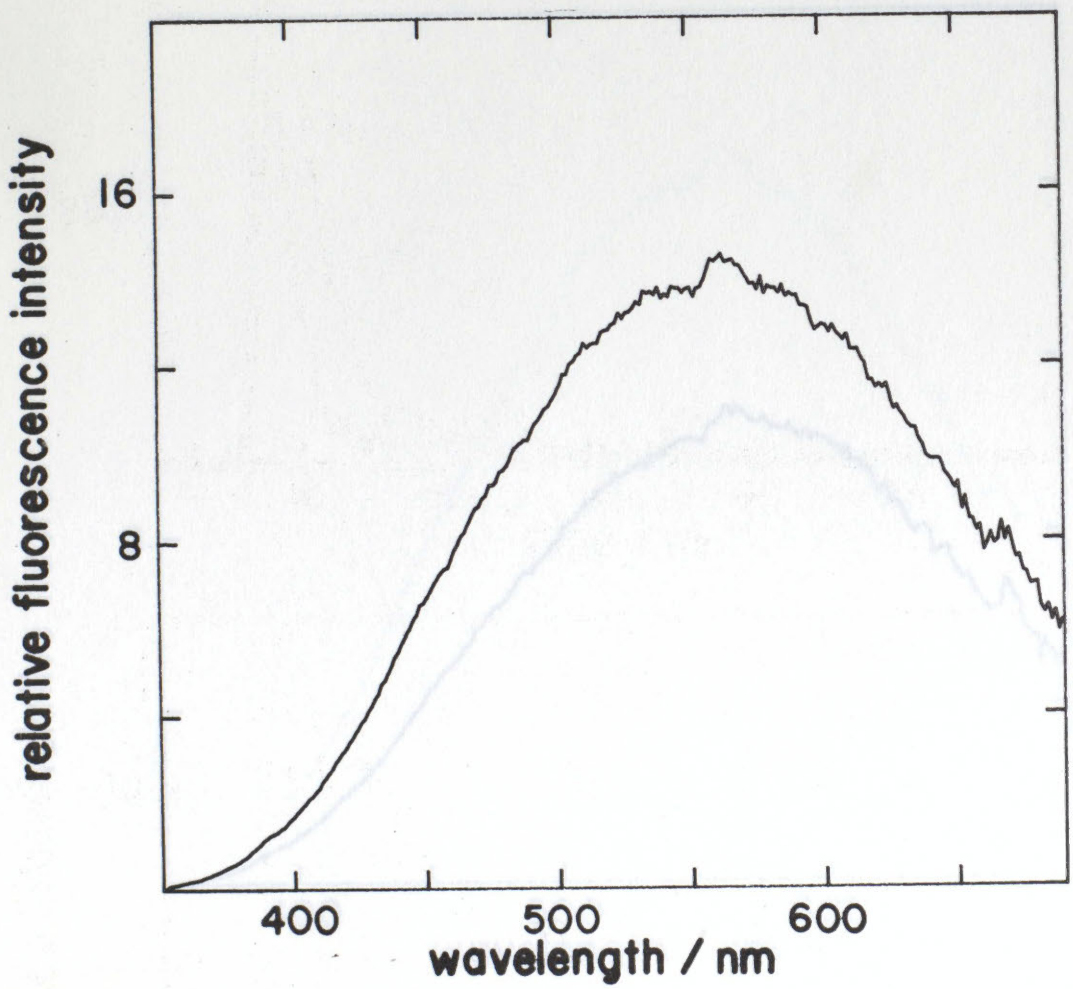

H025. STANDARD OIL LIGHT FUEL OIL (PP79)

400
200
counts
15
30
45
60
75
time \ ns

15
8
relative fluorescence intensity
400
500
600
wavelength \ nm

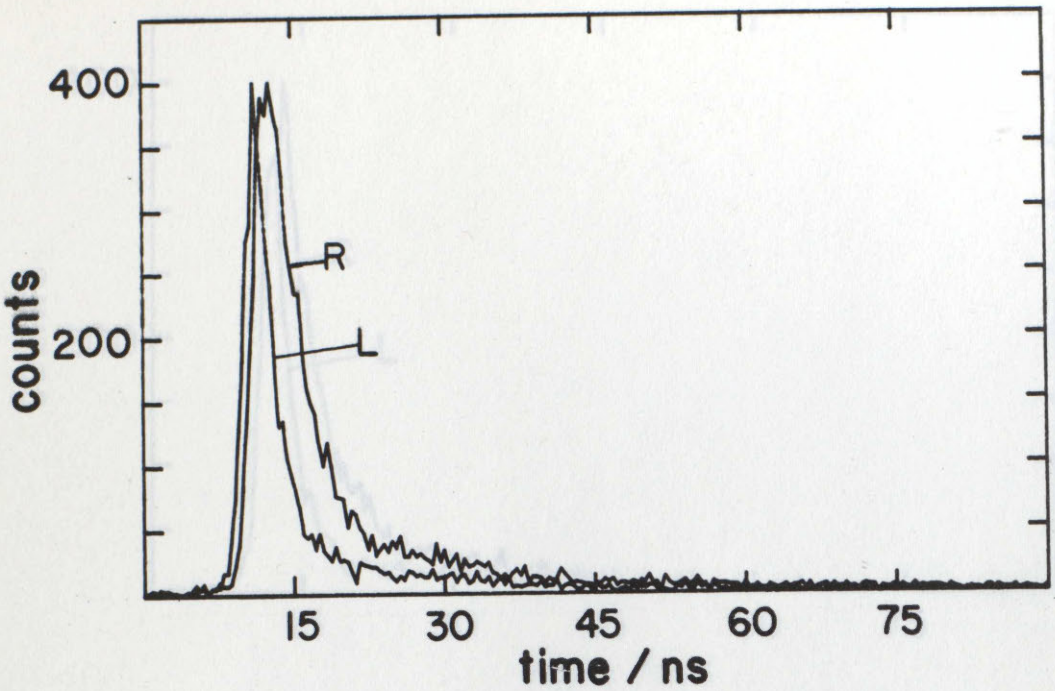

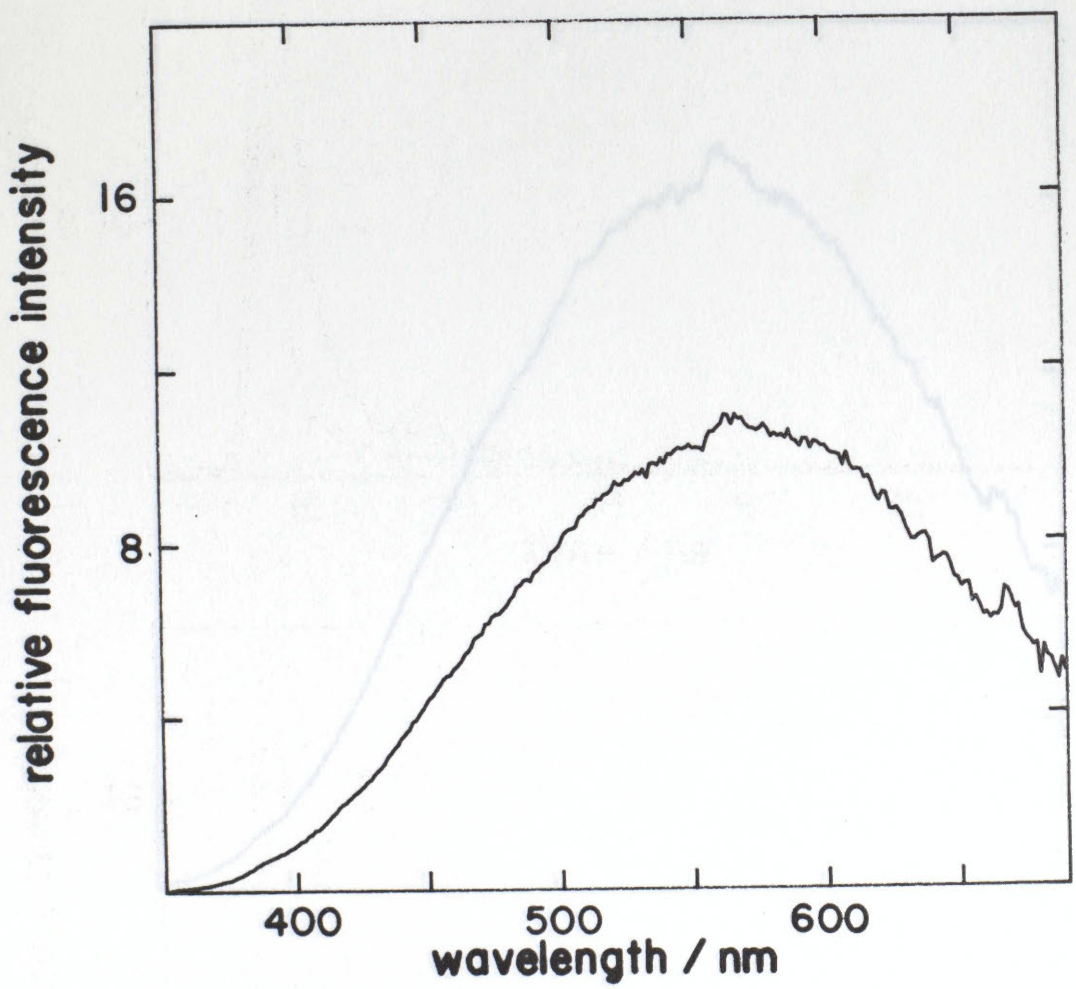

H026. STANDARD FUEL OIL (PP80)

400
200
counts
15
30
45
60
75
time / ns

16
8
relative fluorescence intensity
400
500
600
wavelength / nm

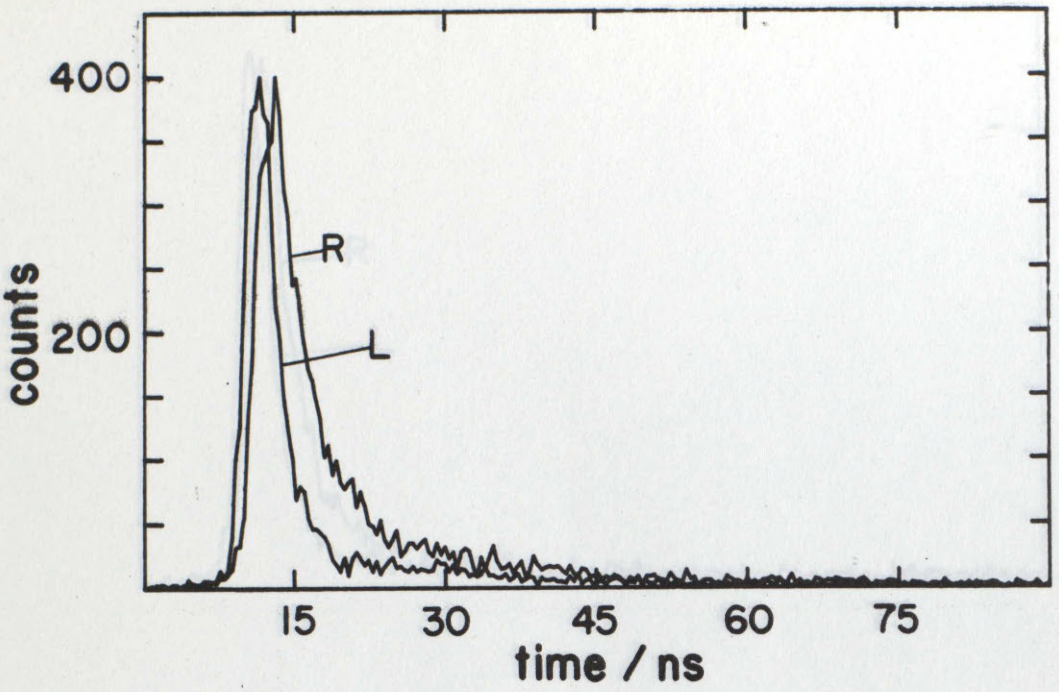

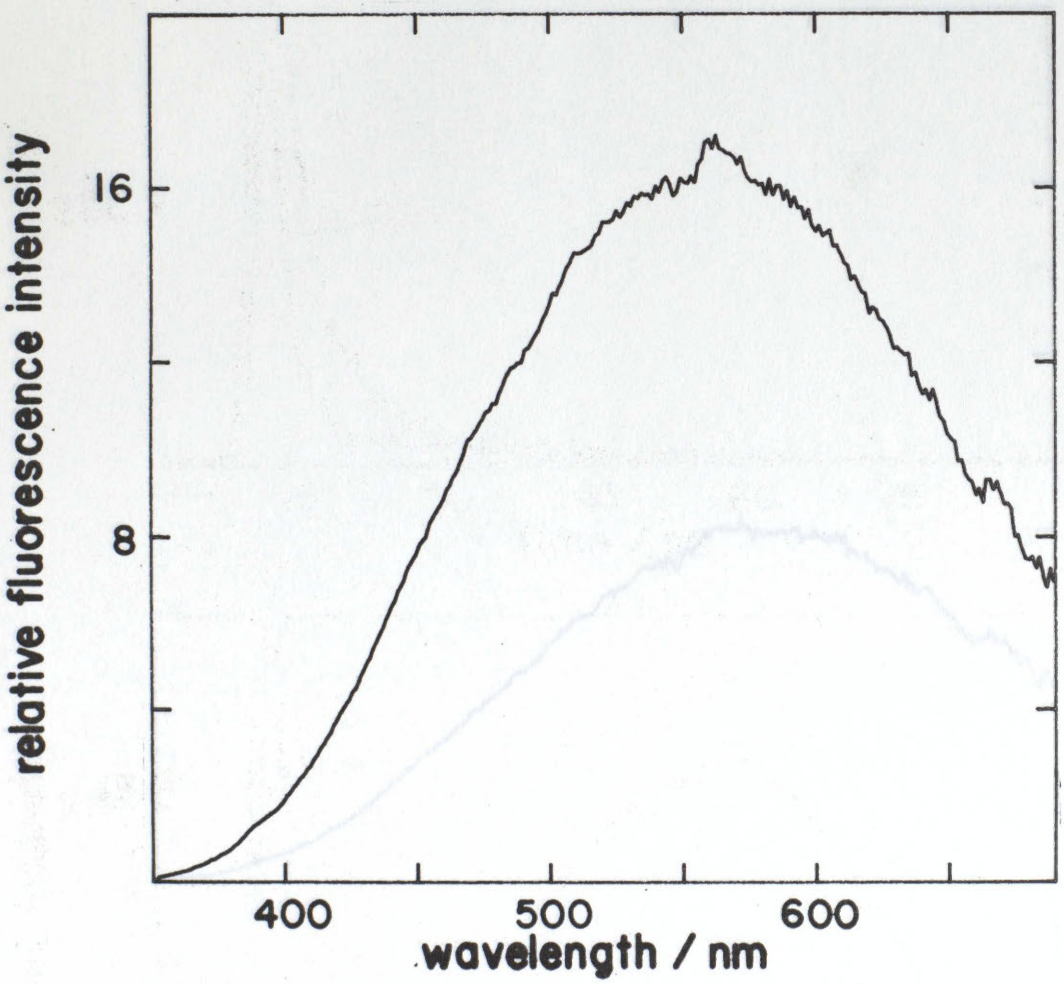

H027. STANDARD OIL CHEVRON INTERMEDIATE BUNKER FUEL 4 (PP81)

400
200
counts
R
L
15
30
45
60
75
time / ns

16
8
relative fluorescence intensity
400
500
600
wavelength / nm

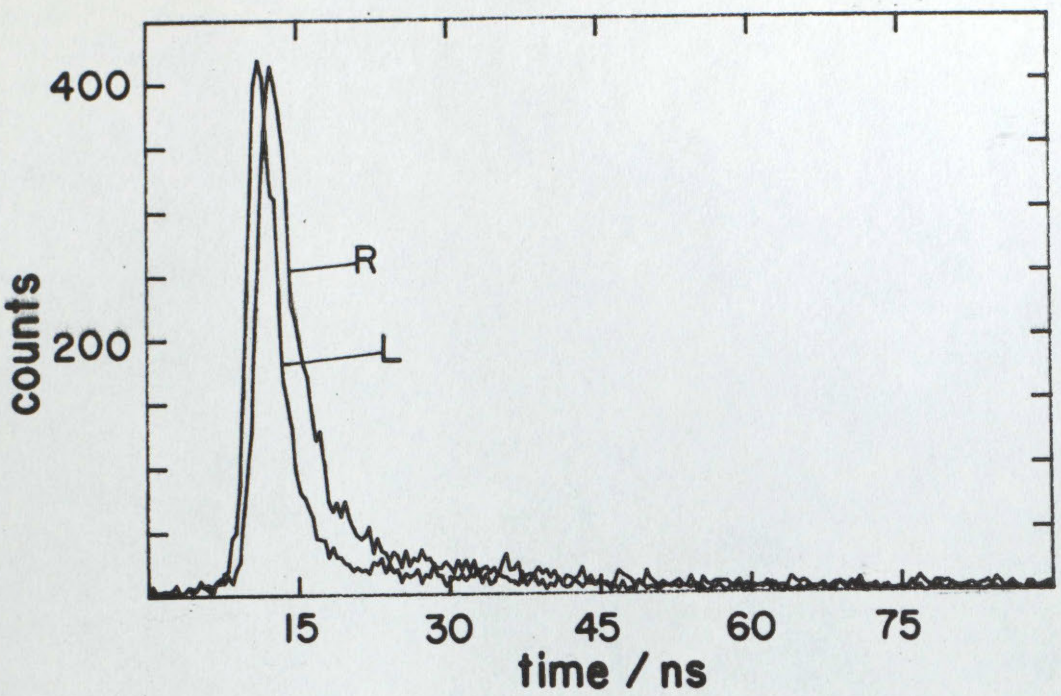

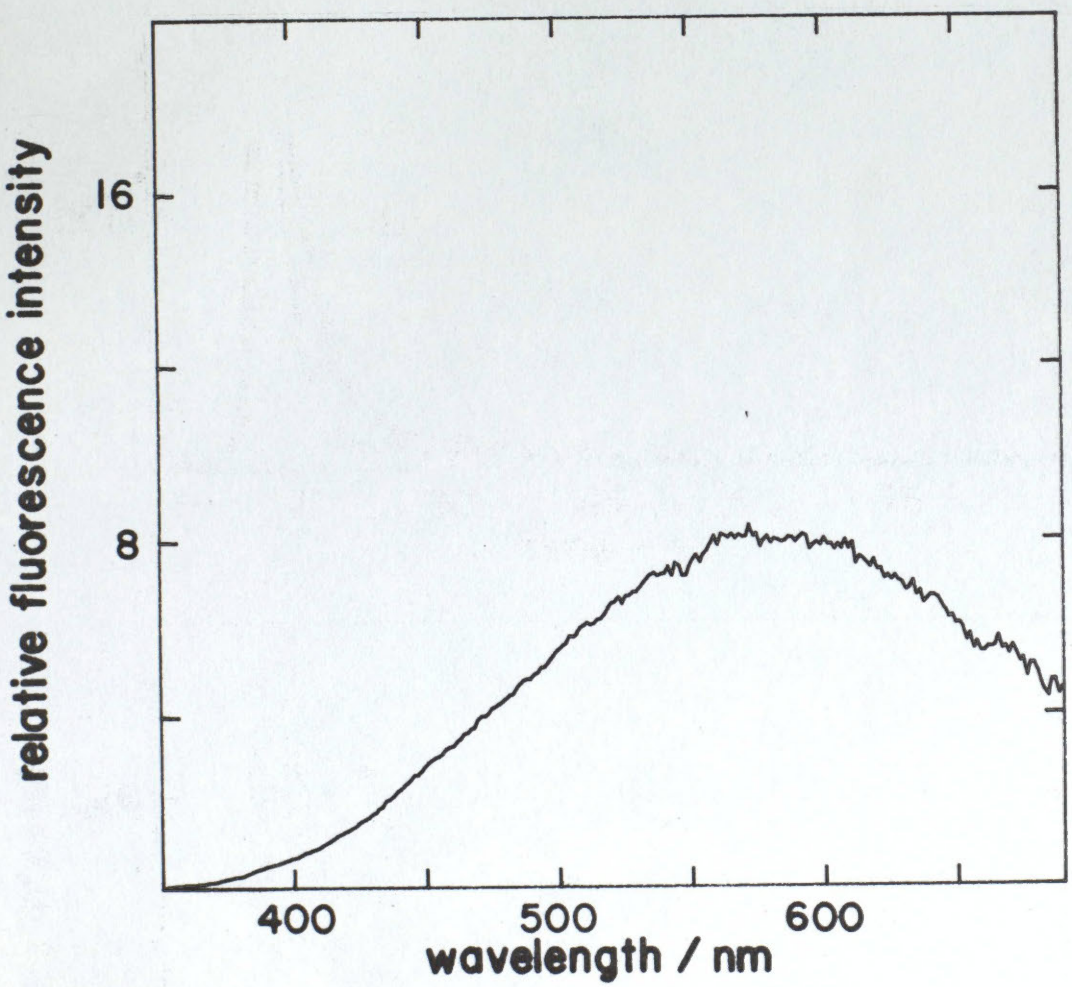

H028. STANDARD OIL CHEVRON INTERMEDIATE BUNKER FUEL 10 (PP82)

400
200
counts
time / ns

16
8
relative fluorescence intensity
wavelength / nm

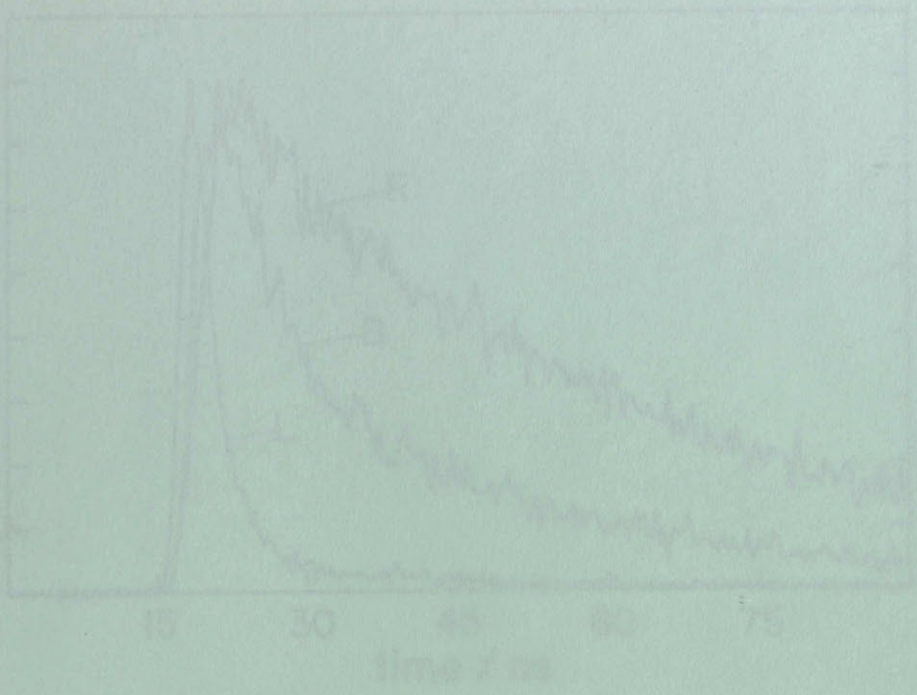
400
200
15
30
45
60
75
time / ns


400
200
400
500
600
wavelength / nm

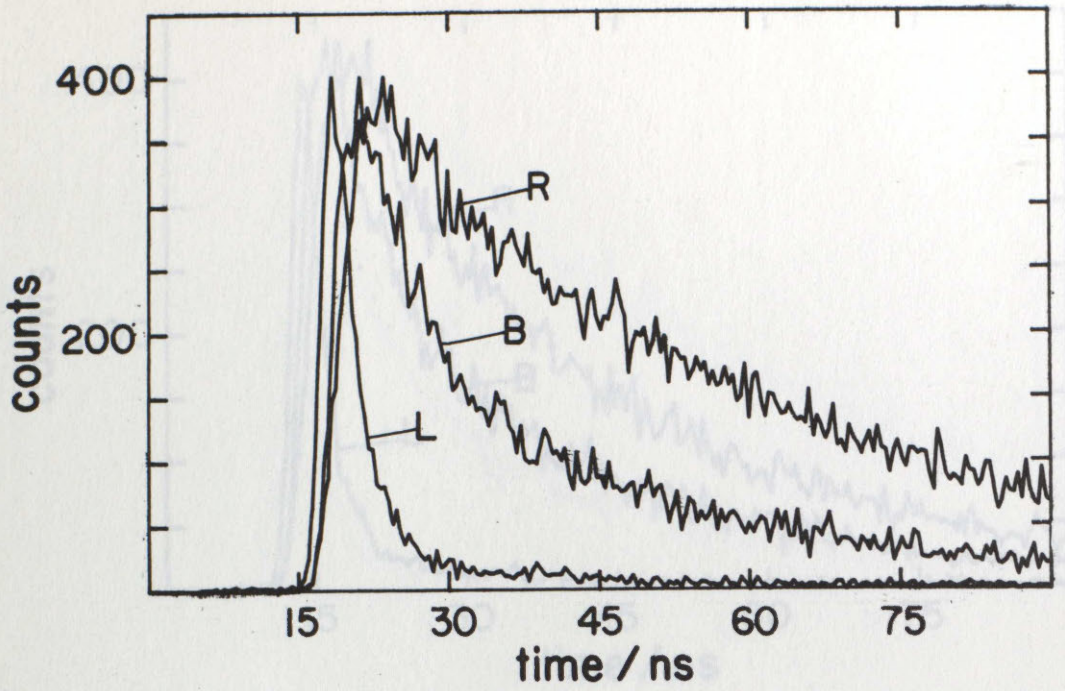

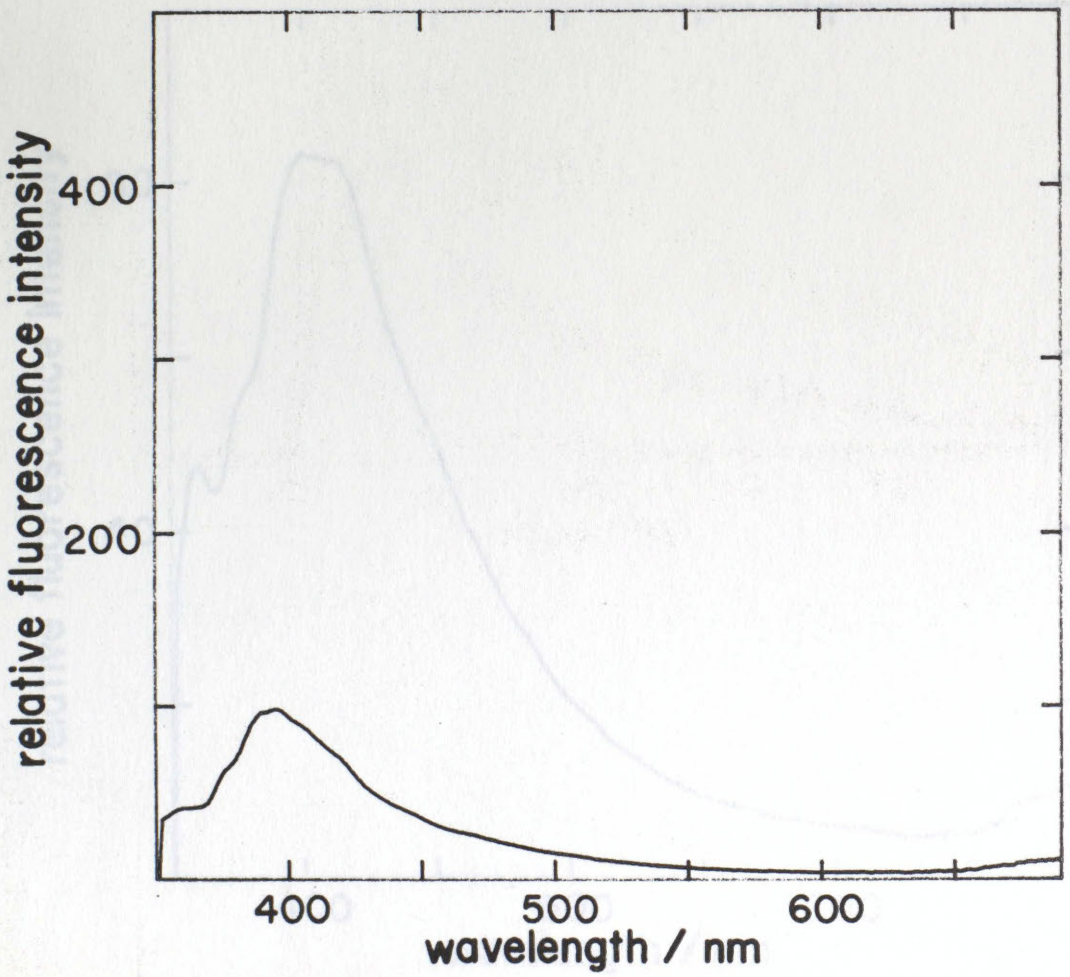

L01. ESSO MARINE GAS/OIL

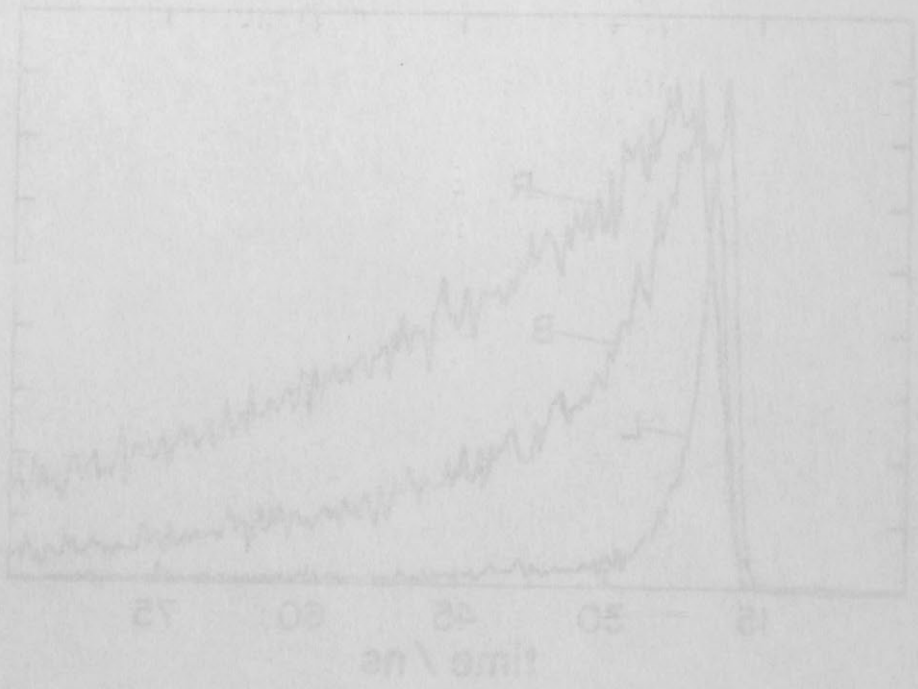
R
S
T

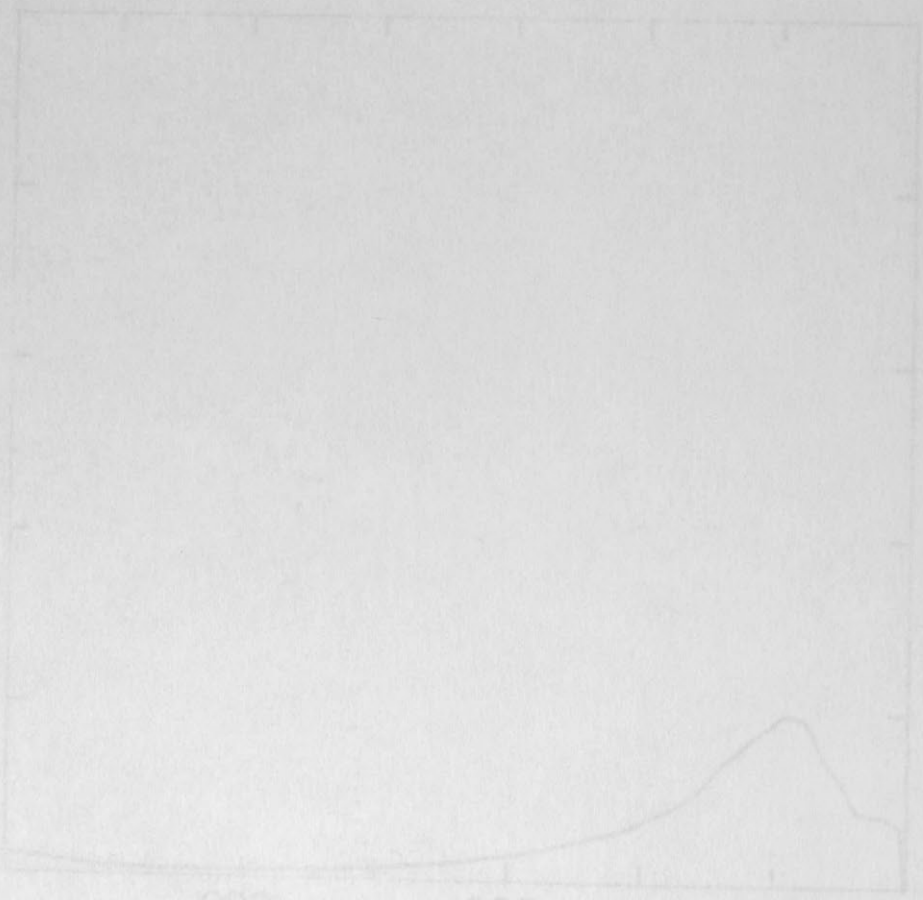

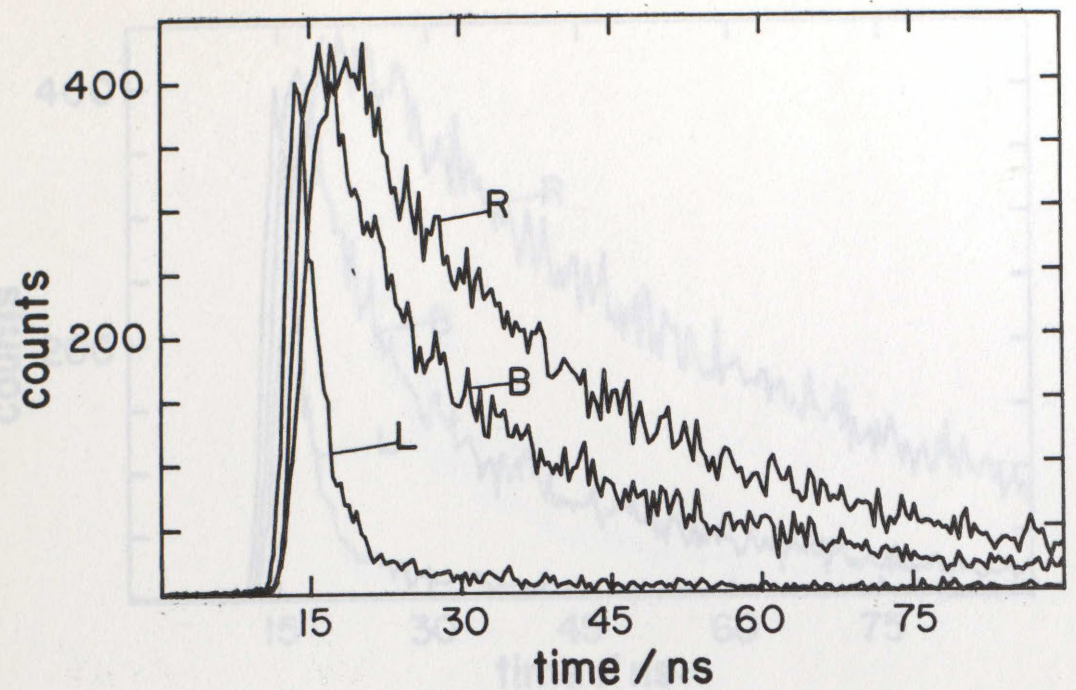

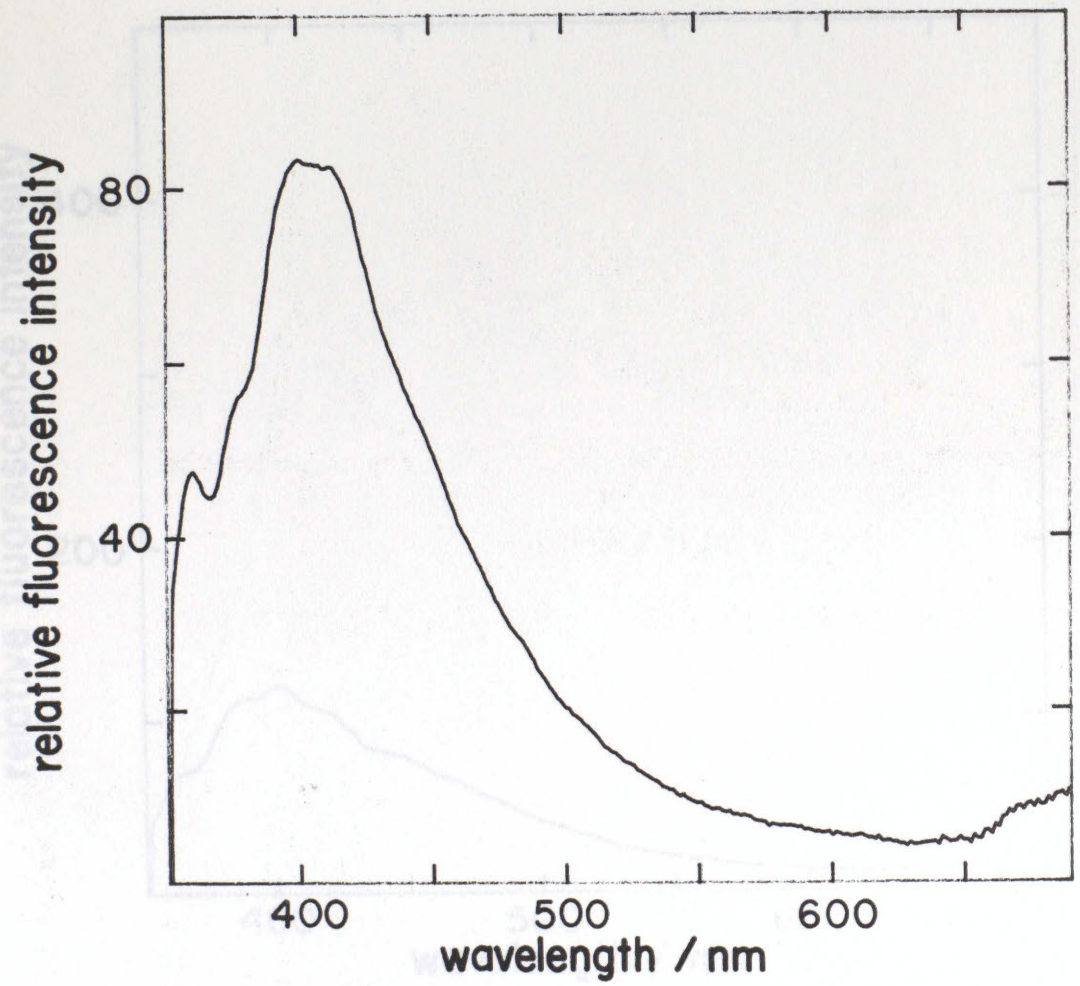

L02. FURNACE FUEL OIL #2B (WINTER)

400
200
counts
R
S
15
30
45
60
75
time / ns

80
40
relative fluorescence intensity
400
500
600
wavelength / nm

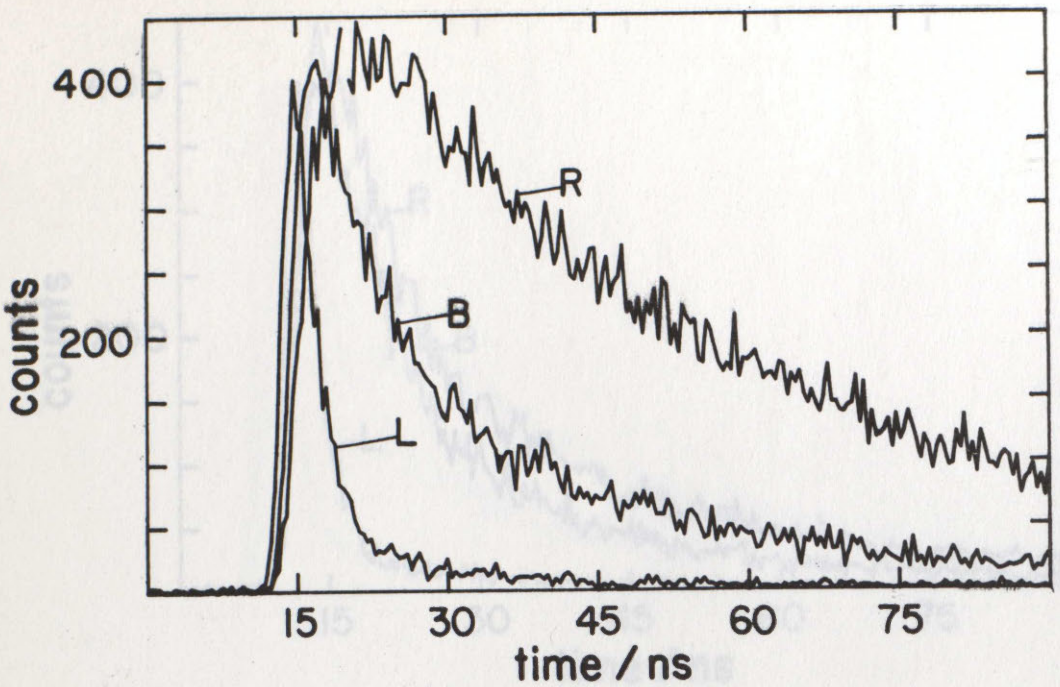

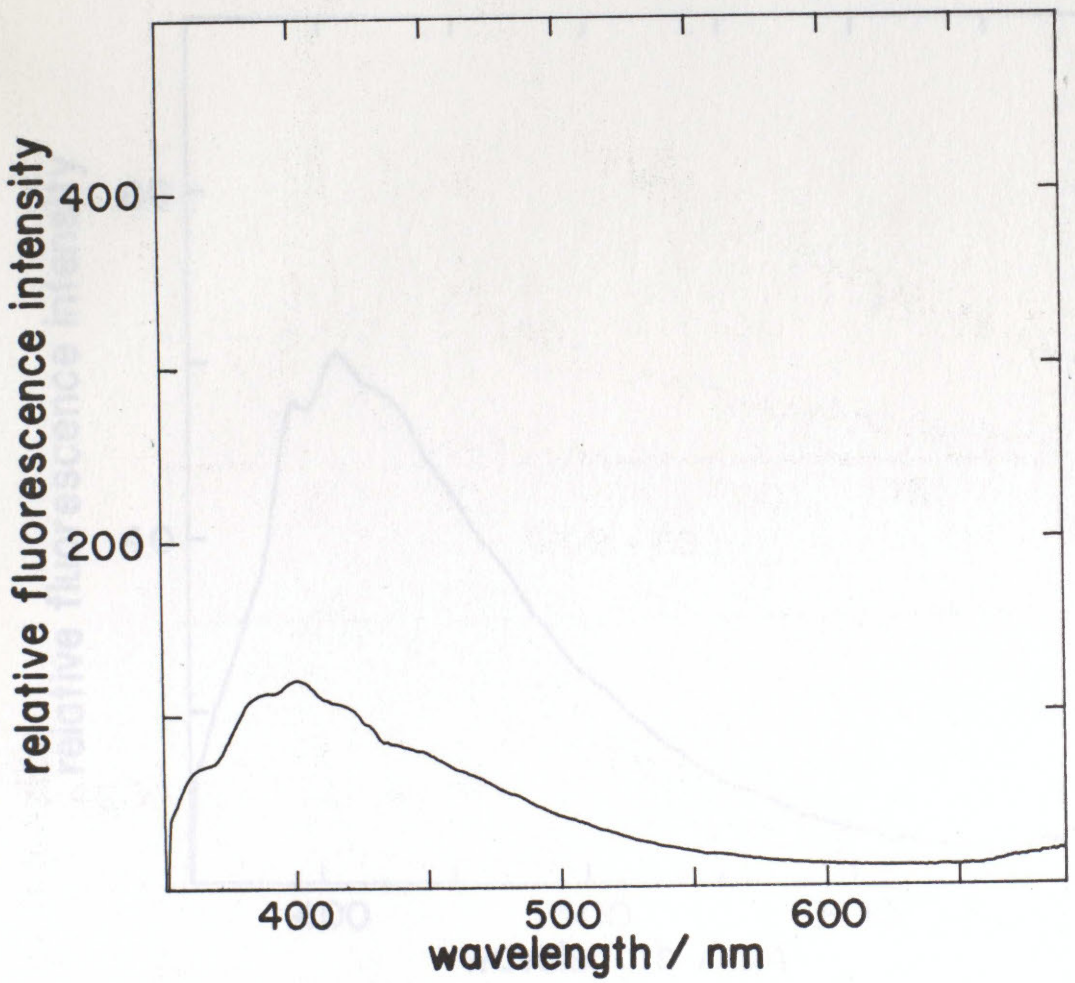

LO3. ESSO MARINE DEISEL

counts
400
200
time / ns
15
30
45
60
75
R
S
I

relative fluorescence intensity
400
200
wavelength / nm
400
500
600

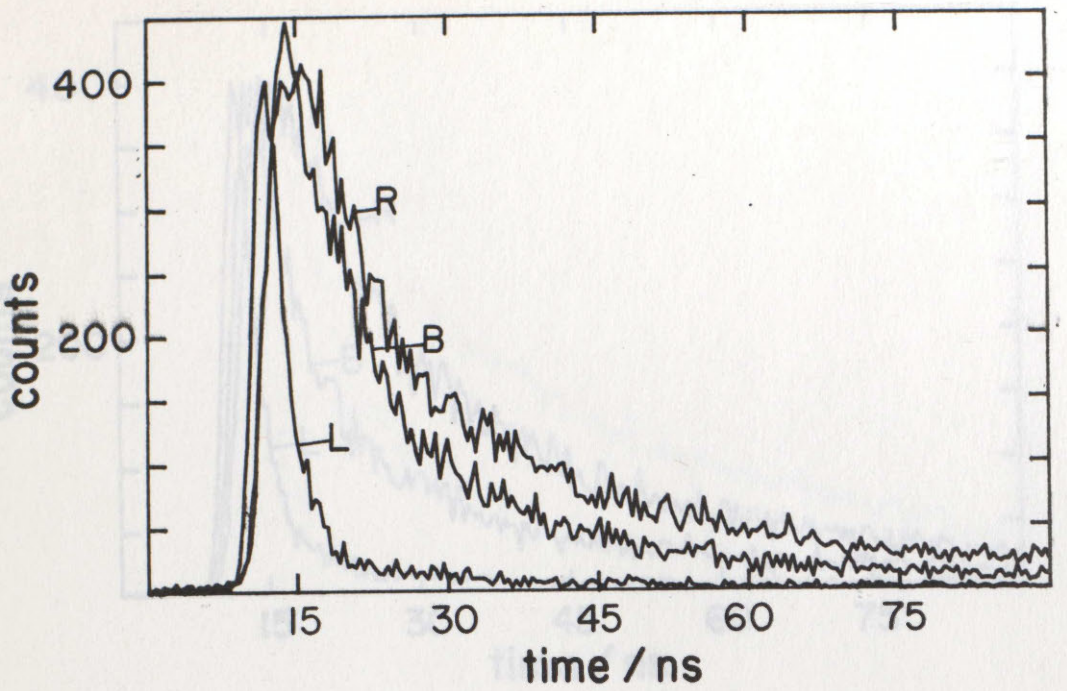

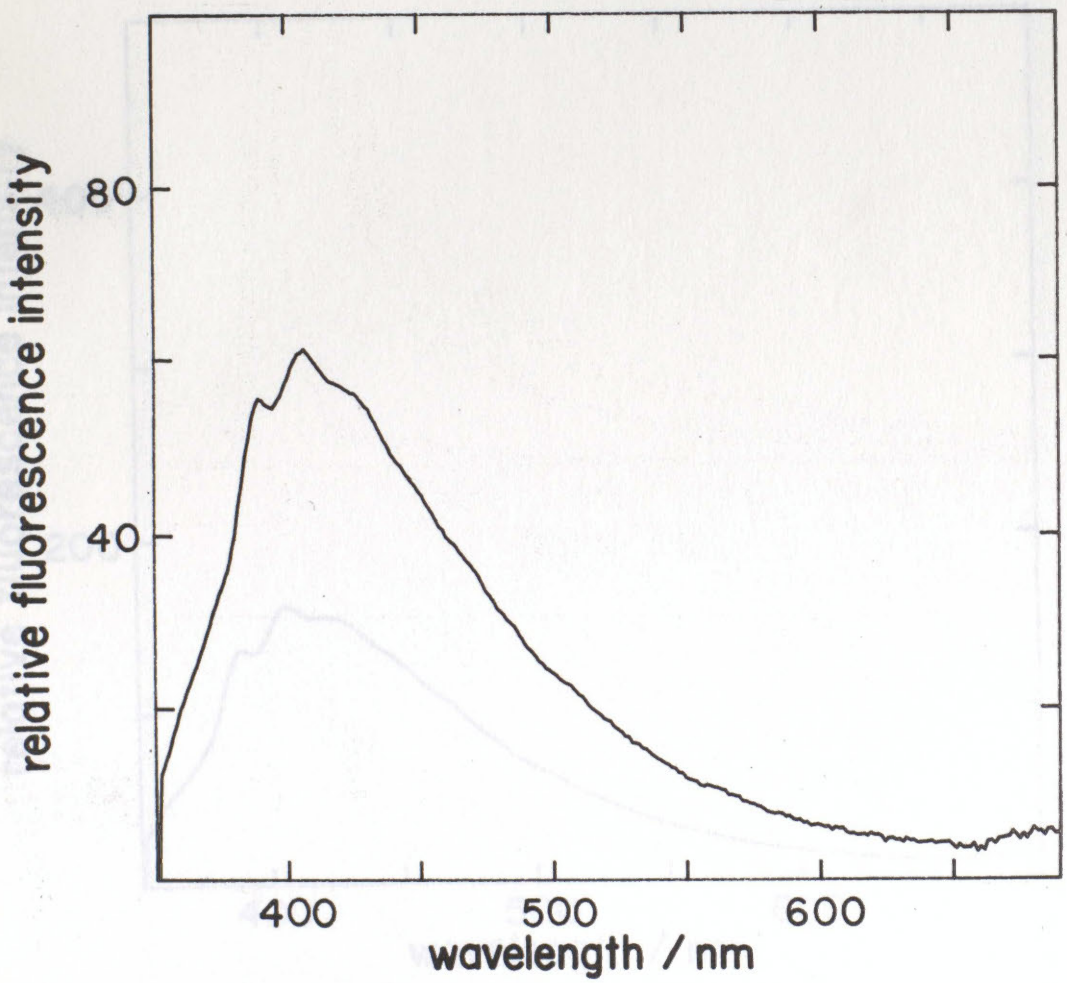

L04. LUBRICATING OIL TAKEN ON ODESSA SOUTH RUSSIAN SHIP "NOVO VORONESH" REG. ILICHEVSK. (PP61)

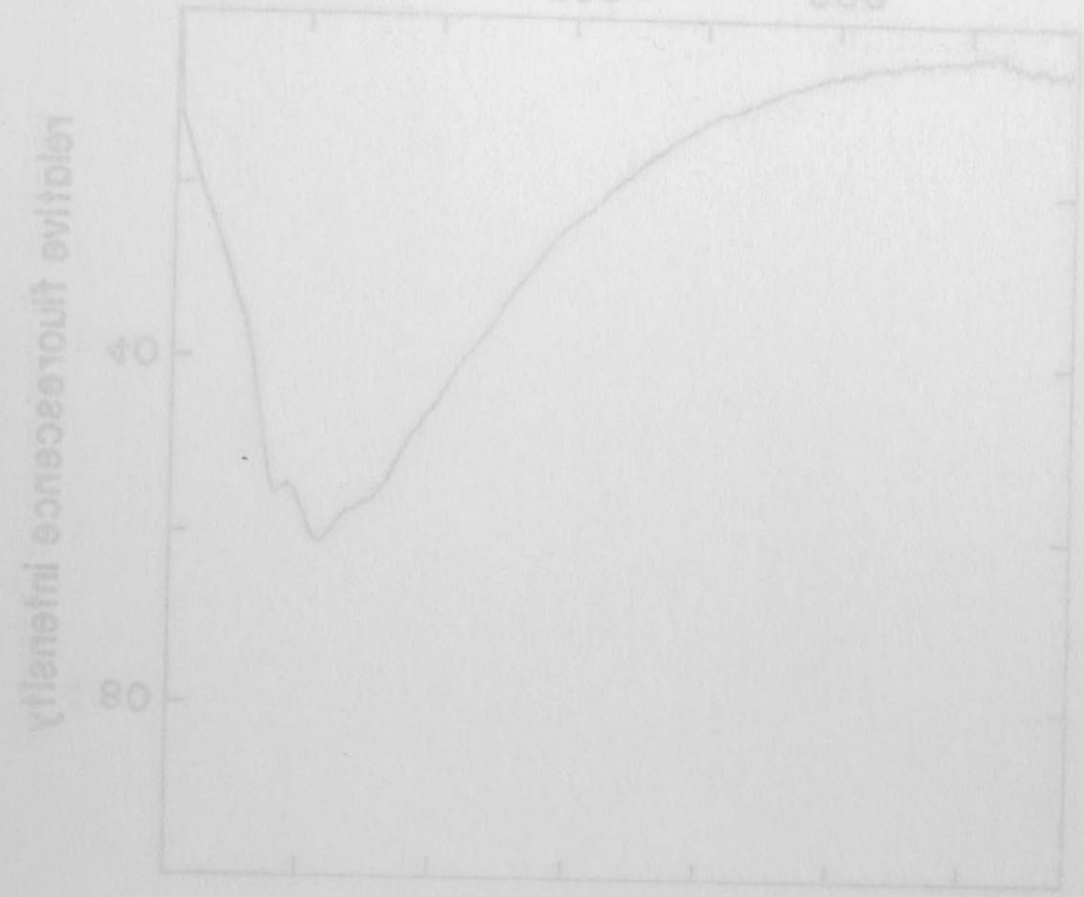
relative fluorescence intensity
0.8
0.4

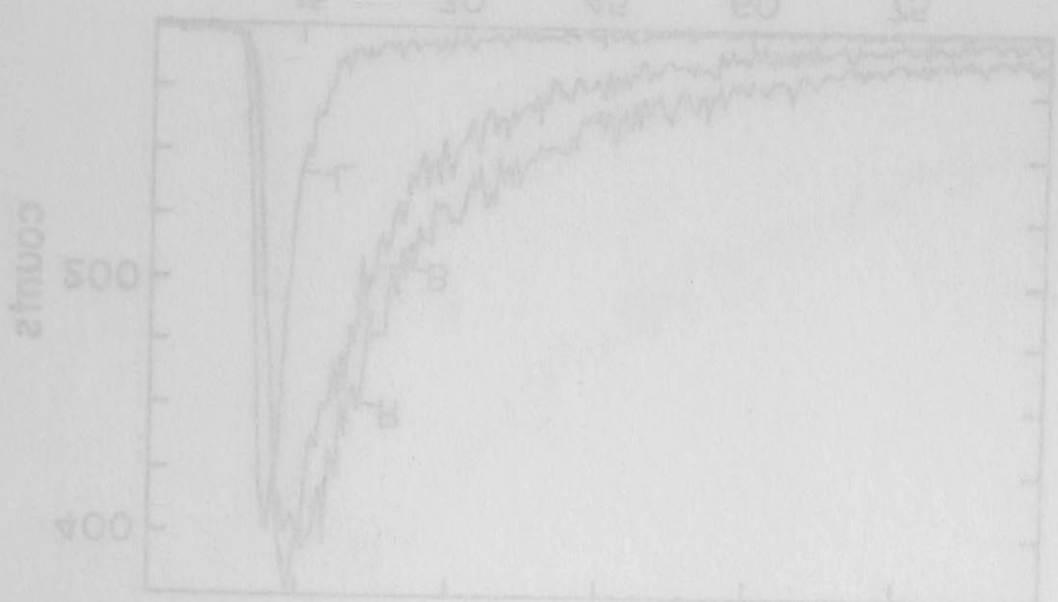
counts
500
T
R

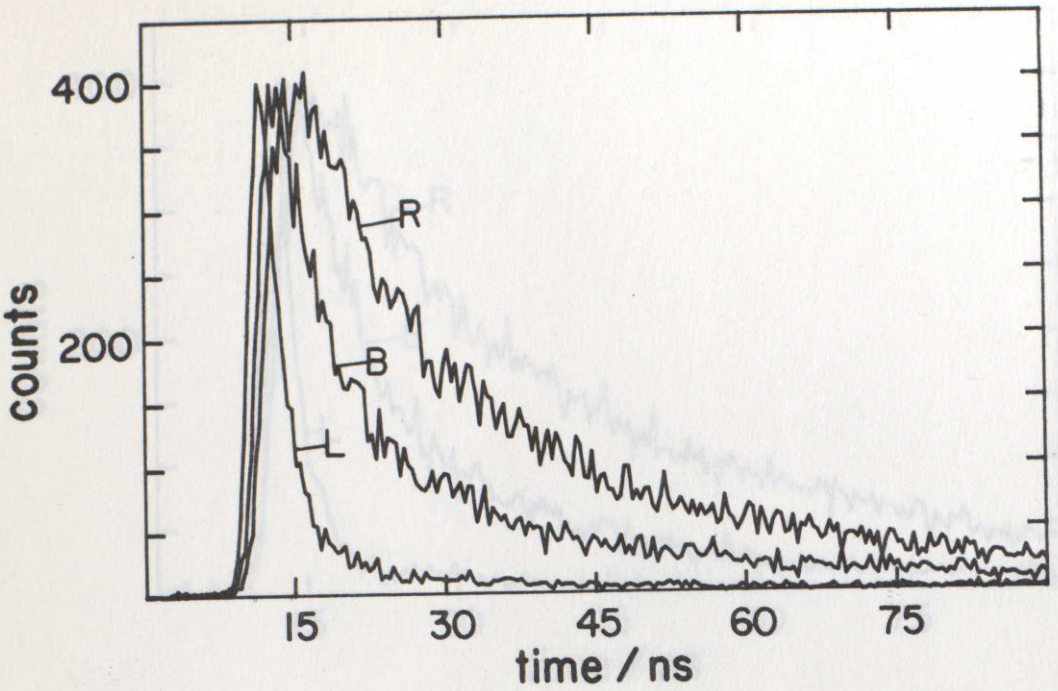

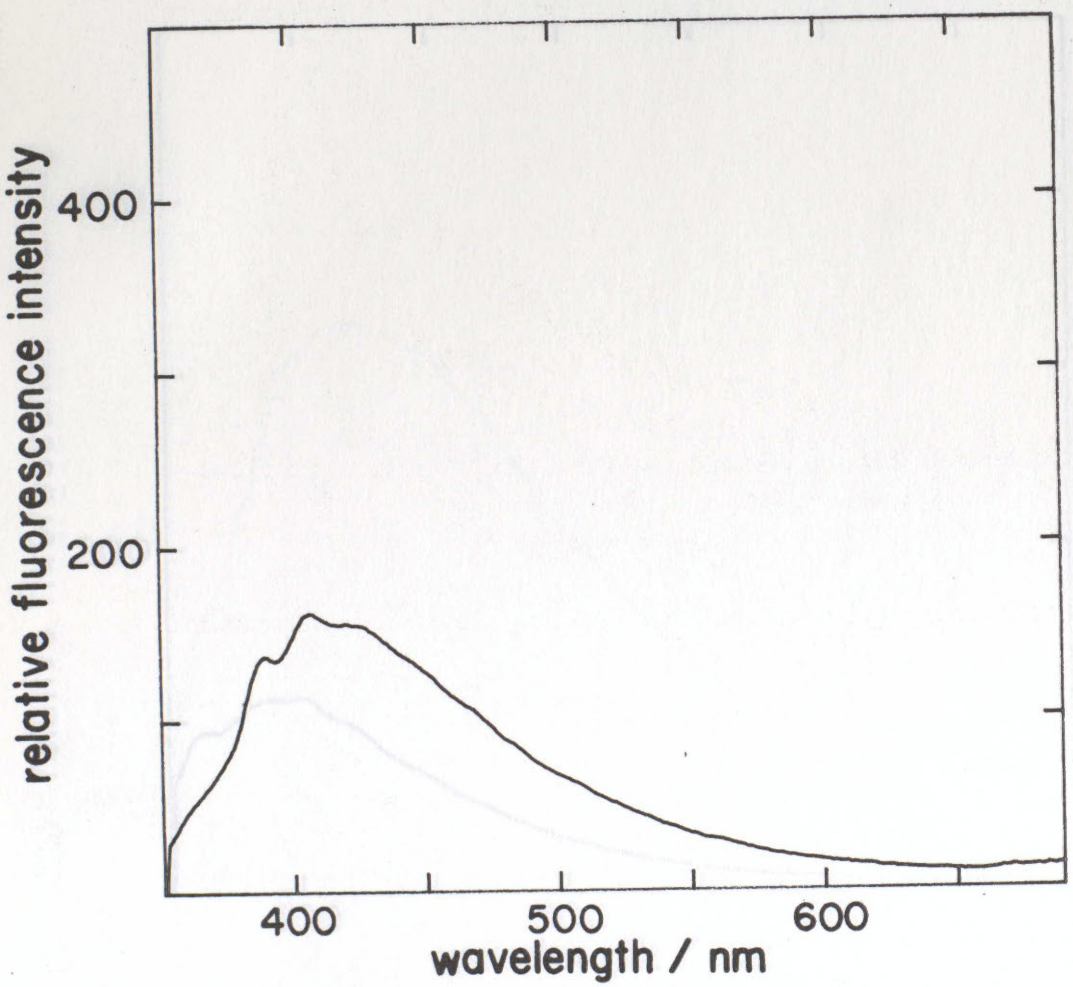

LO5. CIRCULATED LUB OIL TAKEN ON ODESSA SOUTH RUSSIAN SHIP "NOVOVORONESH" REG. ILICHEVSK. (PP62)

400
200
counts
15
30
45
60
75
time / ns

400
200
relative fluorescence intensity
400
500
600
wavelength / nm

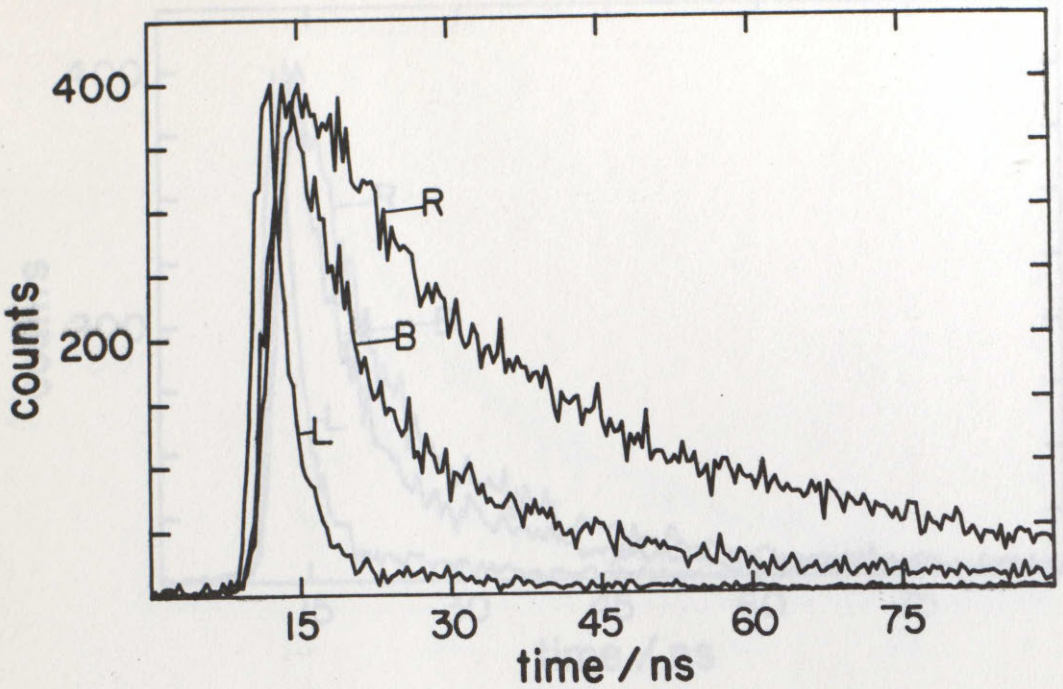

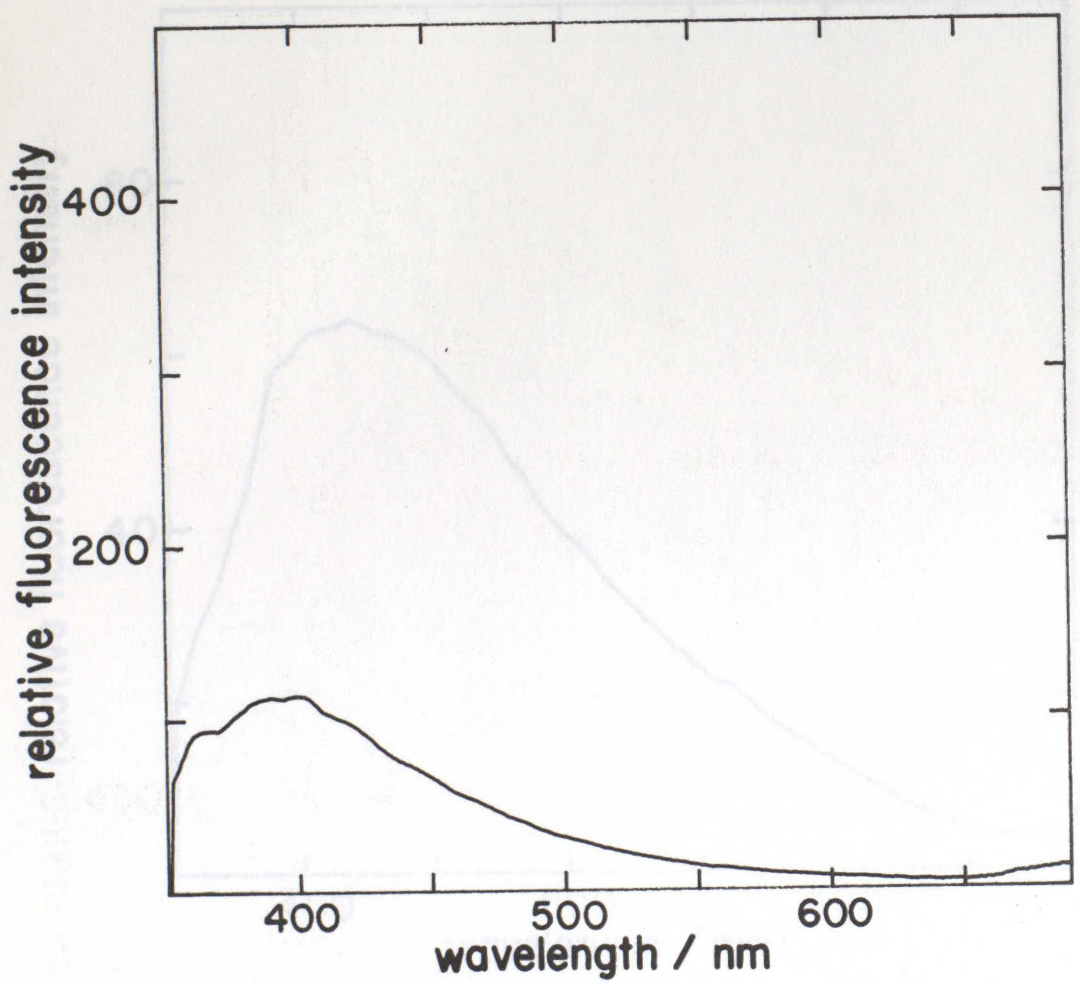

L06. LIGHT DIESEL TAKEN ON MURMANSK, NORTH RUSSIAN SHIP "VASILY KOCHALO REG. MURMANSK. (PP63)

counts
400
200
R
B
I
15
30
45
60
75
time / ns

relative fluorescence intensity
400
200
400
500
600
wavelength / nm

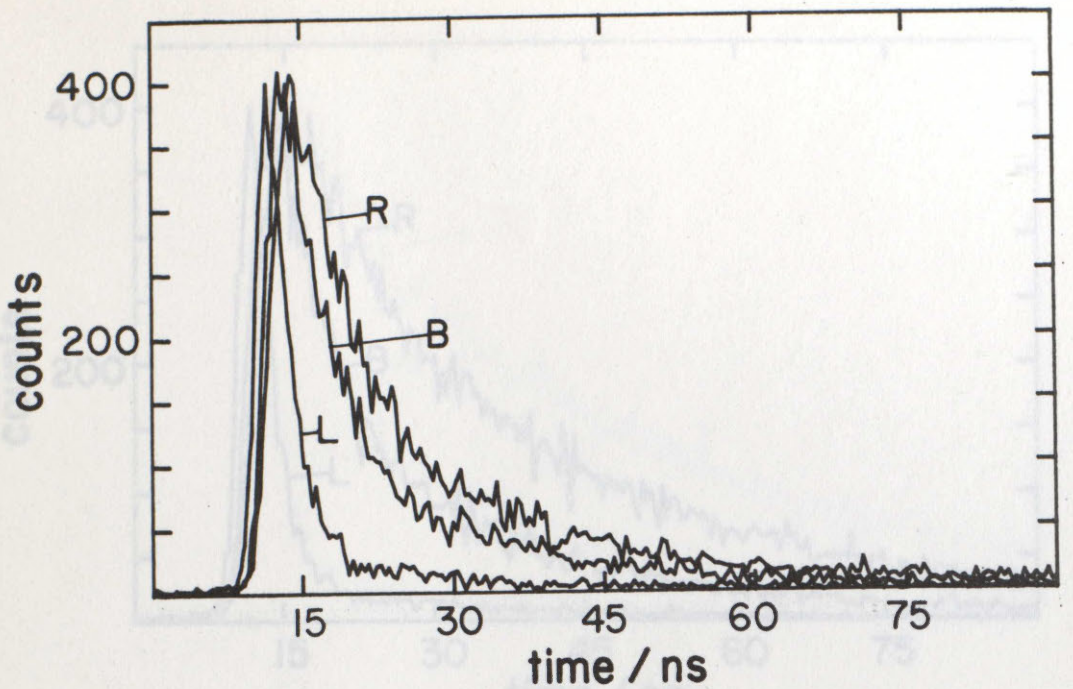

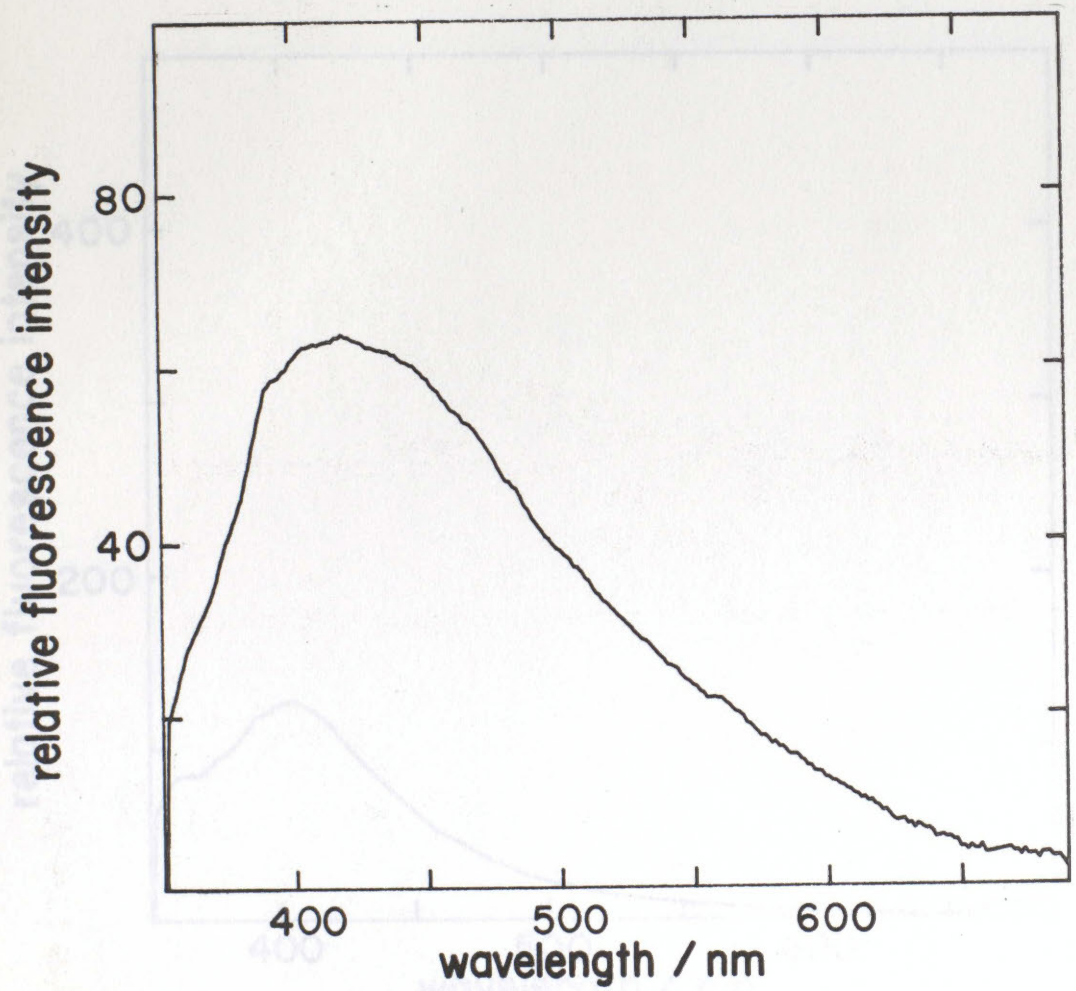

LO7. MARINE DIESEL TAKEN ON GOLHENSBURG SWEDEN
SHIP "MONT LOUIS" REG. LE HAVRE. (PP64)

400
200
counts
R
B
15
30
45
60
75
time / ns

80
40
relative fluorescence intensity
500
600
400
wavelength / nm

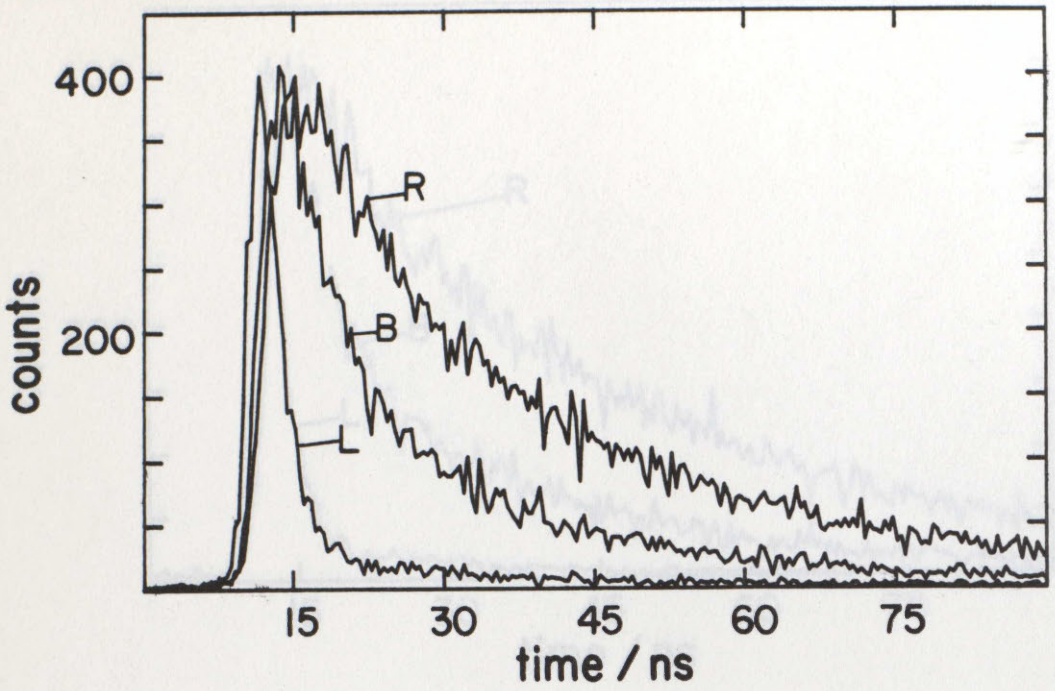

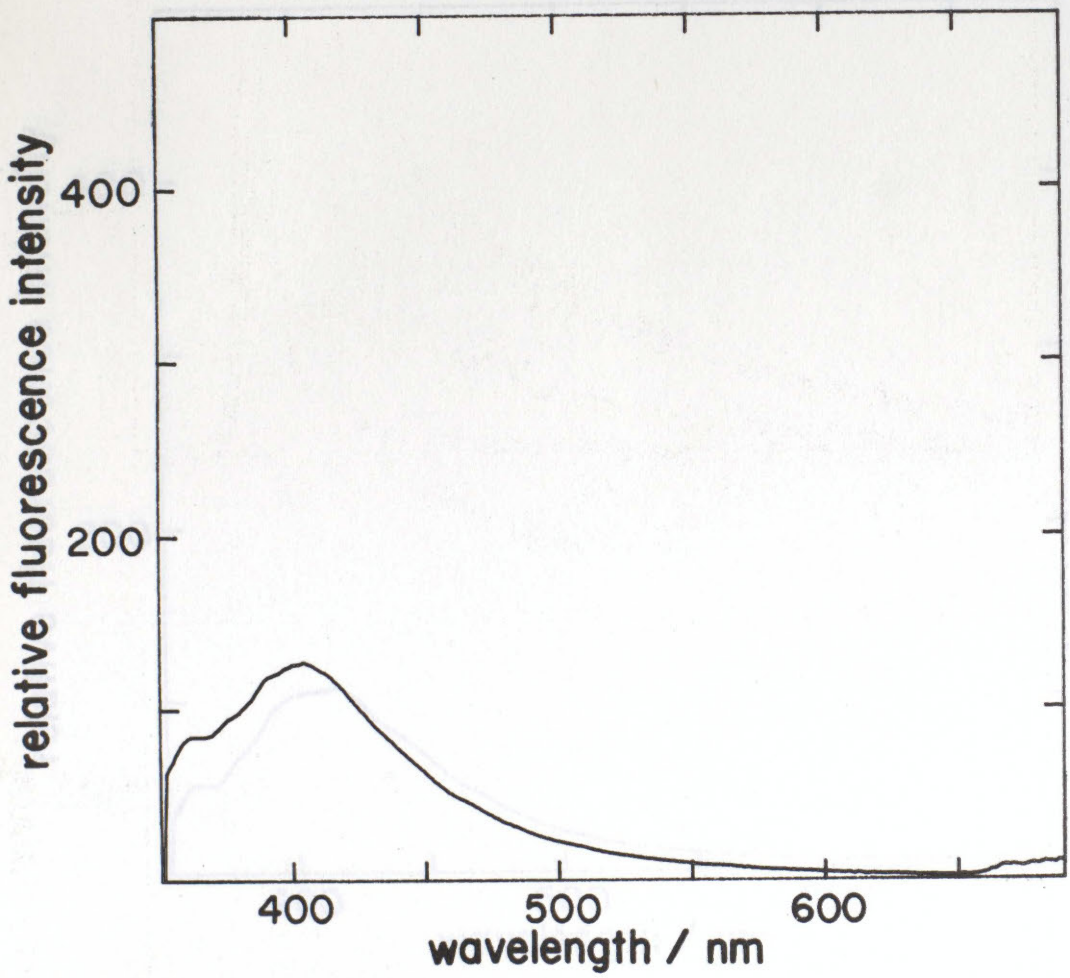

L08. DIESEL (GAS OIL) TAKEN ON ODESSA SOUTH RUSSIA SHIP "NOVOVORONESH" REG. ILICHEVSK. (PP68)

400
200
counts
R
B
T
15
30
45
60
75
time / ns

400
200
fluorescence intensity / arb. units
400
500
600
wavelength / nm

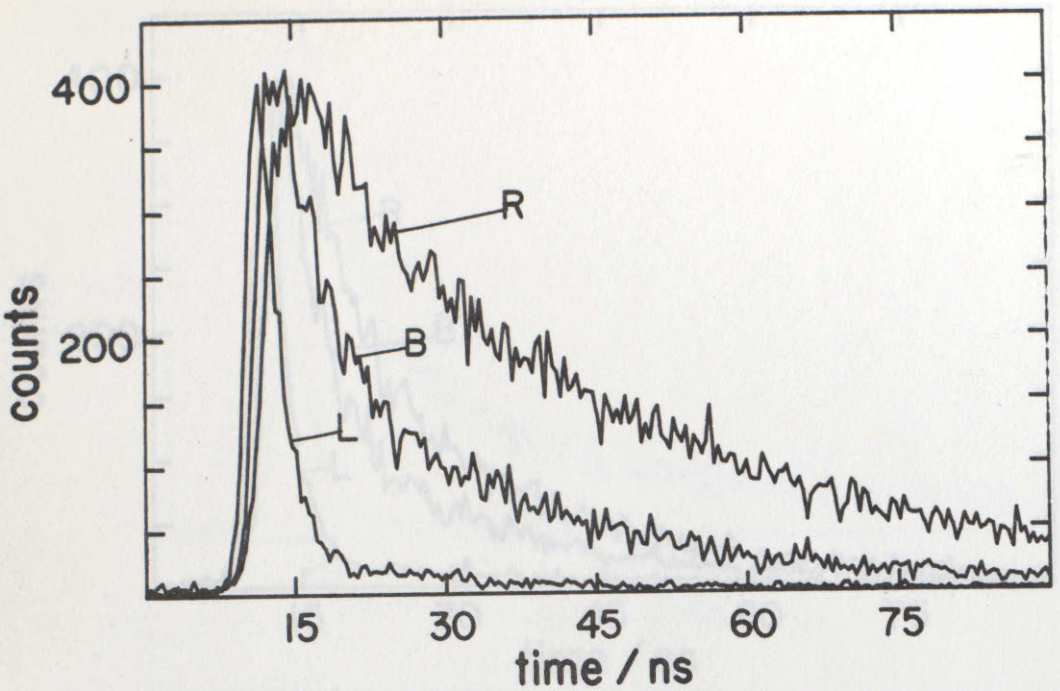

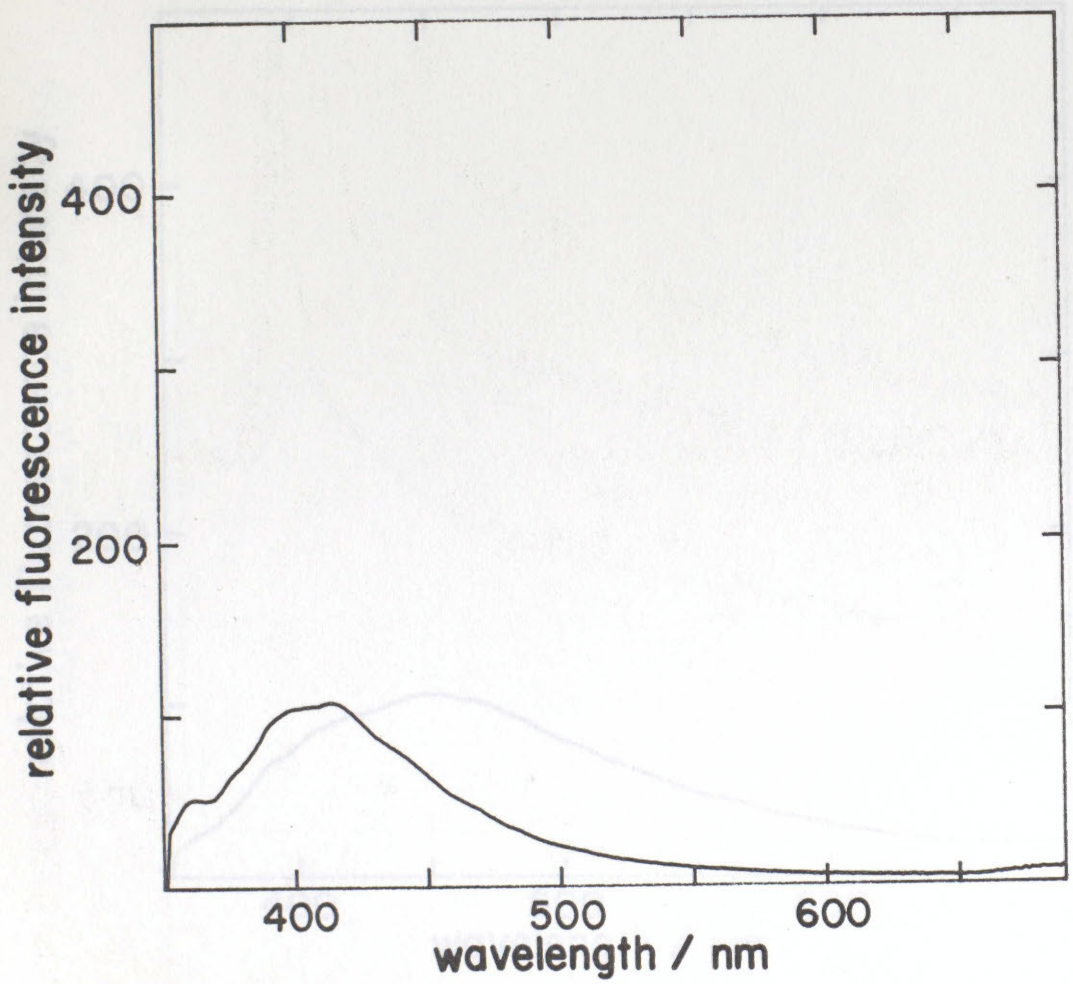

L09. IMPERIAL OIL MARINE DIESEL OIL RECEIVED FROM CDLV OCT/73 (PP84)

counts
400
200
R
S
I
15
30
45
60
75
time \ ns

relative fluorescence intensity
400
200
400
500
600
wavelength \ nm

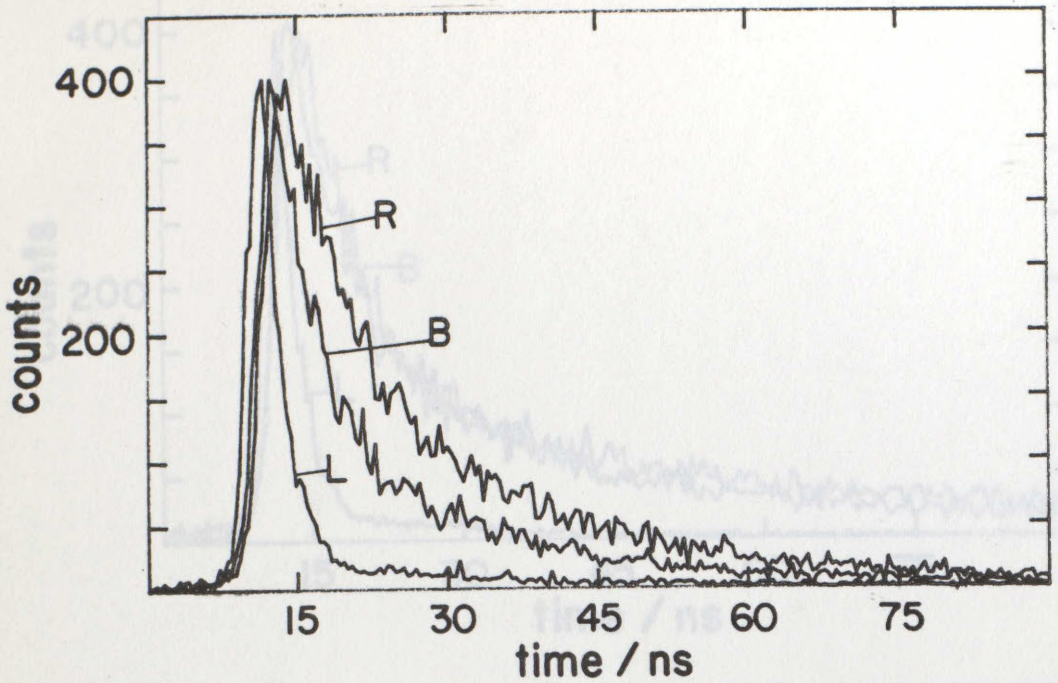

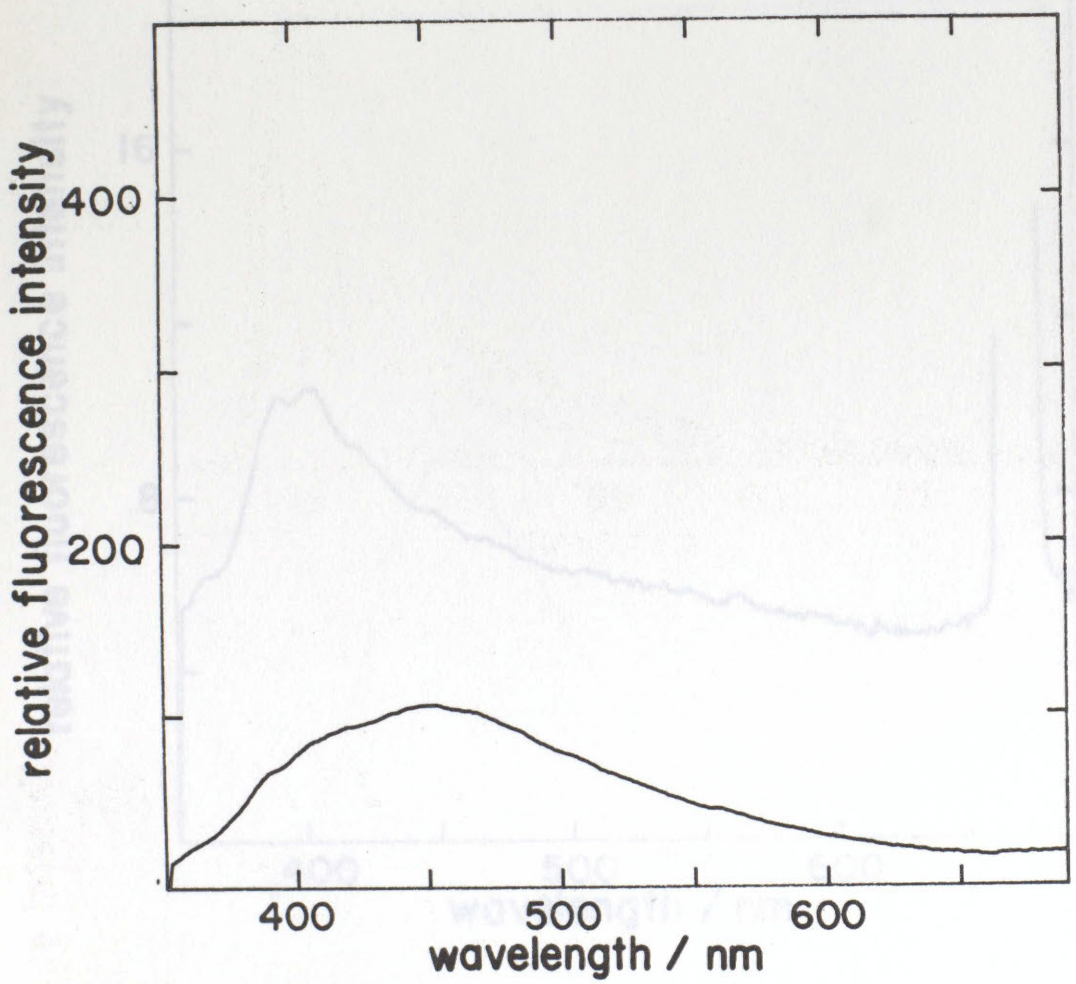

L010. STANDARD OIL CHEVRON MARINE DIESEL FUEL
RECEIVED FROM CDLV OCT/73 (PP84)

400
200
counts
B
A
15
30
45
60
75
time / ns

400
200
relative fluorescence intensity
400
500
600
wavelength / nm

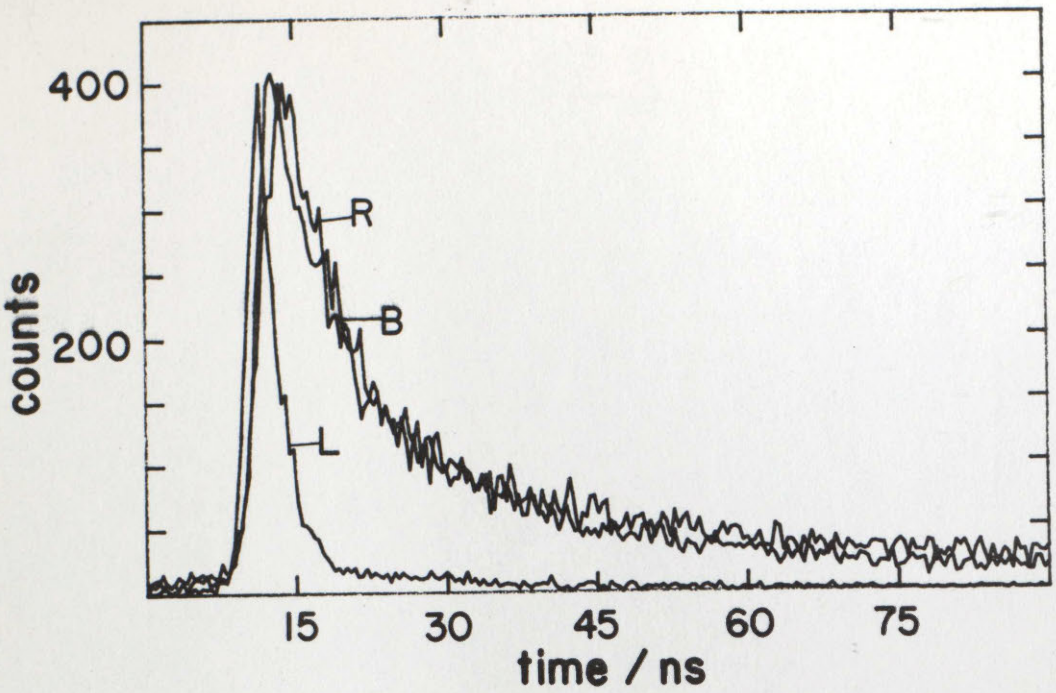
400
200
counts
R
B
L
15
30
45
60
75
time / ns

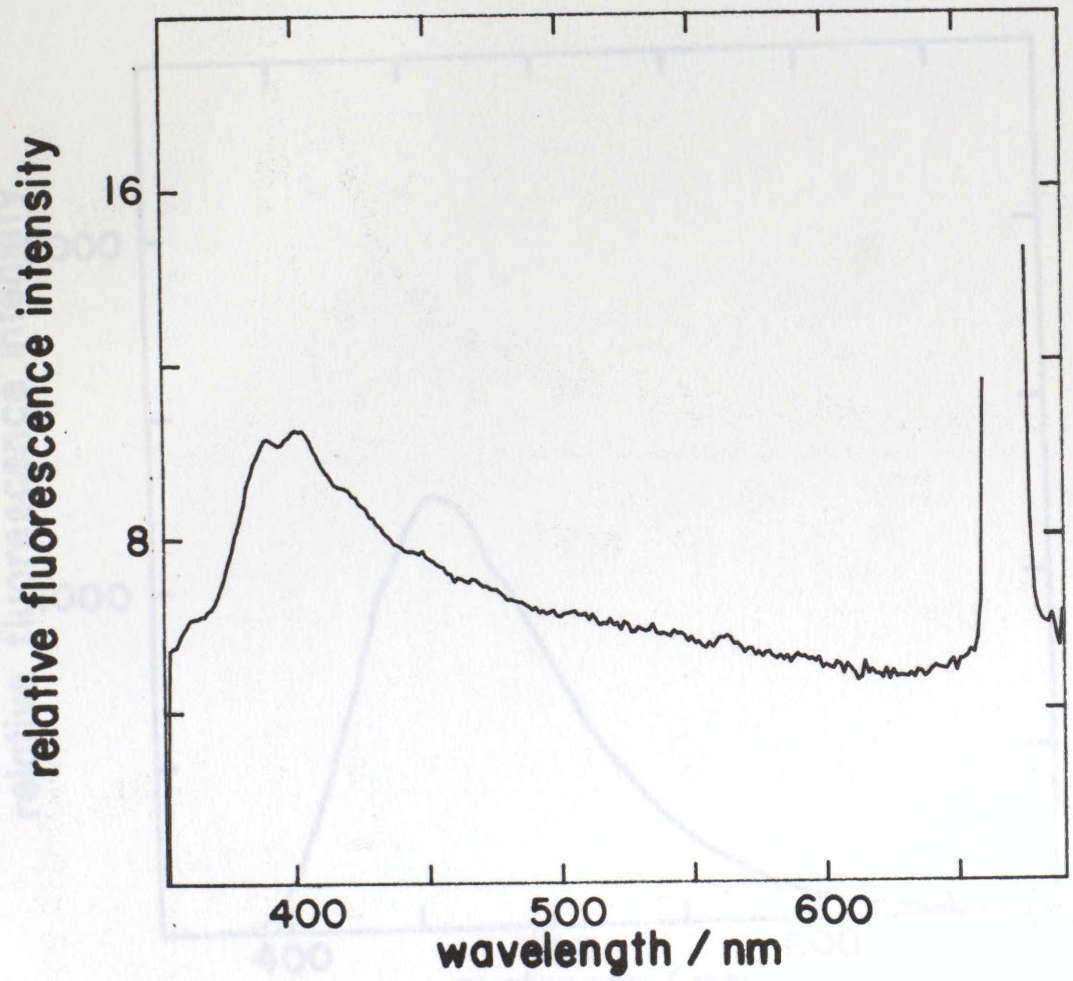
16
8
relative fluorescence intensity
400
500
600
wavelength / nm

U03 (PP91)

400
200
counts
B
A
15
30
45
60
75
time / ns

16
8
differential fluorescence intensity
400
500
600
wavelength / nm

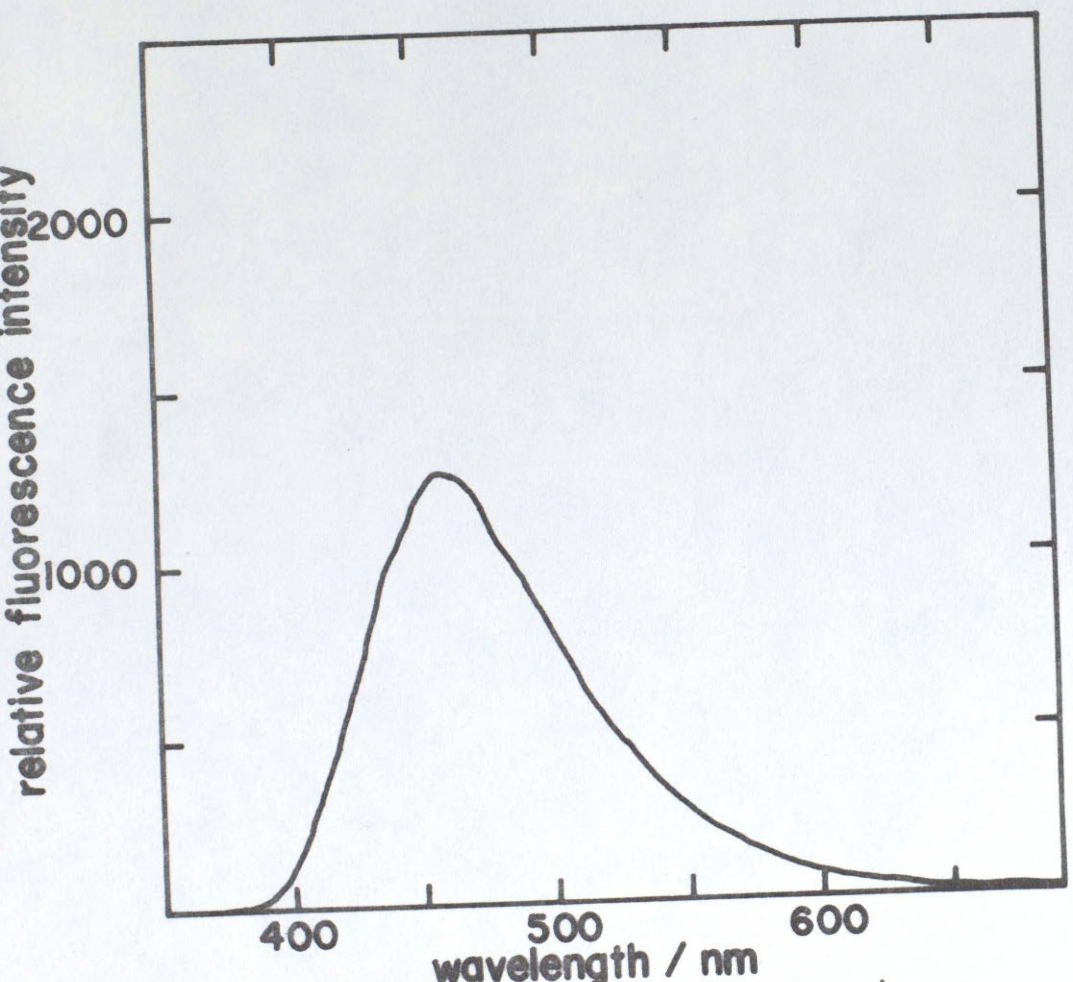

QUININE SULPHATE IN 0.5M H_2SO_4 (0.5 gl^{-1})

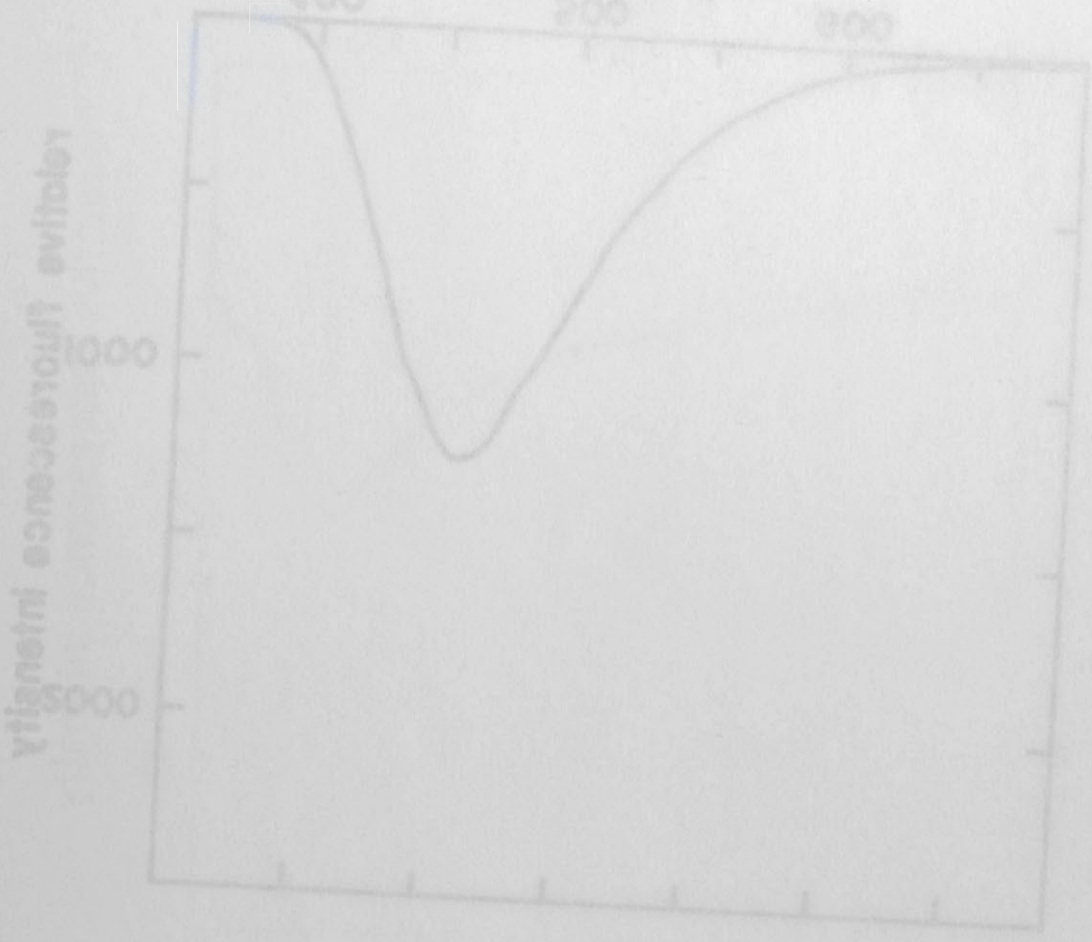

Appendix II

The Effect of Aging on the Fluorescence Properties of Oils

Notes:

i) Whilst the spectra reported in this Appendix are relative to each other they are on different scales to those reported in Appendix I.

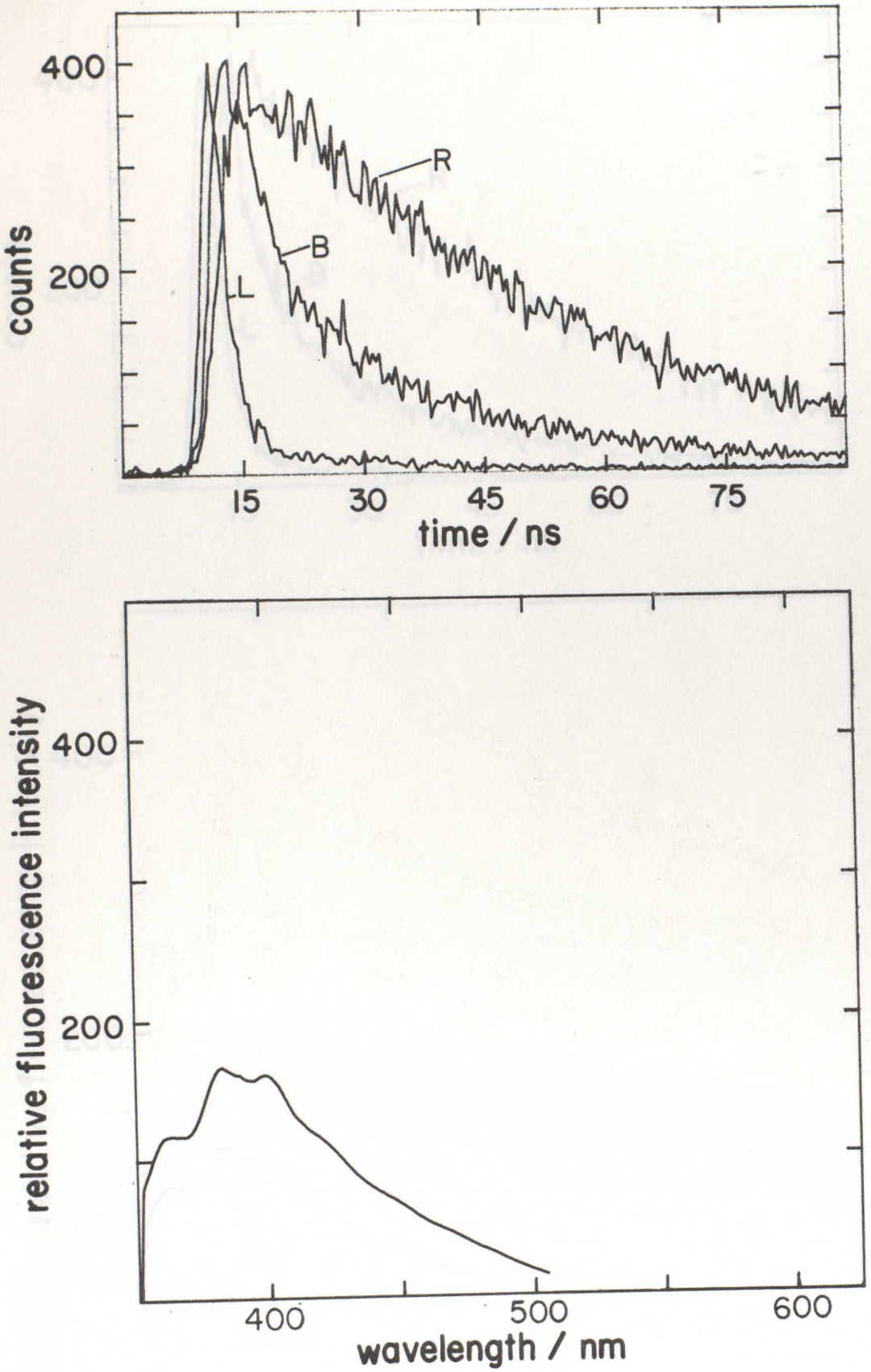

LO3 AFTER 0 HOURS AGING

counts
400
200
15
30
45
60
75
time / ns
relative fluorescence intensity
400
200
400
500
600
wavelength / nm

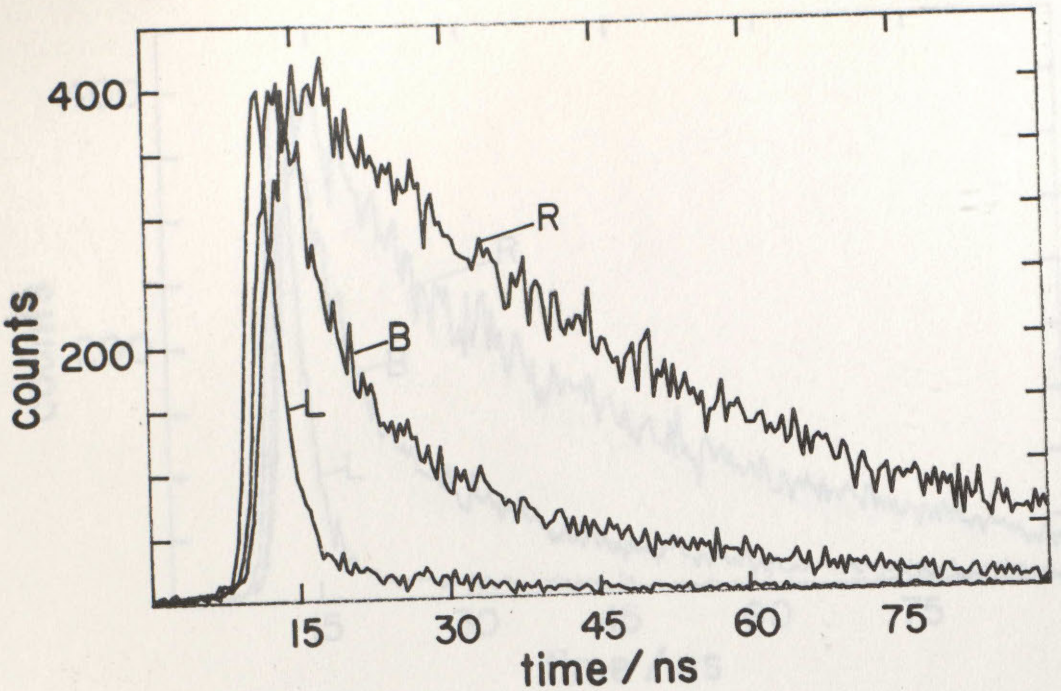

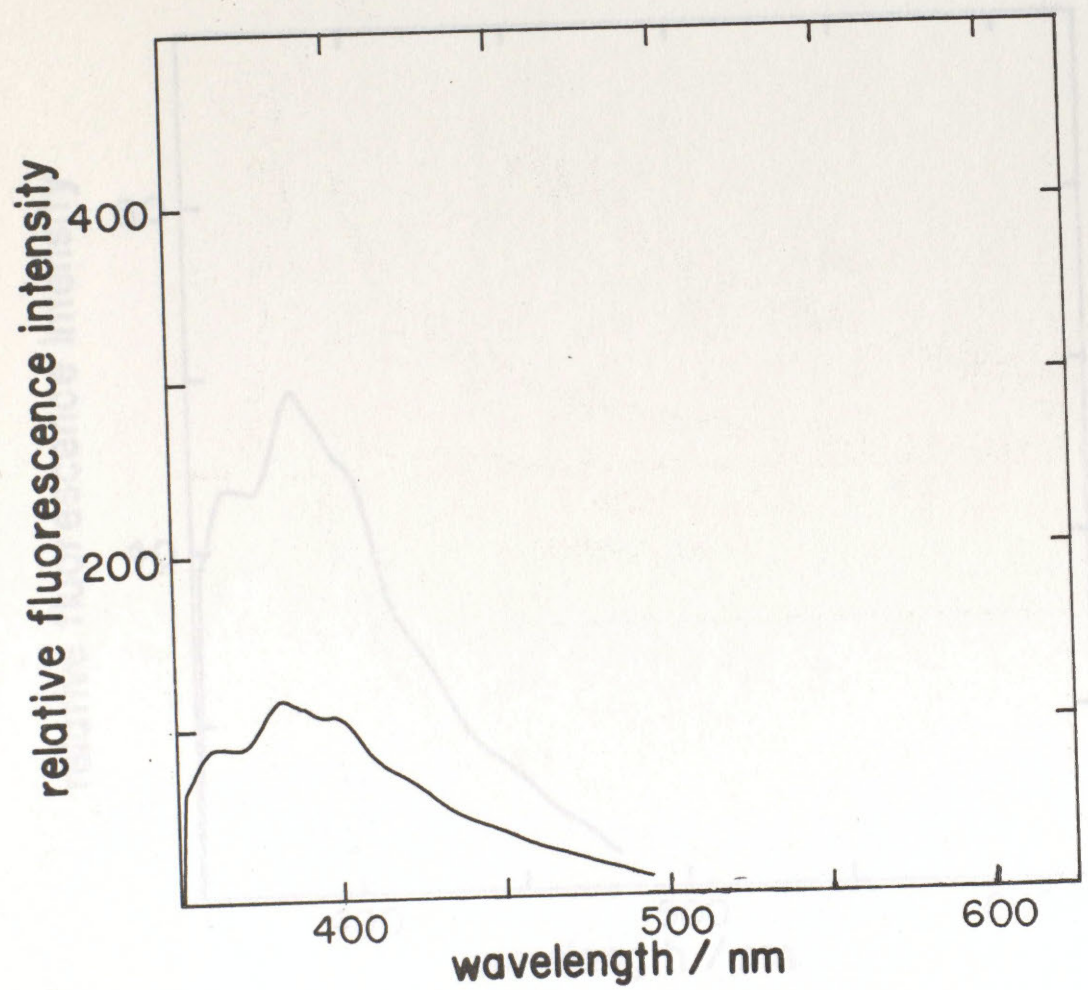

L03 AFTER 24 HOURS AGING

R
S
400
200
counts
15
30
45
60
75
time / ns

400
200
relative fluorescence intensity
400
500
600
wavelength / nm

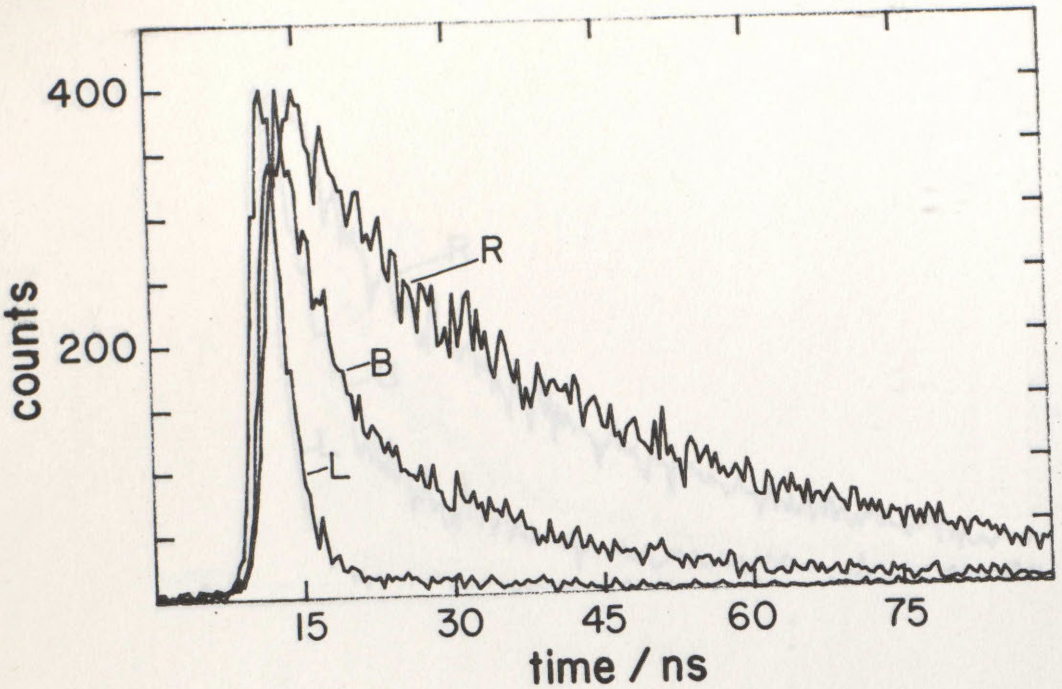

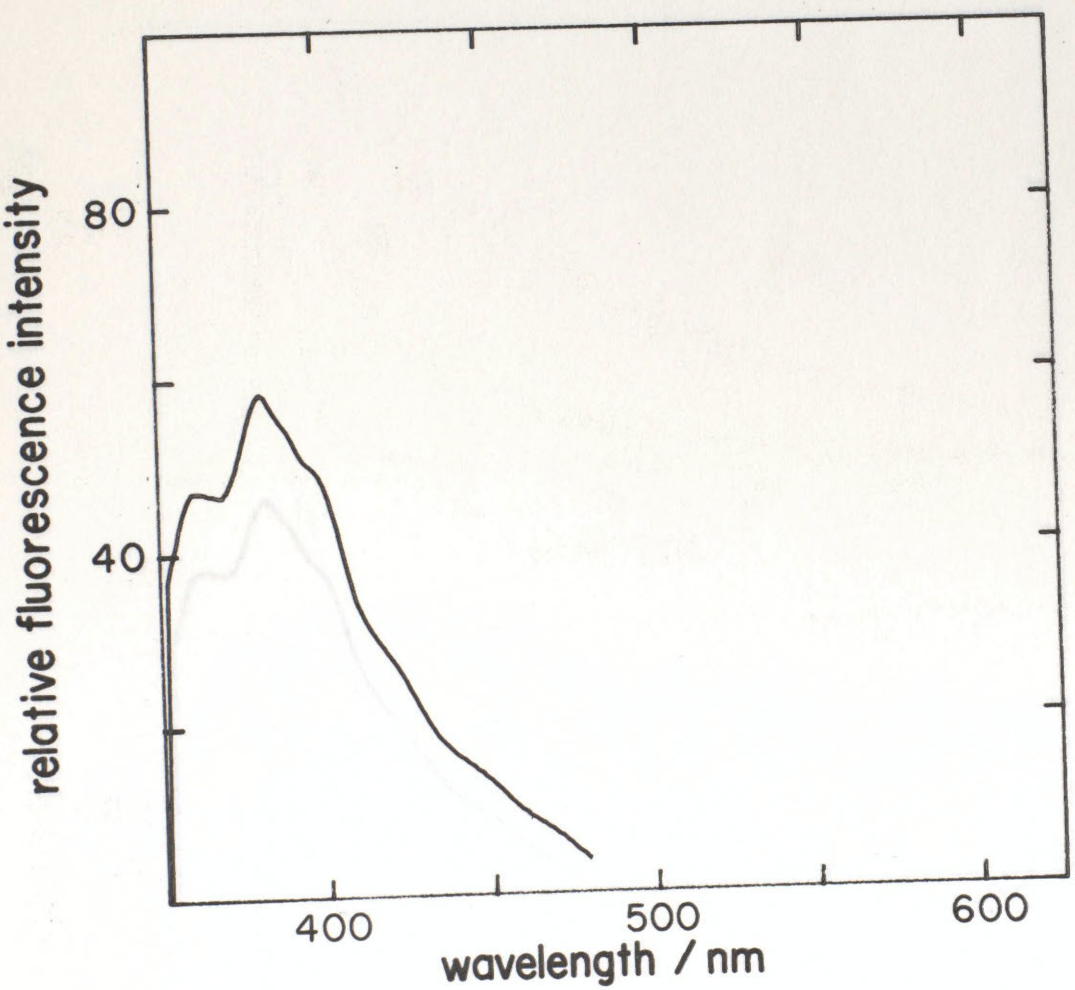

L03 AFTER 48 HOURS AGING

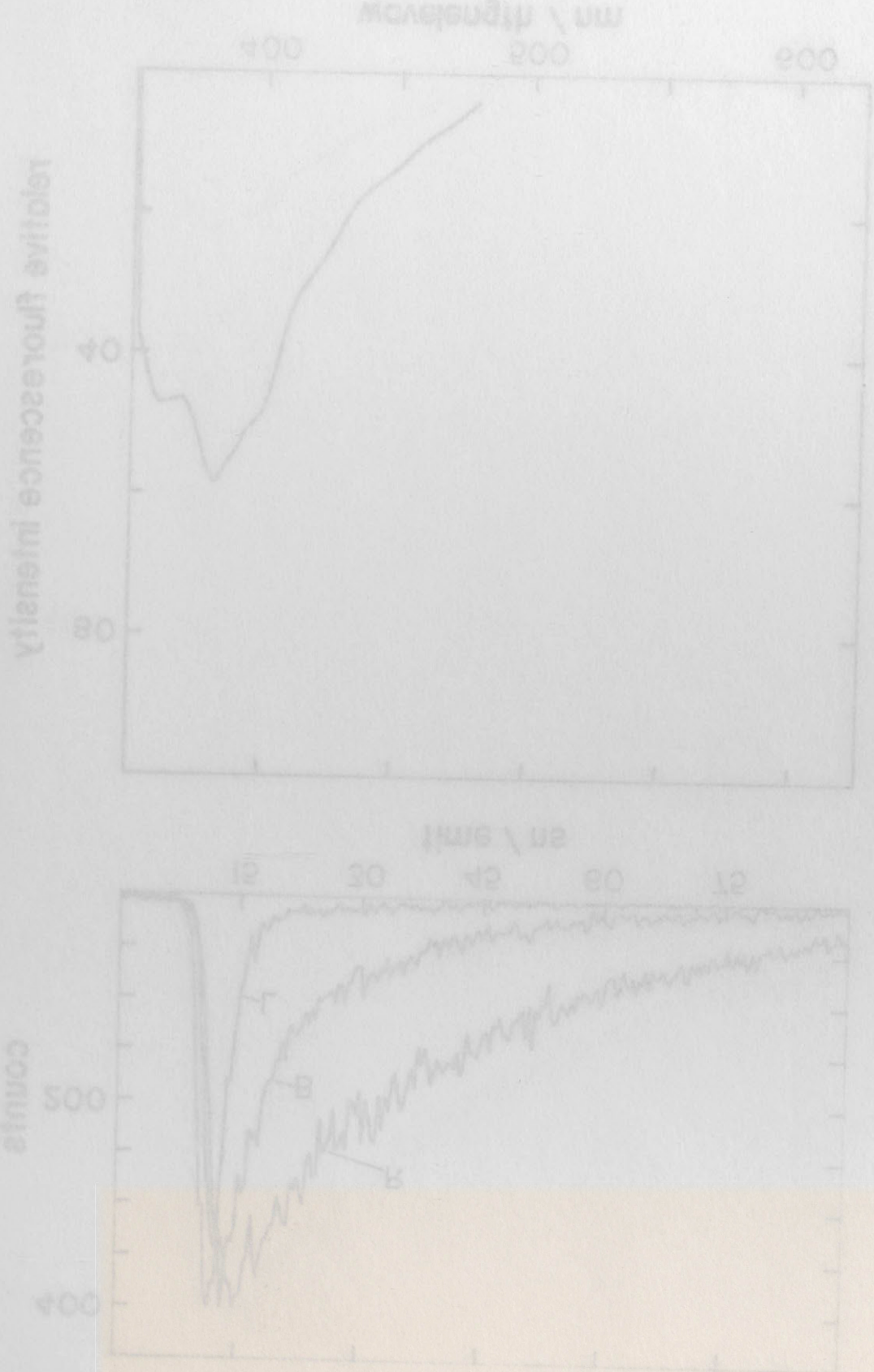
Relative fluorescence intensity
Wavelength / nm
Counts
Time / ns
B
A

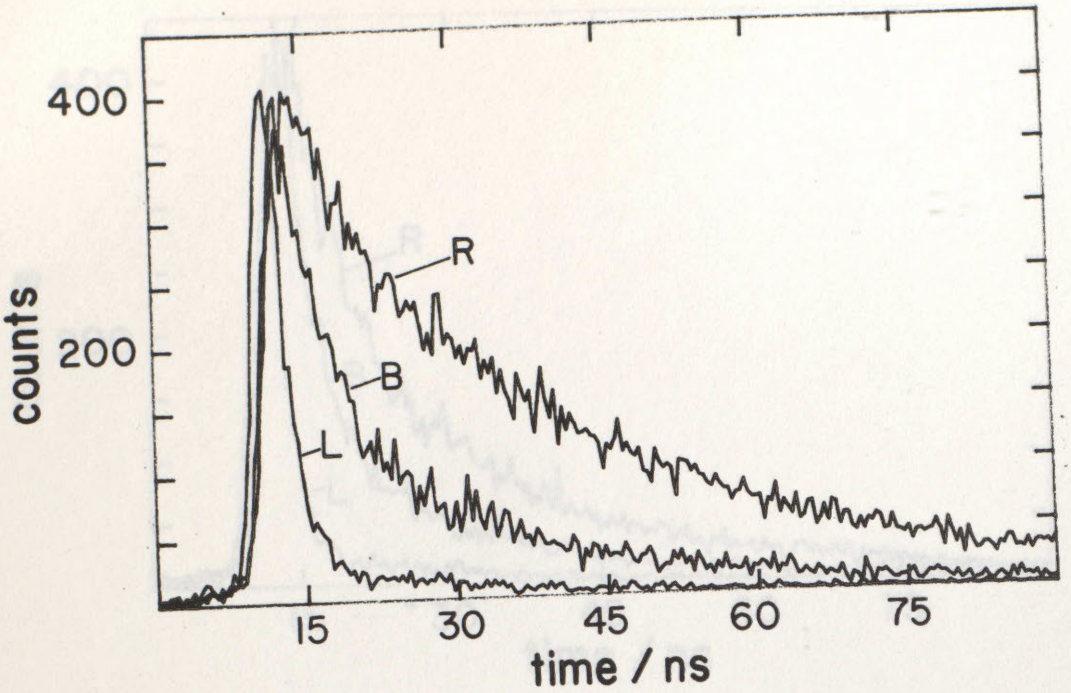

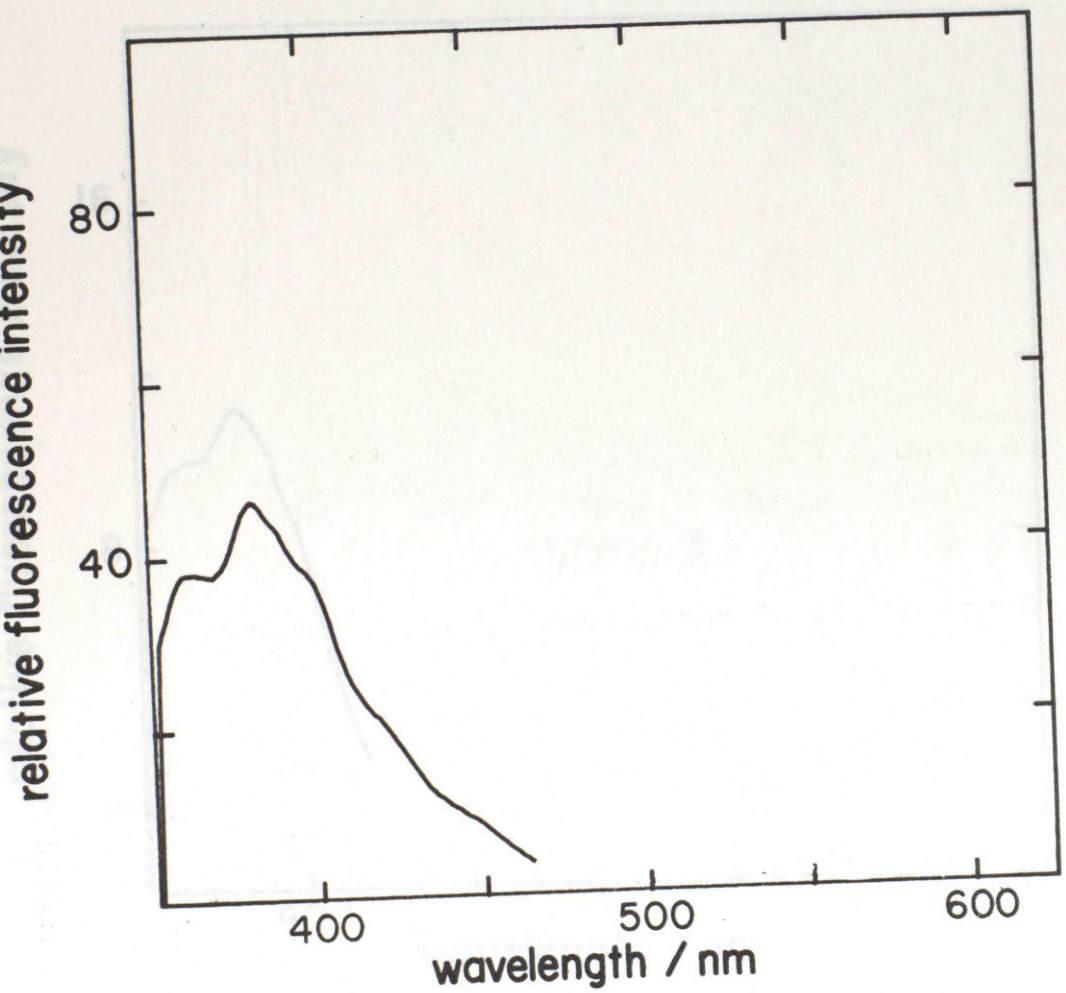

LO3 AFTER 72 HOURS AGING

R
S
L
400
200
counts
15
30
45
60
75
time / ns

80
40
time-integrated emission
600
500
400
wavelength / nm

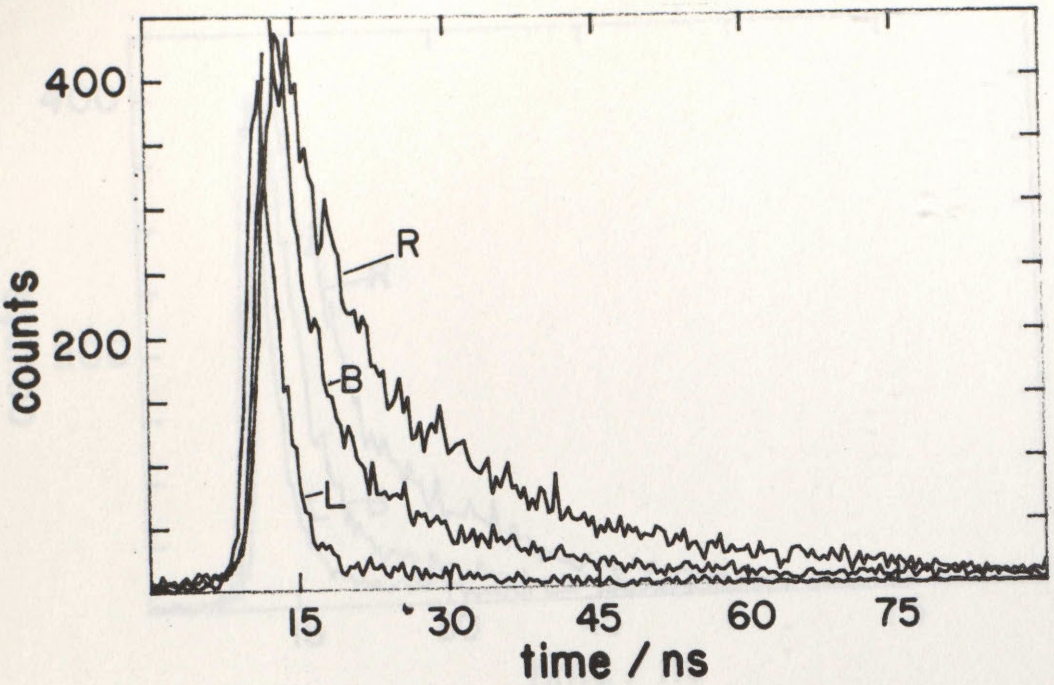

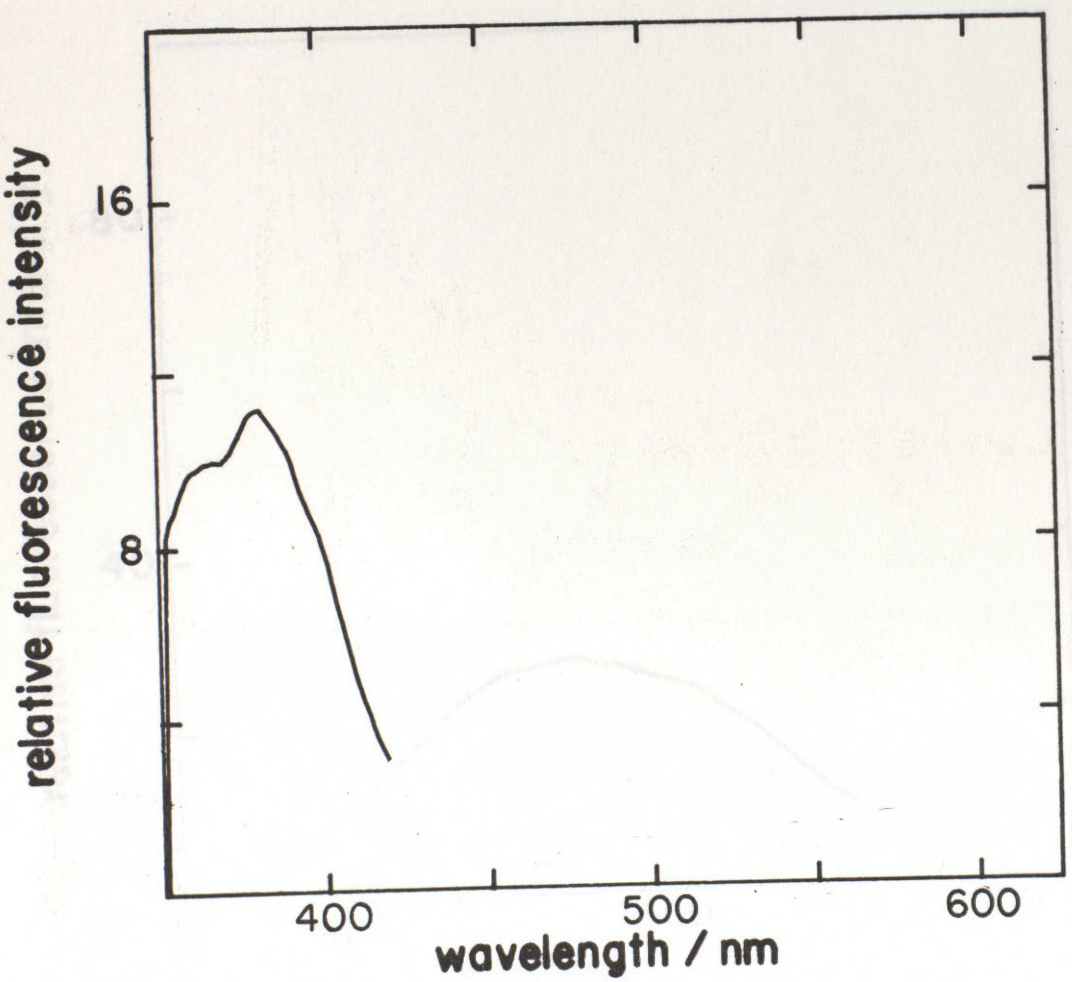

L03 AFTER 114 HOURS AGING

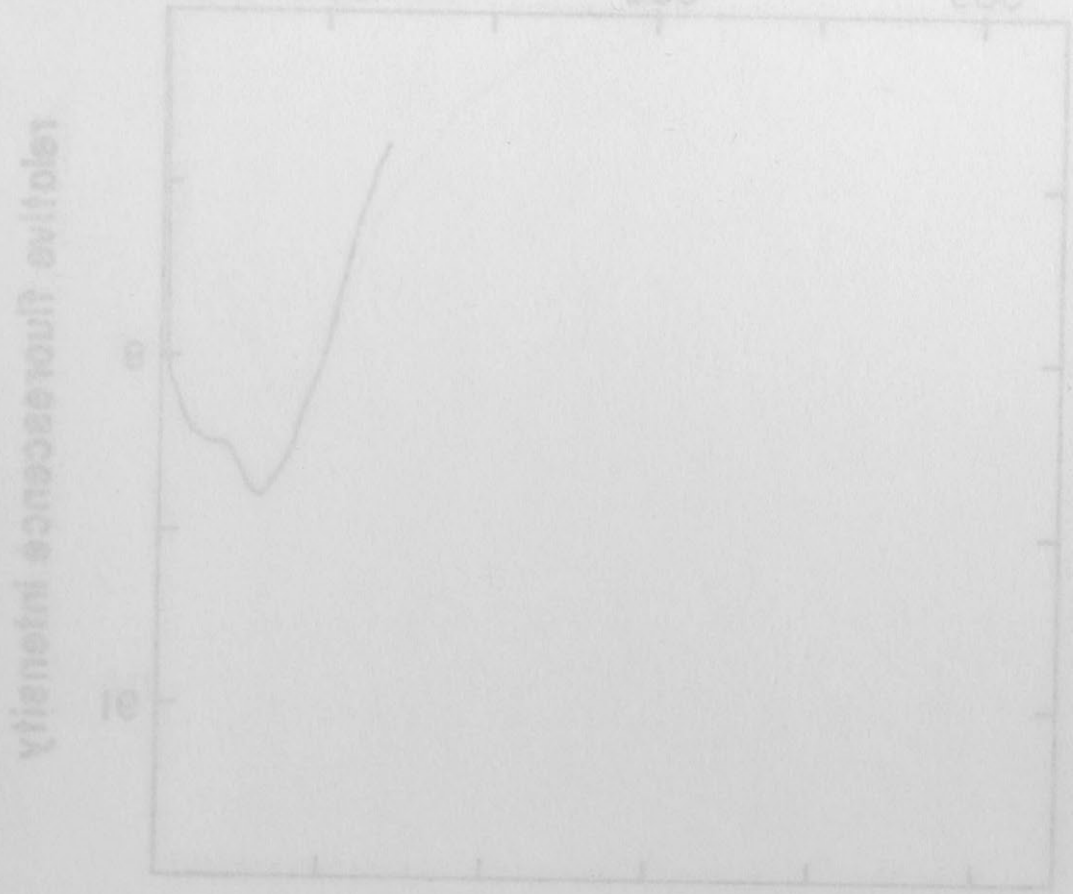
relative fluorescence intensity
wavelength / nm

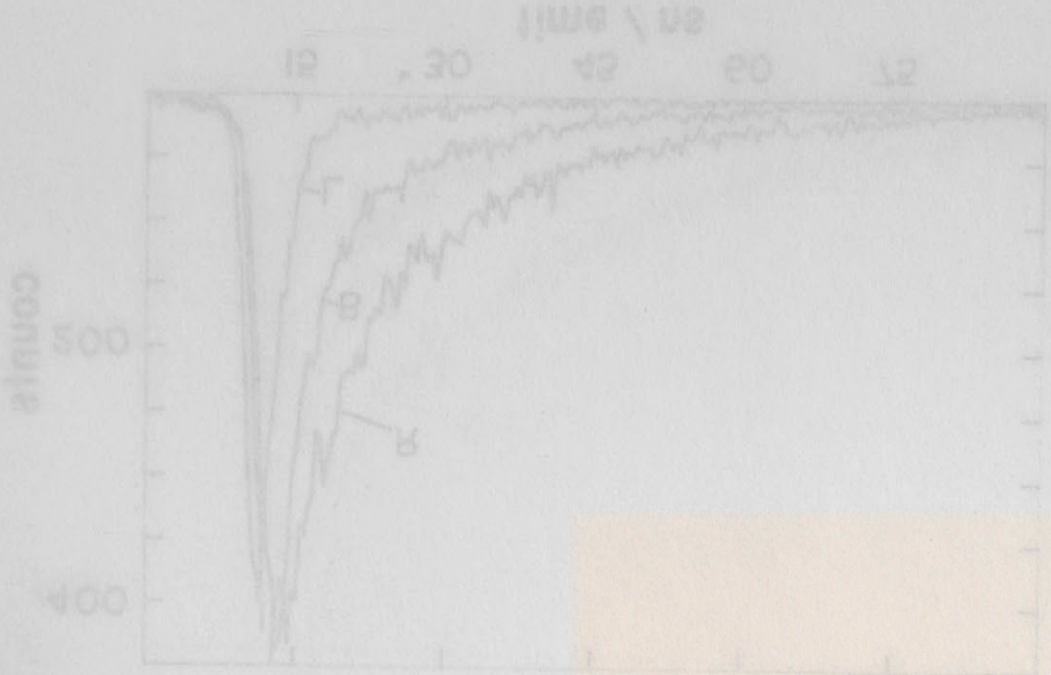
counts
time / ns
A
B
C

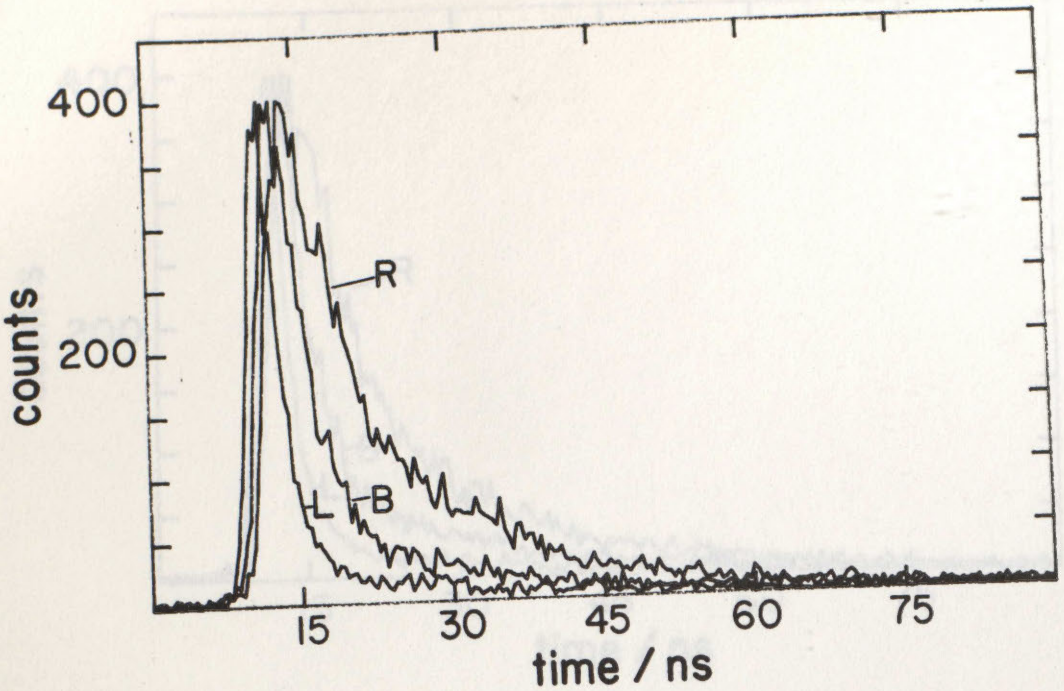

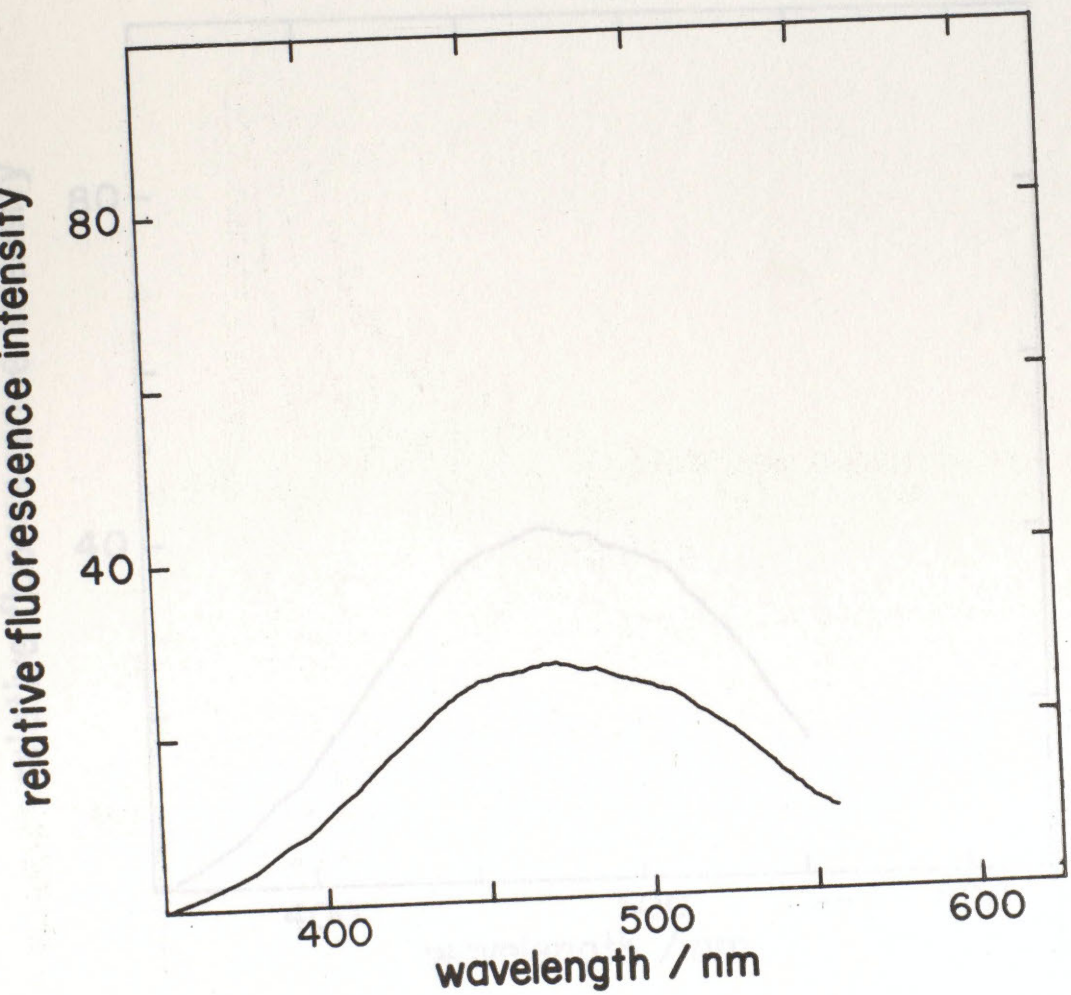

CO2 AFTER 0 HOURS AGING

R
counts
time / ns

relative fluorescence intensity
wavelength / nm

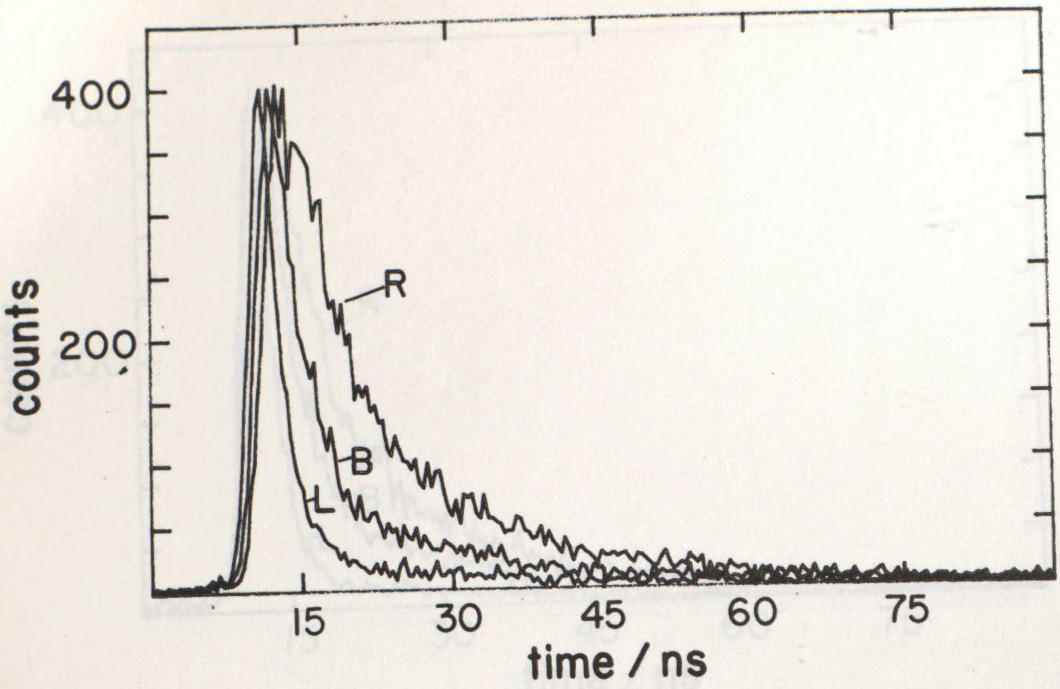

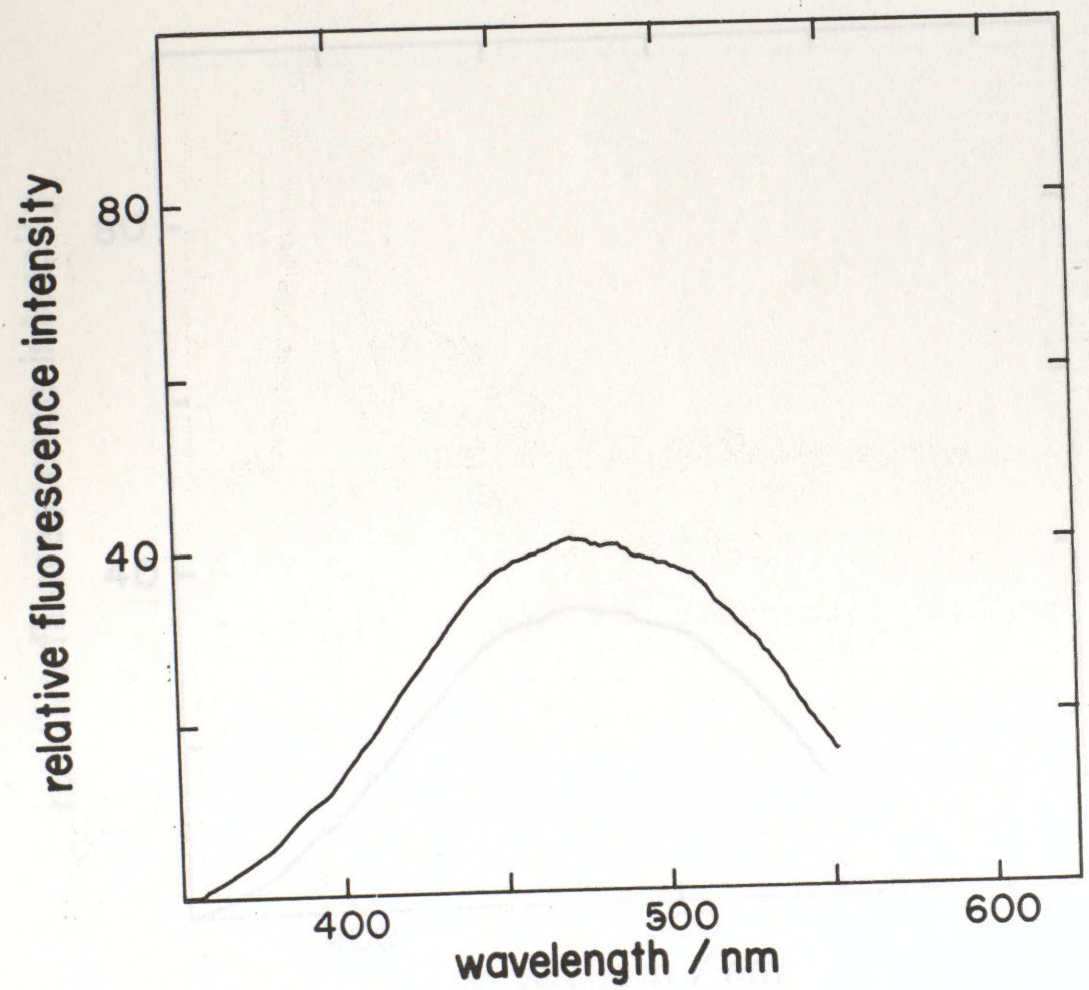

CO2 AFTER 24 HOURS AGING

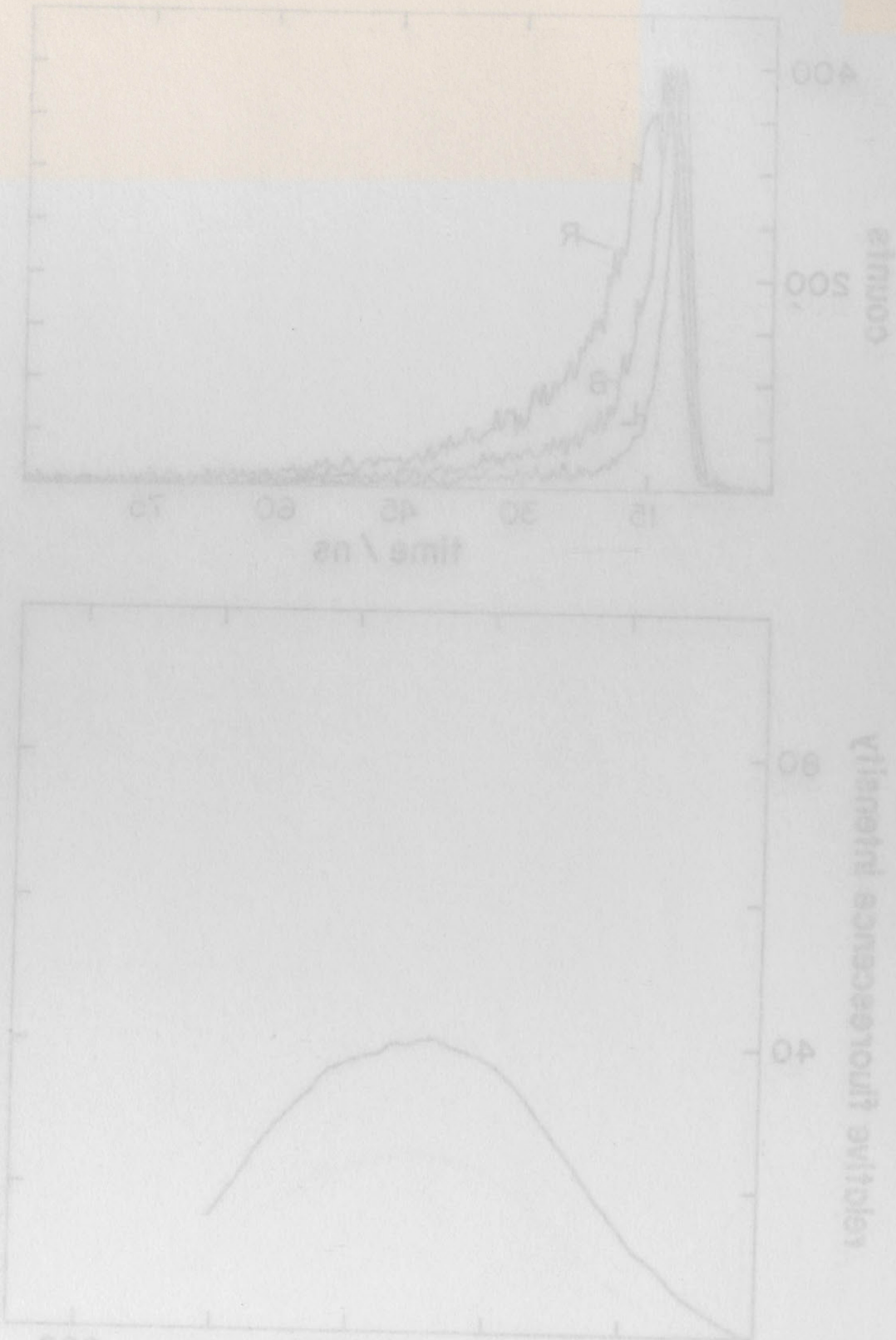
R
B
time / ns
wavelength / nm
relative fluorescence intensity

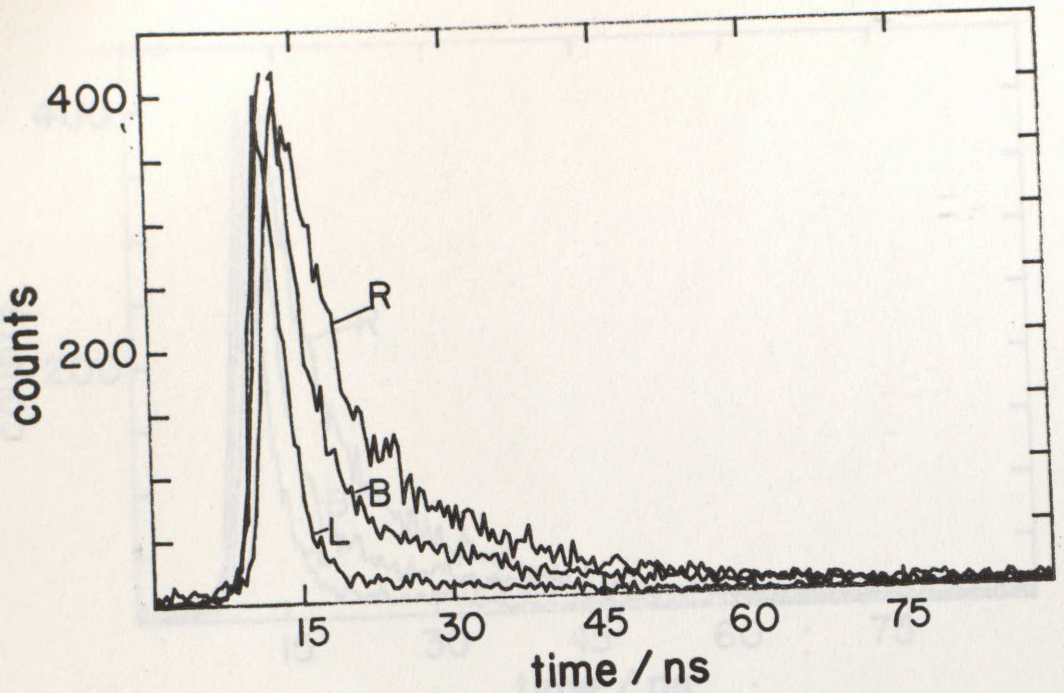

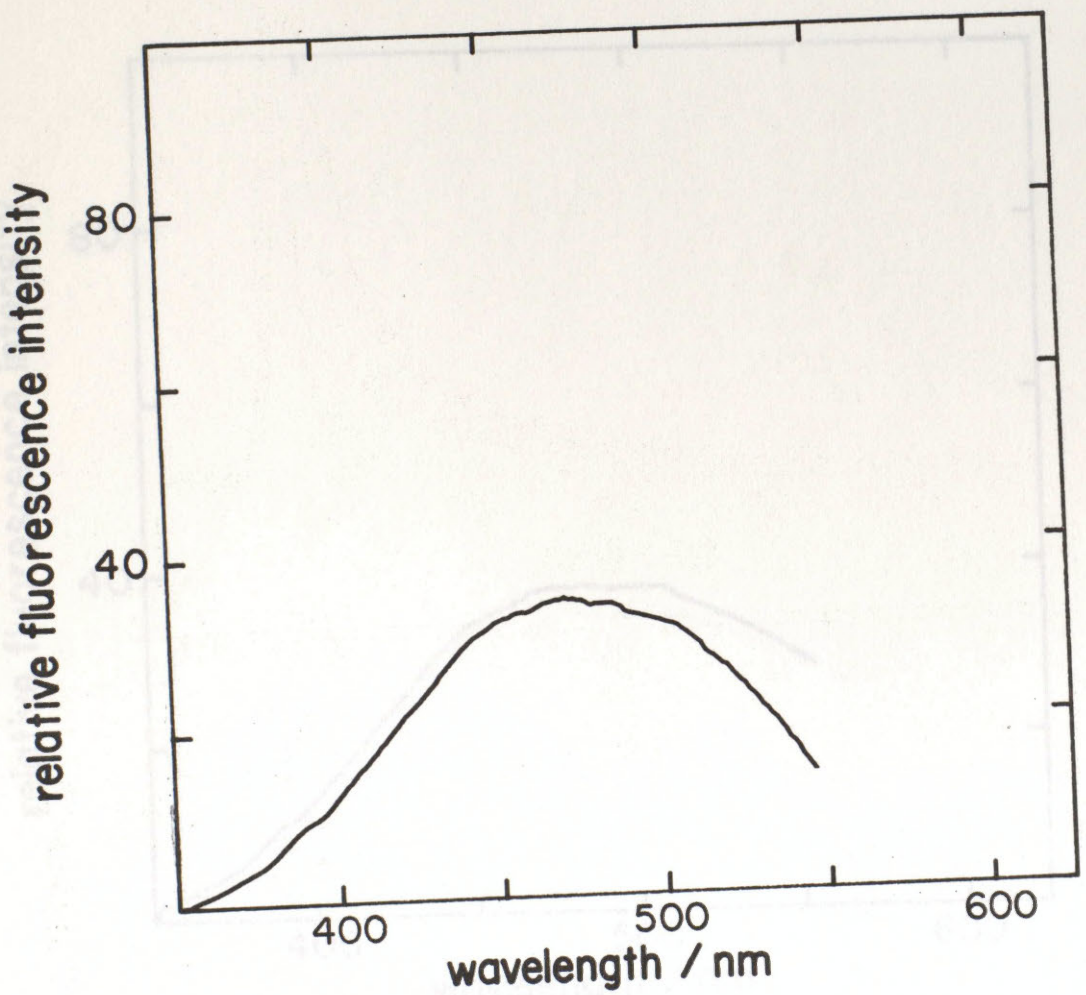

CO2 AFTER 48 HOURS AGING

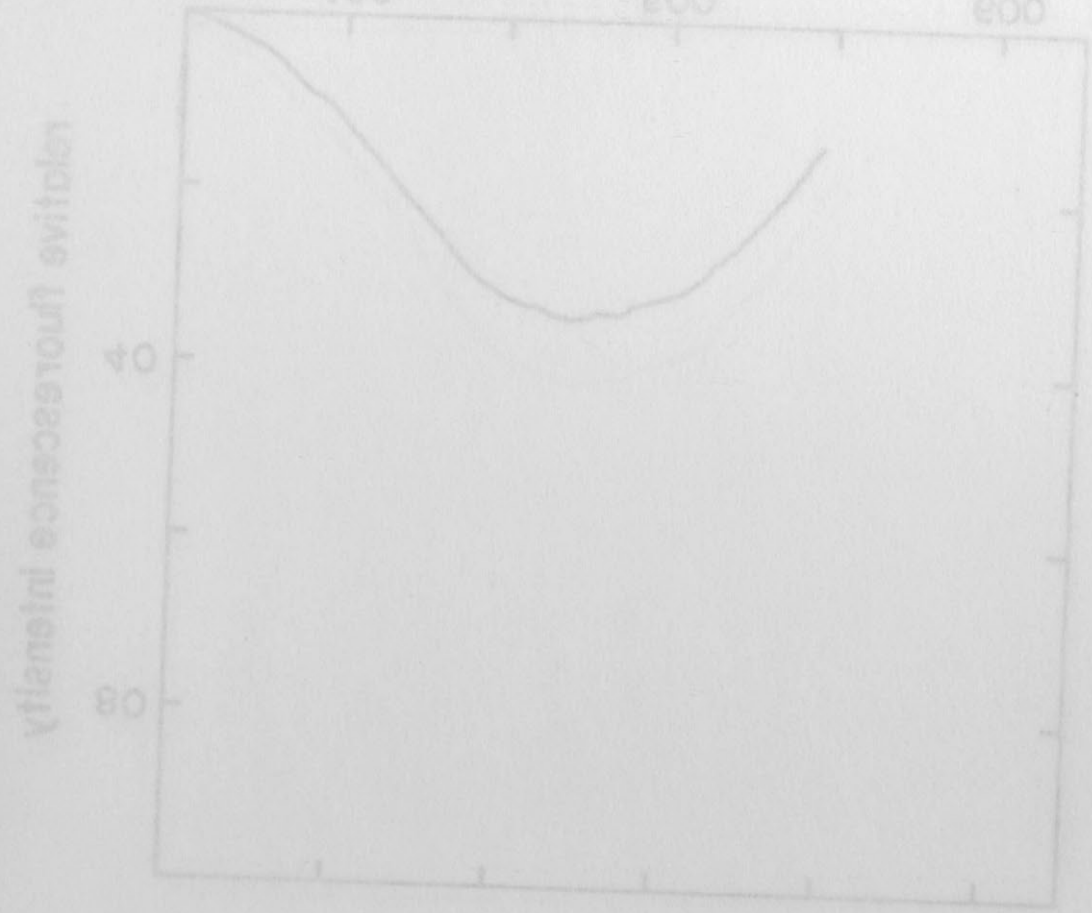
relative fluorescence intensity
0.8
0.4
600
500
400
wavelength / nm

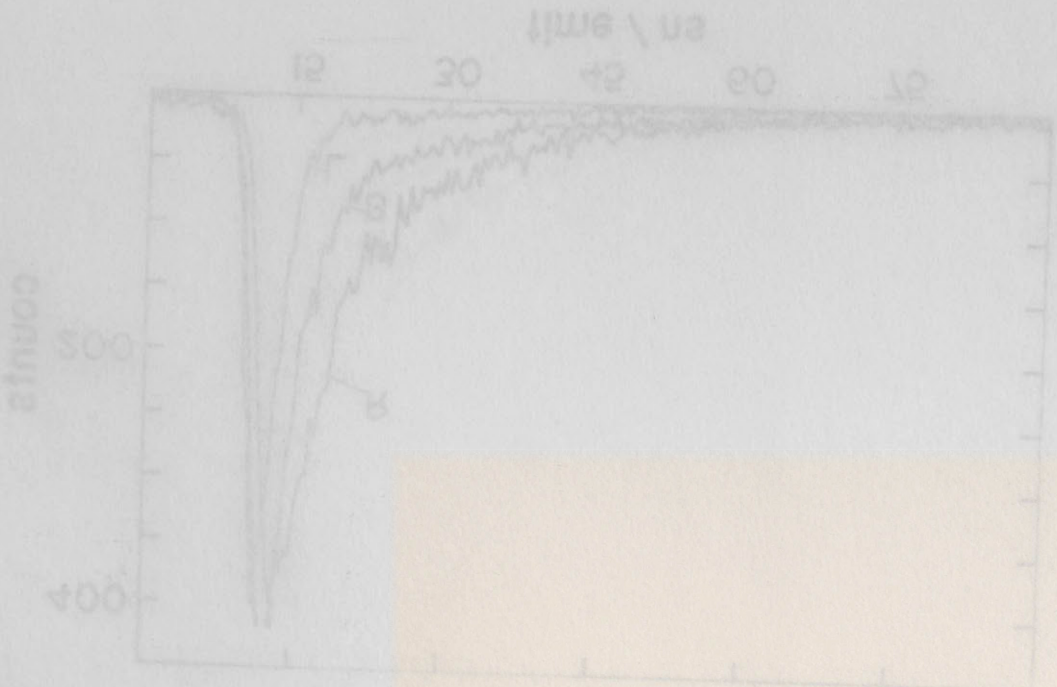
counts
500
400
time / ms
15
30
45
60
75

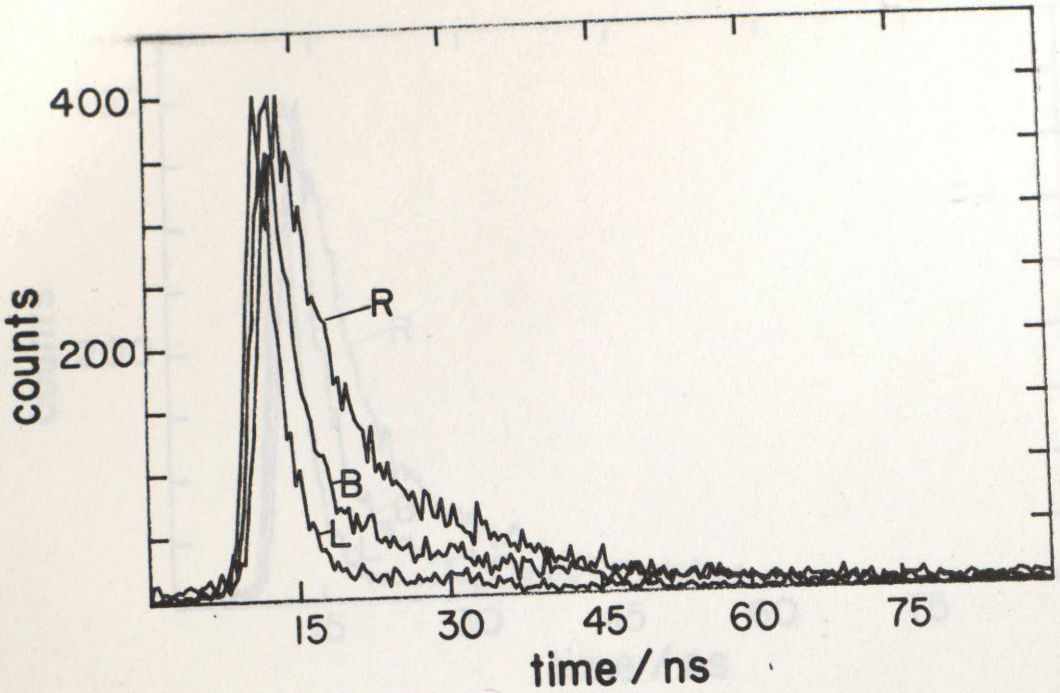

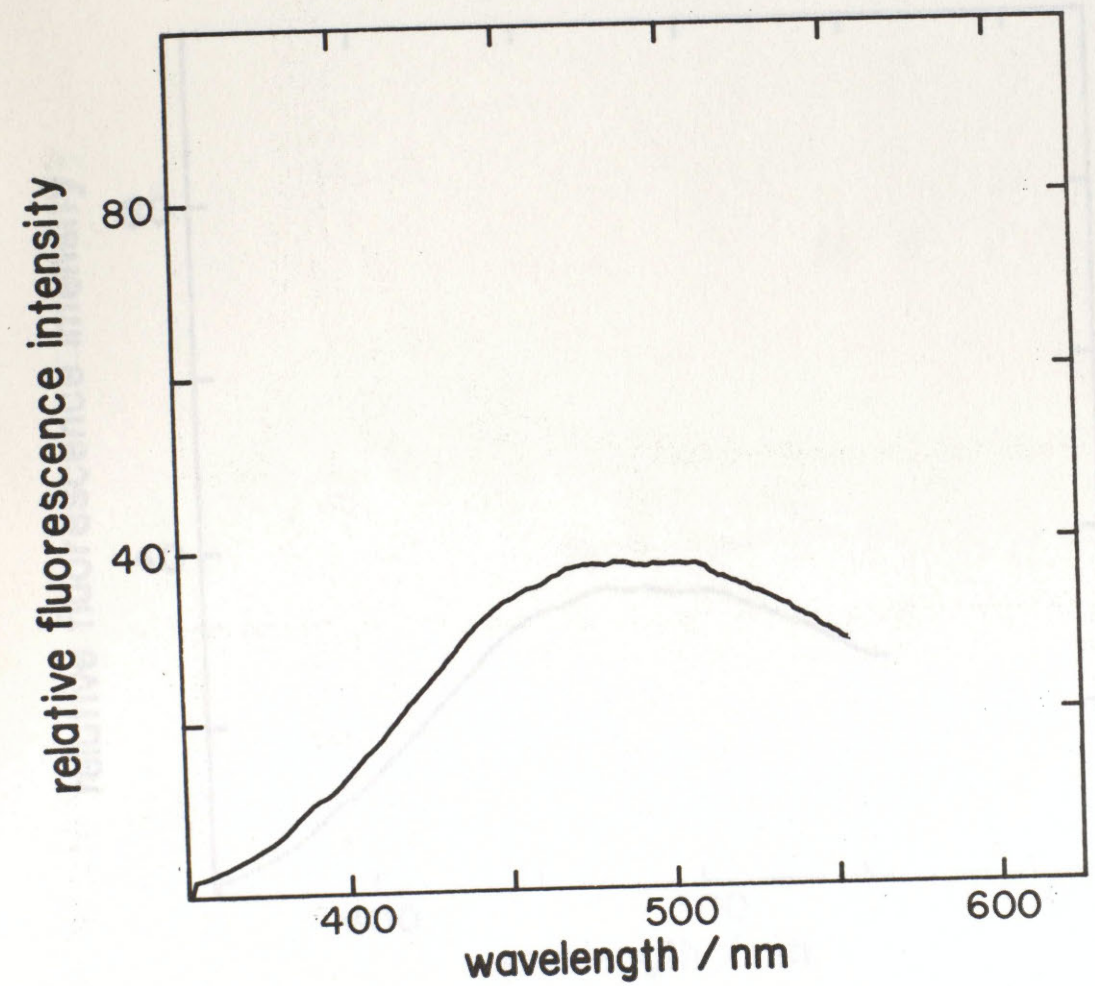

CO2 AFTER 72 HOURS AGING

counts
time / ns

relative fluorescence intensity
wavelength / nm

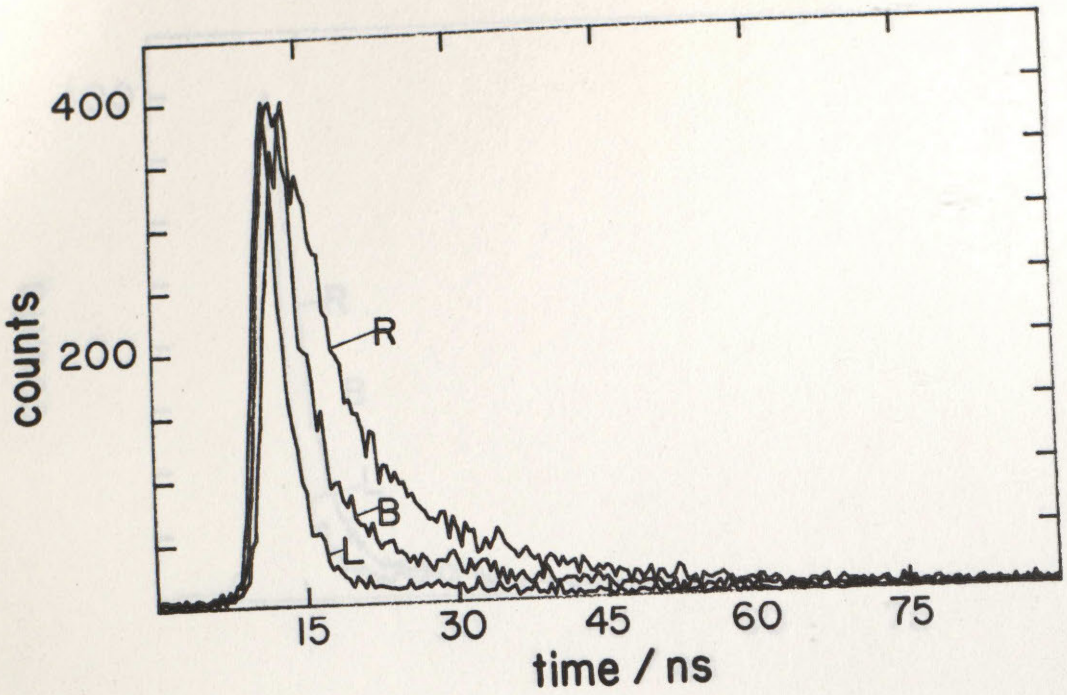

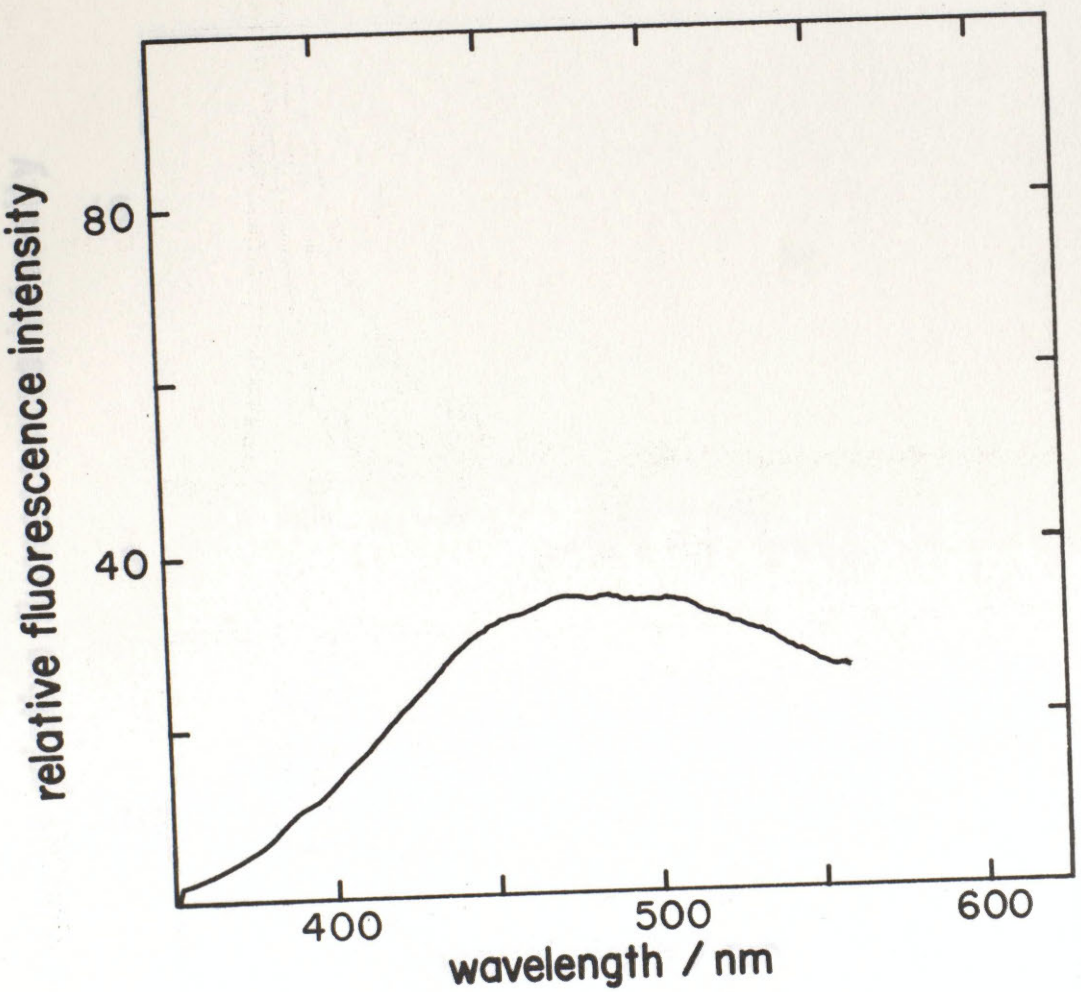

CO2 AFTER 144 HOURS AGING

R
B
time / ns

wavelength / nm

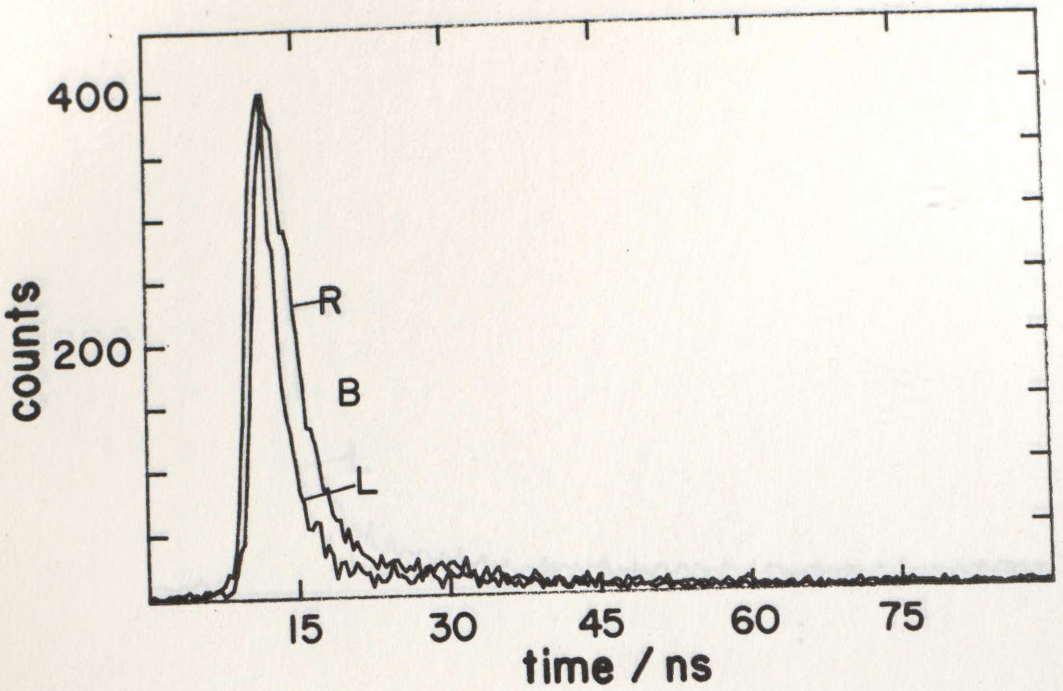

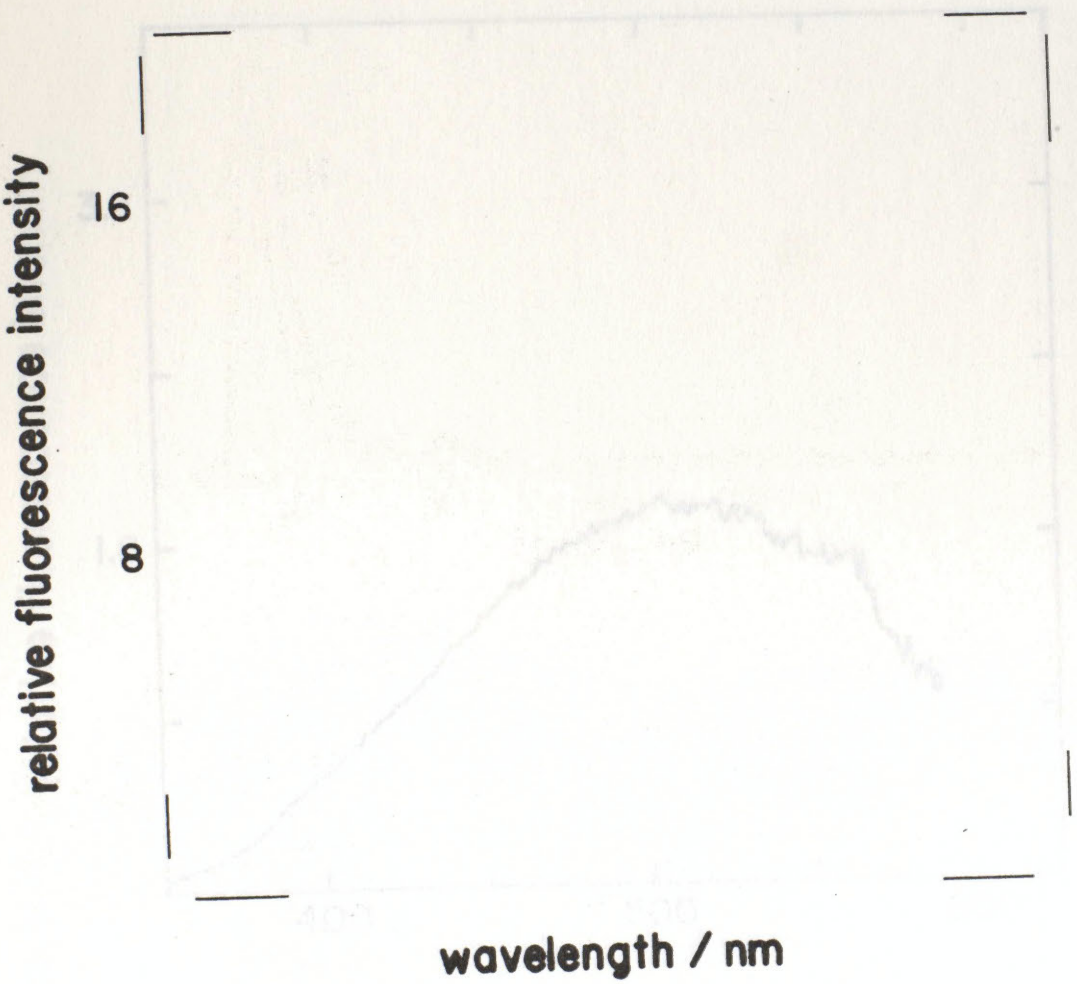

HO2 AFTER 0 HOURS AGING

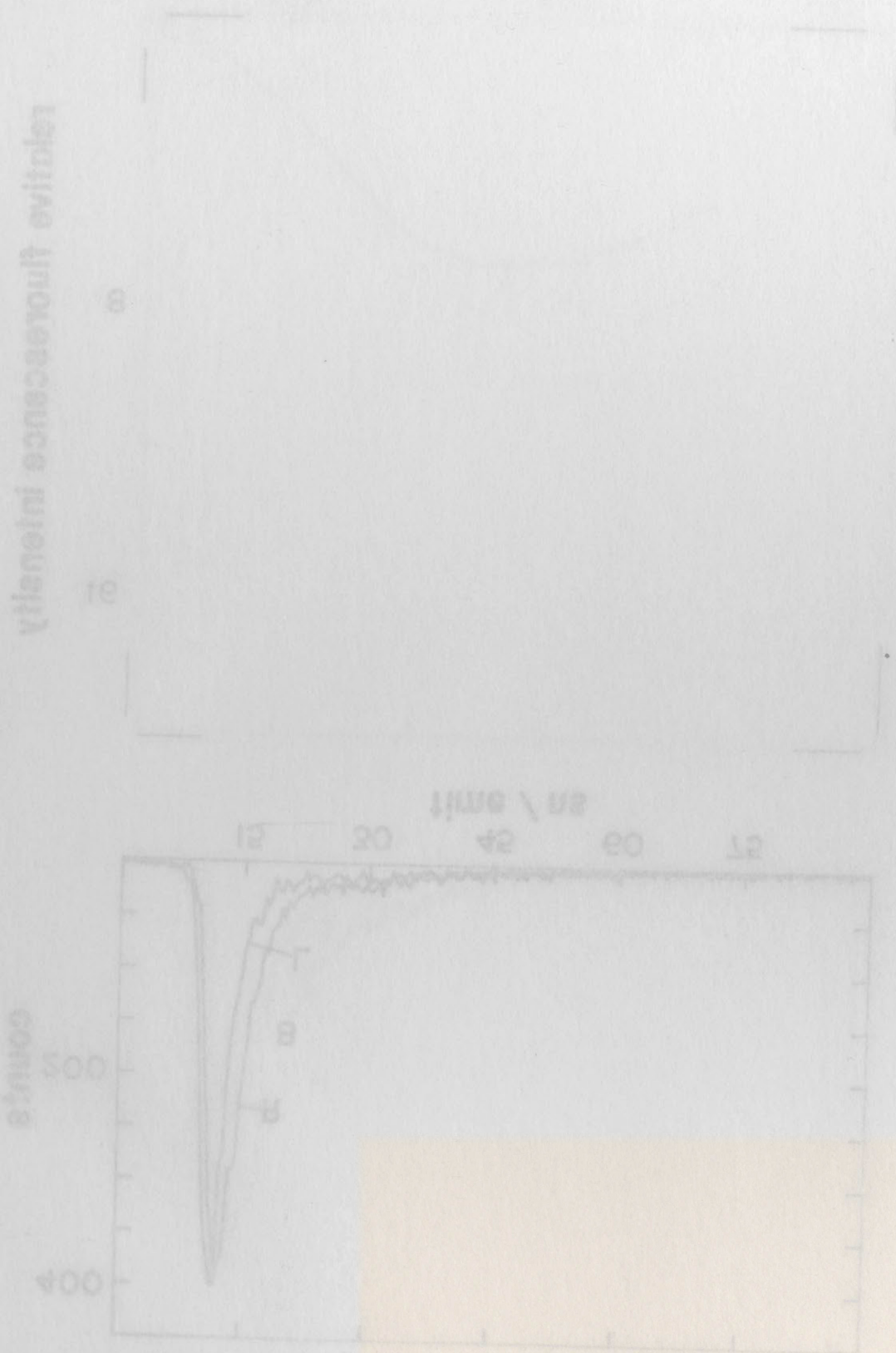

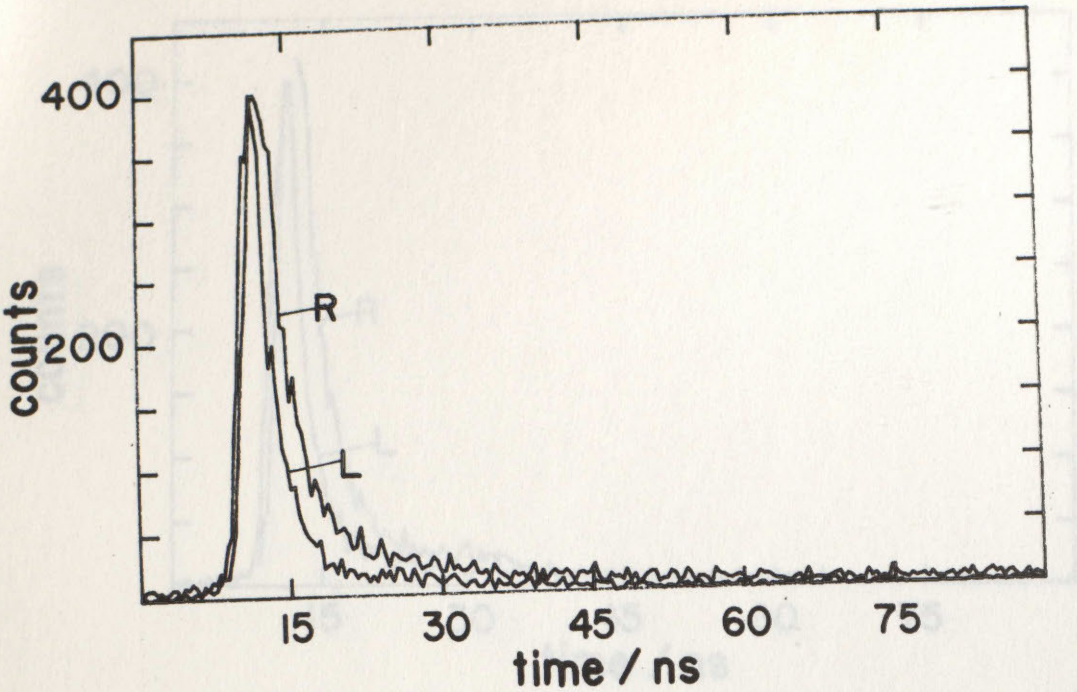

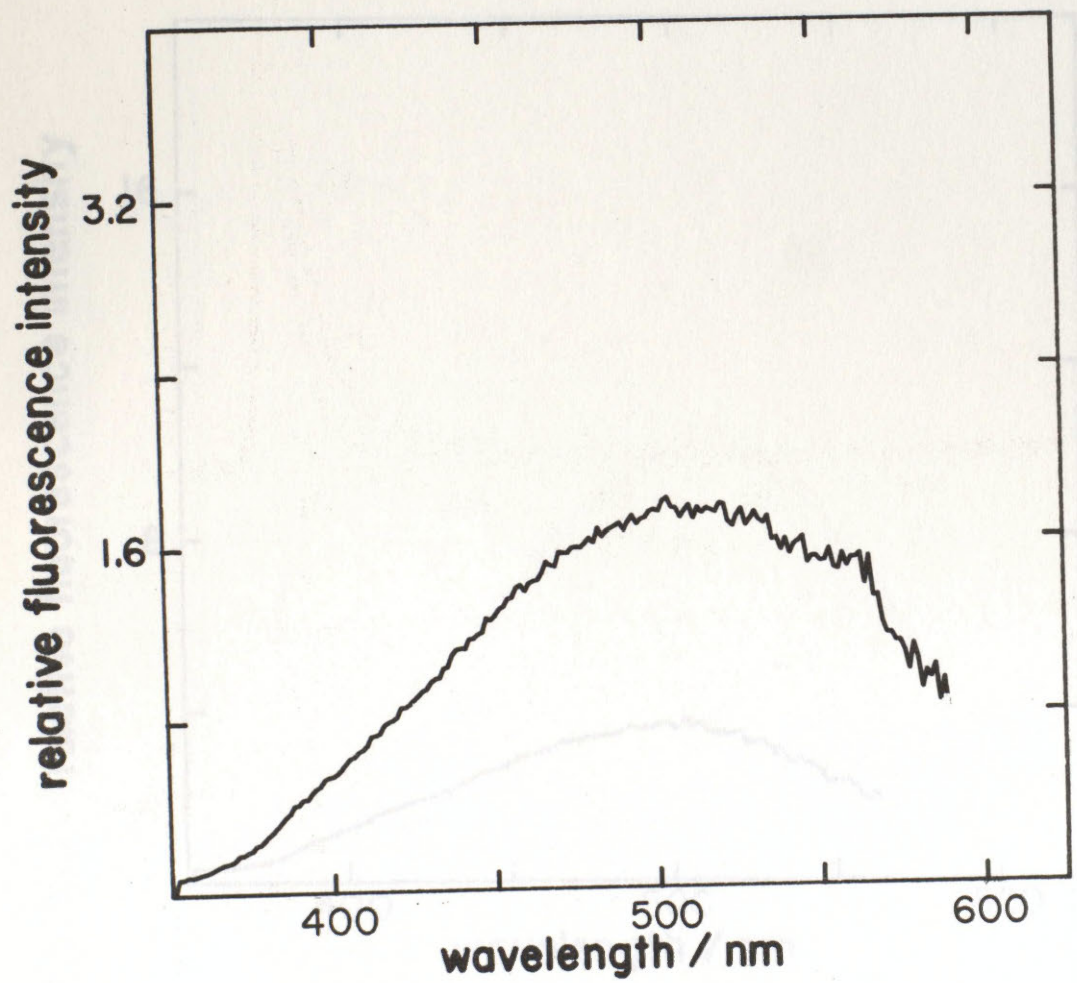

HO2 AFTER 24 HOURS AGING

400
200
counts
15
30
45
60
75
time \ ns

3.2
1.6
relative fluorescence intensity
600
500
400
wavelength \ nm

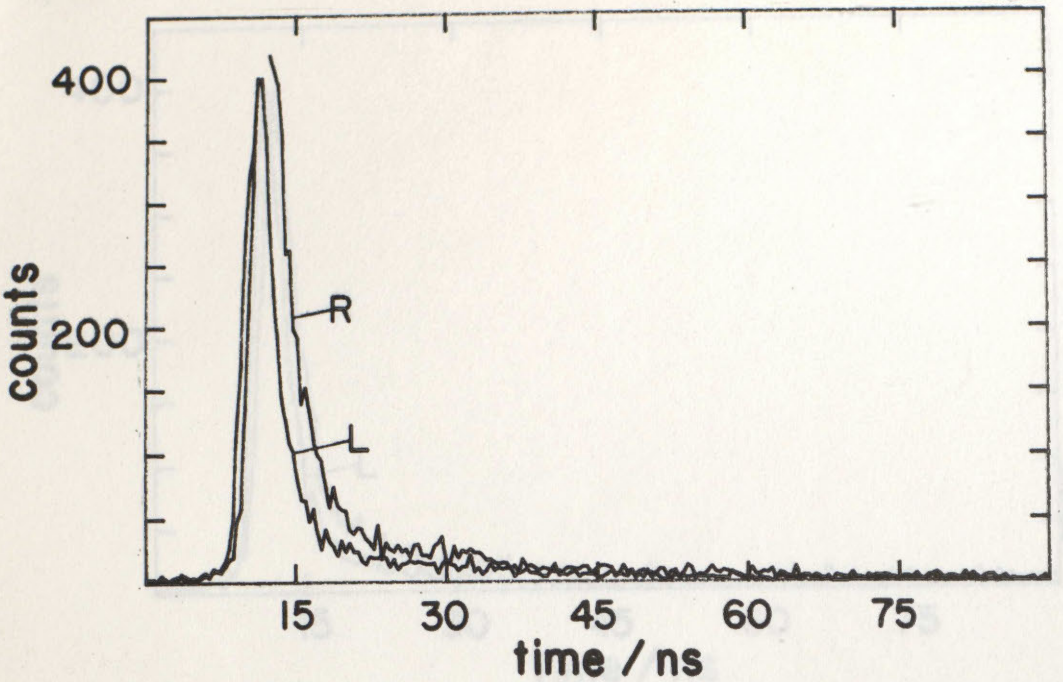

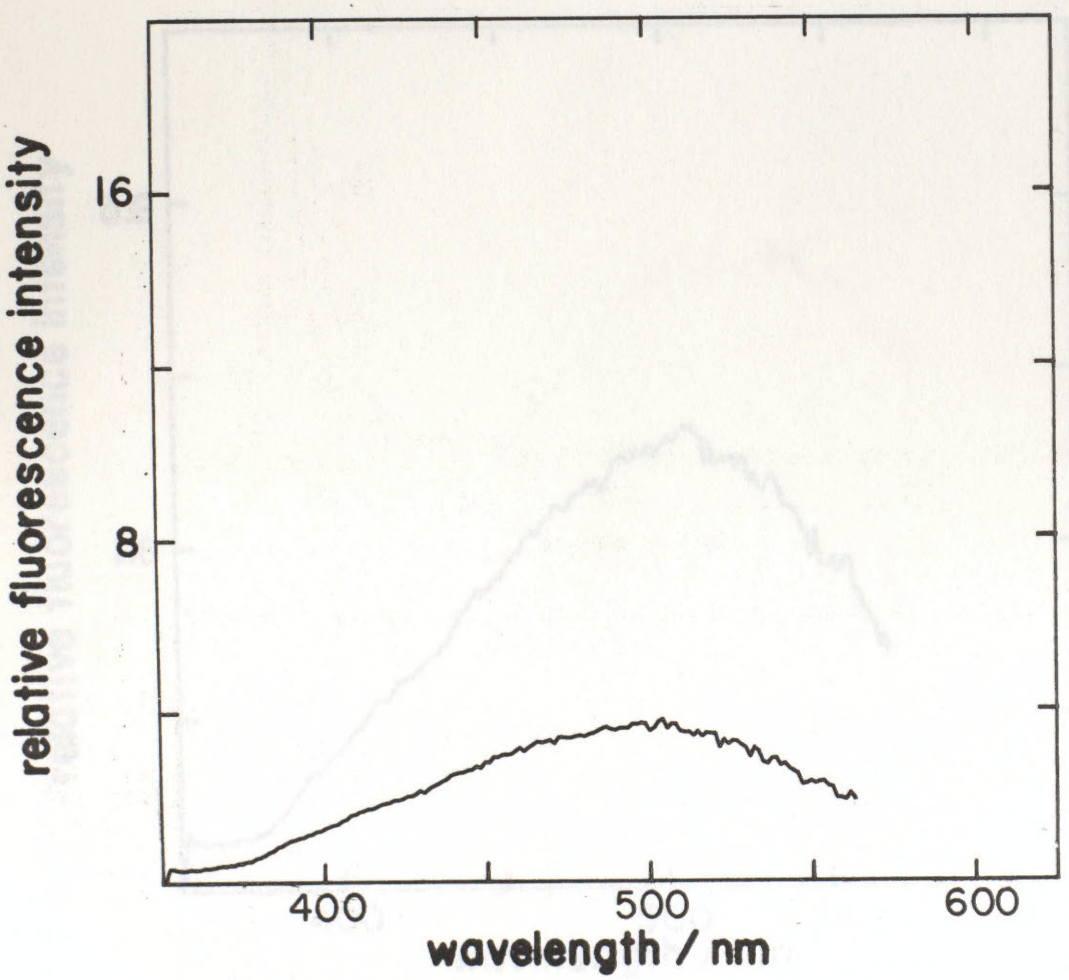

HO2 AFTER 48 HOURS AGING


time / ns

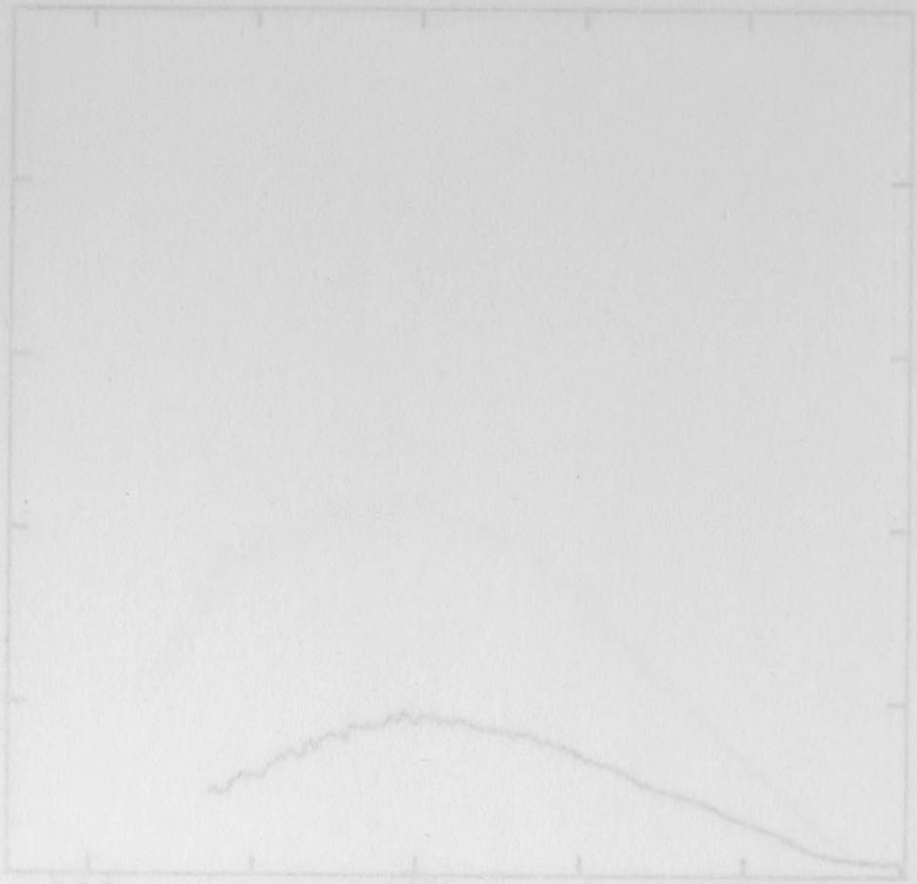
wavelength / nm

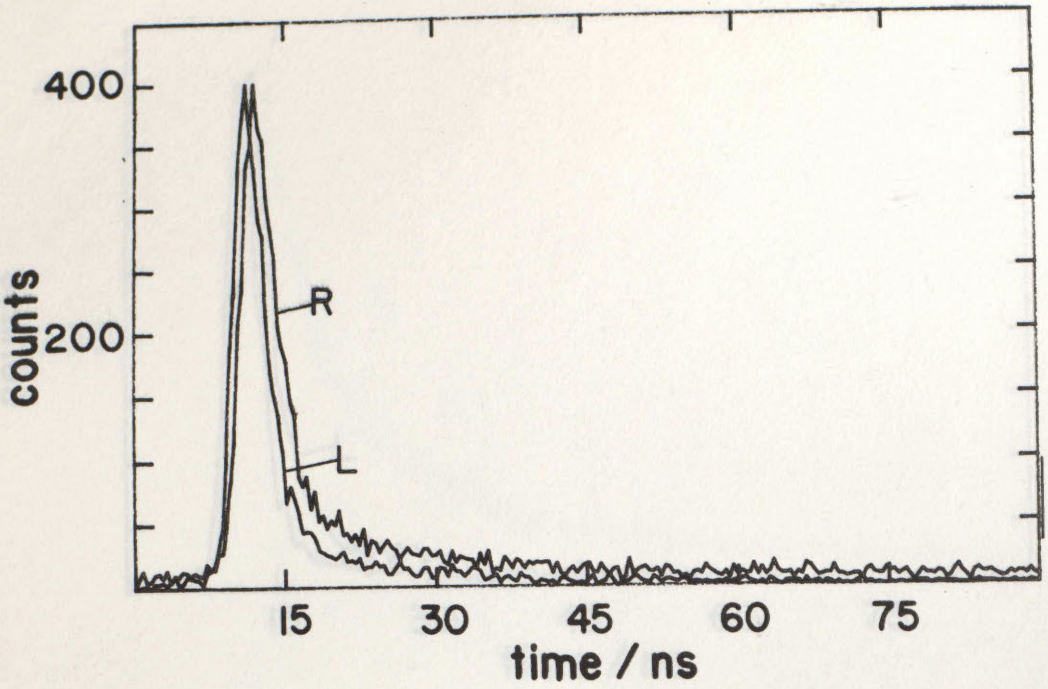

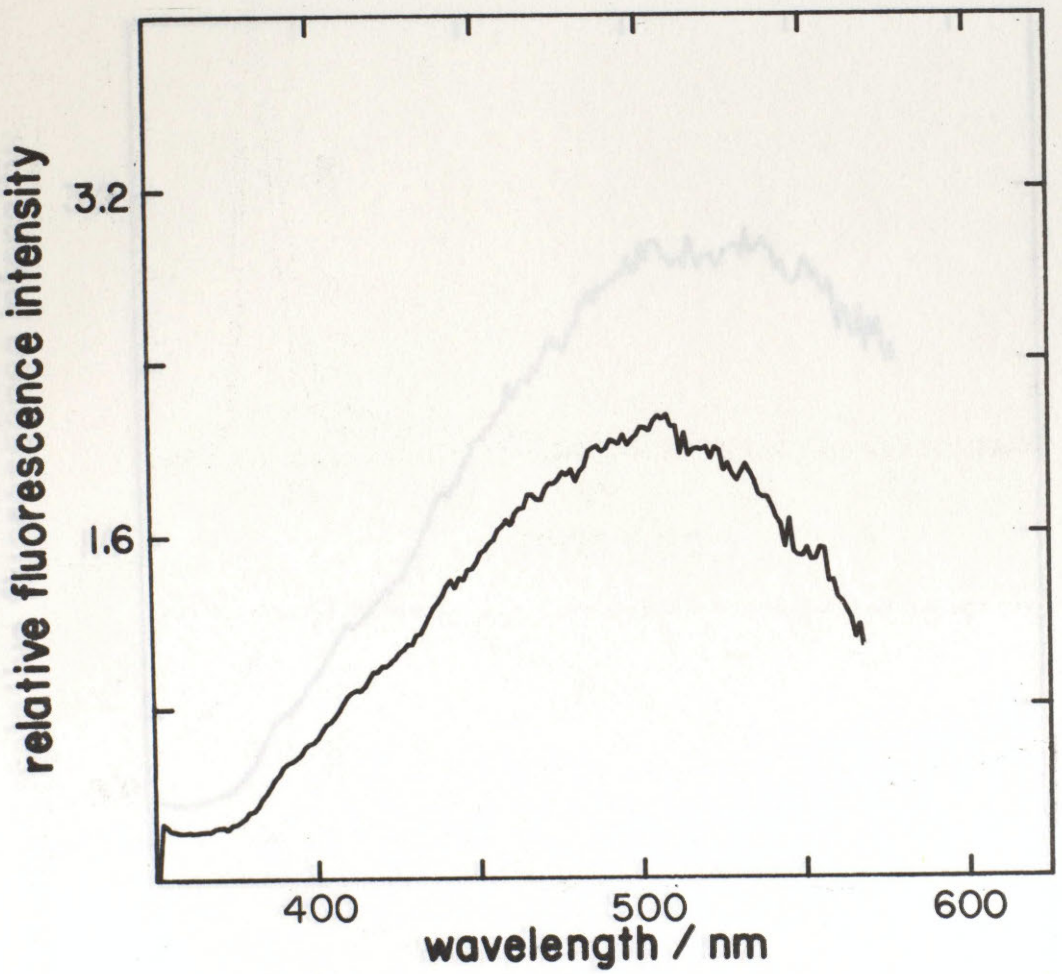

HO2 AFTER 72 HOURS AGING

400
200
counts
R
15
30
45
60
75
time / ns

3.2
1.6
relative fluorescence intensity
400
500
600
wavelength / nm

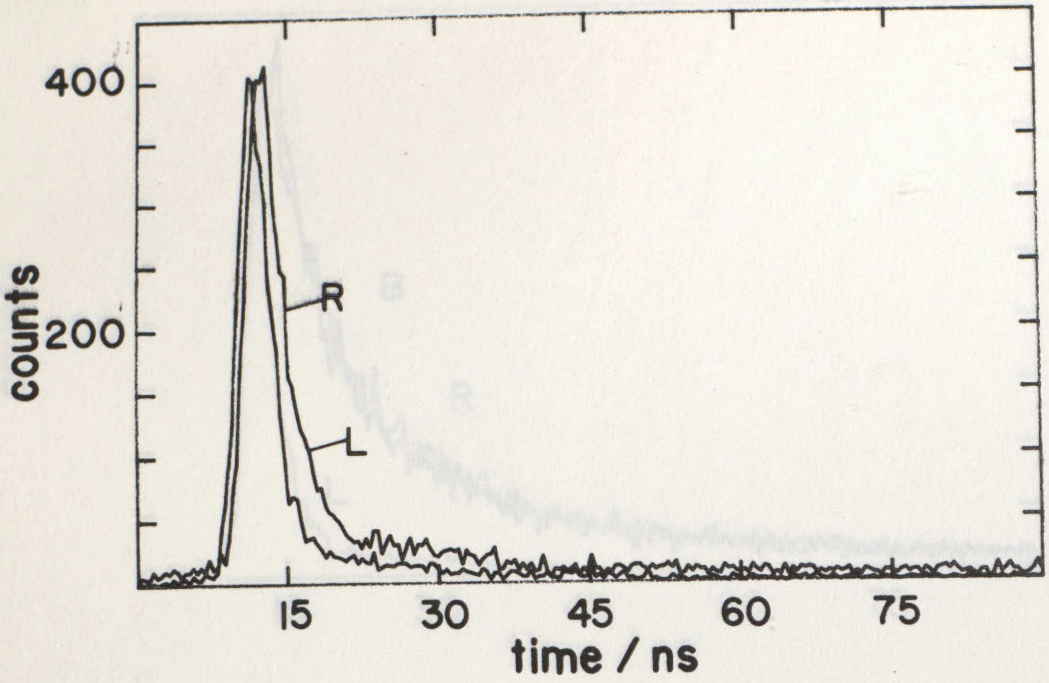

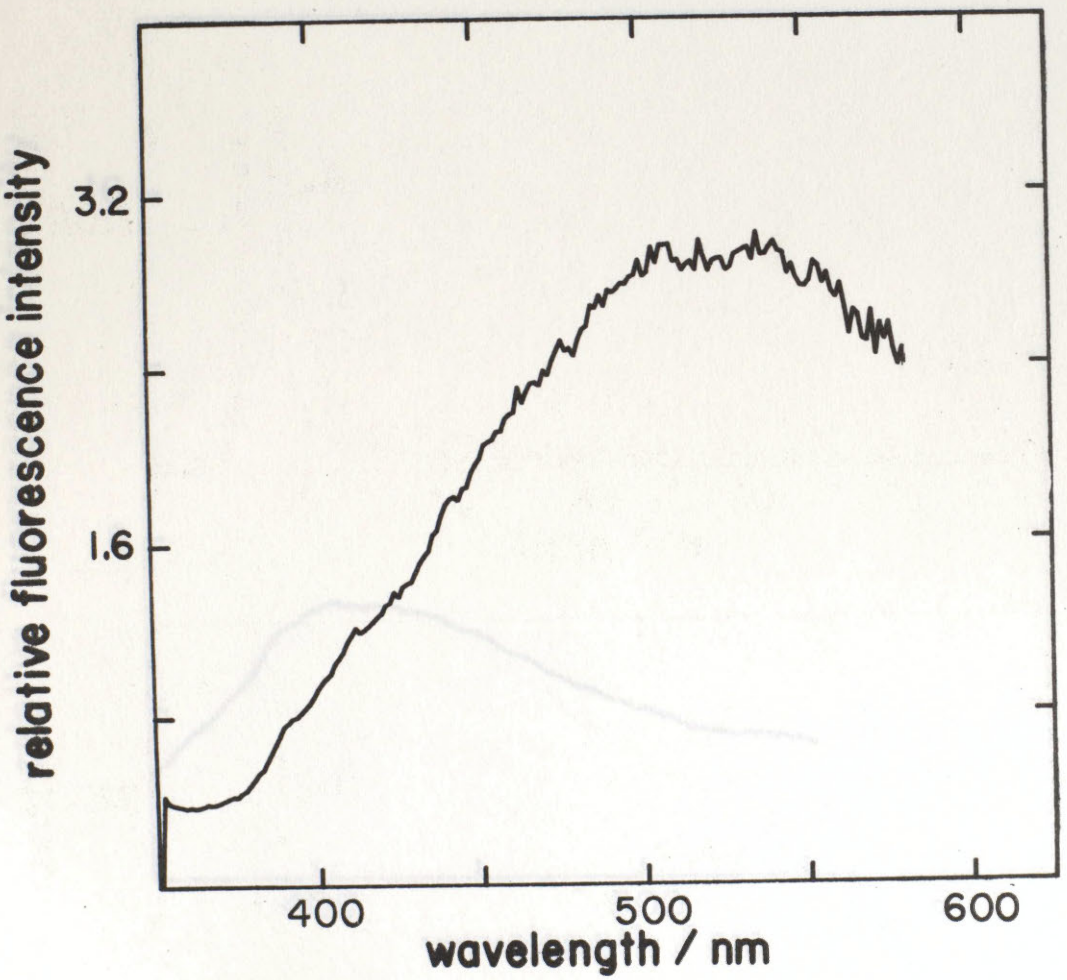

HO2 AFTER 144 HOURS AGING

400
200
counts
IF
IL
15
30
45
60
75
time / ns

3.2
1.6
Relative fluorescence intensity
400
500
600
wavelength / nm

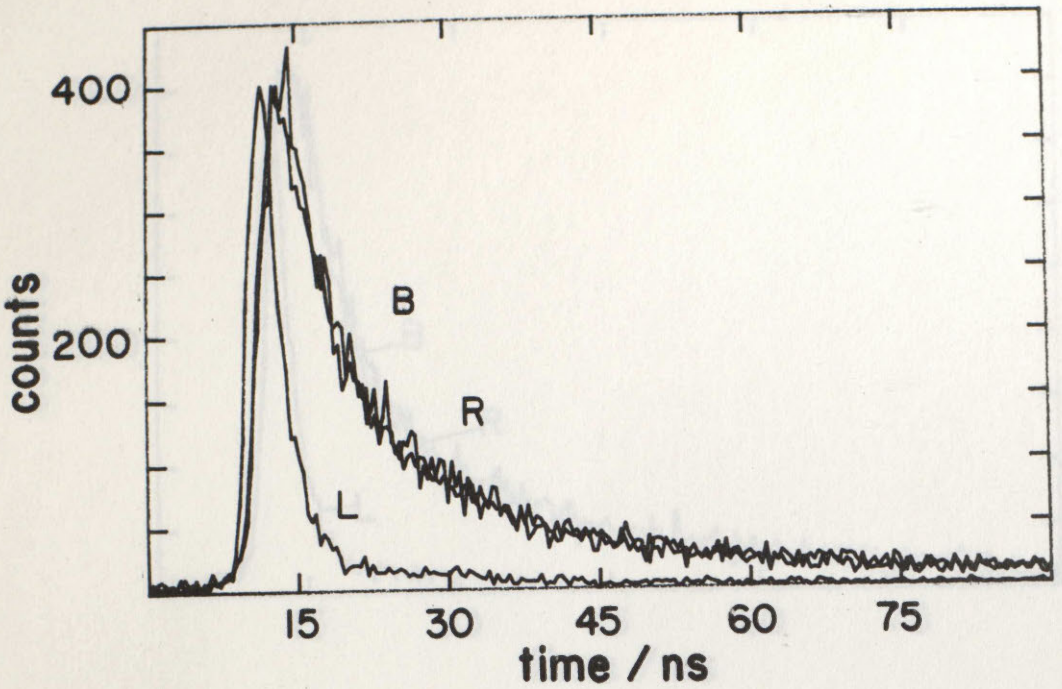

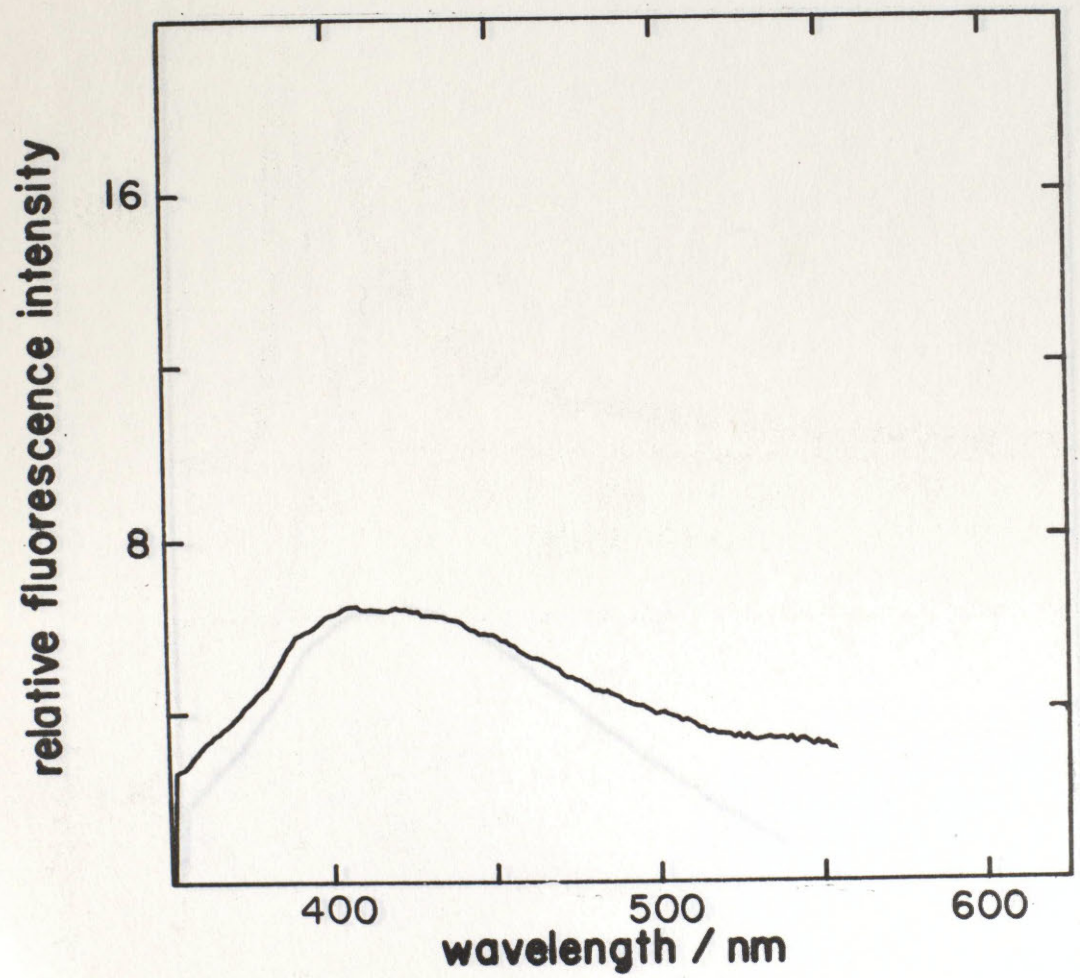

BRINE UNDER L03 AFTER 48 HOURS

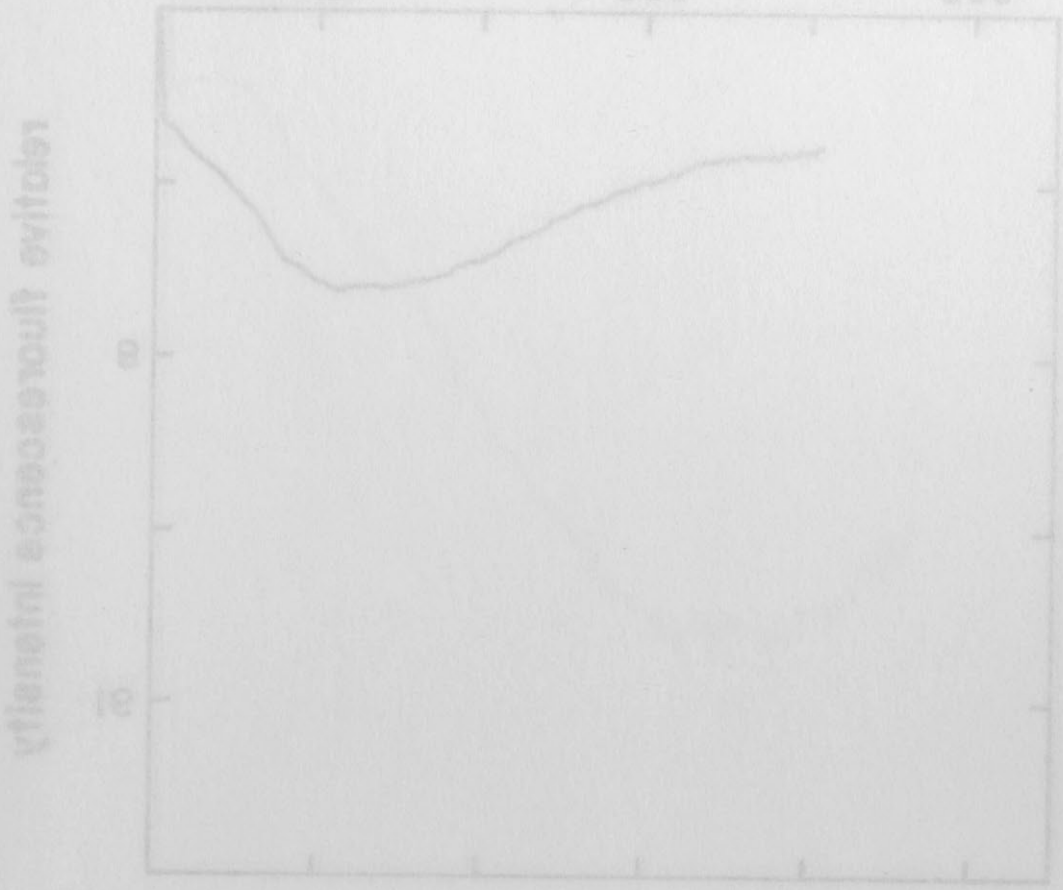

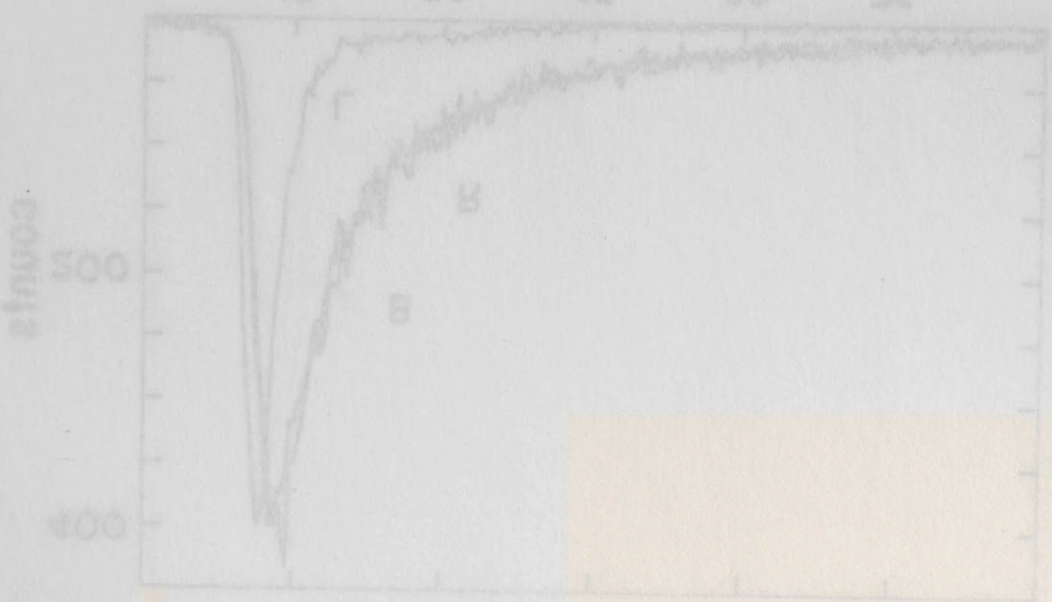

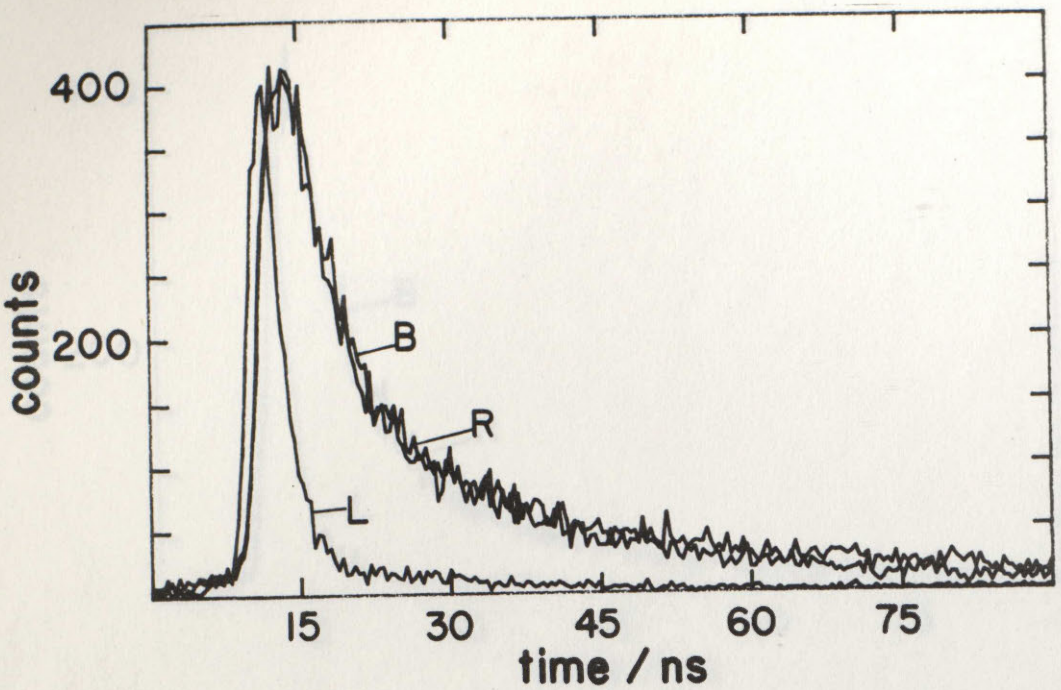

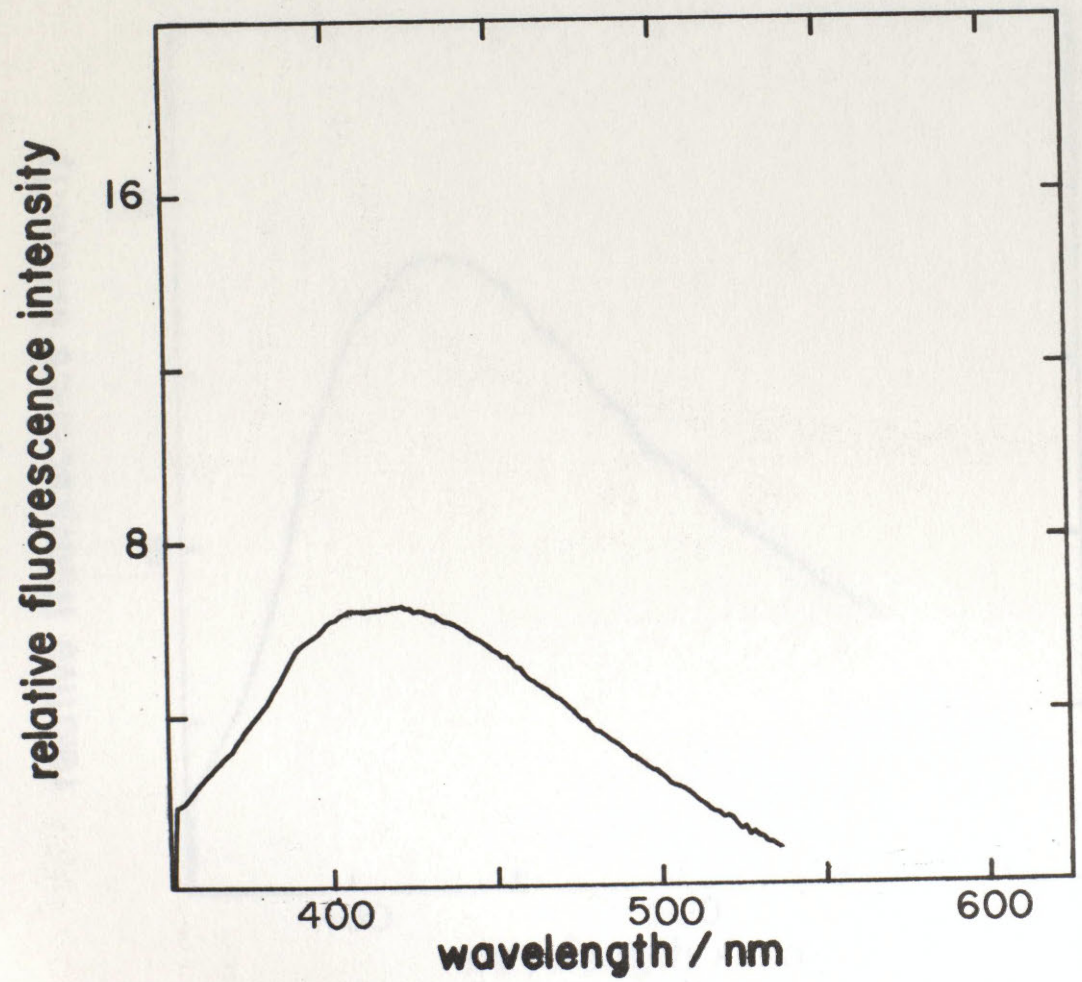

BRINE UNDER L03 AFTER 72 HOURS

counts
400
200
S
R
15
30
45
60
75
time / ns

relative fluorescence intensity
16
8
400
500
600
wavelength / nm

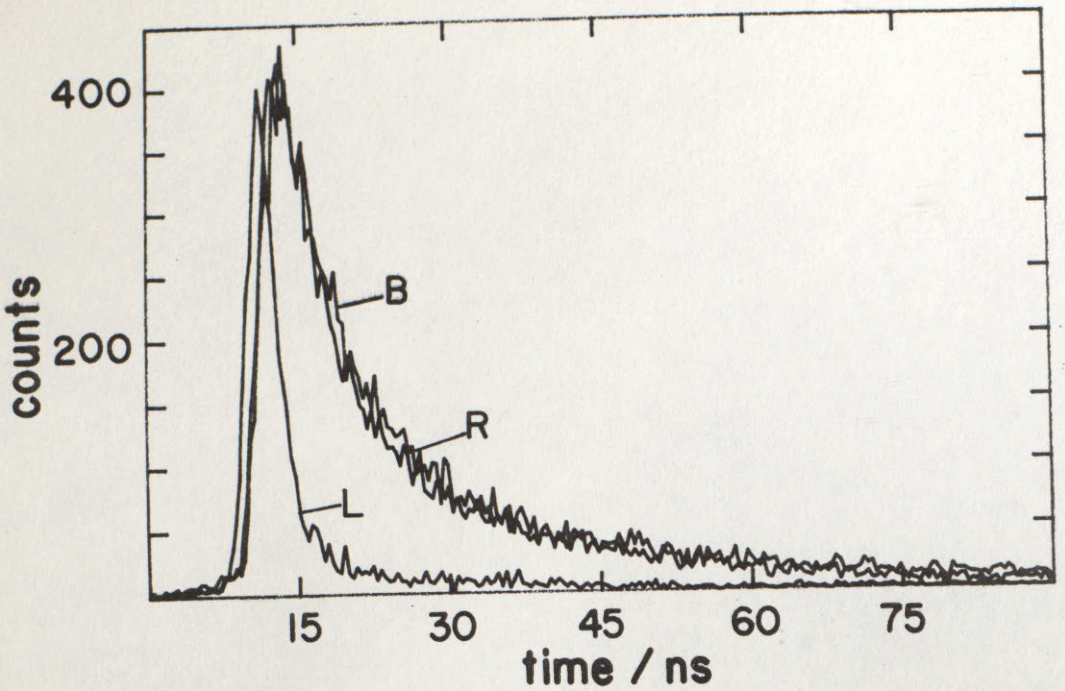

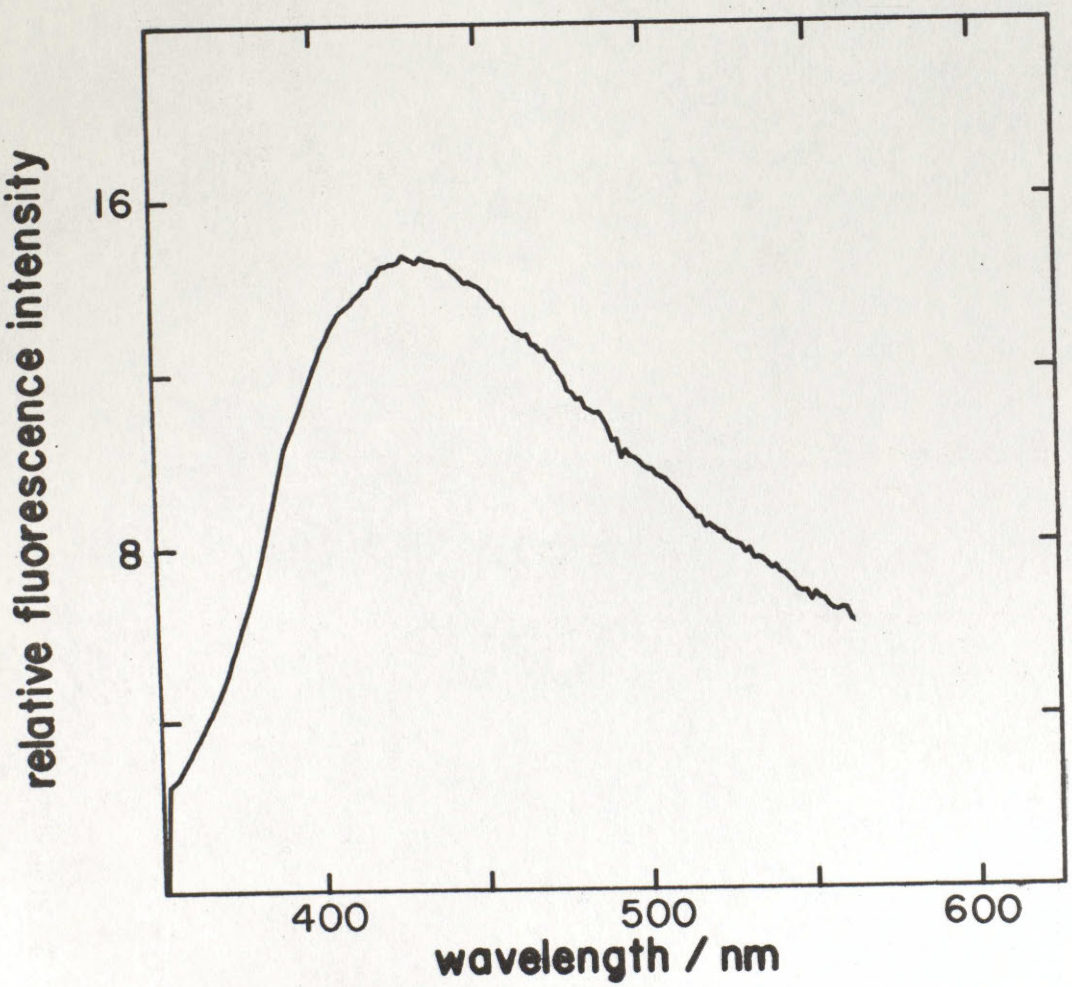

BRINE UNDER L03 AFTER 144 HOURS